# DEVELOPMENT OF A DYNAMIC OUTPUT-FEEDBACK REGULATOR FOR STABILIZATION AND TRACKING OF NON-SQUARE MULTI-INPUT MULTI-OUTPUT SYSTEMS

BY

EseOghene OVIE

B. Eng (UNIBEN) 2006, M. Sc. (INSA Lyon, France) 2012

(PhD/P14EGEE9003/2015-2018)

oveseovese@gmail.com

A THESIS SUBMITTED TO THE SCHOOL OF POSTGRADUATE STUDIES,
AHMADU BELLO UNIVERSITY, ZARIA.

IN PARTIAL FULFILLMENT OF THE REQUIREMENTS FOR THE AWARD OF A DOCTOR OF PHILOSOPHY (PhD.) DEGREE IN CONTROL ENGINEERING.

DEPARTMENT OF COMPUTER ENGINEERING, FACULTY OF ENGINEERING,
AHMADU BELLO UNIVERSITY, ZARIA
NIGERIA

March 2018

## DECLARATION

I EseOghene OVIE, declare that the work in this thesis entitled **"Development of a Dynamic Output-Feedback Regulator for Stabilization and Tracking of Non-square Multi-Input Multi-Output Systems"** has been carried out by me in the Department of Computer Engineering. The information derived from literature has been duly acknowledged in the text and a list of references provided. No part of this dissertation was previously presented for another degree or diploma at this or any other institution.

EseOghene OVIE ..... .....

(Student) Signature Date

## CERTIFICATION

This thesis entitled **"DEVELOPMENT OF AN DYNAMIC OUTPUT-FEEDBACK REGULATOR FOR STABILIZATION AND TRACKING OF NON-SQUARE MULTI-INPUT MULTI-OUTPUT SYSTEMS"** by EseOghene OVIE meets the regulations governing the award of degree of Doctor of Philosophy (PhD.) Degree in Control Engineering of the Ahmadu Bello University, and is approved for its contribution to knowledge and literary presentation.

| | | |
|---|---|---|
| Professor M. B. Muazu | ..... | ..... |
| (Chairman, Supervisory Committee) | Signature | Date |
| Dr. T. H. Sikiru | ..... | ..... |
| (Member, Supervisory Committee) | Signature | Date |
| Dr. I. J. Umoh | ..... | ..... |
| (Member, Supervisory Committee) | Signature | Date |
| Professor M. B. Mu'azu | ..... | ..... |
| (Head of Department) | Signature | Date |
| Professor S. Z. Abubakar | ..... | ..... |
| (Dean School of Postgraduate Studies) | Signature | Date |

## DEDICATION

This work is dedicated to my Dad, who taught me the value of constantly working towards excellence and for his service to his country, family and those ideals that make of men, better men.

## ACKNOWLEDGEMENTS

I give all thanks and praise to God Almighty, who is the foundation upon which all good things are built and the sum total of my existence. In him I live, I move and I have my being.

My most special thanks goes to my supervisory chair Prof. M. B. Mu'azu who I call "the Prof.". Your infectious work ethic and penchant for research excellence made this thesis possible. You have given this document the richness and clarity it possesses which is a testament to your uncanny attention to detail and your ability to keep me focused with the right perspective in view. Every second I had to interact with you was precious and like a sponge, I absorbed every knowledge you had to give from the one-on-one meetings to the discussion group sessions, these were the most valuable times I had in Zaria. I learnt from you in a short time knowledge you had painstakingly acquired over many years. I have developed into a fuller and independent researcher because of you and for this I will be always grateful. My thanks also go to the other members of my supervisory team; Dr. T. H. Sikiru and Dr. I. J. Umoh for your constructive critism, advice and encouragement all through the course of this thesis.

I will like to thank all lecturers and staff of the Department of Electrical and Computer Engineering for making this work possible through the detailed review process of seminar presentations and oral examination. I will like to specifically single out for mention Dr. Adedokun, Dr. Sha'aban, Dr. Sani, Dr. Tekanyi, Tijanni., Bashir, Yusuf, Emmanuel and finally Tukur from the secretariat for all your contribution towards making this thesis a success.

To my Ph.D and M.Sc. colleagues within and outside the department: Mustapha, Hussein, Ben, Abdullahi, Daniel, Ndubuisi, Peter, Atuman, Ajayi, Fatima, Oyibo. Interacting with all of you has been most beneficial, with the times spent bouncing ideas off one another being partly responsible for the final output of this work.

I will like to thank the following individuals who in the spirit of scientific openness acknowledged

my correspondences with them even without knowing me personnally; Prof. Alberto Isidori of the University of Roma in Italy, Prof. Allesandro Astolfi of University College London, Prof. Mitsuji Sampei of the Tokyo Institute of Technology and Dr. Chukwuma James of Digitzed LLC, Houston, USA.

To my teachers who molded me from my early formative years into adulthood; Mrs Arokoyo (N. I. F. F. R. New Bussa), Mall. Saidu (Kontagora), Mr Ukale and Mallam Sule (F. G. C. Kwali), Dr. Anyaeji (UNIBEN), Drs. Grenier, Di Loreto, Moreau and Eberhard, Profs. Bideaux and Hammouri (I. N. S. A. de Lyon, France). The role you have played can not be overemphasized. This continuing story clearly bears the hallmarks and imprints of everyone of you.

To all my friends especially Musty Na Basanko and others in the Psilon group, the former "Navy Captain" and now Commodore Abdullahi, Shola, Felix, Ola, Geoffery, Ochuko, James, your numbers truly underestimate the immensity of your contribution.

To those, whose names I can not remember or even do not know, the cleaners of the Ph.D reading room, the different drivers who made my coming to Zaria safe, the cooks in the various restaurants on campus, the printers and others at my favourite recreational hangout, I say Thank you and may God who alone knows you bless and reward you richly.

To my Director General, S. O. Mohammed (Ph.D) who made my going for this study possible, my departmental Director O. A. Agboola (Ph.D) for his support, Dr. Halidu, Dr. Sadiq, Dr. Momoh and my ever enterprising Coordinator of the Advanced unmanned aerial vehicle laboratory "My Oga" Akachukwu I want to say a big thank you for all the roles you have played individually and collectively. To my other colleagues at NASRDA, thank you for bringing me along on this journey.

Finally, I wish to thank my immediate and extended family, for their beauty, depth and for keeping faith in me through all these years. You are irreplaceable and have been a rich source of inspiration and support. My heartfelt thanks go to my Wife Stacy who during the course of this work tried to

understand geometric symmetry along with me. She has been a most invariant pillar of continued steadiness. To my son, Kome and Jite, who constantly gives me a sense of perspective. I assure you, these times away were not for nothing. To my Dad Dr. S.I. Ovie who is retired but not tired, for his love and support, To my Mum Dr. (Mrs) S.O. Ovie, whose beautiful prayer lines I started this acknowledgement with, I can not thank you enough for your constancy. To my grandmother for her prayers. To my siblings, Nyerovwo, Edesiri, Kevwe and Eguono who contributed in countless ways. Their concern was such that it felt they were also in on this Ph.D journey every step of the way. I am eternally grateful and blessed to have you all as siblings. To Prof. and Prof. (Mrs) Ezemonye, Onyiye, Kosi and Golibe for the blessing of their lovely daughter and sister in the person of my Wife, I say thank you.

**EseOghene "Ibn" OVIE.**

March, 2018.

## ABSTRACT

This research work is aimed at the development of an observer-based dynamic output feedback controller for stabilization and tracking of nonlinear systems. The developed controller is designed after the immersion-invariance and internal model principle (IMP) frameworks and targets non-square systems such as rotational-translational actuator (RTAC), cart-driven inverted pendulum (CIP) and quadrotor unmanned aerial vehicle (UAV). However non-square multiple-input multiple-output (MIMO) systems such as the UAV represented the principal system of choice for their structural properties. Non-square MIMO systems are systems that have more inputs than outputs (over-actuated) or vice-versa (under-actuated) and reflect the structures of many real world systems. The developed immersion invariance error feedback control law(IIEFCL) is used to solve stabilization and robust tracking problems of non-square MIMO non-linear systems. The output feedback internal model based observer is developed and tested with the RTAC, CIP and UAV while the immersion invariance stabilizing controller is developed and tested on the RTAC system. The output feedback controller showed good stability response on the selected models while the immersion invariance method displayed a good transient phase stability and tracking results with the addition of a robust state feedback feature to the underlying controller. The obtained settling times for the output feedback stabilization results were 2.7s, 1.113s and 0.6435s respectively for the three systems. The immersion-invariance control law acting as a robustifier to another controller produced zero percent overshoot and tracking error. The results showed attainment of desired stability and tracking and also quick convergence, disturbance rejection and handling of transient oscillations such as finite time escape or transient instability phenomena, from which many nonlinear systems do not recover after they occur. The IIEFCL was developed for the Quadrotor UAV and the results obtained were compared with some other standard nonlinear controllers that have been used in QUAV control. The metric for comparison was the integral of the squared control input (ISCI) signal. Results obtained compared favourably with existing nonlinear control laws. The IIEFCL showed the most improvement of 92.92% improvement over the backstepping con-

trol law, it had a 72.92% improvement over the feedback linearization control law and the least improvement was with respect to the sliding mode control law where only 66.225% improvement was recorded. Simulations were made using Matlab/Simulink and embedded C++ tools.

## TABLE OF CONTENTS

**Title page** i

**Declaration** ii

**Certification** iii

**Dedication** iv

**Acknowledgments** v

**Abstract** viii

**Table of Contents** x

**List of Figures** xvii

**List of Tables** xx

**List of Acronyms and Symbols** xxi

**Chapter 1: INTRODUCTION** 1

1.1 Background to the Study 1

1.2 Motivation 8

1.3 Significance of Study 10

1.4 Statement of the Problem 10

1.5 Aim and Objectives 12

1.6 Methodology 12

1.7 Thesis Outline 13

**Chapter 2: LITERATURE REVIEW** 15

2.1 Introduction 15

2.2 Review of Fundamental Concepts 15

2.2.1 Output regulation 15

2.2.2 Output feedback-based regulation 27

2.2.3 Stabilization using immersion and invariance 31

2.2.4 Observers for control systems 33

2.2.5 MIMO dynamic model 41

2.3 Review of Similar Works 44

**Chapter 3: METHODOLOGY** 53

3.1 Introduction 53

3.1.1 Development of the output feedback controller 54

3.1.2 RTAC Parameters 61

3.1.3 Output regulation for the CIP system 62

3.1.4 Regulator equations for the CIP 65

3.1.5 CIP Parameters 67

3.1.6 Output regulator for the QUAV 68

3.1.7 Quadrotor UAV Parameters 71

3.2 Development of immersion-invariance stabilizing controller 71

3.2.1 Immersion invariance control of the RTAC or TORA system 72

3.3 Development of the Immersion Invariance Output Error Feedback Regulator for Non-Square Systems 77

3.3.1 Feedback stabilization control design 77

3.3.2 Stabilizing controller by Lyapunov approach 81

3.3.3 Revisiting output error feedback regulator design for the UAV 83

3.3.4 Computation of generalized immersion relations 86

3.3.5 Output error feedback control law 88

3.3.6 Immersion-invariance controller for the quadrotor 89

3.3.7 Actuator model formulation 90

3.3.8 Augmented system model 93

3.3.9 Selection of target dynamic for the quadrotor 94

3.3.10 UAV state feedback controller design for immersion invariance 95

3.3.11 Proof of boundedness and stability of immersion invariance control law 98

3.3.12 Synthesis of immersion invariance output feedback observer-based control 100

3.3.13 Design of the error feedback observer 101

3.4 Validation of the Developed Immersion Invariance Output Feedback Control Law 104

**Chapter 4: RESULTS AND DISCUSSION** 107

4.1 Introduction 107

4.2 Output Regulation Experiments 107

4.2.1 RTAC Regulation Experiments 108

4.2.2 CIP Output Regulation 111

4.2.3 Quadrotor UAV Output Regulation 113

4.2.4 Summary of Output Regulation Experiments 116

4.3 Immersion Invariance Stabilization Experiments 117

4.3.1 RTAC Immersion Invariance 117

4.3.2 RTAC immersion invariance stabilization controller 117

4.3.3 Linear immersion invariance Tracking control with observation 121

4.3.4 Robust RTAC stabilization and tracking experiments with disturbance injection 121

4.4 Immersion Invariance Error Feedback Control Results 125

4.4.1 QUAV unforced stabilization results 126

4.4.2 Exosystem profile 127

4.4.3 Immersion-invariance error feedback regulator results 128

4.4.4 IIEFCL state output results 132

4.4.5 Characterization of the control laws 139

4.4.6 Comparison of results from various control laws 150

**Chapter 5: SUMMARY AND CONCLUSIONS** 152

5.1 Summary 152

5.2 Conclusions 153

5.3 Limitation 155

5.4 Contribution to Knowledge 156

5.5 Recommendation for Future Work 157

**References** 165

**Appendix A: Code listing for the RTAC Output Feedback Regulator Problem** 167

A.0.1 RTAC parameters are defined here from Avis *et al.*, 2013 167

A.0.2 Substitution of params 167

A.0.3 Definition of the exosystem matrix as either constant or variable 167

A.0.4 Computing controllability 167

A.0.5 Discussion 168

A.0.6 Computing observability 168

A.0.7 Computing observability 168

A.0.8 Construct a stabilizing gain Kx for A+BKx 168

A.0.9 Developed method for matching the poles 169

A.0.10 Computing the values in the gains L,L1,L2,G1,G2 169

A.0.11 Computing the gains L=L1 169

A.0.12 Computing the gains L1 and L2 for the matrix G2 170

A.0.13 Compute the L2 gain from developed method 170

A.0.14 Computing Kv 171

A.0.15 Compute the global K matrix Kavis=[Kxavis Kvavis] 171

A.0.16 Solve the sylvester equations from knowlwegde of Kx and Kv 172

A.0.17 Computing the other gain of the observer G1 172

A.0.18 Test for the controllability of Aobsv, Bobsv 172

A.0.19 Test for stability of G1 and G2 matrices 173

A.0.20 Check for Hurwitz stability of the closed loop system matrix below 173

A.0.21 Calling model here 173

**Appendix B: Code listing for the UAV Output Error Feedback Regulator Problem** 174

B.1 QUAV smulation script 174

B.1.1 Symbolic variables used 174

B.1.2 Derived variables from Lefeber, (2015) prepared for linearization 174

B.1.3 Derived variables from Ozbek *et al.*, (2015) prepared for linearization 174

B.1.4 Matrix of vector fields 175

B.1.5 Load system parameter values 175

B.1.6 Evaluating the transmission and input matrices 178

B.1.7 Controllability & observability computation 178

B.1.8 Computation of canonical form matrices 179

B.1.9 Output error feedback regulator design 179

B.1.10 State feedback Kx 180

B.1.11 Compute the augmented Kxi gain 181

B.1.12 Check stability of the gain Kx(i) and global Kx 181

B.1.13 Regulator equations solving the sylvester equations for X and U in the format 181

B.1.14 Check FBI solution results 182

B.1.15 Compute the gains L1 and L2 for the matrix G2 182

B.1.16 Observer gain matrices or internal model matrices can now be formed for G2 182

B.1.17 Internal model design 182

B.1.18 Test the stability of the overall closed loop system 183

B.1.19 Exosystem reference inputs 183

B.1.20 Execution of various commands in script 185

B.1.21 Battery value 186

B.1.22 Inverse matrix for torque generation in plus configuration 186

B.1.23 Compute feedforward generator for the QUAV 186

B.1.24 Gains for the nominal back stepping controller 186

B.1.25 Pole placement for the actuators 187

B.1.26 Stabilizer analysis 187

B.1.27 Khalil's Observer gain 188

**Appendix C: Presentation of Immersion Invariance Script** 192

C.1 Immersion Invariance Controller Design for RTAC System 192

C.1.1 Test for observability or detectability 192

C.1.2 Using matlabs place command find a feedback F with specified poles 192

C.1.3 Using matlabs place command, find an obsrver gain L 192

C.1.4 Call model here 193

C.2 Proof of Immersion Condition 193

## LIST OF FIGURES


| | | |
|---|---|---|
| 1.1 | Standard Regulator Structure (Hoagg and Bernstein, 2006) | 3 |
| 1.2 | Standard Output Feedback Regulator Structure (Valmorbida and Galeani, 2013) | 3 |
| 1.3 | Output Error Feedback Regulator Flowchart | 7 |
| 1.4 | Immersion Invariance Flowchart | 8 |
| 2.1 | Robust Linear Regulation Setup (Kim, 2009) | 18 |
| 2.2 | Robust Non-linear Regulation Setup (Serrani, 2005) | 18 |
| 2.3 | Observer Classification (Luenberger, 1971) | 34 |
| 2.4 | Observer Schematic Showing Interconnection with System (Friedland (nd)) | 36 |
| 2.5 | RTAC or TORA System (Wu and He, 2016) | 42 |
| 2.6 | Cart Driven Inverted Pendulum Diagram (Graham and Turkoglu, 2017) | 43 |
| 2.7 | Quadrotor UAV Diagram (Chovancova *et al.*, 2016) | 44 |
| 3.1 | Experimention Flow Chart | 54 |
| 3.2 | QUAV Control Schematic (Sugawara & Shimada, 2017) | 78 |
| 3.3 | Control Block Diagram | 79 |
| 3.4 | Composite Regulator Controller Schematic (Serrani, 2005) | 102 |
| 4.1 | RTAC OEFR Stabilization with ic=(0.051 0 pi/8 0) | 109 |
| 4.2 | RTAC OEFR Stabilization with ic=(0.2 0 15 0) | 110 |

4.3 CIP OEFR Stabilization with ic=(0.5 2.66 pi/4) 112

4.4 CIP OEFR Stabilization with ic=(0.2 1.3 pi/2) 113

4.5 Regulation Control; ic=(0,0,50,0.785,0.196,0.131) and fc=(0,0,0,0,0,0) 114

4.6 Regulation Control; ic=(0,0,19,7.5,15,0.07) and fc=(0,0,0,0,0,0) 115

4.7 State Output from Immersion Invariance Linear Controller 118

4.8 Plant and Observer Output from Immersion Invariance Linear Controller 118

4.9 Nonlinear State Output from Immersion Invariance Controller without Observer 119

4.10 Nonlinear States Stabilization for 50sec with Observation 120

4.11 Nonlinear States Stabilization for 500sec with Observation 120

4.12 Linear Tracking Control with Conditions; ic=(0,0,0,0), fc1=(0,0,15,0) 121

4.13 Linear Tracking Control with Conditions; ic=(0,0,0,0), fc2=(0,0,7.5,0) 122

4.14 Non-robust Stability Control; ic=(0.051,0,0.393,0), disturbance=0.1units 123

4.15 Robust Stability Control; ic=(0.051,0,0.393,0), disturbance=0.1units 123

4.16 Non-robust Tracking Control; ic=(0,0,0,0), fc=(0,0,15,0) 124

4.17 Robust Tracking Control; ic=(0,0,0,0), fc=(0,0,15,0) 125

4.18 Unforced X-Y-Z Stabilization for the QUAV 126

4.19 Unforced Attitude Roll-Pitch-Yaw Stabilization for the QUAV 127

4.20 Disturbance Generator Profiles 128

4.21 Control Effort of Immersion-Invariance Error Feedback Regulator 129

4.22 Z-axis Output Error 129

4.23 Roll Output Error 130

4.24 Pitch Output Error 130

4.25 Yaw Output Error 131

4.26 Translational Output Response for (x,y,z)=(1,1,10) 132

4.27 Translational Observer Output Error Response for (x,y,z)=(1,1,10) 133

4.28 Attitude (Roll) Output Response for $\phi = \pi/12$ 134

4.29 Roll Observer Output Error Response for $\phi = \pi/12$ 135

4.30 Attitude (Roll) Output Response for $\phi = \pi/12$ 136

4.31 Pitch Observer Output Error Response for $\phi = \pi/12$ 137

4.32 Attitude (Yaw) Output Response for $\phi = \pi/12$ 138

4.33 Yaw Observer Output Error Response for $\phi = \pi/16$ 139

4.34 Smoothed Step Exosystem 140

4.35 Backstepping NLCL for Step Input 140

4.36 EFCL for Step Input 141

4.37 IICL for Step Input 141

4.38 IIEFCL for Step Input 142

4.39 Sinosoidal Exosystem 142

4.40 Backstepping NLCL for Sinusoidal Input 143

4.41 EFCL for Sinusoidal Input 144

4.42 IICL for Sinusoidal Input 144

4.43 IIEFCL for Sinusoidal Input 145

4.44 Impulse Exosystem 145

4.45 Backstepping NLCL for Impulse Input 146

4.46 EFCL for Impulse Input 147

4.47 IICL for Impulse Input 147

4.48 IIEFCL for Impulse Input 148

## LIST OF TABLES


3.1 Table of RTAC Parameters (Nersesov *et al.*, 2010) 62

3.2 Table of CIP Parameters (Elsayed *et al.*, 2015) 67

3.3 Table of QUAV Parameters (Ozbek *et al.*, 2015) 71

4.1 Table of Results for Output Error Feedback Stabilization Control) 117

4.2 RTAC Immersion Invariance Results for Robust-R and Nonrobust-NR 125

4.3 Standard Deviation for a Smoothed Step Exosystem 149

4.4 Standard Deviation Results for a Sinusoidal Exosystem 149

4.5 Standard Deviation Results for an Impulse Exosystem 149

4.6 Average Standard Deviation Results for Each Exosystem 150

4.7 Integral of the Squared Control Input(ISCI) for Three Different Sets of Controllers 151

# CHAPTER 1

# INTRODUCTION

## 1.1 Background to the Study

The design of stabilizing controllers is a major task and requirement for the control engineer. While notions of stability vary from linear to nonlinear systems, the main ideas and goals are the same; which is to force the evolution of the trajectories of a system towards an equilibrium point or an equilibrium set. This is the same goal in either linear bounded-input bounded-output (BIBO) stability or more involved nonlinear counterparts like the Lyapunov stability variants and structural stability. Output regulation, which is the core theme of this proposal, requires that for any system to be successfully controlled, it must first be established to be stabilizable (Byrnes *et al.*, 1990). This stability being enforced in the presence of constraints such as known or unknown disturbances and uncertainties. The system requirement is that all trajectories of interest or system states remain asymptotically close to or converges exactly to the desired equilibrium point and remains there for all time (Isidori & Byrnes, 1990). In the absence of stability, the ultimate desire for affecting the behavior of any system through regulation using suitable control signals is not possible; such regulation being demanded in the presence of the stated constraints which can interact with any real system to cause instability and deviation from correct behavior. Examples of such uncertainties and disturbances include; un-modeled dynamics, high frequency parasitic components, large inputs and other complex coupling phenomena in multiple-input multiple-output (MIMO) systems (Kokotovic, 1985).

The search for a globally stabilizing and asymptotically tracking feedback controller has seen various control schemes put forward for consideration (Andrieu & Praly 2009; Astolfi & Praly 2015). Another name for such a robust stabilization and tracking control scheme is output regulation. Pioneering output regulation control designs include: linear single-input single-output (SISO) and

MIMO systems by Francis and Wonham (1976) and the equivalent nonlinear SISO and MIMO treatment by Byrnes and Isidori (1990). This has also seen the achievement of various results ranging from local, semi-global to global. However, while stabilization in the local sense has been considered for non-linear systems since the early 1990's, it is the stabilization in a large domain such as semi-global stabilization by Teel and Praly (1993), Battilotti (2001) and global stabilization by Chen and Huang (2004), Peixoto *et al.*, (2009) that are good prospects in the search for a global stabilizing feedback compensator. More specifically global robust regulation concerns have dominated the research in many of the literature on stabilization of nonlinear systems (Astolfi & Praly, 2017).

Continuing research in output regulation over the years has seen a stream of new results added by Huang (2004), Chen and Huang (2004), Serrani (2005), Isidori (2011), Khalil and Praly (2014), Astolfi and Praly (2015). These works contributed to the development of workable designs. Specifically considering the analysis of the internal structure of a MIMO system and studies of how this structure was affected by feedback and output injection. The obtained results were used to solve such problems as stabilization, tracking, system decoupling and fault isolation. In the case of non-linear systems, most of the methods for the analysis of the internal structure have been conveniently extended beyond that originally developed by Francis and Wonham (1976). According to Isidori (2011), recent works showed that the study of problems of output feedback design for MIMO nonlinear systems has come to an almost complete stall. Some reasons given for this difficulty in tackling the non-linear MIMO problem include simple and complex interconnections between various states and inputs and difficulty in transferring observer control design from linear to nonlinear MIMO systems (Isidori, 2011; Wang *et al.*, 2014).

Therefore regulation of the output of any system must be preceded by satisfiable stabilization properties in the implemented closed-loop control architecture if regulation of the system output must be achieved. Figure 1.1 depicts such a control architecture that is well known in control systems theory (Hoagg & Bernstein, 2006). The variables $y_c(t)$, $e(t)$, $u(t)$ and $y(t)$ represent the command

or reference input, error signal, control input and output respectively. Such potential instability justifies the case for the presence of a robust regulator that maintains the stability of the system state and regulates the system output towards the asymptotic tracking of reference signals and rejection of unwanted or undesired disturbances. In order to effectively handle a wide range of disturbances

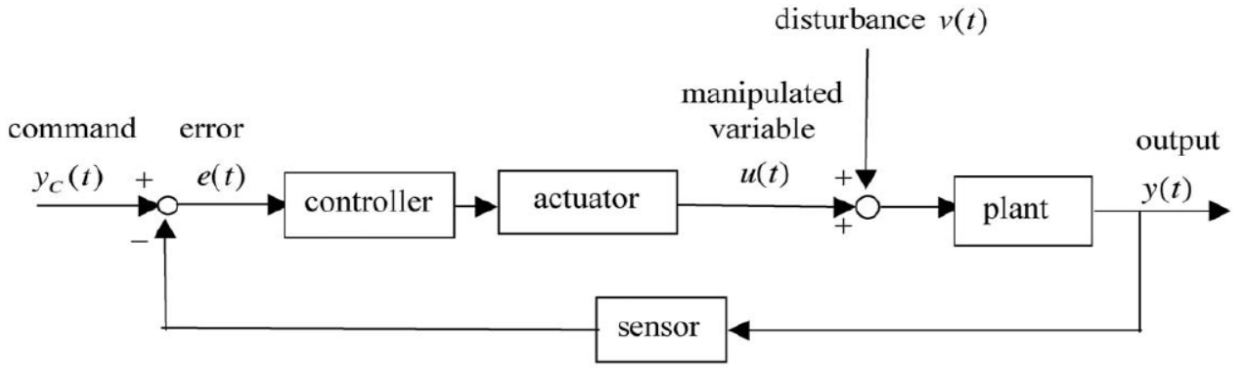



Figure 1.1: Standard Regulator Structure (Hoagg and Bernstein, 2006)

and system uncertainties, a different architecture is needed as given by the internal model-based output feedback controller. The design depicted in Figure 1.2 captures the internal model principle

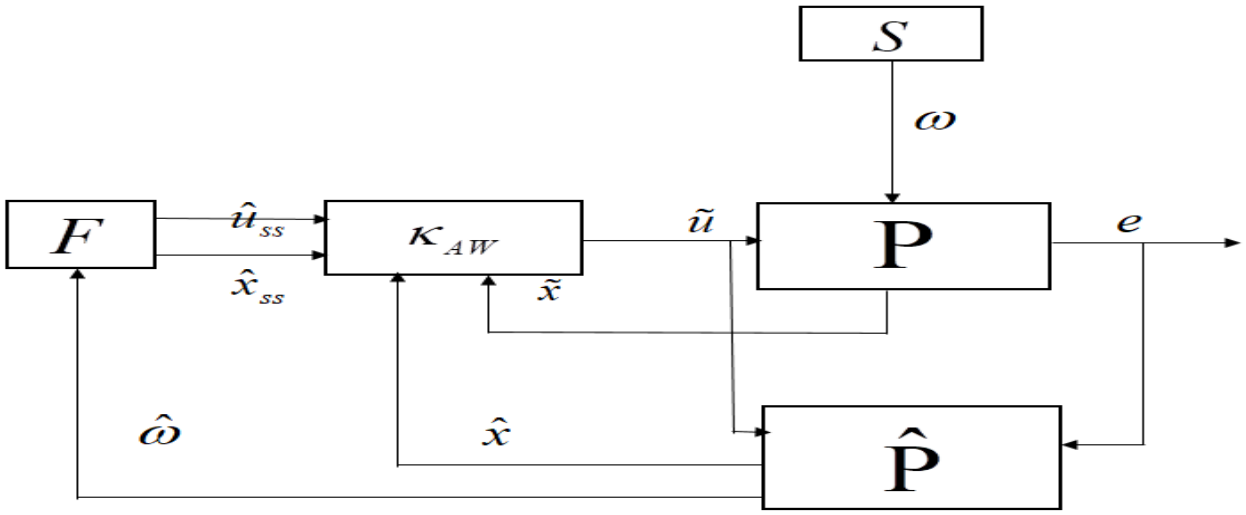



Figure 1.2: Standard Output Feedback Regulator Structure (Valmorbida and Galeani, 2013)

(IMP) philosophy, which requires the resulting controller to have asymptotic tracking and disturbance rejection properties (Kokotovic & Arcak, 2001). The internal model $F$, steady state control and state variables $u_{ss}$ and $x_{ss}$, plant and observer are $P$ and $\hat{P}$ respectively. Observer estimates

$\hat{x}$ and $\hat{\omega}$, unstable states $\tilde{x}$, exogenous signal $\omega$ and output error $e$. This is made possible by embedding a copy of the actual system in the control architecture. This stabilizing control ensures the tracking of a given reference trajectory so that the output error is regulated to zero. The parts of the robust observer-based regulator consist of the plant, the observer which acts as the internal model, the steady state stabilizer and steady state generator ( and respectively) and finally the exosystem supplying the external inputs to the system. This framework also assumes knowledge of the reference signals/disturbances.

In developing an observer-based output feedback control law, specific design methods depend on the kind of information available for feedback (Astolfi & Praly, 2017). In general this technique for robust regulation of a dynamic systems output has been categorized by Serrani (2005) into state and output error feedback. The output feedback approach to regulation of a systems response is more practicable in tackling the robust stabilization and tracking question. Considering that the control system designer is assured of having the entire output present for measurement as against the possibility of having individual state for measurement. Output feedback stabilizing regulator also has other advantages which include; ease of practical implementation, multi-functionality within the single design e.g. a single controller design being able to serve as both stabilizer and steady state regulator for multiple manipulated variables and applicability for disturbance rejection (Astolfi & Praly, 2017; Chang *et al.*, 2015).

Therefore, the developed observer-based output feedback controller is used to achieve robustness, adaptive behavior and importantly, to ensure global asymptotic stability (GAS) of system states. Based on the principle of internal model, the output feedback controller ensures simultaneous robust stabilization and tracking of reference inputs or rejection of reference disturbances (Francis & Wonham, 1976). However, it often achieves this in a local domain of the work space (under small signal perturbation). Another scheme for stabilization is the immersion and invariance method, known for yielding globally stabilizing and adaptive designs for controllers in the presence of parametric uncertainties (Astolfi & Ortega, 2003). Immersion and invariance method does not

however have the robustness characteristics of the internal model output feedback design.

The robust output regulator with structure shown in Figure 1.2 is proposed for modification. This modification is necessary because it is not possible to always know every profile or function of the disturbance or uncertainty to be encountered. Therefore while output measurement by an observer is still necessary, the observer-based output feedback nomenclature remains open to increased robustness and adaptive design features. The development of such stabilizing regulators has seen the use of different implementation architectures using general principles of internal model control (IMC) such as model predictive control (MPC) framework, one example of which is the model predictive regulator of Aguilar and Krener (2014), state and error observer framework by Carnevale *et al.*, (2012), strictly adaptive framework, immersion-invariance framework by Astolfi and Ortega (2003), disturbance observer (Shim *et al.*, 2015).

Extending the treatment to systems with uncertainties, Wiese *et al.*, (2015) and Shim *et al.*, (2015) have also addressed the problem of adaptive control designs. The uncertainties being sources of instability in either the transient or steady operating phase is affected by the observer gains. Whereas high gain designs which are ideal for local or semi-global stabilization are beneficial for quick convergence, high gains have a detrimental effect in the transient regime where large error occurs. High gains also have a detrimental effect on the measurement error in steady state regime where the error (usually small), is derived from model uncertainties. Switched gain observer design has also been studied by Ahrens and Khalil (2008).

Therefore, having established the existence of different approaches and the several attempts made to obtain a globally stabilizing output feedback controller (Andrieu & Praly, 2009), this work proposes another approach for non-square MIMO non-linear systems, based on the identified developments. The approach will make use of a hybridization of techniques from both internal model principle-based output-feedback and immersion-invariance stabilization theory. The developed control scheme shall tradeoff the strengths and weaknesses of each method. While the

output regulation framework requires the unrealistic knowledge of every disturbance and uncertainty, such requirements are absent for Immersion-Invariance stabilization. Therefore the strong stability results from Immersion-Invariance are combined with the strong tracking results from output regulation to produce an improved controller.

This work has given an alternative and detailed development of an immersion and invariance observer-based output feedback regulator that has characteristics of global stability. The design builds on the premise that global asymptotic stabilization implies global asymptotic tracking that assures semi-global stabilization in output feedback (Teel & Praly, 1993). The current synthesis of a stabilizing observer-controller framework has brought together established techniques which are principally from internal model principle and immersion-invariance design. The design specifically addresses stabilization and tracking a non-square MIMO nonlinear systems. Figure 1.3 summarizes the flow of information in an output-regulated feedback controller that is based on the IMP. This flowchart starts with the definition of the plant, exosystem and controller, formation of an autonomous closed loop system, analysis of the resulting structure of the resulting autonomous system, solution of the regulator equations for the system. $A$, $B$ and $C$ are the system transmission matrix, input matrix and output matrix respectively. $W_r$ is the controllability or reachability matrix, $K_x$, $K_v$ are the stabilizing state and disturbance feedback gains. $u$ is the regulator control variable. $L_1$, $L_2$, $G_1$, $G_2$ are observer gains.

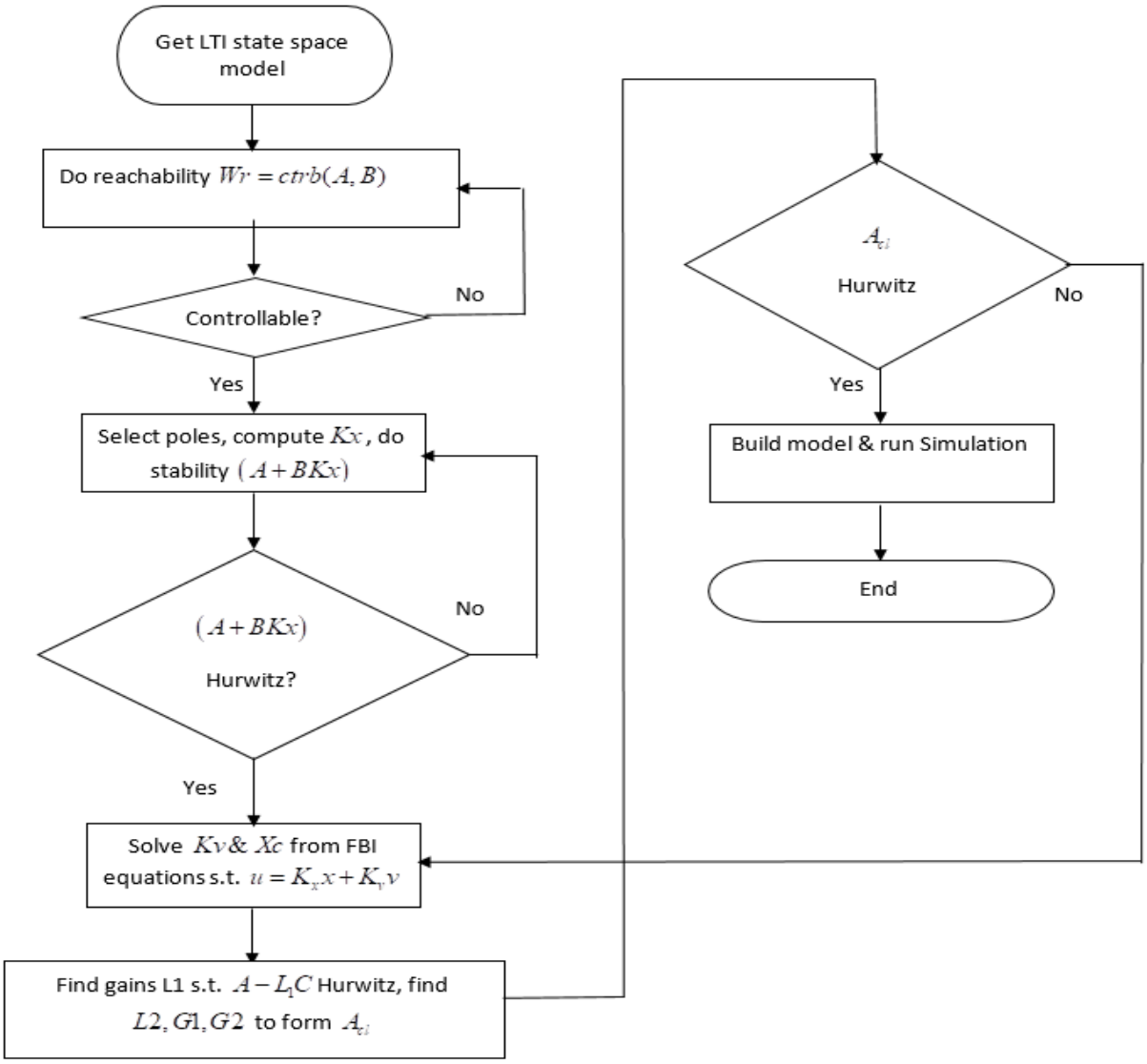



Figure 1.3: Output Error Feedback Regulator Flowchart

Similarly, the flowchart for setting up an Immersion and Invariance stabilization (Astolfi and Ortega, 2003) scheme is shown in Figure 1.4. $x$ is the system state in original coordinates, $\xi$ is system state after immersion, $K$ is stabilizing feedback matrix, $f(.)$ and $g(.)$ are state and input vector fields. $\pi(.)$ is an immersion map and $\phi(.)$ is the zero manifold while $\psi(.,.)$ is the off-manifold control law. Following the establishment of the output regulation scheme using observer output feedback and immersion invariance, a closed loop architecture was implemented. By extending the standard architecture for observer-based output regulation, this work proposed an immersion

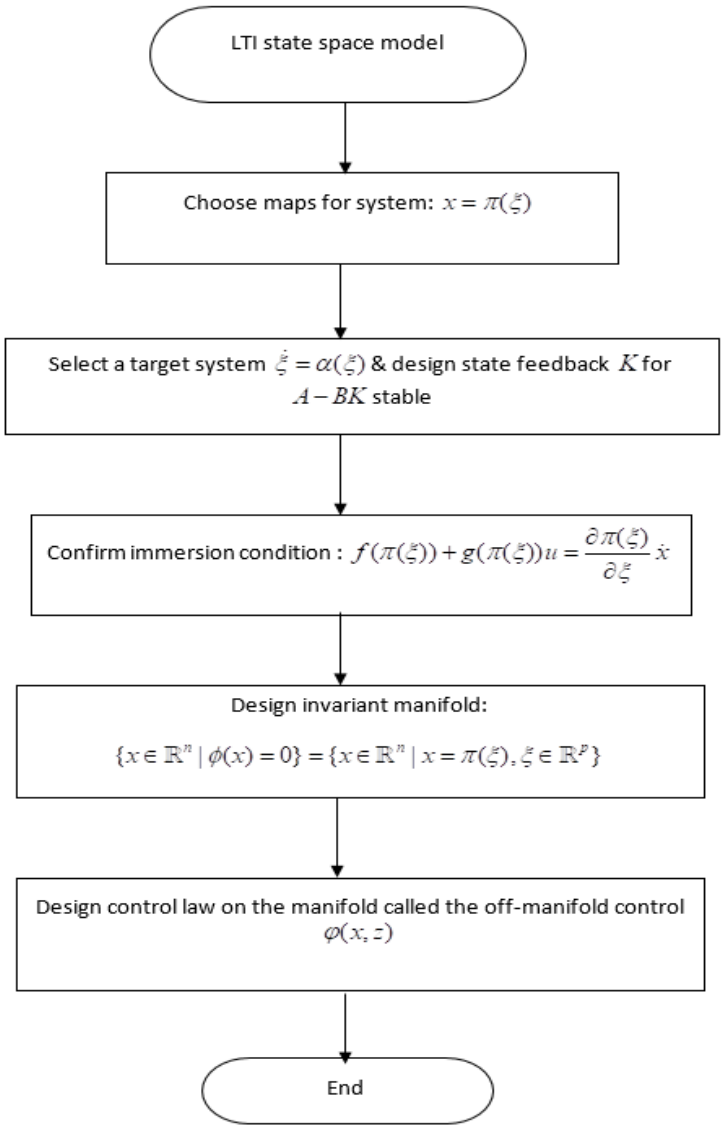



Figure 1.4: Immersion Invariance Flowchart

and invariance output feedback architecture for robust and adaptive stabilization of system state and asymptotic convergence of system output error to zero.

## 1.2 Motivation

Investigations by Wang *et al.*, (2014) in which the dynamic output feedback in MIMO system is achieved in the context of a high gain observer (HGO) forms the principal motivation for this work. Astolfi and Praly (2015) have also looked at the extension of the output feedback problem by in-

vestigating the effects of small un-modeled discrepancies which could also cover external sources arising from reference signals and disturbance inputs. However, practice shows that not all disturbance inputs are of small magnitude. In the case of MIMO non-linear systems that are controlled via output feedback, the problem of asymptotic stabilization, despite of its obvious relevance in dynamic systems remains unresolved. Literature evidence shows that inquiry in this direction has received little attention (Wang *et al.*, 2014). This is moreso for non-square MIMO systems where works addressing observer-based output feedback for non-square uncertain systems are also limited (Isidori, 2011; Shim *et al.*, 2015).

While output feedback presupposes the existence of some form of estimator or observer of state, certain constraints can be identified with the availability of such measurement (Nazrulla & Khalil, 2008). Firstly, not all states are usually available for measurement (Kazantis & Kravaris, 1998; Kaldmae & Kotta, 2013), making the full state information problem of output regulation more ideal than practical for the task. Aside from the full state information being rarely available, design methods based on the availability of partial state information are important (Wang *et al.*, 2014), as well as designs that consider the output error information (Astolfi & Praly, 2017). Such designs have proved to be more practically feasible and have necessitated output feedback techniques which although applied successfully in SISO type systems, have not seen a similar level of progress in nonlinear MIMO systems (Khalil & Praly, 2014; Isidori, 2011). More recent works have utilized immersion (Astolfi and Ortega, 2003), embedding the partial or reduced state output observer as an internal model of the system while respecting certain structural conditions that guarantees system analysis. Other works have utilized non-linear coordinate transformation. These have become more practical approaches to solving the dynamic Output Regulation problem but mainly in square systems. Considering these facts, the problem of achieving robust stabilization-tracking via output feedback is still largely open, especially for non-square MIMO non-linear systems (Wang *et al.*, 2014).

The question therefore becomes, how to achieve GAS in the presence of disturbances and model

uncertainties of varying magnitudes using a control law that is robust and adaptive under all operating conditions? Specifically taking into account the inability to know accurately all possible uncertainties that might enter into a system. One answer to this question was the control law provided by the developed immersion-invariance output feedback controller. The appeal for such a control law follows the established fact that stabilization and tracking without robustness and inherent adaptation leads to instability, reduced control authority, loss of control, increased energy usage and poor transient performance. Therefore the developed scheme did not need to have full information of the possible uncertainties or disturbances to achieve the control goals.

## 1.3 Significance of Study

The significance of this work is the extension of the existing treatment of MIMO output regulation or stabilization-tracking analysis to specifically address non-square MIMO nonlinear systems. The utilized approach firstly, uses output-regulated output feedback control as a basis. Secondly, the current treatment is extended in the particular direction immersion and invariance setting that allows for design of globally stabilizing control laws. Lastly, identifying and making use of relevant design parameters from the two previous techniques. It focuses on the development of a practical framework to be applied towards achieving robust stabilization and tracking irrespective of intervening uncertainties. This new framework is an Immersion-Invariance output feedback strategy. Therefore, elements of the system which might prevent the attainment of global asymptotic stability (GAS) such as finite time escape phenomena like peaking are addressed.

## 1.4 Statement of the Problem

Section 1.2 presented globally stabilizing control laws for nonlinear and linear systems as an open problem in the context of nonlinear, non-square systems utilizing output feedback controllers. One of the difficulties in achieving such stabilizing control laws using output feedback regulation concept remains the existence and uniqueness of solutions to the regulator equations which is not assured for all systems. Because, while it can be checked that such a regulator exists (neces-

sity), obtaining the regulator (sufficiency) remains a difficult task. Moreso, for non-square systems where analysis sometimes requires squaring the plant before output feedback is applied. Seeing the difficulty in achieving stability using the analytical route, certain literature developed a constructive approach using eigenvalue pole placement and gain matrix designs which when properly done, renders the system internally stable. The attraction for such a method rests with the fact that if subsets of the system were designed to be stable then the global system when assembled together retained such stability. The identified difficulty could be described in a sense as structural. This description has meaning in non-square systems with respect to size of inputs and outputs. Also more fundamental was the size reduction in systems with reduced rank leading to nominally uncontrollable and unobservable systems. It has been observed that some of these characteristics that are influenced by the system structure were readily identifiable using differential geometric techniques for analyzing such nonlinear systems.

System stability in the global context requires control laws that are robust for all possible and acceptable inputs. Therefore, the continued demand for controlled systems to have good stability and tracking performance cannot be overemphasized. Also, overcoming the potentially destabilizing effect of disturbances and uncertainties is key to driving the error term in any controlled system to zero. The problem can therefore be summarized as the regulation of any given system's state to an invariant zeroing manifold from which it is impossible to escape and at the lowest possible control cost. The implemented solutions used both state and output feedback principles to ensure the continued internal stability and output regulation of the selected systems' states. This was achieved in the presence of structural imbalance inherent to non-square systems and also in the presence of potential destabilizing factors such as external disturbances and inputs that were captured in the utilized exosystem structure.

## 1.5 Aim and Objectives

The aim of this work is: development and synthesis of a dynamic output feedback observer for stabilization and tracking in non-square MIMO nonlinear systems.
The objectives of the study are therefore as follows:

1. Development of an internal model based output regulation framework for stabilization of non-square MIMO nonlinear systems.

2. Development of an immersion and invariance stabilization framework for non-square MIMO nonlinear systems.

3. Development of an immersion and invariance output feedback control law for stabilization and tracking of non-square MIMO nonlinear systems.

4. Validation of the immersion-invariance output feedback theory and control law using standard benchmark non-square MIMO systems (cart-driven inverted pendulum (CIP) , rotational/translational proof-mass actuator (RTAC) and a fixed rotary wing quadrotor unmanned aerial vehicle (QUAV) .

## 1.6 Methodology

The methodology for implementation of the stated objective items are:

1. Internal model principle(IMP)-based output regulation framework for stabilization and tracking

   (a) Adoption of relevant mathematical background for output regulation

   (b) Analysis of necessary and sufficient conditions for existence of solutions for output regulated control

(c) Implementation of the IMP regulation framework with internal model-based observer on the following non-square dynamic: Rotational Translational Actuator (RTAC), Cart Driven Inverted Pendulum (CIP), Quadrotor Unmanned Aerial Vehicle (QUAV).

(d) Simulation experiments of the output regulated control law in Matlab/Simulink

2. Immersion and invariance (I&I) stabilization framework

   (a) Adoption of relevant mathematical preliminaries for immersion and invariance stabilization

   (b) Analysis of the necessary and sufficient conditions for existence of solutions for an immersion and invariance stabilizing control law

   (c) Implementation of the immersion and invariance framework with standard observer on selected benchmark non-square dynamic

   (d) Simulation experiments of the control law in Matlab/Simulink

3. Development of an immersion and invariance output feedback framework

   (a) Parameter identification for use in developed output regulated output feedback scheme

   (b) Implementation of the immersion and invariance observer output feedback framework on the non-square MIMO QUAV model.

   (c) Simulation in Matlab/Simulink of the developed control law.

4. Validation on selected non-square dynamic system and fine-tuning(using neural tools) where needed of the selected parameters in the developed controller of methodology item (3) to ensure the goal of GAS and perfect tracking

## 1.7 Thesis Outline

The organisation of the thesis is as follows; Chapter One has laid-out in brief the overall goals to be achieved with the introduction, motive, significance of study, statement of the problem, thesis

aim and objectives and ends with a discussion of the method used in achieving the set goals. Chapter Two has given a detailed review of pertinent concepts and literature. Chapter Three has addressed the materials and methods applied in-so-far as this thesis report is concerned, Chapter Four presented the results for discussion and Chapter Five concludes the body of the report. All cited references have been included in the references section while relevant additional material such as codes and certain parameter derivations have been placed in the appendix section.

# CHAPTER 2

# LITERATURE REVIEW

## 2.1 Introduction

This literature review addresses the pertinent topics that concerns the treatment of the non-square MIMO nonlinear system output feedback regulator. The current review first addresses the key fundamental concepts and subsequently makes a detailed review of relevant similar works. In the sections that follow, each of the mentioned parts that make up the controller development is discussed.

## 2.2 Review of Fundamental Concepts

This section highlights concepts that are fundamental to the study like stability, output regulation, IMP, output feedback, observers, immersion and invariance, MIMO systems and peaking phenomenon.

### 2.2.1 Output regulation

The problem of controlling the output of a system so as to achieve asymptotic tracking of prescribed trajectories and/or asymptotic rejection of disturbances is a central problem in control theory. Huang (2004) described the robust servo-mechanism or structurally stable output regulation problem to mean the design of a control law for an uncertain plant such that the closed-loop system satisfies two requirements. The first is the closed-loop stability in the local or nonlocal sense, and the second, is asymptotic tracking and disturbance rejection. This means, the output of the closed-loop system asymptotically tracks a class of reference inputs in the presence of a class of disturbances. For this, there are essentially three different approaches to solving the output regulation (OR) problem. These strategies have been earlier categorized by Isidori *et al.*, (2003),

into three specific approaches, which are:

1. Tracking by dynamic inversion or stable inverse approach, for instance, differential flatness based methods.

2. Adaptive tracking such as utilizing any of the heuristic or artificial intelligence methods.

3. Tracking via internal models, for instance, output feedback or generalized servomechanism approach

Tracking by dynamic inversion or stable inverse approach according to Isidori and Marconi (2007), consists in computing a precise initial state and a precise control input (or equivalently a reference trajectory of the state), such that, if the system is accordingly initialized and driven, its output exactly reproduces the reference signal. The computation of such control input, however, requires perfect knowledge of the entire trajectory which is to be tracked as well as perfect knowledge of the model of the plant to be controlled. Thus, this type of approach is not suitable in the presence of large uncertainties on plant parameters as well as on the reference signal. An example of such an approach is differential flatness (Fleiss *et al.*, 1995). The feasibility of the dynamic inverse method is also predicated upon the availability of an inverse function for any given system. This availability implies that the system must be nonsingular and preferably invertible. A stable inverse should ideally be the perfect way to solve any system of differential equations. However, because of singularity problem and the large size of the matrix to be inverted in such complex systems, this is usually difficult to achieve (Tanwani & Liberzon, 2010).

Adaptive tracking consists of tuning the parameters of a control input computed via dynamic inversion in such a way as to guarantee asymptotic convergence to zero of a tracking error. Utilizing any one of the available tuning methods, it fine tunes the parameters of the control input so as to correctly handle the effect of uncertainties on the system response. Although, this method can successfully handle parameter uncertainties, it still presupposes the knowledge of the entire trajectory which is to be tracked. Therefore an approach of this kind is not suited to the problem of tracking

unknown trajectories (Isidori & Marconi, 2007).

Internal-model-based tracking, on the other hand, is able to handle simultaneously uncertainties in plant parameters as well as in the trajectory which is to be tracked(Isidori & Marconi, 2007; Serrani, 2005). If the trajectory to be tracked belongs to the set of all trajectories generated by some fixed dynamical system, a controller which incorporates an internal model of such a system is able to secure asymptotic decay to zero of the tracking error. This is possible for every trajectory in this set and is done robustly with respect to parameter uncertainties (Chen & Huang, 2004; Huang, 2004). To this group belong the methods of output regulation such as state feedback and output (error) feedback. Output feedback approach to solving a dynamic system has evolved up to the present day as a useful tool for robust output regulation of dynamic systems. The ability to meet the twin goals of stabilization and tracking, which have been set out for robust output regulation, provides one of the strongest reasons yet for its use. Another appeal for this method is that for non-linear systems, it reveals many inherent properties of such systems which are without analogues in the linear case and which provide greater insight into the behavior of such nonlinear dynamic systems. These properties derive from the geometric structural analytic tools (Astolfi & Praly, 2017).

Sample architectures for output regulation and internal model mechanism are shown in Figure 2.1 for the linear regulator. $\omega$ retains its meaning as exogenous signal, $x$, $u$, $v$, $e$ are state, control input, stabilizer output and error output respectively. $K$ , $L$, $M$, $\Phi$, $G$, $H$ are matrices representing stabilizer and internal model. Figure 2.2 gives the nonlinear equivalent of the regulator shown in Figure 2.1. Key points to note in these two representations of the robust regulator are the various parts making up the system which include in either case; a plant, an exosystem which generates the external inputs in form of reference signals and disturbance inputs and a dynamic controller subsystem comprising the stabilizer and steady state generator. The stabilizer and steady state generator are the key parts of any output regulator controller that ensures stable regulation in the presence of external inputs into the system. These are the interacting parts that make up the basic

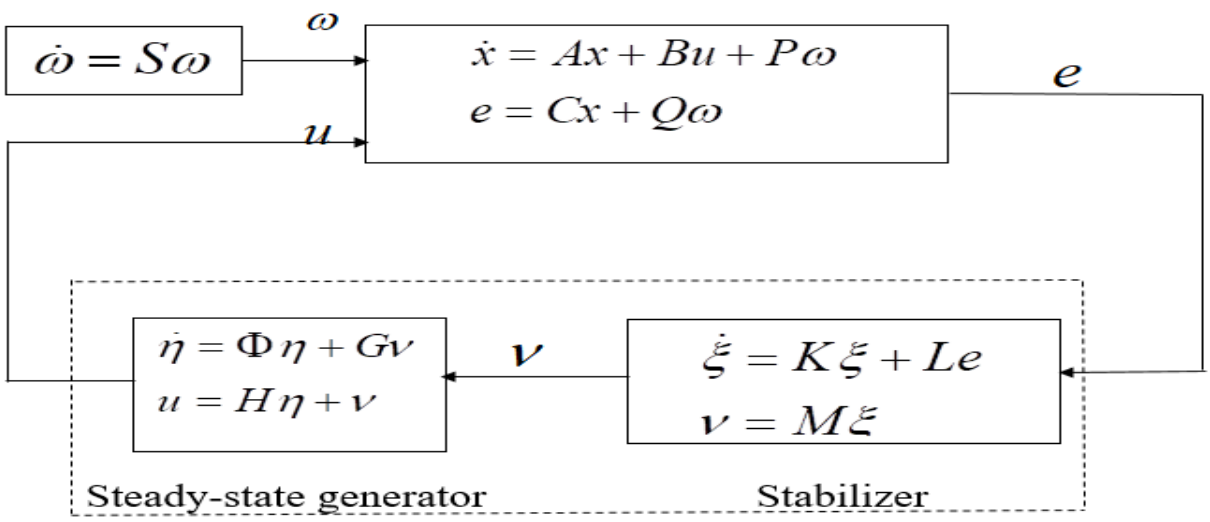



Figure 2.1: Robust Linear Regulation Setup (Kim, 2009)

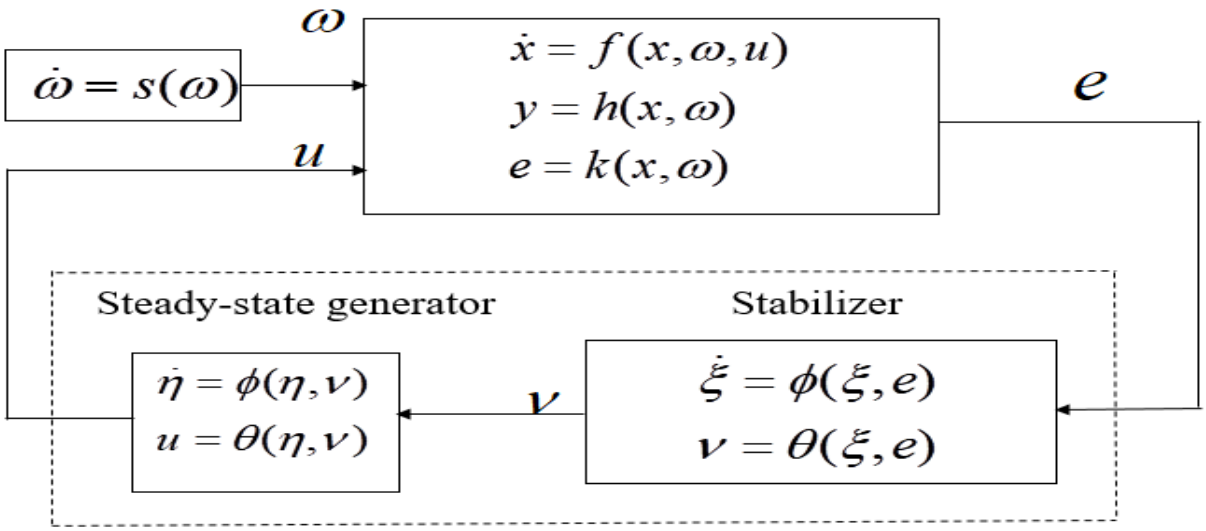



Figure 2.2: Robust Non-linear Regulation Setup (Serrani, 2005)

setup of the robust regulator. In extending this setup to a specific implementation of the output regulation problem, use was made of either state feedback or output feedback approaches. However, due to the merits and demerits of both implementations stated in the background section 1.1, the output-error feedback approach or observer feedback for output regulation is selected (Udrea *et al.*,2012). Another reason for this is that in practice observers are ideally suited to estimate or measure the output and for the specific case of error feedback, error convergence to zero assures asymptotic tracking, irrespective of the uncertainties in the system. These, therefore, satisfy the

demands for output regulation by output-error feedback.

#### *2.2.1.1 Internal model principle (IMP)*

The internal model concept is fundamental in control problems. In linear control systems, internal models have been described in terms of poles in the unstable region of the complex plane which contain the needed information for the control system to attain the desired objective. The concept of internal models is very general and it is applicable in diverse fields such as epistemology, neurology, psychology, and artificial intelligence (Pan *et al.*, 2015). Intuitively, in control theory, the internal model concept can be explained as follows: for acceptable performance, a system needs to have ”enough” information about the conditions under which it has to perform. For example, if a system needs to perform under the effects of undesirable exogenous signals, then acceptable performance is possible if a copy of a model of the dynamics of the exosystem generating the exogenous signals is present in the compensated system. This copy is called an internal model, which provides the necessary information to counteract the effects of the undesirable behavior. Currently, the role of internal models in the regulation of linear, lumped, time invariant, continuous, and discrete time systems is well understood (Gonzalez & Antsalkis, 1989). With development in the late 1990's, extensions to nonlinear systems appeared in several pioneering works (Isidori & Byrnes, 1990; Huang, 2004; Chen & Huang, 2004; Serrani, 2005).

IMP concerns itself with the asymptotic tracking (regulation) and stability (internal state) of the combined system of plant, exogenous signals and a controller subsystem that could be static (linear systems) or dynamic (ideal for non-linear systems). To this end, when the disturbance rejection (output regulation)/internal stability problem is solved, an exact duplicate of the inverse of the denominator matrix of the disturbance (exogenous) signal must be (mathematically) present in the loop at the summation junction where the exogenous signals enter the loop. This is IMP defined in terms of its implementation details. Other merits of the internal model include inherent invertibility of the system and the robust handling of uncertainties arising from within the model and external sources (i.e. matched and unmatched uncertainties. The internal model control principle (IMCP)

therefore combines the abilities of the first two methods of asymptotic tracking discussed in Isidori *et al.*, (2003) and furthermore brings inherent adaptive properties to the designed controller.

The IMP was applied in this work by restricting the analysis to output regulation of uncertain non-square MIMO non-linear systems. Need for more research into the formalization of structural output regulation in such systems has been referenced in several past and current works (Isidori, 2011; Shim *et al.*, 2015). Plausible engineering application domains are process and chemical control, aerospace engineering, that already engage in treatment of the problem of non-square MIMO systems (Wiese *et al.*, 2015), most of the works in this area have proceeded to analyze the stated systems after augmenting the inputs or outputs in some form of squaring routine/algorithm in order to make the problem less daunting and easily amenable to current established techniques for square systems (Udrea *et al.* 2012). Addressing the output regulation in a formalized way, by direct application of the IMP to such systems has been developed with different directions given by Shim *et al.*, (2015). However, the development and standardization of the concept is still not mature (Isidori, 2011).

#### *2.2.1.2 Basic setting of the output regulation IMP framework*

Results for output regulation in the linear and SISO case has been treated very exhaustively starting with the original results by Francis and Wonham (1977), who laid the complete framework for the IMP as a tool for output regulation in linear systems. The basic nonlinear mathematical setting according to Isidori *et al.* (2003), Serrani (2005) and formulation of the problem will now be presented.

Given the linear, time invariant (LTI) system as in Isidori *et al.* (2003):

$$\dot{x} = Ax + B_1 u + B_2 w \tag{2.1}$$

$$z = C_1 x + D_{11} u + D_{12} w \tag{2.2}$$

$$y = C_2 x + D_{21} u + D_{22} w \tag{2.3}$$

where in equations (2.1)-(2.3), $x$ is the vector of state variables, $u$ is the vector of inputs for control purposes, $w$ is vector of inputs which can not be controlled and are viewed as undesired external disturbances, $z$ represents the vector of outputs that need to be controlled and $y$ is the vector of outputs available for measurement and used to feed the devices supplying control action. The following propositions were now made:

**Prop. 1:** $z_{ref}(t)$ is the prescribed behavior in time, $z(t)$ (that the controlled/desired output trajectory) is required to track

**Prop. 2:** What is sought for, is to design a controller which receives $y(t)$ as input and produces $u(t)$ as output, such that it guarantees in the closed loop system the objective of $z(t)$ asymptotically tracking $z_{ref}(t)$. In other words

$$\lim_{t\to\infty} ||z(t) - z_{ref}(t)|| = 0 \tag{2.4}$$

**Prop. 3:** This proposition is more of a prerequisite which requires that the controller must secure proper behavior of all state (including those internal to the system) that characterize the closed loop system and not just the components of the controlled output $z(t)$. This pre-requisite is expressed by imposing the property that the internal (state) variables $w(t)$ and $z_{ref}(t)$ are bounded. This proposition is guaranteed for linear systems and follows from classical BIBO stability concept.

**Prop. 4:** The ability to successfully address this problem very much depends on how much the controller is allowed to know about the external stimuli $w(t)$ and $z_{ref}(t)$ and on their specific shape.

**Prop. 5:** If the external stimuli $w(t)$ and $z_{ref}(t)$ are allowed to be thought of as belonging to a fixed family of functions of time with the initial conditions varying over a given prescribed set, then the following assumptions can be safely made:

1. There is no need to keep them separate as done in equation (2.3)

2. They can be thought of as components belonging to a larger (augmented) vector of Exoge-

nous inputs given in Isidori *et al.*, (2003) by

$$w_a = \begin{pmatrix} w \\ z_{ref} \end{pmatrix} \tag{2.5}$$

3. Accordingly, this allows $z$ in equation (2.3) to be replaced with the tracking error $e = z - z_{ref}$ i.e.

$$e = C_1^a x + D_{11}^a u + D_{12}^a w^a \tag{2.6}$$

which is itself a linear function of the state.

**Prop. 6:** This linear function of state therefore depends on a linear differential equation in which the composite external stimuli $w^a$ in equation (2.5) evolves by

$$\dot{w} = S^a w^a \tag{2.7}$$

**Prop. 7:** This exosystem provides a model of all possible exosystem signals to be taken into account in the design problem with respect to reference outputs $(z_{ref}(t))$, that the plant might be required to track, as well as disturbance inputs $(w(t))$ that might affect its behavior. $S^a$ , is a fixed matrix. Cast in these terms, the design problem reduces to that of finding a feedback controller such that, for all initial conditions in the state spaces of the plant and of the controller (if the controller has an internal dynamics), and for all initial conditions in the prescribed subset of the state space of the exosystem, all trajectories of the resulting closed-loop system are bounded (if also are those of the augmented exosystem given by equation (2.7) and error converges to zero in positive time

$$\lim_{t \to \infty} e(t) = 0 \tag{2.8}$$

*2.2.1.3 Internal model principle for linear and nonlinear systems*

The formulation of the internal model principle for two specific classes (linear and nonlinear) of systems is now presented before presentation of the output feedback problem.

1. The Case of Linear Systems:

   Consider the LTI system described by Serrani (2005):

$$\dot{x} = Ax + Bu + Pw \tag{2.9}$$

$$y = Cx + Qw \tag{2.10}$$

$$e = C_e x + Q_e w \tag{2.11}$$

   with $x$ is the state vector, $u$ is the control input, $w$ is the disturbance input, $y$ is the measured output, and $e$ is the tracking error, i.e., the regulated output. The disturbance input $w$ affecting this system is generated by an autonomous LTI system (Serrani, 2005):

$$\dot{w} = Sw \tag{2.12}$$

   which following the terminology introduced in Section 2.2.1.1, is referred to as the exosystem.

   The control of equations (2.9)-(2.11) is achieved by means of a dynamic feedback controller, which processes the measured output $y$ and generates the control input $u$. This controller is itself an LTI system, modeled by equations of the form described by Serrani, (2005):

$$\dot{\xi} = F\xi + Gy \tag{2.13}$$

$$u = H\xi + Ky \tag{2.14}$$

   Otherwise, equation (2.14) can be expressed in terms of the regulated (tracking) output error

given as (Serrani, 2005):

$$\dot{\xi} = F\xi + Ge \tag{2.15}$$

$$u = H\xi + Ke \tag{2.16}$$

with, $\xi \in R^v$.

2. The Case of Nonlinear Systems:

   The non-linear equivalent internal model design has been given sufficient treatment (Byrnes & Isidori, 2000; Byrnes & Isidori, 2003), with particular implementation being subject to the specific type or class of nonlinear system being considered. Serrani (2005), gives a detailed expose of the output regulation problem for MIMO nonlinear systems; the basic setting, necessary and sufficient conditions for the output regulation problem and the scope of regulation to be achieved as required in the local or global sense. With some slight modification made by ignoring the uncertain terms, the non-linear output regulation problem is reproduced here. Given a non-linear plant model of the form given by Serrani (2005).

$$\dot{x} = f(x, u, w) \tag{2.17}$$

$$e = h(x, w) \tag{2.18}$$

   $\forall x \in R^n$, control input $u \in R^m$ and error to be regulated $e \in R^p$. The signal $w$, is generated by a nonlinear exosystem of the form

$$\dot{w} = s(w) \tag{2.19}$$

   With state $w \in R^r$. The plant model is assumed to satisfy the following assumptions (Serrani, 2005):

(a) The functions $f(:)$ and $g(:)$ are smooth $(C^{\infty})$

(b) $f(0;0;0) = 0$ and $h(0;0) = 0$ are initial conditions

(c) The pair $(A, B)$ is stabilizable and the pair $(C, A)$ is detectable, where $A = [\partial f/\partial x]_0$, $B = [\partial f/\partial u]_0$ , $C = [\partial h/\partial x]_0$

(d) the exosystem is assumed to be neutrally stable: meaning

i. The equilibrium $w = 0$ is stable in the sense of Lyapunov

ii. each initial state $w_0 \in W$ is stable in the sense of Poisson

(e) This implies that $S = [\partial s/\partial w]_0$ has all eigenvalues on the imaginary axis. The problem of local and structurally stable regulation is to find a smooth ($C^{\infty}$) controller of the form

$$\dot{\xi} = \phi(\xi, e) \tag{2.20}$$

$$u = \theta(\xi) \tag{2.21}$$

With $\xi \in R^v$ , satisfying $\phi(0,0) = 0$, $\theta(0,0) = 0$ and the associated linear maps $F = [\partial\phi/\partial\xi]_0$, $G = [\partial\phi/\partial e]_0$ and $H = [\partial\theta/\partial\xi]_0$ such that

(f) The **origin** is a locally exponentially stable equilibrium of the unforced closed loop system

$$\dot{x} = f(x, \theta(\xi), 0) \tag{2.22}$$

$$\dot{\xi} = \phi(\xi, h(x, 0)) \tag{2.23}$$

(g) The trajectories of the closed loop system

$$\dot{w} = Sw \tag{2.24}$$

$$\dot{x} = f(x, \theta(\xi), 0) \tag{2.25}$$

$$\dot{\xi} = \phi(\xi, h(x, 0)) \tag{2.26}$$

$$e = h(x, w) \tag{2.27}$$

which originate within the neighbourhood, $Wx\chi x\Xi \in R^{r+n+v}$ are bounded and satisfies equation (2.8).

(h) Finally the closed loop system after linearization about the origin was given by Serrani (2005) as

$$\dot{x} = Ax + BH\xi + Pw + \varphi(x, \xi, w) \tag{2.28}$$

$$\dot{\xi} = GCx + F\xi + GQw + \chi(x, \xi, w) \tag{2.29}$$

$$\dot{w} = Sw + \Psi(w) \tag{2.30}$$

$\forall(x, \xi, w) \in \chi x\Xi xW$. With $\chi x\Xi xW$ representing a compact set and where $\varphi(x, \xi, w), \chi(x, \xi, w)$ and $\Psi(w)$ vanish at the origin with their first derivatives.

It was established that for output regulation to be considered effective in the real sense, uncertainties have to be addressed and this should form a central part of any practical general solution to the output regulation problem (Serrani, 2005). Possible uncertainties that could impact on a systems performance can be classified to include parametric and non-parametric uncertainties, matched and unmatched uncertainties. With their sources being of diverse origins but usually being categorized as either inherent (internally generated by system model) to the model or external to system (coming from uncontrolled sources).

### 2.2.2 Output feedback-based regulation

Existing output feedback approaches are restricted to certain classes of systems as no one solution fits all types of nonlinear characteristics. Research in this field has continued to be uniquely tailored for individual nonlinear dynamical system architectures. A reason for this is due to the rich complexity of behaviors found in non-linear systems. However, whatever the approach adopted for output feedback, the goal remains to enforce stabilization and tracking of system states and trajectories respectively (Ortega *et al.*, 1994). Some of these different architectures include: SISO, MIMO, linear and nonlinear, forced and unforced systems, affine and non-affine systems, certain and uncertain systems, minimum and non-minimum phase, square and non-square systems etc. Chang *et al.*, (2015) reported two ways to design an output feedback controller. They were: firstly, through the direct utilization of the system output to design a controller followed by robust stability analysis of the closed-loop system. The second method constructs an observer to estimate the system states before the controller is then designed according to the observed estimates. Previous work by Serrani (2005), stated that the output regulation problem can be solved via robust output feedback in basically two ways:

1. State feedback or the full information (FI) output regulator problem

2. Error feedback (EF) output regulator problem

A review of these two basic methodologies as given by Serrani (2005) is discussed in the sections that follow:

#### *2.2.2.1 State feedback or full information (FI) output regulator*

This approach is a more ideal method (i.e., if it was possible to have all states available for measurement, but also more unrealistic in terms of implementation) for carrying out Output regulation via output feedback. This is because assuming the availability (through measurements) of all the state in the closed loop autonomous system comprising of the plant and exosystem is at best ideal and in practice quite unrealistic. This is borne out by the fact that certain plant parameters remain

largely unknown; either partially or completely, and are therefore unavailable for measurement and control purposes. Implementation of this method requires development of state dependent controllers that use all of the system states in the controller that is static (Serrani, 2005).

In general, the tracking error of equation (2.11) does not naturally converge to zero, hence it is necessary to determine an input signal $u(t)$ which drives it to zero. The simplest possible way to construct such an input signal is to assume that it is generated via static feedback of the state $x(t)$ of the system to be controlled and of the state $w(t)$ of the exosystem, (Serrani, 2005) i.e.

$$u = Kx + Lw \tag{2.31}$$

However it has been identified from practice, that it is unrealistic to assume that both $x(t)$ and $w(t)$ are measurable. Hence it may be more natural to assume that the input signal $u(t)$ is generated via dynamic feedback of the error signal only. This is a more feasible requirement for any dynamic system that considers measuring the entire output (in which strictly speaking is embedded the state variables). This has given rise to the more feasible and realistic alternative of error feedback which is discussed in the next paragraph.

*2.2.2.2 Error feedback (EF) implementation of the output regulator*

This problem relies on the more realistic scenario of output measurement and regulation. A goal that is more in line with the overall aim of output regulation i.e. stabilization and tracking in the presence of exogenous inputs into a system (Astolfi & Praly, 2017). This is achieved because the steady state requirements from a controller to help the system output track a specified reference trajectory is satisfied when the regulated output achieves this result without isolating any particular state but with the entire output being considered for asymptotic tracking and global regulation. Error feedback is a particular implementation of the output feedback solution when the output to be tracked is the error generated from comparison between a model reference system such as a dynamic observer and the nominal plant (Serrani, 2005). Implementation of this method entails

output/error dependent controllers such as observer-based controller designs. The observer itself being a dynamic system, its input values are the values of measured outputs from the original system, and its state vector generates missing information about the state of the original system. The observer can be regarded as a dynamic device that, when connected to the available system outputs, generates the entire state. This is the advantage of incorporating the observer as an internal model. The behavior of error parameter decaying to zero determines the nature of the observation as approximate, exact, asymptotic or exponential.

For the case when the control is generated by the dynamic feedback of the error signal only, the dynamic controller system is given by equation (2.16). For some $t > 0$ , $F, G, H$ and $K$ are matrices with constant entries. This setup defines the dynamic controller for use in the regulator.

*2.2.2.3 Necessary and Sufficient Conditions for Solution to Output Regulation Problem*

Necessary and sufficient conditions for a solution to the regulator problem are now posed for the system set out in equation (2.11). Two key requirements are demanded to be met for the solution to the full information or error feedback regulator problem to have a solution. These conditions are here described by (Serrani, 2005):

1. Stability condition (S)
2. Regulation condition (R)

Following the problem formulation approach in Serrani, (2005), Krener, (1998), the two basic types of output regulation problems are discussed next within the context of the necessary and sufficient conditions for solution to the output regulation problem to hold.

1. Full Information Regulator Problem

   Consider the system in equation (2.11), driven by the exosystem in equation (2.12) and connected with the controller in equation (2.31). The full information regulator problem is the

problem of determining the matrices $K$ and $L$ of the controller such that (Serrani, 2005):

(a) (S) the system

$$\dot{x} = (A + BK)x \tag{2.32}$$

$$\dot{\xi} = F\xi + GCx \tag{2.33}$$

is asymptotically stable;

(b) (R) all trajectories of the system

$$\dot{w} = Sw \tag{2.34}$$

$$\dot{x} = (A + BK)x + (P + BL)w \tag{2.35}$$

$$e = Cx + Qw \tag{2.36}$$

such that $\lim_{t\to\infty} e(t) = 0$

2. Error Feedback Regulator Problem

Again, consider the system in equation (2.11), driven by the exosystem equation (2.12) and connected with the controller. The error feedback regulator problem is the problem of determining the matrices $F, G$ and $H$ of the controller described by Serrani, (2005):

(a) (S) the system given by equation (2.33) is asymptotically stable;

(b) (R) all trajectories of the system

$$\dot{w} = Sw \tag{2.37}$$

$$\dot{x} = Ax + BK\xi + Pw \tag{2.38}$$

$$\dot{\xi} = F\xi + G(Cx + Qw) \tag{2.39}$$

$$e = Cx + Qw \tag{2.40}$$

such that $\lim_{t\to\infty} e(t) = 0$

Having described the global requirements for a solution to the output regulation problem to exist, necessary and sufficient conditions for the solution to the problem is required. Without explicit description of the mathematically rigorous presentation of these conditions, it is sufficient to state here that, in the linear multivariable case the solution to the output regulation problem has been given by Francis (1977) in the form of an extension to the Sylvester equations (usually taking the form of linear matrix inequalities). For the non-linear equivalent solution, results by Isidori and Byrnes (1990), showed that the solution to the problem required solving a set of partial differential equations which are called Francis-Byrnes-Isidori (FBI) equations (Aguilar & Krener, 2013).

### 2.2.3 Stabilization using immersion and invariance

Having already discussed the robust regulation of systems using output feedback stable designs, a similar stabilization method is the immersion-invariance adaptive method (Astolfi & Ortega, 2003). The basic idea behind immersion-invariance is to project the given dynamic system into a system with pre-specified properties. Examples of this include the immersion of a generic (theoretical) non-linear system into a linear and controllable system using static/dynamic state feedback. If this immersion is possible, then robust regulation is achievable provided the exosystem can be immersed into a linear and observable system.

*2.2.3.1 Formulation of the immersion-invariance stabilization scheme*

Consider the system given in Astolfi and Ortega (2003) by

$$\dot{x} = f(x, u) \tag{2.41}$$

And the basic stabilization problem of finding (whenever possible) a state feedback control law such as: $u = u(x)$. Such that the closed loop system is locally or globally asymptotically stable. The immersion-invariance approach proceeds in two steps as follows (Astolfi & Ortega, 2003):

1. Find a target dynamical system

$$\dot{\xi} = \alpha(\xi) \tag{2.42}$$

   This is locally or globally asymptotically stable and of dimension strictly smaller than the dimension of the full plant defined by $\dot{x}$ . This dynamical system can be obtained by the application of the functional maps given by

$$x = \pi(\xi) \tag{2.43}$$

$$u = c(x) \tag{2.44}$$

   such that

$$f(\pi(\xi), c(\pi(\xi))) = \frac{\partial \pi}{\partial \xi}\dot{\xi} \tag{2.45}$$

   Significant points to note about this concept are

   (a) Any trajectory $x(t)$ of the system $\dot{x} = f(x, c(x))$ is the image through the mapping $\pi(.)$ of a trajectory of the target system.

   (b) The mapping $\pi : \xi \to x$ is an immersion. This means that, rank of the map $\pi$ equals the dimension of $\xi$

2. Apply a control law, which renders the manifold $x = \pi(\xi)$ attractive and keeps the closed

loop trajectories bounded. The significance of this second step is that the closed loop system will asymptotically behave like the desired target system and stability is ensured. The implementation of a controller becomes a trivial task after this.

This same idea is applied in sliding mode control (SMC), where the target dynamics are the dynamics of the system on the sliding manifold. SMC ensures manifold attractivity is enforced with the aid of a discontinuous or nominal control law in one part while the second part of the control law is made complete by the equivalent control law. This is a similar procedure to immersion but with significant difference being that SMC uses a change of coordinates and not an immersion. The applied control law remains one that renders the manifold invariant (Astolfi & Ortega, 2003).

### 2.2.4 Observers for control systems

Observers are dynamic constructs that could be either linear or non-linear, stochastic as in the Kalman/extended Kalman filter or deterministic as in the Luenberger observer, low gain as in the traditional Luenberger observer (Luenberger, 1971; Luenberger, 1979) or high gain as in extensions to the standard Luenberger observers by Khalil and Praly (2013), Gauthier *et al.*, (1992) and Andrieu *et al.*, (2007). They can be used as soft sensing, measuring and estimation tools (identity observer for identification of nonlinear systems), in fault detection and isolation, disturbance rejection, in synthesis of an adaptive internal model used in model predictive control, model reference control or output regulation stabilization. The role of the observer as an estimator which was used in this work seeks to ensure convergence of the system state estimates or observed output to the desired or true state. To this end therefore, observers can also be described as partial or reduced state and full state or expanded state observers (Krener, 2004) depending on the subset of the state space being estimated or sensed and the convergence properties of the observer. Figure 2.3 is a simplified tree structure for observer classification as described by Luenberger (1971). This classification is done to highlight the possibilities from which this work choses output feedback observer-based implementation.

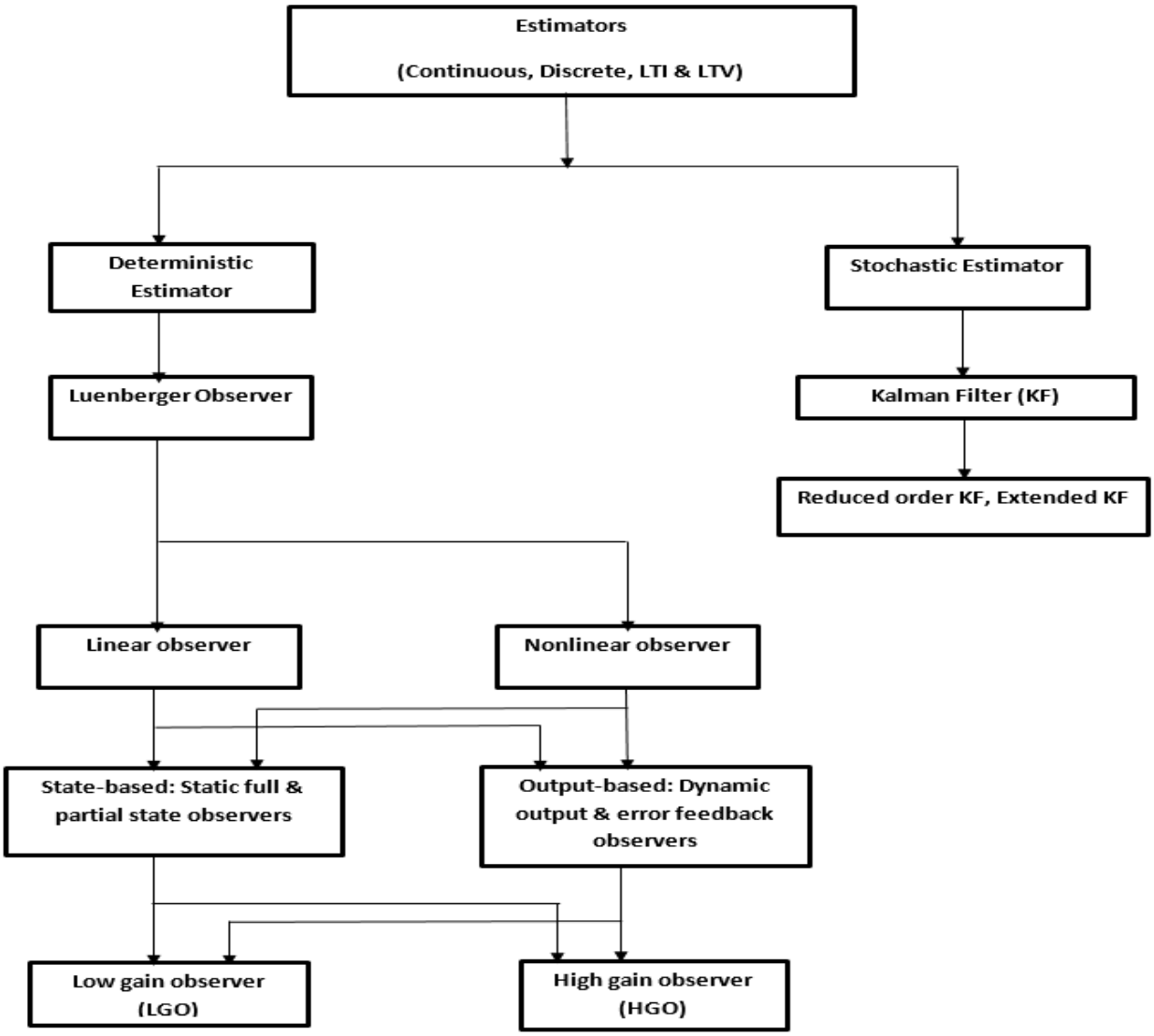



Figure 2.3: Observer Classification (Luenberger, 1971)

*2.2.4.1 Linear observer design review*

Given a general linear time invariant (LTI) system in state space form

$$\dot{x} = Ax + Bu \tag{2.46}$$

$$y = Cx + Du \tag{2.47}$$

and assuming the disturbance input term was zero such that $D = 0$, the system in equation (2.47) becomes

$$\dot{x} = Ax + Bu \tag{2.48}$$

$$y = Cx \tag{2.49}$$

A suitable observer for the LTI system in equation (2.49) would be the linear Luenberger-type observer dynamic system of the form (Friedland, nd):

$$\dot{\hat{x}} = A\hat{x} + Hu + L(y - \hat{y}) \tag{2.50}$$

$$\hat{y} = C\hat{x} \tag{2.51}$$

where $x, \hat{x}, y, \hat{y}$ represent the true system state, observer state, system output, observer output respectively. $A, B, C, H\&L$ are appropriate system and observer matrices and the observer gain to be designed for which renders the closed loop system stable. The overall dynamics of the autonomous/compound system reduces to that of the error dynamics given by (Friedland, nd):

$$\dot{e} = \hat{A}e \tag{2.52}$$

in which $\hat{A} \equiv A - LC$, which is the closed loop matrix that must be rendered stable via an appropriate choice of the design parameter $L$ (implying that all eigenvalues of the matrix $\hat{A}$ have negative real part or the spectrum of the matrix $\hat{A}$ all lie in the open left half plane of the complex plot) and the error which is the output to be regulated to zero if the state estimation is to be made correctly. It is obvious from equation (2.52), that the error dynamic is linear and asymptotically stable thereby rendering the system trajectory stable also, guaranteeing a steady state behavior that is ultimately bounded and invariant (Isidori & Marconi, 2007). The implementation structure for such an observer is shown in Figure 2.4.

Extending this consideration to the nonlinear observer for nonlinear systems, the dynamical sys-

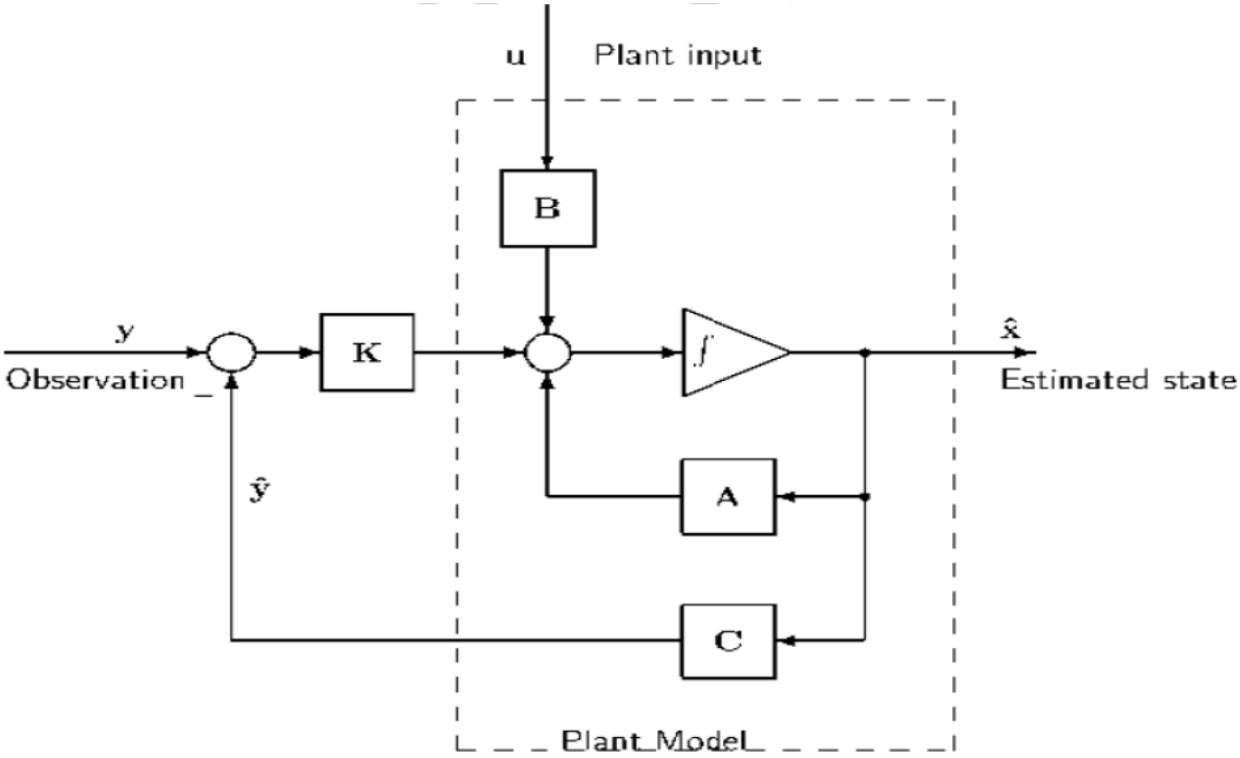



Figure 2.4: Observer Schematic Showing Interconnection with System (Friedland (nd))

tem whose input is the measured vector variables $[u \quad y]'$ and output is the state estimate $\hat{x}$ given by Primbs (1996):

$$\dot{\hat{x}} = \hat{f}(t, z, u, y) \tag{2.53}$$

$$y = \hat{h}(t, z, u, y) \tag{2.54}$$

More specifically as developed in Primbs (1996), having a non-linear system of the form

$$\dot{x} = f(x); x \in R^n \tag{2.55}$$

$$y = h(x); y \in R^p \tag{2.56}$$

and proceeding as in the linear case with output injection, a first approximation to the nonlinear observer can be written as in Primbs (1996):

$$\dot{\hat{x}} = f\hat{x} + L(y - \hat{y}) \tag{2.57}$$

$$\hat{y} = h(\hat{x}) \tag{2.58}$$

With $L \in R^{nxp}$. Considering the error between our estimated state $\hat{x}$ and true state $x$ i.e. $x - \hat{x}$

$$\dot{e} = f(x) - f(\hat{x}) + L(h(x) - h(\hat{x})) \tag{2.59}$$

Since the error dynamics in equation ( 2.59) are non-linear, the stability of the error dynamics become unclear due to nonlinear and uncertain terms occuring in the vector fields $f(x), f(\hat{x})$. Motivated by the fact that stability of a linearized system about a fixed point, implies local stability of the corresponding non-linear system about that fixed point, linearizing the error dynamics about its fixed point, $e = 0$, results in the following set of equations (Primbs, 1996):

$$\dot{e} = f(x) - f(\hat{x}) + L(h(x) - h(\hat{x})) \tag{2.60}$$

$$\dot{e} = f(x) - f(x + e) + L(h(x) - h(x + e)) \tag{2.61}$$

$$\dot{e} = \left(\frac{\partial f}{\partial x}(x) - L\frac{\partial h}{\partial x}(x)\right) e + O(e^2) \tag{2.62}$$

so that, the linearized system given in Primbs (1996) is:

$$\dot{e} = \left(\frac{\partial f}{\partial x}(x) - L\frac{\partial h}{\partial x}(x)\right) e \tag{2.63}$$

with the nonlinear terms $O(e^2)$ ignored. Unfortunately, the above linearization is a function of the true state $x$ which, firstly, is not a fixed quantity, and secondly, is unknown (Primbs, 1996). Making any estimate by such an observer only approximate. This clearly shows that techniques beyond the realm of linear theory are needed to analyze the error dynamics in equation (2.63),

thereby necessitating the introduction of non-linear design techniques for the non-linear observer design as discussed in the next section.

*2.2.4.2 Nonlinear observer design techniques*

Progress in nonlinear output feedback design has been slower (Kokotovic & Arcak, 2001). For the development of an observer-based output feedback controller, Primbs (1996), gives a good expose and summary of some of the nonlinear observer design techniques used for non-linear systems to include:

1. Lyapunov approach (Kazantzis & Kravaris, 1998)
2. Method of extended linearization (Primbs, 1996)
3. Differential geometry or Lie-algebraic approach (Srinivasa, 2002).

Utilizing differential algebra and geometric techniques, the Lie-algebraic approach to non-linear observer design is selected and applied for the non-linear observer synthesis. The observer will preferably be of high gain (HGO) while serving as an internal adaptive model and a detector of the system output/system error. The class of systems being targeted are those for which a global state transformation exists such that $x = T(z)$ , with $T$ being the system observability matrix that is invertible. A review of lie-algebraic method for observer design is given in Primbs, (1996), Srinivasa, (2002).

Given a non-linear dynamic system, the first step in observer design is to check if the system is observable by computing the rank of the observability matrix rank (Srinivasa, 2002):

$$rank \begin{pmatrix} dh(x) \\ dL_f^{(1)}h(x) \\ \vdots \\ dL_f^{(n-1)}h(x) \end{pmatrix} = n \tag{2.64}$$

Where $dh(x)$, is the grad of $h(x)$ and $L_f h(x)$ is the Lie derivative of h(x) with respect to $f(x)$. In a multi-output system, the observation space $O$ is the linear space of the functions $h_1, h_2, \ldots, h_p$ and all repeated Lie derivatives $L_{x1}, L_{x2}, \ldots, L_{xi}h_j$. Intuitively, $O$ comprises of the output functions and the magnitude of their derivatives along all possible system trajectories (in infinitesimal time). According to Srinivasa (2002), given a nonlinear system that flows according to:

$$\dot{x} = f(x) \tag{2.65}$$

$$y = h(x) \tag{2.66}$$

it is now left to consider a smooth one-to-one global mapping (as in immersion approach) or non-linear transformation that gives the new partially-linear system a global observer canonical form (GOCF). The GOCF permits a nonlinear state transformation as given by (Srinivasa, 2002):

$$\dot{z} = Az + \phi(y); z \in R^n \tag{2.67}$$

$$y = Cz; y \in R \tag{2.68}$$

This is a good candidate for an observer of the form in (Srinivasa, 2002):

$$\dot{\hat{z}} = Az + \phi(y) + L(\hat{y} - y); \hat{z} \in R^n \tag{2.69}$$

$$\hat{y} = C\hat{z}; \hat{y} \in R \tag{2.70}$$

That produces the linear error dynamics ($e = z - \hat{z}$) of the form in (Srinivasa, 2002):

$$\dot{e} = (A + LC)\, e \tag{2.71}$$

The utilization of the Lie-algebraic approach (Primbs, 1996) is premised on the idea that given an arbitrary non-linear system such as equation (2.66), if there exists a transformation $x = T(z)$,

that takes equation (2.66) to equation (2.68), then equation (2.66) can be transformed to equation (2.68). The development can then proceed according to Krener and Xiao (2002), by designing an observer for equation (2.68) as in equation (2.70) by using linear observer results, and then transform back to obtain an observer for the non-linear system equation (2.66).

#### *2.2.4.3 Peaking phenomenon*

The implementation of output feedback for system stabilization has established the use of observers. High-gain observers have been utilized owing to their robustness to plant uncertainties and arbitrarily small estimation error. However, the price to be paid is the generation of peaking which may potentially lead to finite time escape instability when the peaking signal is transmitted to the plant (Oliviera *et al.*, 2008a, Oliviera *et al.*, 2008b). This is a major obstacle to the desired goal of output regulation (Sussmann & Kokotovic, 1991; Lobry & Sari, 2000) which is, GAS and asymptotic convergence to zero of the output error. Established sources of peaking phenomenon include interconnections in cascade systems, MIMO complex systems, non-linear terms, observer-based high gains, etc. The peaking problem could alternatively be described as a stabilization problem as the onset of peaking is synonymous with potentially unstable system response behavior. In linear systems, a peaking phenomenon occurs when high-gain feedback is used to produce eigenvalues with very negative real parts (Sussmann & Kokotovic, 1991). Then some states peak to very large values, before they rapidly decay to zero. In partially linear systems, peaking states act as destabilizing inputs to the nonlinear part and may even cause some of its states to escape to infinity in finite time. Therefore Peaking free designs have been sought for implementation in such systems with some of the more established methods utilizing input damping, sliding mode observers, adaptive neural techniques such as fuzzy, neural network methods, stabilizers and invariant manifold approach(Oliveira *et al.* 2008; Pan *et al.* 2015). The immersion and invariance output regulator being developed combines the ability to handle uncertainties and also drive the error to zero. If convergence is not achieved, several techniques exist in literature to force this convergence such as: heuristic and metaheauristic methods, neural and adaptive neural methods and

generally computational and artificial intelligent techniques which can be introduced to optimize the controller behavior.

### 2.2.5 MIMO dynamic model

The general form for an input affine MIMO nonlinear system is given as in Udrea *et al.* 2012:

$$\dot{x} = f_i(x) + g_i(x)u_i \tag{2.72}$$

$$y_i = h_i(x) \tag{2.73}$$

with $i \geq 2$ in the control inputs and outputs for the MIMO systems being considered for validation. The variables have dimensions $x \in R^n$, $u \in R^m$ and $y \in R^p$ , with the non-square form to be considered being that for which the size of $m > p$ and $m < p$.

#### *2.2.5.1 Square and non-square MIMO system*

Following the discussion in section 2.2.5, when the size of $u_i$ equals that of $y_i$, the system has square dimension and the resulting MIMO system assumes square shape. On the other hand, if the size of $u_i$ is less than or greater than that of $y_i$, the resulting MIMO system is of non-square dimension (Shead & Rossiter, 2006). For the MIMO system such as the QUAV considered in this work, it is required that the size of u and y be at least equal to or greater than two. The case in which the number of inputs is less than the corresponding numbers of outputs (or degrees of freedom) is referred to as under actuated case, while that in which the number of inputs is greater than number of outputs is referred to as over actuation. This work has applied the developed controllers to the general case of nonlinear MIMO systems and also specifically targeted strictly non-square MIMO systems as presented in the following models.

*2.2.5.2 Working models*

This work selected from among three working models which represented standard benchmark systems utilized for control law studies. The models include the cart-driven inverted pendulum (CIP), rotational-translational actuator (RTAC) system and the quadrotor UAV. These systems are now described, before the presentation of the developed controllers in methodology items (1c) and (2c).

1. The Rotational-Translational Actuator (RTAC)

   The RTAC is a standard benchmark system used in control systems theory and practice to demonstrate various control law designs and synthesis in either linear or nonlinear formulations. It is a standard MIMO system that allows for MIMO system controller designs. Also known as the the translational oscillator with a rotational actuator (TORA), it is shown in Figure 2.5. The system consists of an actuated rotary arm which drives the translation of

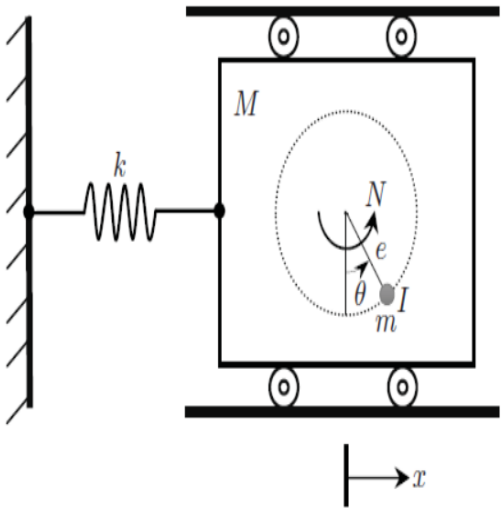



Figure 2.5: RTAC or TORA System (Wu and He, 2016)

   the larger mass by transfer of force or torque using the coriolis effect. The control force that moves the arm is supplied by a DC motor. The real world equivalent of this benchmark system can also be found in the aerospace industry in the form of spin-stabilized spacecraft, in drill bits found in oil rigs.

2. The Cart-Driven Inverted Pendulum (CIP)

   The CIP is a standard benchmark system used in control systems theory and practice to demonstrate various control law designs and synthesis in either linear or nonlinear formulations. The CIP is shown in Figure 2.6, the system consists of an inverted pendulum driven

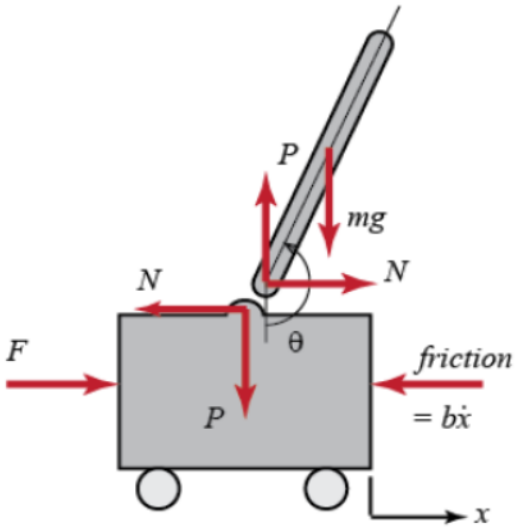



Figure 2.6: Cart Driven Inverted Pendulum Diagram (Graham and Turkoglu, 2017)

   by an actuated cart. The control force that moves the cart is supplied by a system of DC motor and railing. The real world equivalent of this benchmark system can be found in the aerospace industry in the form of rockets on their launch pads, a standing human or humanoid robot.

3. The Quadrotor Unmanned Aerial Vehicle (QUAV)

   The QUAV is a standard benchmark system used in control systems theory and practice to demonstrate various control law designs for linear and nonlinear formulations of MIMO systems. It is a nonlinear, non-square, multivariable and under actuated system having 6 degrees-of-freedom (DOF) and only 4 actuators. The QUAV is as shown in Figure 2.7. The system is a fly-by-wire system because it uses electricity for its propulsion. It consists of

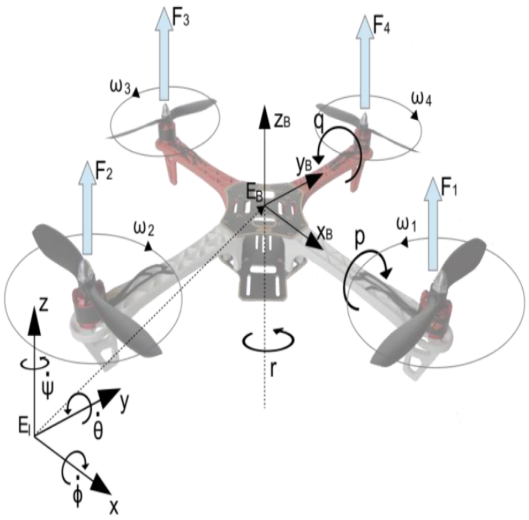



Figure 2.7: Quadrotor UAV Diagram (Chovancova *et al.*, 2016)

four DC motor driven rotors that are placed on the four corners of an imaginary square. The rotors provided the thrust and also provided the output that ensured the proper attitude (position and orientation) control of the QUAV. The control force that moves the QUAV was applied in a series of steps that makes manouvering possible. Various magnitudes of applied voltages to the DC motors makes possiible different flight modes of the quadrotor QUAV. The real world equivalent of this benchmark system can be found in the aerospace industry, robotics industry, and hobbyists or toys. The QUAV has been used to perform functions as varied as surveillance of pipelines, dams, package delivery, warfare, movie making, and humanitarian work like search operations.

## 2.3 Review of Similar Works

Having already seen various aspects and components of the stabilization and tracking problem. The current review takes a critical look at the state of the art in this regard. Particular emphasis being given to the problem of global asymptotic stability and robust output tracking as seen in non-square MIMO nonlinear system.

**Teel and Praly (1995)** investigated conditions for the stabilizability of nonlinear system using output feedback. Particularly, nonlinear systems with possibility for finite time escape were addressed

as being only semi-globally stabilizable by output feedback. This was so even in the event when the system has stabilizable and observable properties as sufficient conditions. The work extended two results (stabilizability and stabilizability + observability) by combining, in the controller, the observability property, dynamic extension, with the high gain observer and the saturated state estimates. Stability analysis here utilized lyapunov methods. However, because the controller involved a high-gain observer, the practical interest for this approach is somewhat limited and unclear. Because this was one of the pioneering works on semi-global stabilization, an important feature in the approach used considered the issue of bounded solutions separate from convergence to the equilibrium. To guarantee convergence a sufficient condition was imposed, but not necessary, small gain condition which generalizes local exponential stability assumptions. The method was able to show that semi global stabilizability by uniformly completely observable state feedback is a sufficient condition for semi-global practical stabilization by output feedback. The method was however specifically targeted at feedback linearizable systems or systems which are called uniformly completely observable. This fact in conjunction with the state or static feedback control law limits the achievable stability region to at best, semi-global domains.

**Battilotti (1996)** developed concepts pertinent to the global output regulation problem. Emphasis was on the role of output injection (observer design) in achieving global stabilization via output feedback in a certain class of systems. Key to the implementation is the synthesis of a two part control lyapunov function. The implementation considered both static and dynamic output feedback. Using dynamic output feedback, it was shown that for the same class of systems the global output regulation problem (in particular, the global stabilization problem) and the disturbance attenuation problem can be split up into two sub-problems: one is the problem via full information and the other is the problem via output injection. From solving the two sub problems, one obtains two Lyapunov functions which, combined, give a candidate Lyapunov function for solving the output feedback stabilization problem. Proofs and the procedure for identifying candidate lyapunov functions was laid down.

**Marconi** *et al.*, **(2007)** addressed the problem of existence of an (output) feedback law for the purpose of asymptotically steering to zero a given controlled variable, while keeping all state variables bounded, for any initial conditions in a given compact set. The problem was viewed as an extension of the classical problem of semi-globally stabilizing the trajectories of a controlled system to a compact set which is similar to requirements in classical problem of output regulation. The crucial observation that made the advances developed in the work possible was the realization that the two issues of forcing the existence of an invariant set (on which the regulated variable vanishes) and of making the latter attractive are intimately related to, and actually can be cast as, the problem of designing a (non-linear) observer. The design method suggested relied almost entirely on the construction of a nonlinear high-gain and nonlinear adaptive Luenberger-type observer. The obtained results were applicable to a wide class of non-minimum-phase nonlinear systems not tractable in existing frameworks. The treatment was however left at a theoretical stage.

**Astolfi** *et al.*, **(2010)** identified speed observation as a longstanding problem and gave a complete solution to the speed observation problem. Description and proof was given for the development involving the construction of the observer that relied on the use of the immersion and invariance technique. Using the method of immersion-invariance, the observer design was recast as the problem of rendering attractive a suitably selected invariant manifold dened in the extended statespace of the plant and the observer. Overall, a denite afrmative answer was given to the question of existence of a globally convergent speed observer for general mechanical systems with non-holonomic constraints. No assumption was made on the existence of an upper bound for the inertia matrix, hence the results were applicable to robots with prismatic joints. The only requirement was that the system be forward complete, i.e., that trajectories of the system exist for all times t  0; which was adjudged to be a rather weak condition. A restriction on the solution given here was that in addressing the problem of global convergence, the treatment discussed was limited to speed observation only.

**Udrea** *et al.*, **(2012)** addressed in theory, the output regulation problem in square and non-square

MIMO systems based on suitably selected normal forms. Crucial to the solution developed was the observation that the problem of achieving the asymptotic regulation-stabilization was closely related to, and actually could be cast as, the problem of designing a nonlinear observer. For MIMO nonlinear systems, the observer design was found to be more difficult technically (where suitable system structure that enable observability conditions to be adjudged are needed). The observer designs drew inspiration from two broadly identified classes i.e. those based on immersion (they imply rather strong assumptions) and newest results that drop the immersion/observability condition. Drawback of the aforementioned methods was that they were not general, meaning they can only be applied to particular classes of systems, under specific hypotheses.

**Sarras** *et al.*, **(2012)** gave a method for combining observers and controller in output feedback framework. The combination made use of an immersion and invariance observer with a proportional plus damping controller to solve the problem of unmeasurable velocity estimation in teleoperators. The specic choice of the immersion and invariance observer was justied by the fact that it was applicable to general Euler-Lagrange systems and that, in comparison to other schemes that provide an asymptotic estimate; it provided a globally exponentially convergent estimate of velocities. This work highlighted the fact that proving the interconnected closed-loop system possesses the desired stability properties which is not trivial for general non-linear mechanical systems. Specifically, the work contributed to two key modications in observer design that were necessary and gave results which are hinged upon the modication of the observer design in a way that the observer dynamics could be straightforwardly derived and that the interconnection of the closed-loop system with the observer does not lose its stability properties. The proof of the results however required Lyapunov approach to design the output feedback law which is not a straight forward task. It has also been stated that, external forces which were not considered here need to be considered for a more robust solution.

**Aguilar and Krener (2013)** continued the search for feasible solutions to the partial differential equations (PDE) known as FBI equation. Solution to the FBI equation meant the existence of a

regulator for such a system. Specific case of the system tested required characteristics of the system to be real analytic and control affine, an exosystem of order two and the zero dynamics to be hyperbolic. This meant the solution technique was based on the periodic nature of two-dimensional analytic center manifold which gave better approximations (i.e. uniform convergence), than when Taylor polynomial was applied. The reliance on control affine form and two-dimensionality was however not general enough to approximate conditions found in other real world MIMO non-linear systems.

**Isidori, (2013)** revisited the zero dynamics concept and the main motivation for introducing this concept was the ambition to develop systematic methods for asymptotic stabilization, with guaranteed region of attraction, when the dynamics in question are globally asymptotically stable. The review considered various dimensions of zero dynamics study which have been undertsood such as; high-gain feedback, feedback linearization, stable non-interacting control, output regulation, passivity, limits of performance. Also addressed were problems for which zero dynamics approach was a potential analytical solution technique such as strongly minimum-phase systems, robust stabilization via dynamic output feedback, coordinate-free setting for nonlinear stabilization problems, output redesign for non-minimum phase systems, MIMO systems, internal model design for MIMO systems. After having reviewed the highlights of the historical development of this concept, an existing current challenge or development of a coordinate free version of the standard output-feedback design paradigm was made evident. The analysis of problems of stabilization and tracking in the presence of unstable zero dynamics, and extensions to multivariable non-square systems was however left untreated but suggested for further study.

**Aguilar and Krener (2014)** introduced a model predictive regulation (MPR) control scheme whose development combined principles from model predictive control (MPC) and output regulation. The solution method added a cost functional to the classical output regulation problem, thereby removing the need to solve offline Francis-Byrnes-Isidori (FBI) equations. The online solution of MPR guarantees the existence of a stabilizable and observable system in the linear part of

the system when the system is minimum phase. The solution is also dependent on the linear part of the exosystem being neutrally stable (in the sense of Poisson). Therefore couched as an optimal control problem, the usual infinite horizon optimal cost and feedback problem was approximated and used as the terminal cost and feedback in the finite horizon optimal control problem of MPR. The method adopted targeted linearized systems which automatically limited the system response to a local or at best semi-global domain due to linearization about an operating point.

**Moshksar and Guay (2015)** developed a similar method to immersion and invariance. The alternative technique based on invariant manifolds was developed for a class of nonlinear systems with periodic and aperiodic uncertainties. The method utilized a number of high-gain estimators and filters leading to the generation of an almost invariant manifold. This property of almost invariance provided explicit functions that relate the known variables and the unknown variables implicitly, as is usually done with immersion and invariance method. A parameter update law was also designed that guaranteed exponential convergence of the estimated parameters to a small region of the true values of the time-varying parameters. Extension of the algorithm to the estimation of uncertain periodic disturbances with a known number of distinct, but unknown frequencies provided an exact invariant manifold instead of an almost invariant manifold. The approach has provided a formal scheme which relied on the definition of an almost invariant manifold from which the boundedness of the parameter estimation error is achieved for sufficiently large values of the gain in the estimator. The obtained results showed that the designed invariant manifold provided estimates of the upper bound of periodic parameters and their corresponding time derivatives. The effectiveness of the method proved to be the dependence on only a single tuning parameter which was the estimator gain. This work was targeted at estimation only and was inconclusive as to the global nature of stability and the requirement for error convergence to zero.

**Abdelkhalek *et al.*, (2015)** presented the dynamics and control system for a linearized model of quadcopter. The control part gave implementation details of a new control action which considered the angular acceleration plus PD controller (PD-A) and comparing it with regular PD controller.

The PD-A controller is aimed to enhance the response of a system than the regular PD. In order to show the effectiveness of the PD-A over the PD, theoretical and experimental studies were carried out based on one degree of freedom quadcopter model. The main objectives for the design of this controller were the quadrotor stability and its tracking to a desired trajectory. The challenge is how to control the system and perform the mission while there are uncertainties in the control system such as external disturbances, sensor error, actuator degradation and time delays. The comparison between the theoretical and experimental results revealed a significant stability improvement for the developed control methodology in comparison with the conventional PD methodology. However assumptions of linearity made limited the scope of the controller to non-global coverage.

**Wiese** *et al.***, (2015)** developed a new method of synthesizing an output feedback adaptive controller for a class of uncertain, non-square, MIMO systems that often occur in hypersonic vehicle models. Key features of the design included a baseline controller that used a Luenberger observer, a closed-loop reference model (CRM), which could be considered as an internal model, manipulations of a bilinear matrix inequality, and the Kalman-Yakubovich(KY) Lemma. The controller was composed of a baseline control gain augmented with an adaptive component to accommodate control effectiveness uncertainty and matched plant uncertainty, and made use of the closed-loop reference model to improve the transient properties of the overall adaptive system. The adaptive controller required the underlying error dynamics be made strictly positive real (SPR) through the synthesis of the post compensator and CRM gain. The procedure did not require the plant first be squared-up. It is computationally simple, and it required only the calculation of some generalized inverses, the solution of the Lyapunov equation, and the solution of a reduced order state feedback problem. Identified drawbacks with this design philosophy is the need for achieving strict positive realness (SPR) property, computation of generalized inverse which has been and still is a problem for large MIMO systems and need to solve a Lyapunov equation.

**Qu** *et al.***, (2016)** developed an adaptive controller that includes a baseline design based on observers and closed-loop reference model (CRM). The observer served as a measurement feedback

tool while the CRM was used for parameter adaptation. The developed controller was applicable to a class of underactuated non-square MIMO plants. In particular, the developed controller allowed the plant to have first-order actuator dynamics and parametric uncertainties in both plant and actuator dynamics while maintaining robust stabilization and tracking. The design method is however staged so that the Conditions are delineated under which this controller can guarantee stability and asymptotic reference tracking unlike the approach in output regulated internal model control which combines both processes.

**Sun** *et al.***, (2016)** presented the stabilization of the benchmark Rotational-translational actuator (RTAC) system. This paper made the claim to being the first continuous controller, which is designed and analyzed without linearizing/approximating the original nonlinear dynamical equations, to globally stabilize both the rotation and translation of RTAC systems inuenced by nonvanishing matched disturbances. The solution technique utilized a new sliding manifold that was elaborately synthesized such that the state variables on the manifold are always bounded and globally asymptotically converge to the desired equilibria, which is rigorously guaranteed by applying Lyapunov-based theoretical analysis. The drawbacks identified by the authors included the fact that for such an underactuated RTAC system, the tracking control problem although very important a research direction and also of signicant importance in practical applications has not been sufficiently treated. This was identified for resolution in future efforts. Also it has been well documented that sliding mode design introduces chattering effect which is detrimental to the operation of most systems. Using Lyapunov techniques for analysis also removes the certainty desired by most control designs as Lyapunov approach is known to be without formalized design approach.

**Astolfi and Praly (2017)** addressed the problem of utilizing integral action in the design of a stabilizing output feedback for MIMO nonlinear systems. In addressing the particular problem of output regulation for MIMO nonlinear systems,the interest was making the stability of an equilibrium point and the regulation to zero of an output, robust to (small) unmodelled discrepancies between design model and actual system, in particular those introducing an offset. The developed

method was intended to be relevant to real life systems. Overall, the technique used, borrowed from well established methods. The methods were used as building blocks to obtain global asymptotic stability in the presence of small disturbance injection. An identified drawback of the developed controller was the restriction of the type of disturbances to only small signals without considering effect of large disturbances which could be realistically encountered in practice. Thereby placing the claim of global asymptotic stability in question

In conclusion, the reviewed works showed some major problems with the observer-based output feedback implementation of output regulated control. Some of these problems are, the localization of the output response, the presence of steady state error, uncertainties and disturbances, transient instability, separation of the design steps of the stabilizer from the regulator and gain selection amongst others. These drawbacks all constitute reason to improve on the control law using a combination of robust-adaptive control methods that ensures the control action effects control in a larger invariant set (semi-global or global domain) with the complete removal of the steady state error. This work has tested the developed algorithms in methodology items (1) and (2) on general non-square dynamic systems which have one or more inputs and outpits. However the final validation is made on only strictly non-square MIMO systems having two or more inputs or outputs. Example becnhmark dynamic models include DC machine, UAV, satellite Attitude orbit control system(AOCS).

# CHAPTER 3

# METHODOLOGY

## 3.1 Introduction

The controllers in chapter two are implemented with the help of Matlab and Simulink software application. The various models adopted from literature were built using Matlab, while simulation experiments were carried out to specification, as set out in the selected literature. The steps used to develop the objective items in 1.5 for all working models were itemized in section 1.6 that detailed the methodology to be followed. Items in this methodology form the sequence of tasks in the development of objective items (1) to (4) . In this report, methodology items 1(a-d), 2(a-d), 3(a-d) and (4) have been completed. Overall, the sequence of methodology implementation and experiments to be made in this thesis is given in Figure 3.1 The flowchart in Figure 3.1, implements the output feedback observer regulator of methodology item (1) on three different non-square control test benches which are RTAC, CIP and UAV. Methodology item (2) introduces the concept of immersion invariance control and the proof of concept is carried out on the RTAC system. Methodology item (3) contains the development of the proposed immersion invariance output feedback control law while methodology item (4) validates via simulation the developed control law. While methodlogy items(1) and (2) focused generally on MIMO systems, methodology item (3) and (4) are dedicated to addressing the output feedback problem for strictly non-square MIMO system candidates such as the UAV, field excited DC machine or satellite attitude control system. This last choice was made because for the type of non-square systems being considered, only models that met the MIMO specification of having at least two or more control inputs and output states to work with are considered.

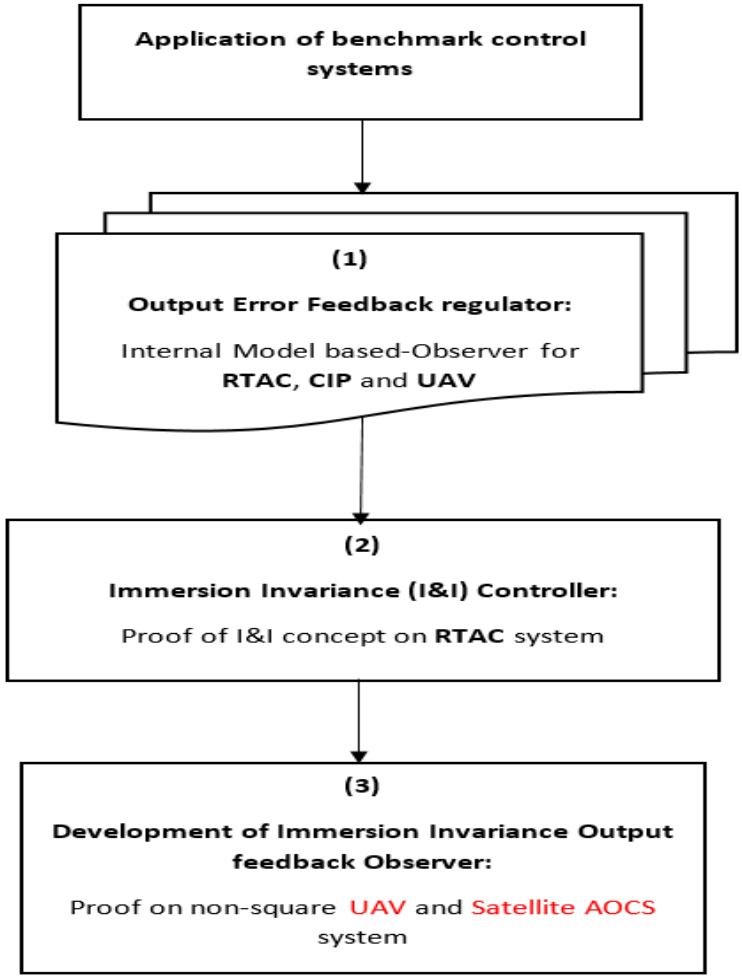



Figure 3.1: Experimention Flow Chart

### 3.1.1 Development of the output feedback controller

The output feedback controller has been developed for the Rotational Translational Actuator (RTAC), Cart driven inverted pendulum (CIP) system and the quadrotor unmanned aerial vehicle (QUAV).

#### *3.1.1.1 Output regulator for the RTAC system*

The nonlinear mathematical model of the RTAC system adopted from Avis *et al.*, (2010), was used

$$(M+m)\ddot{q} + kq = ml sin\theta\dot{\theta}^2 - ml cos\theta\ddot{\theta} + F \tag{3.1}$$

$$(I+ml^2)\ddot{\theta} = -ml cos\theta\ddot{q} + N \tag{3.2}$$

where $q$, $\dot{q}$, $\theta$ and $\dot{\theta}$ are variables representing translational displacement, translational velocity, angular displacement and angular velocity respectively. Substituting $M_1 = M + m$ and $M_2 = I + ml^2$, in equation (3.1)-(3.2),

$$\ddot{q} = \frac{1}{M_1}(mlsin\theta\dot{\theta}^2 - mlcos\theta\ddot{\theta} - kq + F) \tag{3.3}$$

and from equation (3.2)

$$\ddot{\theta} = \frac{1}{M_2}(-mlcos\theta\ddot{q} + N) \tag{3.4}$$

substituting equation (3.3) into equation (3.2) and equation (3.4) into equation (3.1) produced the model

$$\ddot{q} = \frac{-M_2kq}{D_{nl}} + \frac{mlM_2\dot{\theta}^2sin\theta}{D_{nl}} - \frac{mlNcos\theta}{D_{nl}} + \frac{M_2F}{D_{nl}} \tag{3.5}$$

$$\ddot{\theta} = \frac{mlkqcos\theta}{D_{nl}} - \frac{m^2l^2\dot{\theta}^2sin\theta cos\theta}{D_{nl}} + \frac{M_1N}{D_{nl}} - \frac{mlFcos\theta}{D_{nl}} \tag{3.6}$$

with the parameter $D_{nl} = M_1M_2 - m^2l^2cos^2\theta$, $N$ is the control input torque and $F$ is the disturbance input or force which enters the system. The torque $N$, is produced by a servo motor system which has the standard form given by the model:

$$\dot{i} = -\frac{R}{L}i - \frac{K_m}{L}\omega + \frac{V}{L} \tag{3.7}$$

$$\dot{\omega} = \frac{K_e}{J}i - \frac{bc}{J}\omega \tag{3.8}$$

with $i$, the current, $\omega$, the angular velocity and $V$, the control voltage. The control torque supplied by the actuator, $N$, is given as $J\dot{\omega} = K_ei - b_cw$. The state space form with $x = [q, \dot{q}, \theta, \dot{\theta}] \equiv$

$[x_1, x_2, x_3, x_4]$, is

$$\begin{pmatrix} \dot{x}_1 \\ \dot{x}_2 \\ \dot{x}_3 \\ \dot{x}_4 \end{pmatrix} = \begin{pmatrix} x_2 \\ \frac{-M_2 k x_1}{D_{nl}} + \frac{mlM_2 x_4^2 sinx_3}{D_{nl}} - \frac{mlNcosx_3}{D_{nl}} + \frac{M_2 F}{D_{nl}} \\ x_4 \\ \frac{mlkx_1 cosx_3}{D_{nl}} - \frac{m^2 l^2 x_4^2 sinx_3 cosx_3}{D_{nl}} + \frac{M_1 N}{D_{nl}} - \frac{mlFcosx_3}{D_{nl}} \end{pmatrix} \tag{3.9}$$

*3.1.1.2 RTAC linearization*

The linearized dynamics of the RTAC system is obtained using Taylor's expansion

$$\ddot{q} = \frac{-M_2 kq}{D_l} - \frac{mlN}{D_l} + \frac{M_2 F}{D_l} \tag{3.10}$$

$$\ddot{\theta} = \frac{mlkq}{D_l} + \frac{M_1 N}{D_l} - \frac{mlF}{D_l} \tag{3.11}$$

with $D_l = M_1 M_2 - m^2 l^2$, and state space:

$$\begin{pmatrix} \dot{x}_1 \\ \dot{x}_2 \\ \dot{x}_3 \\ \dot{x}_4 \end{pmatrix} = \begin{pmatrix} x_2 \\ \frac{-M_2 k x_1}{D_l} - \frac{mlN}{D_l} + \frac{M_2 F}{D_l} \\ x_4 \\ \frac{mlkx_1}{D_l} + \frac{M_1 N}{D_l} - \frac{mlF}{D_l} \end{pmatrix} \tag{3.12}$$

which when expanded further results in

$$\begin{pmatrix} \dot{x}_1 \\ \dot{x}_2 \\ \dot{x}_3 \\ \dot{x}_4 \end{pmatrix} = \begin{pmatrix} x_2 \\ \frac{-M_2 k x_1}{D_l} \\ x_4 \\ \frac{mlkx_1}{D_l} \end{pmatrix} + \begin{pmatrix} 0 & 0 \\ -\frac{ml}{D_l} & \frac{M_2}{D_l} \\ 0 & 0 \\ \frac{M_1}{D_l} & \frac{-ml}{D_l} \end{pmatrix} \begin{pmatrix} u_1 \\ u_2 \end{pmatrix} \tag{3.13}$$

with $u_1 = N$ and $u_2 = F$. The various system matrices are now given by

$$\frac{\partial f}{\partial x} \equiv A = \begin{pmatrix} 0 & 1 & 0 & 0 \\ \frac{M_2 k}{D_l} & 0 & 0 & 0 \\ 0 & 0 & 0 & 1 \\ \frac{mlk}{D_l} & 0 & 0 & 0 \end{pmatrix} \tag{3.14}$$

with $A$, being the linear transmission matrix

$$\frac{\partial g}{\partial x} \equiv B = \begin{pmatrix} 0 & 0 \\ \frac{-ml}{D_l} & \frac{M_2}{D_l} \\ 0 & 0 \\ \frac{M_1}{D_l} & \frac{-ml}{D_l} \end{pmatrix} \tag{3.15}$$

and $B$, the input matrix.

#### *3.1.1.3 Some notes on the linearized system*

From literature and practice, a direct consequence of linearization is the possibility of loosing certain aspects of the system dynamics. This is very true in the case of the RTAC system, where after linearization, the third element of the state space is left out of the system model as seen in the transmission matrix. The implication of this, is the reduction of the system in rank so that the system matrix becomes singular to working precision. This means that in practice this matrix is not invertible.

#### *3.1.1.4 Regulator equations for the RTAC*

The formulation of the regulator equations for the linear RTAC system is now presented. However the following assumptions were made to fit with the design target for tracking.

1. The states for regulation are $x_1$, $x_3$ and $x_4$

2. The error associated with each regulated state is $e_1 = x_1 - w1 \quad e_2 = x_3 - w3 \quad e_3 = x_4 - w4$

3. Since the exosystem is neutrally stable, hypothesis H1 in Vaidyanathan (2013) demanded Lyapunov stability in both forward and backward time at $w = 0$.

4. A second hypothesis (H2) according to Vaiyanathan, (2013) required that every uncontrollable eigenvalue be stabilizable by appropriate choice of state feedback.

5. Since these two hypotheses were satisfied for the RTAC system, a feedback regulator exists if there can be found a homomorphism or continuously differentiable mapping defined by $x_i = \pi_i(w)$. The choice of mapping must satisfy the FBI equations, which for any dynamic system represents a set of unique equations that completely spell out the solution of the developed regulator or compensator. Vaidyanathan, (2011; 2013) gives the regulator equations as

$$\frac{\partial \pi}{\partial w} s(w) = f(\pi(w)) + g(\pi(w))\varphi(w) + p(\pi(w))w \tag{3.16}$$

$$h(\pi(w)) - q(w) = 0 \tag{3.17}$$

which are analogous to the Sylvester equations

$$\Pi Sexo = A\Pi + BU + P \tag{3.18}$$

$$0 = C\Pi + Q \tag{3.19}$$

6. For the RTAC the mappings are $x_1 = \pi_1(w) \quad x_2 = \pi_2(w) \quad x_3 = \pi_3(w) \quad x_4 = \pi_4(w)$.

For the RTAC linear system, the constant tracking problem for $x_1$

$$\begin{pmatrix} \dot{x}_1 \\ \dot{x}_2 \\ \dot{x}_3 \\ \dot{x}_4 \\ e_1 \end{pmatrix} = \begin{pmatrix} x_2 \\ \frac{-M_2 k x_1}{D_l} - \frac{mlN}{D_l} + \frac{M_2 F}{D_l} \\ x_4 \\ \frac{mlkx_1}{D_l} + \frac{M_1 N}{D_l} - \frac{mlF}{D_l} \\ x_1 - w \end{pmatrix} \tag{3.20}$$

After some computation, the (unique) set of solutions to the regulator equations while tracking $x_1$ were obtained as:

$$\pi_1(w) = w \quad \pi_2(w) = 0 \quad \pi_3(w) = 0 \quad \pi_4(w) = 0 \quad \varphi_1(w) = \frac{M_2 w}{ml}(1-k) \quad \varphi_2(w) = \frac{ml}{M_1}(w-k) \tag{3.21}$$

The constant tracking problem for $x_3$

$$\begin{pmatrix} \dot{x}_1 \\ \dot{x}_2 \\ \dot{x}_3 \\ \dot{x}_4 \\ e_2 \end{pmatrix} = \begin{pmatrix} x_2 \\ \frac{-M_2 k x_1}{D_l} - \frac{mlN}{D_l} + \frac{M_2 F}{D_l} \\ x_4 \\ \frac{mlkx_1}{D_l} + \frac{M_1 N}{D_l} - \frac{mlF}{D_l} \\ x_3 - w \end{pmatrix} \tag{3.22}$$

which generated the (unique) set of solutions to the regulator equations for tracking $x_3$ as;

$$\pi_1(w) = 0 \quad \pi_2(w) = 0 \quad \pi_3(w) = w \quad \pi_4(w) = 0 \quad \varphi(w) = \frac{M_2 mlw(1+k)}{M_1 M_2 + m^2 l^2 k} \tag{3.23}$$

The constant tracking problem for $x_4$

$$\begin{pmatrix} \dot{x}_1 \\ \dot{x}_2 \\ \dot{x}_3 \\ \dot{x}_4 \\ e_3 \end{pmatrix} = \begin{pmatrix} x_2 \\ \frac{-M_2 k x_1}{D_l} - \frac{mlN}{D_l} + \frac{M_2 F}{D_l} \\ x_4 \\ \frac{mlkx_1}{D_l} + \frac{M_1 N}{D_l} - \frac{mlF}{D_l} \\ x_4 - w \end{pmatrix} \tag{3.24}$$

which generated the (unique) set of solutions to the regulator equations for tracking $x_4$ as;

$$\pi_1(w) = 0 \quad \pi_2(w) = 0 \quad \pi_3(w) = 0 \quad \pi_4(w) = w \quad \varphi(w) = \frac{M_2 mlw(1+k)}{M_1 M_2 + m^2 l^2 k} \tag{3.25}$$

which resulted in the state feedback defined by

$$u = \varphi(w) + K(x - \pi(w)) \tag{3.26}$$

where $\varphi(w), \quad \pi(w)$, are defined as in equations (3.21), (3.23) and (3.25) in accordnace with equations (3.16) and (3.17). $K$, is the feedback gain matrix that renders $A + BK$ Hurwitz stable.

*3.1.1.5 Observer-based internal model for the RTAC system*

The observer internal model subsystem for the RTAC model and generally for any system has the following form given by

$$\dot{\xi} = \begin{pmatrix} A & E \\ 0 & S \end{pmatrix} \xi + \begin{pmatrix} B \\ 0 \end{pmatrix} u + L\left(y_m - [C_m \quad Q_m]\xi - D_m u\right) \tag{3.27}$$

alternatively given as follows

$$\begin{pmatrix} \dot{\xi}_0 \\ \dot{\xi}_1 \end{pmatrix} = \begin{pmatrix} A & E \\ 0 & S \end{pmatrix} \begin{pmatrix} \xi_0 \\ \xi_1 \end{pmatrix} + \begin{pmatrix} B \\ 0 \end{pmatrix} u + L\left(y_m - [C_m \quad Q_m]\xi - D_m u\right) \tag{3.28}$$

The internal IMP and the role it played was described in section 2.2.1.1. However the structure of equation (3.27), according to Serrani (2005) consists of not just an observer estimator, but can be precisely divided into two parts given in equation (3.28); an internal model or steady state generator and a stabilizer. In a nutshell, the estimator is an interconnection between an internal model and a stabilizer(Serrani, 2005).

#### *3.1.1.6 Practicability of the compensator*

Finally the test for practicabilty of the designed compensator is made with respect to the closed loop system formed by the plant and observer This test has been referenced in equation (**??**). The test basically reduces to an eigenvalue analysis of the following matrix

$$J_{cllp} = \begin{pmatrix} A & BH \\ GC & F \end{pmatrix} \tag{3.29}$$

where having each eigenvalue in the LHCP means the successful design of the output regulator. This Hurwitz test remains applicable to any system being stabilized by output error feedback observer regulation (Serrani, 2005). The implication were, conditions for an asymptotic regulation has been met and unique solutions were found for the FBI regulator equations (3.17) or equivalently equation (3.19).

### 3.1.2 RTAC Parameters

The parameters for the underactuated RTAC system were adopted from two main literature. Avis *et al.*,(2010) addressed the comparison of different control laws for the RTAC system while Sun *et al.*, (2016) addressed the nonlinear continuous global stabilization of the RTAC system. Table 3.1 shows the parameters of the RTAC used by Nersesov *et. al.,*2010.

Table 3.1: Table of RTAC Parameters (Nersesov *et al.*, 2010)

| Description | Parameter | Value | Units |
|---|---|---|---|
| Cart mass | M | 1.7428 | kg |
| Eccentric mass | m | 0.2739 | kg |
| Arm eccentricity | la | 0.0537 | m |
| Arm inertia | Ia | 0.000884 | $kgm^2$ |
| Spring stiffness | k | 339.4 | $N/m$ |

### 3.1.3 Output regulation for the CIP system

The nonlinear dynamic model of the CIP was adopted from Elsayed *et al.*,(2015). The model of the cart driven inverted pendulum with generalized coordinates $(x, \theta)$ was:

$$(M+m)\ddot{x} + mlsin\theta\dot{\theta}^2 - mlcos\theta\ddot{\theta} - \psi(\dot{x}) = \tau + w1(t) \tag{3.30}$$

$$(I+ml^2)\ddot{\theta} - mlcos\theta\ddot{x} - mglsin\theta - \varphi(\dot{\theta}) = +w2(t) \tag{3.31}$$

The frictional terms $\psi(\dot{x})$ and $\varphi(\dot{\theta})$ were represented by $F_{fr}$ and $q\dot{\theta}$ respectively.

#### *3.1.3.1 Nonlinear model of CIP*

When the system is represented as a system of first order differential equations, the nonlinear CIP becomes;

$$\dot{x}_1 = x_2 \tag{3.32}$$

$$\dot{x}_2 = -\frac{m^2l^2gsinx_3cosx_3}{Dnl} + \frac{M_2mlsinx_3x_4^2}{Dnl} + \frac{M_2u}{Dnl} + \frac{M_2w_1}{Dnl} + \frac{mlcosx_3w_2}{Dnl} \tag{3.33}$$

$$\dot{x}_3 = x_4 \tag{3.34}$$

$$\dot{x}_4 = \frac{-m^2l^2sinx_3cosx_3x_4^2}{Dnl} + \frac{M_1mglsinx_3}{Dnl} - \frac{mlcosx_3u}{Dnl} + \frac{mlcosx_3w_1}{Dnl} + \frac{M_1w_2}{Dnl} \tag{3.35}$$

Equations( 3.32)-( 3.35) represent the first order ODE form of the inverted pendulum nonlinear dynamics model given in equation (3.31). The term $Dnl = M_1M_2 - m^2l^2cos^2x_3$, is nonlinear in

$x_3$.

### *3.1.3.2 Linear model of CIP*

For the simulation work, a first linear model was used. This linearized equivalent of the CIP system was given for two scenarios;

1. pendulum-down model given by

$$(M+m)\ddot{x} - ml\ddot{\theta} - c(\dot{x}) = \tau + w1(t) \tag{3.36}$$

$$(I+ml^2)\ddot{\theta} - ml\ddot{x} - mgl\theta - q(\dot{\theta}) = w2(t) \tag{3.37}$$

2. pendulum-up position model.

$$(M+m)\ddot{x} + ml\ddot{\theta} - c(\dot{x}) = \tau + w1(t) \tag{3.38}$$

$$(I+ml^2)\ddot{\theta} + ml\ddot{x} + mgl\theta - q(\dot{\theta}) = w2(t) \tag{3.39}$$

where equations ( 3.37) and ( 3.39) represent the pendulum arm at angles of 0 $\deg$ and 180 $\deg$ respectively.

### *3.1.3.3 State space realization of CIP*

After some re-arrangement of equation (3.37) where the frictional terms were ignored, the dynamic equations for the CIP in the pendulum-down position were obtained as

$$\ddot{x} = \frac{m^2l^2g}{D_l}\theta + \frac{M_2}{D_l}\tau + \frac{M_2}{D_l}w_1 + \frac{ml}{D_l}w_2 \tag{3.40}$$

$$\ddot{\theta} = \frac{M_1mgl}{D_l}\theta + \frac{ml}{D_l}\tau + \frac{ml}{D_l}w_1 + \frac{M_1}{D_l}w_2 \tag{3.41}$$

with the full dynamics given by

$$\begin{pmatrix} \dot{x}_1 \\ \dot{x}_2 \\ \dot{x}_3 \\ \dot{x}_4 \end{pmatrix} = \begin{pmatrix} x_2 \\ \ddot{x} = \frac{m^2 l^2 g}{D_l} x_3 + \frac{M_2}{D_l}\tau + \frac{M_2}{D_l} w_1 + \frac{ml}{D_l} w_2 \\ x_4 \\ \ddot{\theta} = \frac{M_1 mgl}{D_l} x_3 + \frac{ml}{D_l}\tau + \frac{ml}{D_l} w_1 + \frac{M_1}{D_l} w_2 \end{pmatrix} \tag{3.42}$$

Selected state space coordinates are $x = [x, \dot{x}, \theta, \dot{\theta}] \equiv [x_1, x_2, x_3, x_4]$

$$\begin{pmatrix} \dot{x}_1 \\ \dot{x}_2 \\ \dot{x}_3 \\ \dot{x}_4 \end{pmatrix} = \begin{pmatrix} 0 & 1 & 0 & 0 \\ 0 & 0 & \frac{m^2 l^2 g}{D_l} & 0 \\ 0 & 0 & 0 & 1 \\ 0 & 0 & \frac{M_1 mgl}{D_l} & 0 \end{pmatrix} \begin{pmatrix} x_1 \\ x_2 \\ x_3 \\ x_4 \end{pmatrix} + \begin{pmatrix} 0 \\ \frac{M_2}{D_l} \\ 0 \\ \frac{ml}{D_l} \end{pmatrix} u + \begin{pmatrix} 0 & 0 \\ \frac{M_2}{D_l} & \frac{ml}{D_l} \\ 0 & 0 \\ \frac{ml}{D_l} & \frac{M_1}{D_l} \end{pmatrix} \begin{pmatrix} w_1 \\ w_2 \end{pmatrix} \tag{3.43}$$

Similar modification of equation (3.39) resulted in the dynamic equations for the pendulum-up position

$$\ddot{x} = \frac{m^2 l^2 g}{D_l}\theta + \frac{M_2}{D_l}\tau + \frac{M_2}{D_l} w_1 - \frac{ml}{D_l} w_2 \tag{3.44}$$

$$\ddot{\theta} = -\frac{M_1 mgl}{D_l}\theta - \frac{ml}{D_l}\tau - \frac{ml}{D_l} w_1 + \frac{M_1}{D_l} w_2 \tag{3.45}$$

with the full pendulum-up dynamics given by

$$\begin{pmatrix} \dot{x}_1 \\ \dot{x}_2 \\ \dot{x}_3 \\ \dot{x}_4 \end{pmatrix} = \begin{pmatrix} x_2 \\ \ddot{x} = \frac{m^2 l^2 g}{D_l} x_3 + \frac{M_2}{D_l}\tau + \frac{M_2}{D_l} w_1 - \frac{ml}{D_l} w_2 \\ x_4 \\ \ddot{\theta} = -\frac{M_1 mgl}{D_l} x_3 - \frac{ml}{D_l}\tau - \frac{ml}{D_l} w_1 + \frac{M_1}{D_l} w_2 \end{pmatrix} \tag{3.46}$$

with state space realization given as

$$\begin{pmatrix} \dot{x}_1 \\ \dot{x}_2 \\ \dot{x}_3 \\ \dot{x}_4 \end{pmatrix} = \begin{pmatrix} 0 & 1 & 0 & 0 \\ 0 & 0 & \frac{m^2 l^2 g}{D_l} & 0 \\ 0 & 0 & 0 & 1 \\ 0 & 0 & -\frac{M_1 mgl}{D_l} & 0 \end{pmatrix} \begin{pmatrix} x_1 \\ x_2 \\ x_3 \\ x_4 \end{pmatrix} + \begin{pmatrix} 0 \\ \frac{M_2}{D_l} \\ 0 \\ -\frac{ml}{D_l} \end{pmatrix} u + \begin{pmatrix} 0 & 0 \\ \frac{M_2}{D_l} & -\frac{ml}{D_l} \\ 0 & 0 \\ -\frac{ml}{D_l} & \frac{M_1}{D_l} \end{pmatrix} \begin{pmatrix} w_1 \\ w_2 \end{pmatrix} \tag{3.47}$$

In every case the denominator $D_l$, has been given as $M_1 M_2 - m^2 l^2$

### 3.1.4 Regulator equations for the CIP

Formulation for the regulator equations of linear CIP pendulum-up system were made and presented as follows:

1. the states for regulation are $(x_1 \quad x_2 \quad x_3)$
2. the error associated with each regulated state is $e_1 = x_1 - w1 \quad e_2 = x_2 - w2 \quad e_3 = x_3 - w3$
3. the same hypotheses H1 and H2, described in section 3.1.1.4 are satisfied for the CIP system. Therefore a feedback regulator exists if there can be found a homomorphism or continuously differentiable mapping defined by $x_i = \pi_i(w)$.
4. For the CIP the mappings are $x_1 = \pi_1(w) \quad x_2 = \pi_2(w) \quad x_3 = \pi_3(w) \quad x_4 = \pi_4(w)$.

For the CIP linear system, the constant tracking problem for $x_1$ is developed as follows;

$$\begin{pmatrix} \dot{x}_1 \\ \dot{x}_2 \\ \dot{x}_3 \\ \dot{x}_4 \\ e_1 \end{pmatrix} = \begin{pmatrix} x_2 \\ \frac{m^2 l^2 g}{D_l} x_3 + \frac{M_2}{D_l}\tau + \frac{M_2}{D_l} w_1 - \frac{ml}{D_l} w_2 \\ x_4 \\ -\frac{M_1 mgl}{D_l} x_3 - \frac{ml}{D_l}\tau - \frac{ml}{D_l} w_1 + \frac{M_1}{D_l} w_2 \\ x_1 - w \end{pmatrix} \tag{3.48}$$

After some computation, the (unique) set of solutions to the regulator equations was obtained for regulation of state $x_1$ as;

$$\pi_1(w) = w \tag{3.49}$$

$$\pi_2(w) = 0 \tag{3.50}$$

$$\pi_3(w) = \frac{(m^2l^2 - M_1M_2)w_2}{m^3l^3g - M_1M_2mgl}; \frac{(M_1M_2 - m^2l^2)w_2}{M_1M_2mgl + m^3l^3g} \tag{3.51}$$

$$\pi_4(w) = 0 \tag{3.52}$$

$$\varphi(w) = \frac{(-M_1M_2 + m^2l^2)w_1}{M_1M_2 - m^2l^2} \tag{3.53}$$

which resulted in the state feedback defined by

$$u = \varphi(w) + K(x - \pi(w)) \tag{3.54}$$

where $\varphi(w), \quad \pi(w)$, are defined as in equations (3.49)-(3.53) and $K$, is the feedback gain that renders $A + BK$ Hurwitz stable.

Replacing the output error $x_1 - w$ in equation (3.48) by $e = x_2 - w$, the constant tracking problem for $x_2$ yielded the following solution to the regulator equations

$$\pi_1(w) = 0 \tag{3.55}$$

$$\pi_2(w) = w \tag{3.56}$$

$$\pi_3(w) = \frac{(m^2l^2 - M_1M_2)w_2}{m^3l^3g - M_1M_2mgl}; \frac{(M_1M_2 - m^2l^2)w_2}{M_1M_2mgl + m^3l^3g} \tag{3.57}$$

$$\pi_4(w) = 0 \tag{3.58}$$

$$\varphi(w) = \frac{(-M_1M_2 + m^2l^2)w_1}{M_1M_2 - m^2l^2} \tag{3.59}$$

thereafter the feedback is synthesized as previously done for $x_1$ using equation (3.54) with terms defined by equations (3.55)-(3.59).

Finally constant tracking problem for $x_3$ also yields the following solution to the regulator equa-

tions for $e = x_3 - w$

$$\pi_1(w) = 0 \tag{3.60}$$

$$\pi_2(w) = 0 \tag{3.61}$$

$$\pi_3(w) = w \tag{3.62}$$

$$\pi_4(w) = 0 \tag{3.63}$$

$$\varphi(w) = -M_1 g w - w - 1 + \frac{M_1 w_2}{ml}; \frac{-m^2 l^2 g w}{m_2} - w_1 + \frac{m l w_2}{M_2} \tag{3.64}$$

with a similar state feedback synthesis used as given by equation (3.54) and defined by equations (3.60)-(3.64).

### 3.1.5 CIP Parameters

The parameters for the CIP used in the simulation experiments are presented in Table 3.2.

Table 3.2: Table of CIP Parameters (Elsayed *et al.*, 2015)

| Description | Parameter | Value | Units |
|---|---|---|---|
| Cart mass | M | 0.882 | kg |
| Pendulum mass | m | 0.32 | kg |
| Acc. due to gravity | g | 9.81 | $kg/m^2$ |
| Length of pendulum | l | 0.3302 | m |
| MOI of pendulum | I | $7.88 * 10^{-8}$ | $kgm^2$ |
| Coeff. of friction | $F_{fr}$ | 1.3 | $Ns/m$ |
| Pendulum damping coeff | q | 0.0001 | $N.s/rad$ |
| Armature inductance | La | $0.18 * 10^{-3}$ | H |
| Armature resistance | Ra | 2.6 | ohm |
| MOI of rotor | J | $3.9 * 10^{-7}$ | $kgm^2$ |
| Pendulum damping coeff | q | $8 * 10^{-7}$ | $N.m.s/rad$ |

### 3.1.6 Output regulator for the QUAV

The nonlinear QUAV equations as adopted from Lefeber & Biever, (2015) were given in the original coordinates as
$x = [p_1 \;\; p_2 \;\; p_3 \;\; \phi \;\; \theta \;\; \psi \;\; v_1 \;\; v_2 \;\; v_3 \;\; p \;\; q \;\; r]$ as

$$\begin{pmatrix} \dot{p}_1 \\ \dot{p}_2 \\ \dot{p}_3 \\ \dot{\phi} \\ \dot{\theta} \\ \dot{\psi} \\ \dot{v}_1 \\ \dot{v}_2 \\ \dot{v}_3 \\ \dot{p} \\ \dot{q} \\ \dot{r} \end{pmatrix} = \begin{pmatrix} c\psi c\theta v_1 + (-s\psi c\phi + c\psi s\theta s\phi)v_2 + (s\psi s\phi + c\psi s\theta c\phi)v_3 \\ s\psi c\theta v_1 + (c\psi c\phi + s\psi s\theta s\phi)v_2 + (-s\phi c\psi + s\psi s\theta c\phi)v_3 \\ -s\theta v_1 + s\phi c\theta v_2 + c\theta c\phi v_3 \\ p + qs\phi tan\theta + rc\phi tan\theta \\ qc\phi - rs\phi \\ qs\phi\frac{1}{c\theta} + rc\phi\frac{1}{c\theta} \\ rv_2 - qv_3 - gs\theta \\ -rv_1 + pv_3 + gs\phi c\theta \\ qv_1 - pv_2 + gc\theta c\phi - f/m \\ qr\frac{J_y - J_z}{J_x} + \gamma_1/J_x \\ pr\frac{J_z - J_x}{J_y} + \gamma_2/J_y \\ pq\frac{J_x - J_y}{J_z} + \gamma_3/J_z \end{pmatrix} \tag{3.65}$$

Equation (3.65) is transformed into new coordinates of
$x = [x_1 \;\; x_2 \;\; x_3 \;\; x_4 \;\; x_5 \;\; x_6 \;\; x_7 \;\; x_8 \;\; x_9 \;\; x_{10} \;\; x_{11} \;\; x_{12}]$ as

$$\begin{pmatrix} \dot{x}_1 \\ \dot{x}_2 \\ \dot{x}_3 \\ \dot{x}_4 \\ \dot{x}_5 \\ \dot{x}_6 \\ \dot{x}_7 \\ \dot{x}_8 \\ \dot{x}_9 \\ \dot{x}_{10} \\ \dot{x}_{11} \\ \dot{x}_{12} \end{pmatrix} = \begin{pmatrix} cx_6cx_5x_7 + (-sx_6cx_4 + cx_6sx_5sx_4)x_8 + (sx_6sx_4 + cx_6sx_5cx_4)x_9 \\ sx_6cx_5x_7 + (cx_6cx_4 + sx_6sx_5sx_4)x_8 + (-sx_4cx_6 + sx_6sx_5cx_4)x_9 \\ -sx_5x_7 + sx_4cx_5x_8 + cx_5cx_4x_9 \\ x_{10} + x_{11}sx_4tanx_5 + x_{12}cx_4tanx_5 \\ x_{11}cx_4 - x_{12}sx_4 \\ x_{11}sx_4\frac{1}{cx_5} + x_{12}cx_4\frac{1}{cx_5} \\ x_{12}x_8 - x_{11}x_9 - gsx_5 \\ -x_{12}x_7 + x_{10}x_9 + gsx_4cx_5 \\ x_{11}x_7 - x_{10}x_8 + gcx_5cx_4 - u_1/m \\ x_{11}x_{12}\frac{J_y - J_z}{J_x} + u_2/J_x \\ x_{10}x_{12}\frac{J_z - J_x}{J_y} + u_3/J_y \\ x_{10}x_{11}\frac{J_x - J_y}{J_z} + u_4/J_z \end{pmatrix} \tag{3.66}$$

#### *3.1.6.1 Linearized QUAV model*

The equivalent linearized QUAV model has the state space form given by

$$\begin{pmatrix} \dot{x}_1 \\ \dot{x}_2 \\ \dot{x}_3 \\ \dot{x}_4 \\ \dot{x}_5 \\ \dot{x}_6 \\ \dot{x}_7 \\ \dot{x}_8 \\ \dot{x}_9 \\ \dot{x}_{10} \\ \dot{x}_{11} \\ \dot{x}_{12} \end{pmatrix} = \begin{pmatrix} x_7 \\ x_8 \\ x_9 \\ x_{10} \\ x_{11} \\ -x_{12} \\ -9.8100x_5 \\ 9.81x_4 \\ 0 \\ 0 \\ 0 \\ 0 \end{pmatrix} + \begin{pmatrix} 0 & 0 & 0 & 0 \\ 0 & 0 & 0 & 0 \\ 0 & 0 & 0 & 0 \\ 0 & 0 & 0 & 0 \\ 0 & 0 & 0 & 0 \\ 0 & 0 & 0 & 0 \\ 0 & 0 & 0 & 0 \\ 0 & 0 & 0 & 0 \\ -1.2658 & 0 & 0 & 0 \\ 0 & 250.0000 & 0 & 0 \\ 0 & 0 & 250.0000 & 0 \\ 0 & 0 & 0 & 119.0476 \end{pmatrix} \begin{pmatrix} u_1 \\ u_2 \\ u_3 \\ u_4 \end{pmatrix} \tag{3.67}$$

equation (3.67) has the general affine form

$$\dot{x} = f(x) + g(x)u \tag{3.68}$$

For outpiut regulation studies, the possible disturbance inputs impacts each of the desired output states. When the disturbance term was included, the equation transformed into the augmented form given by

$$\dot{x} = f(x) + g(x)u + p(x)w \tag{3.69}$$

In which $p(x)$, was a matrix of appropriate size to the intended disturbance entering the system with $w$ a vector.

### *3.1.6.2 QUAV regulator equations*

The regulator equations for the QUAV are here presented. They are obtained from the linear UAV model of equation (3.67) and the FBI equations presented in equation (3.17) The following error

maps are defined for the selected output signals

$$e_1 = x_3 - w \tag{3.70}$$

$$e_2 = x_4 - w \tag{3.71}$$

$$e_3 = x_5 - w \tag{3.72}$$

$$e_4 = x_6 - w \tag{3.73}$$

with the exosystem defined as a constant $\dot{w} := s(w) = 0$ and maps $x_1 := \pi_1(w), x_2 := \pi_2(w), x_3 := \pi_3(w), x_4 := \pi_4(w), x_5 := \pi_5(w), x_6 := \pi_6(w), x_7 := \pi_7(w), x_8 := \pi_8(w), x_9 := \pi_9(w), x_{10} := \pi_{10}(w), x_{11} := \pi_{11}(w), x_{12} := \pi_{12}(w)$,, the regulator equations obtained for the tracking of set-points $x_3, x_4, x_5, x_6$, were:

$\pi_3(w), \ldots, \pi_6(w) := \omega$, $\pi_7(w), \ldots, \pi_{12}(w) := 0$, $c_{1x} := c_{1y} := 0$, $c_{1z} := -mg$ and finally $c_\phi := c_\theta := c_\psi := 0$ where the exosystem variable $w$, could possess different characteristic profiles from simple linear combinations of terms to more complex polynomial, trigonometric or nonlinear superimposed terms. The derived regulator equations above were found to be only a particular solution to the FBI equations for the quadrotor. They were however not unique. This non-uniqueness is explainable by the sparseness of the linearized quadrotor model. This non-uniqueness was expressed by freedom to assign certain regulator terms as given by $*$.

### *3.1.6.3 Closed loop dynamic for the QUAV*

At the end of all the analytical designs, with all the gains designed for, the closed loop system is obtained. The closed loop system matrix is described as:

$$A_{cl} = \begin{pmatrix} A + BK_x & BK_x & BK_v \\ 0 & A - L1C & P - L1Q \\ 0 & -L2C & S - L2Q \end{pmatrix} \tag{3.74}$$

It is an augmented matrix with the following parts, the original plant, internal model (IM) and also the exosystem state. It is required that the closed loop system has all its eigenvalues well placed on the left hand complex plane (LHCP) for the plant and internal model eigenvalues. The exception being the eigenvalues of the exosystem which are Poisson stable and are located on the imaginary axis of the complex plane. Having satisfied this condition, the system states became asymptotically stable or the closed loop system is described as globally asymptotically stable.

#### *3.1.6.4 Internal model observer design for the QUAV*

The design parameters for the QUAV internal model-based observer in the ouput feedback regulator or compensator were the gains $Kx, \quad Xsyl \quad Usyl \quad Kv \quad G_1, \quad G_2$. These parameters which have been synthesized can be seen in section B.1.13 of the Appendix.

### 3.1.7 Quadrotor UAV Parameters

The parameters for the quadrotor used in the simulation experiments are presented in Table3.3.

Table 3.3: Table of QUAV Parameters (Ozbek *et al.*, 2015)

| Description | Parameter | Value | Units |
|---|---|---|---|
| UAV mass | m | 0.8 | kg |
| Acc. due to gravity | g | 9.81 | $kg/m^2$ |
| Arm length of vehicle | la | 0.3 | m |
| PMIx | Ixx | $15.67 * 10^-3$ | $kgm^2$ |
| PMIy | Iyy | $15.67 * 10^-3$ | $kgm^2$ |
| PMIz | Izz | $23.34 * 10^-3$ | $kgm^2$ |
| Thrust coeff | b | $192 * 10^-7$ | $Ns^2$ |
| Drag coeff | d | $4.003 * 10^-5$ | $Nm^2$ |

## 3.2 Development of immersion-invariance stabilizing controller

The immersion invariance controller was developed and demonstrated for the RTAC system. This report now proceeds to give details of this development.

### 3.2.1 Immersion invariance control of the RTAC or TORA system

The immersion and invariance control scheme for the RTAC is presented as follows. The working model is the nonlinear model of equation (3.9). The consideration made in the following development are drawn from Astolfi and Ortega, (2003).

1. selection of target system was flexible with certain factors informing the choice. These factors include the presence of slow or fast subsystem, bending modes, applications with low, medium or high power applications

2. For low power applications, the actuator dynamics have been safely neglected as shown in equation (3.9). However for medium to low-power applications, the actuator dynamics were considered. This required an extension of the state space.

3. The state space was expanded to accomodate the actuator dynamics which is not explicit in the nonlinear version of equation (3.9). The new state space is $x = [q, \dot{q}, \theta, \dot{\theta}, i]$ equivalent to $x = [x_1, x_2, x_3, x_4, x_5]$, with the new variable selected as the DC motor current dynamic which has input voltage as one of its parameters. This is shown in the actuator model of equation (3.8).

The dynamics of this expanded system is given as

$$\dot{x}_1 = x_2 \tag{3.75}$$

$$\dot{x}_2 = -\frac{M_2 k x_1}{D} + \frac{mlM_2 x_4^2 sinx_3}{D} - \frac{mlK_m x_5 cosx_3}{D} + \frac{M_2 F}{D} \tag{3.76}$$

$$\dot{x}_3 = x_4 \tag{3.77}$$

$$\dot{x}_4 = \frac{mlkx_1 cosx_3}{D} - \frac{m^2 l^2 x_4^2 sinx_3 cosx_3}{D} + \frac{M_1 K_m x_5}{D} - \frac{mlcosx_3 F}{D} \tag{3.78}$$

$$\dot{x}_5 = -\frac{R}{L}x_5 - \frac{K_m}{L}x_4 + \frac{V}{L} \tag{3.79}$$

where the control torque $N$ in equation (3.2) has been replaced by the equivalent motor torque, $K_m i = K_m x_5$ in equation (3.118).

*3.2.1.1 Selection of target dynamic for RTAC*

From this system, a suitable target system was constructed in the form $\xi = \alpha(\xi)$. This form is derived from the following maps $x_1 = \pi(\xi_1), x_2 = \pi(\xi_2), x_3 = \pi(\xi_3), x_4 = \pi(\xi_4), x_5 = \pi(\omega_5(\xi))$. Where $\omega_5(\xi)$, is any stabilizing state feedback to be computed as a function of the remaining system states $x_1, x_2, x_3, x_4$. This implies a possible solution of the Francis-Byrnes-Isidori(FBI) equation is given by the functional map $\pi(\xi) = col(\xi_1, \xi_2, \xi_3, \xi_4, \omega(\xi))$. The target system is now presented:

$$\dot{\xi}_1 = \xi_2 \tag{3.80}$$

$$\dot{\xi}_2 = -\frac{M_2 k \xi_1}{D} + \frac{mlM_2\xi_4^2 sin\xi_3}{D} - \frac{mlK_m\omega(x)cos\xi_3}{D} + \frac{M_2 F}{D} \tag{3.81}$$

$$\dot{\xi}_3 = \xi_4 \tag{3.82}$$

$$\dot{\xi}_4 = \frac{mlk\xi_1 cos\xi_3}{D} - \frac{m^2l^2\xi_4^2 sin\xi_3 cos\xi_3}{D} + \frac{M_1K_m\omega(x)}{D} - \frac{mlcos\xi_3 F}{D} \tag{3.83}$$

The selected maps and target system were verified by using the Francis-Byrnes-Isidori or Immerson equations to test for immersion condition. This test has been given by Astolfi & Ortega, (2003) as:

$$f(\pi(\xi)) + g(\pi(\xi))c(\pi(\xi)) = \frac{\partial\pi}{\partial\xi}\alpha(\xi) \tag{3.84}$$

The equations were found to all satisfy the immersion condition. A suitable manifold was then selected as $z \equiv \phi(x) = x_5 - \omega(x)$, which was used to derive the control $U = \psi(x, z)$ (input voltage $V$ in equation (3.79) is set to this $U$), that drives the off-the-manifold coordinate $z$ to zero

while simultaneously keeping the system bounded. This derivation was made as follows

$$z = \phi(x) = x_5 - \omega(x) \tag{3.85}$$

$$\dot{z} \equiv \dot{\phi}(x) = \frac{\partial \phi}{\partial x_5}\dot{x_5} - \dot{\omega}(x) \tag{3.86}$$

$$\dot{z} = -\frac{R}{L}x_5 - \frac{k_m}{L}x_4 + \frac{U}{L} - \dot{\omega}(x) \tag{3.87}$$

$$\dot{z} = -\frac{R}{L}x_5 - \frac{k_m}{L}x_4 + \frac{\psi(x,z)}{L} - \dot{\omega}(x) \tag{3.88}$$

$$\psi(x,z) = L\dot{z} + Rx_5 + k_m x_4 + L\dot{\omega}(x) \tag{3.89}$$

$$\frac{\psi}{R} = \frac{L}{R}\dot{z} + x_5 + \frac{K_m}{R}x_4 + \frac{L}{R}\dot{\omega}(x) \tag{3.90}$$

$$\frac{\psi}{R} = x_5 - z + \frac{K_m}{R}x_4 + \frac{L}{R}\dot{\omega}(x) \tag{3.91}$$

$$\psi = R(x_5 - z) + K_m x_4 + L\dot{\omega}(x) \tag{3.92}$$

where $\dot{z} = -\frac{R}{L}z$, $\omega(x) = x_5 - z$ and if $z = x_5 - \omega(x)$, then $\dot{x_5} = \dot{z} + \dot{\omega}(x) \equiv -\frac{R}{L}z + \dot{\omega}(x)$. It is now shown that for the selected state feedback $w(x_1, x_2, x_3, x_4)$, the trajectories of the system with coordinates given by $(z, x_1, x_2, x_3, x_4, x_5)$, is bounded

$$\dot{z} = -\frac{R}{L}z \tag{3.93}$$

$$\dot{x}_1 = x_2 \tag{3.94}$$

$$\dot{x}_2 = -\frac{M_2 k x_1}{D} + \frac{mlM_2 x_4^2 sinx_3}{D} - \frac{mlK_m x_5 cosx_3}{D} + \frac{M_2 F}{D} \tag{3.95}$$

$$\dot{x}_3 = x_4 \tag{3.96}$$

$$\dot{x}_4 = \frac{mlkx_1 cosx_3}{D} - \frac{m^2 l^2 x_4^2 sinx_3 cosx_3}{D} + \frac{M_1 K_m x_5}{D} - \frac{mlcosx_3 F}{D} \tag{3.97}$$

$$\dot{x}_5 = -\frac{R}{L}z + \dot{\omega}(x) \tag{3.98}$$

A further change of coordinates given by $(z, \eta, x_1, x_2, x_3, x_4)$ was made, such that $\eta = x_5 - \omega(x)$, $\dot{\eta} = \dot{x_5} - \dot{\omega(x)}$. But $\dot{z} = \dot{x_5} - \dot{\omega(x)}$ and $\dot{z} \equiv -\frac{R}{L}z$, therefore $\dot{\eta} = -\frac{R}{L}z$

$$\dot{z} = -\frac{R}{L}z \tag{3.99}$$

$$\dot{\eta} = -\frac{R}{L}z \tag{3.100}$$

$$\dot{x}_1 = x_2 \tag{3.101}$$

$$\dot{x}_2 = -\frac{M_2 k x_1}{D} + \frac{mlM_2 x_4^2 sinx_3}{D} - \frac{mlK_m cosx_3}{D}\eta - \frac{mlK_m cosx_3}{D}\omega + \frac{M_2 F}{D} \tag{3.102}$$

$$\dot{x}_3 = x_4 \tag{3.103}$$

$$\dot{x}_4 = \frac{mlkx_1 cosx_3}{D} - \frac{m^2 l^2 x_4^2 sinx_3 cosx_3}{D} + \frac{M_1 K_m}{D}\eta + \frac{M_1 K_m}{D}\omega - \frac{mlcosx_3 F}{D} \tag{3.104}$$

which has shown $z$ converged to zero exponentially fast, assuring that $\eta$ is bounded. The control law is finally obtained as

$$u = R\omega(x_1, x_2, x_3, x_4) + k_m x_4 + L\dot{\omega}(x) \tag{3.105}$$

where $\omega(x_1, x_2, x_3, x_4)$, is any stablizing state feedback for the target system and $\dot{\omega}$, is obtained from the full state dynamic as $\dot{x_5}$ in this case.

#### *3.2.1.2 RTAC state feedback controller design for immersion invariance*

Having understood the need for a suitable state feedback controller given by $w(x)$, as presented in section 3.2.1.1, the design of this controller was achieved, selecting from known available feedback design methods such as; pole placement, polynomial matching. Since the designed feedback is

derived from the target system, this system has been reproduced here;

$$\dot{\xi}_1 = \xi_2 \tag{3.106}$$

$$\dot{\xi}_2 = -\frac{M_2 k \xi_1}{D} + \frac{mlM_2 \xi_4^2 sin\xi_3}{D} - \frac{mlK_m \omega(x) cos\xi_3}{D} + \frac{M_2 F}{D} \tag{3.107}$$

$$\dot{\xi}_3 = \xi_4 \tag{3.108}$$

$$\dot{\xi}_4 = \frac{mlk\xi_1 cos\xi_3}{D} - \frac{m^2 l^2 \xi_4^2 sin\xi_3 cos\xi_3}{D} + \frac{M_1 K_m \omega(x)}{D} - \frac{mlcos\xi_3 F}{D} \tag{3.109}$$

Given that the system is in its nonlinear form, linearization of the system was performed (using either Jacobian linearization or Taylor's seris expansion) and the following linear equivalent dynamic model resulted;

$$\dot{x}_1 = x_2 \tag{3.110}$$

$$\dot{x}_2 = -\frac{M_2 k x_1}{D} - \frac{mlK_m x_5}{D} + \frac{M_2 F}{D} \tag{3.111}$$

$$\dot{x}_3 = x_4 \tag{3.112}$$

$$\dot{x}_4 = \frac{mlkx_1}{D} + \frac{M_1 K_m x_5}{D} - \frac{mlF}{D} \tag{3.113}$$

$$\dot{x}_5 = -\frac{R}{L} x_5 - \frac{K_m}{L} x_4 + \frac{V}{L} \tag{3.114}$$

having target dynamics;

$$\dot{\xi}_1 = \xi_2 \tag{3.115}$$

$$\dot{\xi}_2 = -\frac{M_2 k \xi_1}{D} - \frac{mlK_m \omega(\xi)}{D} + \frac{M_2 F}{D} \tag{3.116}$$

$$\dot{\xi}_3 = \xi_4 \tag{3.117}$$

$$\dot{\xi}_4 = \frac{mlk\xi_1}{D} + \frac{M_1 K_m \omega(\xi)}{D} - \frac{mlF}{D} \tag{3.118}$$

with state space realization

$$\begin{pmatrix} \dot{\xi}_1 \\ \dot{\xi}_2 \\ \dot{\xi}_3 \\ \dot{\xi}_4 \end{pmatrix} = \begin{pmatrix} 0 & 1 & 0 & 0 \\ \frac{-M_2 k}{D_l} & 0 & 0 & 0 \\ 0 & 0 & 0 & 1 \\ \frac{mlk}{D_l} & 0 & 0 & 0 \end{pmatrix} \begin{pmatrix} \xi_1 \\ \xi_2 \\ \xi_3 \\ \xi_4 \end{pmatrix} + \begin{pmatrix} 0 \\ -\frac{ml}{D_l} \\ 0 \\ \frac{M_1}{D_l} \end{pmatrix} u + \begin{pmatrix} 0 \\ \frac{M_2}{D_l} \\ 0 \\ \frac{-ml}{D_l} \end{pmatrix} w \tag{3.119}$$

This obtained state space realization will now be used to derive the relevant feedback and observer gains for the target system given by $F$ and $L$ respectively.

## 3.3 Development of the Immersion Invariance Output Error Feedback Regulator for Non-Square Systems

Methodology items (1) and (2) were addressed in section 3.1.1 and 3.2. The problem statement and knowledge gap were discussed in section 1.4 of chapter two. It has identified strictly non-square MIMO systems as a subset of nonlinear systems which has not received much attention and generalized formulation of feedback regulator designs. The chart in Figure 3.1 has given the final design tasks for this work to be the synthesis of the immersion invariance and output feedback regulator principles for strictly non-square MIMO systems itemized in methodology item (3) and its subsequent validation. The following sections has addressed this design and was only targeted at achieving stabilization and tracking of a strictly non-square MIMO QUAV system.

### 3.3.1 Feedback stabilization control design

The QUAV model to be controlled has been implemented in Matlab/Simulink. The generalized control diagram for the closed loop control is given in Figure 3.2. It shows the various blocks that form the complete UAV simulation diagram.

The variables in the diagram are: reference $r$,attitude reference $U_{f1,x,y}$, pseudo control input

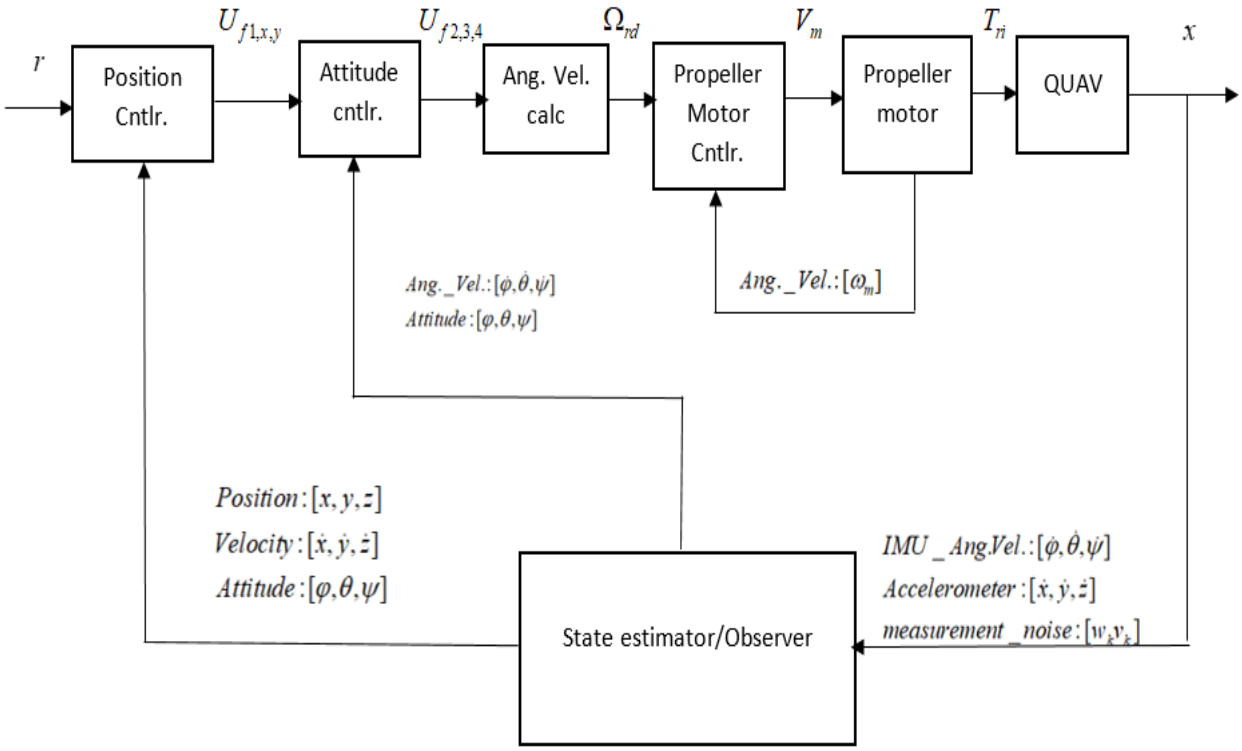



Figure 3.2: QUAV Control Schematic (Sugawara & Shimada, 2017)

$U_{f2,3,4}$, velocity reference $\Omega_{rd}$, voltage reference $V_m$, true control torque input $T_{ri}$, UAV states $X = x, y, z, \phi, \theta, \psi, \dot{x}, \dot{y}, \dot{z}, \dot{\phi}, \dot{\theta}, \dot{\psi}$ and finally the measurement noise $\omega_k, v_k$. The QUAV physical model of the QUAV forces the system to have four inputs with six possible DOF as outputs. These six outputs are translation along and rotation about the x-axis (2-DOF), y-axes (2-DOF) and z-axes (2-DOF). Subsequent validation work made important modifications to this structure as explained in section 3.4 using the model given in Figure 3.3. The changed features include the propeller motor limited pole placement controler which has been replaced by a hybrid PID-pole placement controller and the kalman estimator which is replaced by a Khalil high gain observer (HGO) which formed part of the designed error feedback observer regulator. The QUAV control diagram given in Figure 3.3 was implemented in Matlab/Simulink and has the following blocks: A signal generating block, a nonlinear backstepping controller in green, a motor reference velocity generating block in light blue, a motor control block in brown, a torque computation block in red, the QUAV sysytem

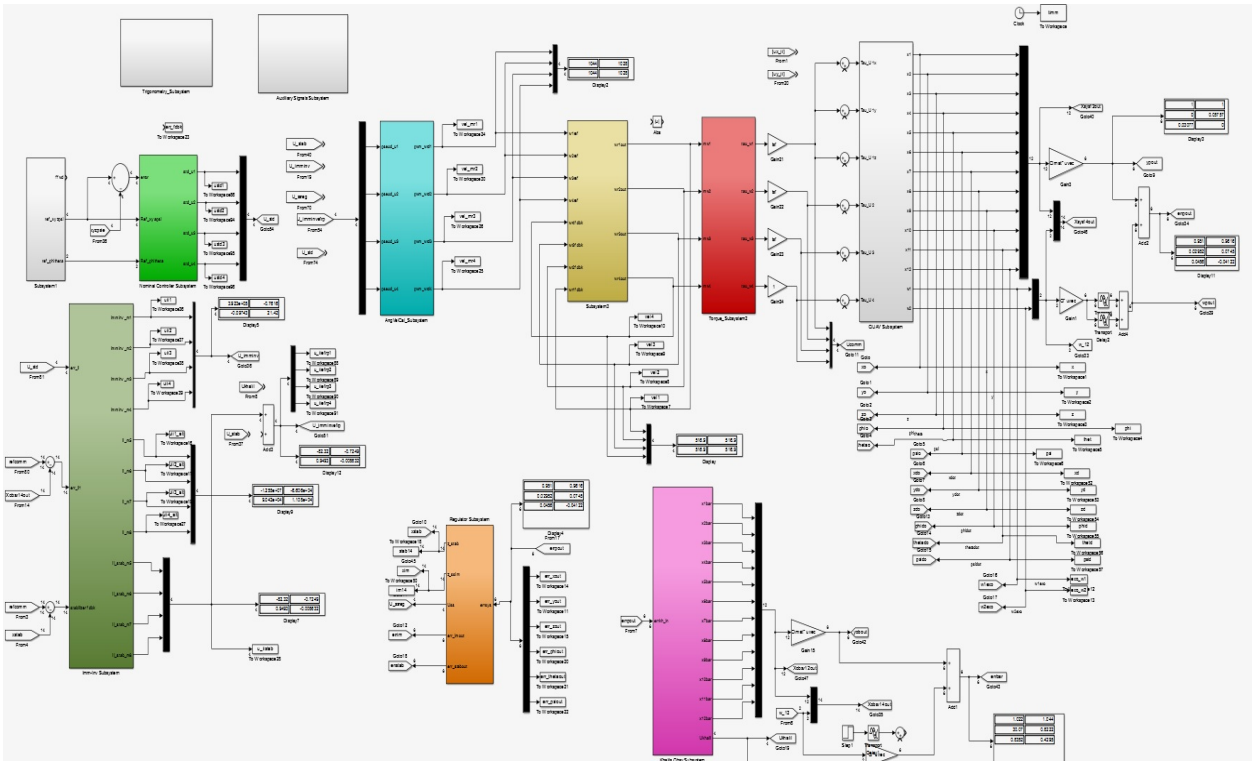


Figure 3.3: Control Block Diagram

in white, the high gain observer in Magenta, the output feedback regulator block in orange and the immersion invariance controller block in dark green.

However, the adopted dynamic model and parameters of the QUAV used in the remainder of this thesis was given by Ozbek *et al.*, (2015)

$$\begin{pmatrix} \dot{x}_1 \\ \dot{x}_2 \\ \dot{x}_3 \\ \dot{x}_4 \\ \dot{x}_5 \\ \dot{x}_6 \\ \dot{x}_7 \\ \dot{x}_8 \\ \dot{x}_9 \\ \dot{x}_{10} \\ \dot{x}_{11} \\ \dot{x}_{12} \end{pmatrix} = \begin{pmatrix} x_7 \\ x_8 \\ x_9 \\ x_{10} \\ x_{11} \\ x_{12} \\ (cx_4sx_5cx_6 + sx_4sx_6)\frac{u_1}{m} \\ (cx_4sx_5sx_6 - sx_4cx_6)\frac{u_1}{m} \\ -g + (cx_4cx_5)\frac{u_1}{m} \\ x_{11}x_{12}\frac{J_y - J_z}{J_x} - \frac{J_r}{J_x}x_{11}\Omega_r + \frac{L}{J_x}u_2 \\ x_{10}x_{12}\frac{J_z - J_x}{J_y} + \frac{J_r}{J_y}x_{10}\Omega_r + \frac{L}{J_y}u_3 \\ x_{10}x_{11}\frac{J_x - J_y}{J_z} + \frac{u_4}{J_z} \end{pmatrix} \tag{3.120}$$

With the state variables given by $x, y, z, \phi, \theta, \psi, \dot{x}, \dot{y}, \dot{z}, \dot{\phi}, \dot{\theta}, \dot{\psi} \equiv x_1, x_2, x_3, x_4, x_5, x_6, x_7, x_8, x_9, x_{10}, x_{11}, x_{12}$. The structure of this model is that of the standard input affine form $\dot{x} = Ax + Bu$. In developing the stabilizing controller, the error dynamic of the QUAV was deduced. Jeurgens, (2016), developed the following type of feedback stabilizing QUAV controller;

$$e_1 = x_r - x \tag{3.121}$$
$$e_2 = \dot{x}_r - \dot{x} + k_1 e_1 \tag{3.122}$$
$$e_3 = y_r - y \tag{3.123}$$
$$e_4 = \dot{y}_r - \dot{y} + k_3 e_3 \tag{3.124}$$
$$e_5 = z_r - z \tag{3.125}$$
$$e_6 = \dot{z}_r - \dot{z} + k_5 e_5 \tag{3.126}$$
$$e_7 = \phi_r - \phi \tag{3.127}$$
$$e_8 = \dot{\phi}_r - \dot{\phi} + k_7 e_7 \tag{3.128}$$
$$e_9 = \theta_r - \theta \tag{3.129}$$
$$e_{10} = \dot{\theta}_r - \dot{\theta} + k_9 e_9 \tag{3.130}$$
$$e_{11} = \psi_r - \psi \tag{3.131}$$
$$e_{12} = \dot{\psi}_r - \dot{\psi} + k_{11} e_{11} \tag{3.132}$$

The equations are given such that equations (3.121) - (3.122) represents the error and filtered error for the translational $x$-component of the system state. Similarly, equations (3.123)-(3.126) represents the error and filtered error for the translational $y$- and $z$-component of the state space vector. Equations (3.127) - (3.132) describe the error and filtered error signals for the $\phi$, $\theta$ and $\psi$ attitude components of the state space. The derivative of equations (3.121) - (3.132) generated a new set of equations;

$$\dot{e}_1 = e_2 - k_1 e_1 \tag{3.133}$$
$$\dot{e}_2 = \ddot{x}_r - \ddot{x} + k_1 \dot{e}_1 \tag{3.134}$$
$$\dot{e}_3 = e_4 - k_3 e_3 \tag{3.135}$$
$$\dot{e}_4 = \ddot{y}_r - \ddot{y} + k_3 \dot{e}_3 \tag{3.136}$$
$$\dot{e}_5 = e_6 - k_5 e_5 \tag{3.137}$$
$$\dot{e}_6 = \ddot{z}_r - \ddot{z} + k_5 \dot{e}_5 \tag{3.138}$$
$$\dot{e}_7 = e_8 - k_7 e_7 \tag{3.139}$$
$$\dot{e}_8 = \ddot{\phi}_r - \ddot{\phi} + k_7 \dot{e}_7 \tag{3.140}$$
$$\dot{e}_9 = e_{10} - k_9 e_9 \tag{3.141}$$
$$\dot{e}_{10} = \ddot{\theta}_r - \ddot{\theta} + k_9 \dot{e}_9 \tag{3.142}$$
$$\dot{e}_{11} = e_{12} - k_{11} e_{11} \tag{3.143}$$
$$\dot{e}_{12} = \ddot{\psi}_r - \ddot{\psi} + k_{11} \dot{e}_{11} \tag{3.144}$$

From equations (3.133)-(3.144), it can be clearly seen that the dynamic representing the input appears in the equations as the various second derivatives. Adopting a Lyapunov approach, a stabilizing controller was synthesized.

### 3.3.2 Stabilizing controller by Lyapunov approach

For the error dynamics represented by the states $e_1 \dots e_{12}$, a candidate Lyapunov function for the QUAV is given by the following positive definite quadratic relation

$$V_e = \frac{1}{2}\left(e_1^2 + e_2^2 + e_3^2 + e_4^2 + e_5^2 + e_6^2 + e_7^2 + e_8^2 + e_9^2 + e_{10}^2 + e_{11}^2 + e_{12}^2\right) \tag{3.145}$$

which on derivation gave

$$\dot{V}_e = e_1\dot{e}_1 + e_2\dot{e}_2 + e_3\dot{e}_3 + \ldots + e_{12}\dot{e}_{12} \tag{3.146}$$

that by lyapunov principle is required to be negative definite. After substitution of the equations (3.133)-(3.144) into equation (3.146), the various affine control inputs for the QUAV were obtained

in the nonlinear case as;

$$U_x = \frac{m}{cx_4sx_5cx_6 + sx_4sx_6}\left((1-k_1^2)e_1 - (k_1+k_2)e_2 + \ddot{x}_r\right) \tag{3.147}$$

$$U_y = \frac{m}{cx_4sx_5sx_6 - sx_4cx_6}\left((1-k_3^2)e_3 - (k_3+k_4)e_2 + \ddot{y}_r\right) \tag{3.148}$$

$$U_z = \frac{m}{cx_4cx_5}\left(g + (1-k_5^2)e_5 - (k_5+k_6)e_6 + \ddot{z}_r\right) \tag{3.149}$$

$$U_\phi = \frac{J_x}{L}\left(-x_{11}x_{12}I_{yzx} + \frac{J_r}{I_x}x_{11}\Omega_r + (1-k_7^2)e_7 - (k_7+k_8)e_8 + \ddot{\phi}_r\right) \tag{3.150}$$

$$U_\theta = \frac{J_y}{L}\left(-x_{10}x_{12}I_{zxy} + \frac{J_r}{I_y}x_{10}\Omega_r + (1-k_9^2)e_9 - (k_9+k_{10})e_{10} + \ddot{\theta}_r\right) \tag{3.151}$$

$$U_\psi = J_z\left(-x_{10}x_{11}I_{xyz} + (1-k_{11}^2)e_{11} - (k_{11}+k_{12})e_{12} + \ddot{\psi}_r\right) \tag{3.152}$$

and for the equivalent linear setup, the control signals were obtained as

$$U_x = * \tag{3.153}$$

$$U_y = * \tag{3.154}$$

$$U_z = m\left((1-k_5^2)e_5 - (k_5+k_6)e_6 + \ddot{z}_r\right) \tag{3.155}$$

$$U_\phi = \frac{J_x}{L}\left((1-k_7^2)e_7 - (k_7+k_8)e_8 + \ddot{\phi}_r\right) \tag{3.156}$$

$$U_\theta = \frac{J_y}{L}\left((1-k_9^2)e_9 - (k_9+k_{10})e_{10} + \ddot{\theta}_r\right) \tag{3.157}$$

$$U_\psi = J_z\left((1-k_{11}^2)e_{11} - (k_{11}+k_{12})e_{12} + \ddot{\psi}_r\right) \tag{3.158}$$

The variables $k_1, k_2, \ldots, k_{12}$, represent positive constant control parameters which must be carefully selected in order to derive the correct performance from the nonlinear controller. The nonlinear stabilizing controller will therefore be derived from the derivative of equation ( 3.145) as

$$\dot{V}_e = -k_1e_1^2 - k_2e_2^2 - k_3e_3^2 - k_4e_4^2 - k_5e_5^2 - k_6e_6^2 - k_7e_7^2 - k_8e_8^2 - k_9e_9^2 - k_{10}e_{10}^2 - k_{11}e_{11}^2 - k_{11}e_{11}^2 - k_{12}e_{12}^2 \tag{3.159}$$

In summary, since equation (3.145) is strictly positive definite and the derivative equation (3.159) is strictly negative definite, the origin of the controlled error dynamic is asymptotically stable

(Jeurgens, 2016). The control signals $U_x, U_y, U_z, U_\phi, U_\theta, U_\psi$, through this design also ensured the Lyapunov stability of the closed loop system(Ozbek *et al.*, 2015).

### 3.3.3 Revisiting output error feedback regulator design for the UAV

In order to study the behavior of the dynamic output error feedback regulator, the system of equations for the UAV will be repeated. Recall the dynamic model of the quadrotor given in equation (3.120). However, the model is augmented with a disturbance term on each equation which resulted into the general output feedback form given by $\dot{x} := Ax + Bu + Pw$ with $P$ being a random Gaussian noise matrix.

$$\begin{pmatrix} \dot{x}_1 \\ \dot{x}_2 \\ \dot{x}_3 \\ \dot{x}_4 \\ \dot{x}_5 \\ \dot{x}_6 \\ \dot{x}_7 \\ \dot{x}_8 \\ \dot{x}_9 \\ \dot{x}_{10} \\ \dot{x}_{11} \\ \dot{x}_{12} \end{pmatrix} = \begin{pmatrix} x_7 + P_1\omega \\ x_8 + P_2\omega \\ x_9 + P_3\omega \\ x_{10} + P_4\omega \\ x_{11} + P_5\omega \\ x_{12} + P_6\omega \\ (c\phi s\theta c\psi + s\phi s\psi)\frac{u_1}{m} + P_7\omega \\ (c\phi s\theta s\psi - s\phi c\psi)\frac{u_1}{m} + P_8\omega \\ -g + (c\phi c\theta)\frac{u_1}{m} + P_9\omega \\ \dot{\theta}\dot{\psi}\frac{J_y - J_z}{J_x} - \frac{J_r}{J_x}x_{11}\Omega_r + \frac{L}{J_x}u_2 + P_{10}\omega \\ \dot{\phi}\dot{\psi}\frac{J_z - J_x}{J_y} + \frac{J_r}{J_y}x_{10}\Omega_r + \frac{L}{J_y}u_3 + P_{11}\omega \\ \dot{\phi}\dot{\theta}\frac{J_x - J_y}{J_z} + \frac{u_4}{J_z} + P_{12}\omega \end{pmatrix} = \begin{pmatrix} x_7 + P_1\omega \\ x_8 + P_2\omega \\ x_9 + P_3\omega \\ x_{10} + P_4\omega \\ x_{11} + P_5\omega \\ x_{12} + P_6\omega \\ (cx_4sx_5cx_6 + sx_4sx_6)\frac{u_1}{m} + P_7\omega \\ (cx_4sx_5sx_6 - sx_4cx_6)\frac{u_1}{m} + P_8\omega \\ -g + (cx_4cx_5)\frac{u_1}{m} + P_9\omega \\ x_{11}x_{12}\frac{J_y - J_z}{J_x} - \frac{J_r}{J_x}x_{11}\Omega_r + \frac{L}{J_x}u_2 + P_{10}\omega \\ x_{10}x_{12}\frac{J_z - J_x}{J_y} + \frac{J_r}{J_y}x_{10}\Omega_r + \frac{L}{J_y}u_3 + P_{11}\omega \\ x_{10}x_{11}\frac{J_x - J_y}{J_z} + \frac{u_4}{J_z} + P_{12}\omega \end{pmatrix} \tag{3.160}$$

while the exosystem supplying the disturbance term is given by a Poisson stable oscillator that is unlike the constant exosystem described in section 3.1.6.2,

$$\dot{w}_1 = \alpha w_2 \tag{3.161}$$

$$\dot{w}_2 = -\alpha w_1 \tag{3.162}$$

Introduction of the following immersion maps was made to capture the relationship between the plant states and the exosystem; $x_1 := \pi_1(w), x_2 := \pi_2(w), x_3 := \pi_3(w), x_4 := \pi_4(w), x_5 := \pi_5(w), x_6 := \pi_6(w), x_7 := \pi_7(w), x_8 := \pi_8(w), x_9 := \pi_9(w), x_{10} := \pi_{10}(w), x_{11} := \pi_{11}(w), x_{12} :=$

$\pi_{12}(w), e_1 := x_1 - w_1, e_2 := x_2 - w_1, e_3 := x_3 - w_1, e_4 := x_4 - w_1, e_5 := x_5 - w_1, e_6 := x_6 - w_1.$

$$\begin{pmatrix} \dot{x}_1 \\ \dot{x}_2 \\ \dot{x}_3 \\ \dot{x}_4 \\ \dot{x}_5 \\ \dot{x}_6 \\ \dot{x}_7 \\ \dot{x}_8 \\ \dot{x}_9 \\ \dot{x}_{10} \\ \dot{x}_{11} \\ \dot{x}_{12} \\ e_1 \\ e_2 \\ e_3 \\ e_4 \\ e_5 \\ e_6 \end{pmatrix} = \begin{pmatrix} x_7 \\ x_8 \\ x_9 \\ x_{10} \\ x_{11} \\ x_{12} \\ (cx_4sx_5cx_6 + sx_4sx_6)\frac{u_1}{m} + \omega \\ (cx_4sx_5sx_6 - sx_4cx_6)\frac{u_1}{m} + \omega \\ -g + (cx_4cx_5)\frac{u_1}{m} + \omega \\ x_{11}x_{12}\frac{J_y - J_z}{J_x} - \frac{J_r}{J_x}x_{11}\Omega_r + \frac{L}{J_x}u_2 + \omega \\ x_{10}x_{12}\frac{J_z - J_x}{J_y} + \frac{J_r}{J_y}x_{10}\Omega_r + \frac{L}{J_y}u_3 + \omega \\ x_{10}x_{11}\frac{J_x - J_y}{J_z} + \frac{u_4}{J_z} + \omega \\ x_1 - w \\ x_2 - w \\ x_3 - w \\ x_4 - w \\ x_5 - w \\ x_6 - w \end{pmatrix} \tag{3.163}$$

Solution of the regulator equations (Castillo-Toledo *et al.*, 2004 ; Vaidyanathan, 2013) for the QUAV system in equation (3.163) employs the FBI relations of Isidori and Byrnes, (1990) given by equation (3.17).

For the nonlinear representation, the following set equality relations were obtained: $\pi_1 = \pi_2 = \pi_3 = \pi_4 = \pi_5 = \pi_6 = \alpha\omega_1$ while, $\pi_7 = \pi_8 = \pi_9 = \pi_{10} = \pi_{11} = \pi_{12} = \alpha\omega_2$. From which is derived the following relations

$$\frac{\partial \pi_1}{\partial w_1}\dot{w}_1 = \pi_7 \equiv \alpha w_2 \tag{3.164}$$

by a similar reasoning, $\pi_8 = \pi_9 = \pi_{10} = \pi_{11} = \pi_{12} \equiv \alpha w_2$. From which is also found

$$\frac{\partial \pi_7}{\partial w}\dot{w}_2 = -\alpha^2 w_1 \tag{3.165}$$

giving also by a similar reasoning the relations $\frac{\partial \pi_8}{\partial w}\dot{w}_2 = \frac{\partial \pi_9}{\partial w}\dot{w}_2 = \frac{\partial \pi_{10}}{\partial w}\dot{w}_2 = \frac{\partial \pi_{11}}{\partial w}\dot{w}_2 = \frac{\partial \pi_{12}}{\partial w}\dot{w}_2 \equiv -\alpha^2 w_1$. The following represent the steady state input which makes invariant the steady state zero

output manifold. They are also used to compute the generalized immersion (Castillo-Toledo *et al.*, 2004), here given for the case where $\alpha := 1$.

$$c_{1x}(w) = \frac{-m\alpha^2\omega_1}{c^2\omega_1 s\omega_1 + s^2\omega_1} \tag{3.166}$$

$$c_{1y}(w) = \frac{-m\alpha^2\omega_1}{s^2\omega_1 c\omega_1 - s\omega_1 c\omega_1} \tag{3.167}$$

$$c_{1z}(w) = \frac{m}{c^2\omega_1}(g - \alpha^2\omega_1) \tag{3.168}$$

$$c_2(w) = \frac{J_x}{L}(-\alpha^2\omega_2^2 Jyzx + \frac{J_r}{J_x}\alpha\omega_2\Omega_r - \alpha^2\omega_1) \tag{3.169}$$

$$c_3(w) = \frac{J_y}{L}(-\alpha^2\omega_2^2 Jzxy - \frac{J_r}{J_y}\alpha\omega_2\Omega_r - \alpha^2\omega_1) \tag{3.170}$$

$$c_4(w) = J_z(-\alpha^2\omega_2^2 Jxyz - \alpha^2\omega_1) \tag{3.171}$$

while for the linear QUAV model given by

$$\begin{pmatrix} \dot{x}_1 \\ \dot{x}_2 \\ \dot{x}_3 \\ \dot{x}_4 \\ \dot{x}_5 \\ \dot{x}_6 \\ \dot{x}_7 \\ \dot{x}_8 \\ \dot{x}_9 \\ \dot{x}_{10} \\ \dot{x}_{11} \\ \dot{x}_{12} \\ e_1 \\ e_2 \\ e_3 \\ e_4 \\ e_5 \\ e_6 \end{pmatrix} = \begin{pmatrix} x_7 \\ x_8 \\ x_9 \\ x_{10} \\ x_{11} \\ x_{12} \\ gx_5 \\ -gx_4 \\ \frac{\delta U_1}{m} \\ \frac{L}{I_x}U_2 \\ \frac{L}{I_y}U_3 \\ \frac{1}{I_z}U_4 \\ x_1 - w \\ x_2 - w \\ x_3 - w \\ x_4 - w \\ x_5 - w \\ x_6 - w \end{pmatrix} \tag{3.172}$$

using the linear analogue of the FBI regulator relations given in equation (3.19), the following

solution to the regulator equations were obtained:

$$c_1(w) = -m\alpha^2\omega_1 \tag{3.173}$$

$$c_2(w) = -\frac{I_x}{L}\alpha^2\omega_1 \tag{3.174}$$

$$c_3(w) = -\frac{I_y}{L}\alpha^2\omega_1 \tag{3.175}$$

$$c_4(w) = -\frac{1}{I_z}\alpha^2\omega_1 \tag{3.176}$$

from the nonlinear and linear expressions in equation (3.166) - (3.171) and (3.173)-(3.176), the necessary condition for regulation $\pi(0) = c(0) = 0$ was satisfied in every case. These expressions satisfying the conditions for the existence and computation of the required generalized immersions (Castillo-Toledo *et al.*, (2004)).

### 3.3.4 Computation of generalized immersion relations

The generalized immersion is necessary for proper formation of the error feedback regulator. The following used the input map $c(w)$ as an example of the immersion map development

1. let $c_1(w) = m\frac{\omega_2+g}{c^2\omega_1} =: z_1$. After repeated derivatives, the generalized immersion is obtained as a polynomial defined by the following general expressions;

$$\begin{pmatrix} c(w) \\ L_{s(w)}c(w) \\ L^2_{s(w)}c(w) \\ \vdots \\ L^{q-1}_{s(w)}c(w) \end{pmatrix} \tag{3.177}$$

equation ( 3.177) gives the Lie algebra formulation of such a map. It is required that the polynomial formed from this matrix map, be of the form

$$L^q_s c(w) + a_{q-1}L^{q-1}_s c(w) + \cdots + a_1 L_s c(w) + a_0 c(w) = 0 \tag{3.178}$$

$\forall \quad \omega \in W$, (Serrani, 2005).

2. An example of such derivation in practice is usually cumbersome and sometimes impossible to find according to Castillo-Toledo *et al.*, (2004). Insight is gained as to the development of such a generalized immersion from the following analysis made on the generalized input of equation (3.168):

$$c_1(w) = m\frac{\omega_2 + g}{c^2\omega_1} =: z_1 \tag{3.179}$$

$$z_2 = \dot{z_1} = \frac{m\omega_1 c^2\omega_1}{c^4\omega_1} + \frac{2\omega_2 s\omega_1 c\omega_1}{c^2\omega_1} z_1 \tag{3.180}$$

$$z_3 = \dot{z_2} = z_2 - \frac{2\omega_1 s\omega_1}{c\omega_1} z_1 + \frac{2\omega_2^2 s^2\omega_1}{c^2\omega_1} z_1 + 2\omega_2^2 \tag{3.181}$$

$$z_4 = \dot{z_3} = \frac{2\omega_2 s\omega_1}{c\omega_1} z_3 - z_2 - \frac{2\omega_2 s\omega_1}{c\omega_1} z_2 - 2\omega_1\omega_2 z_1 \tag{3.182}$$

$$... + \frac{4\omega_2^3 s\omega_1}{c\omega_1} z_1 - \frac{2\omega_1\omega_2 s^2\omega_1}{c^2\omega_1} z_1 - 4\omega_1\omega_2 - \frac{m\omega_1}{c^2\omega_1} - \frac{4\omega_2^3 s\omega_1}{c\omega_1} \tag{3.183}$$

Equation (3.180) - (3.183), gives an example of how such a computation was performed. The first two derivatives of the input functional for $c_1(w)$ were computed towards the acquisition of a generalized immersion map. Details and characteristics of this map can be found in Serrani (2005). The result is however significantly incomplete and not posible to find a closed form solution for a large system like the QUAV with trigonometric terms in the input map (Castillo-Toledo *et al.*, 2004).

3.

$$c_2(w) = J_x(\omega_2 - \omega_2^2 Jyzx - \omega_1) =: z_1 \tag{3.184}$$

$$\vdots \tag{3.185}$$

$$z4 = \dot{z_3} = (2Jw_2 + 2Jw_2^3/k - 8Jw_1w_2^2/k - 2w_1^2/k - 4Jw_1^3/k)z_1 \ldots \tag{3.186}$$

$$+2Jw_2z_2 \ldots \tag{3.187}$$

$$+(2Jw_2^3/k - 8Jw_1w_2^2/k - 2w_1^2/k - 4Jw_1^3/k)z_3 \tag{3.188}$$

note that here $k = (w_2^2 - 2w_1^2)$ and $J_2 = Jyzx$. Similarly, the immersion polynomial for

$c_3(w)$ and $c_4(w)$ are computable to give $J_2 = Jzxy$ and $J_4 = Jxyz$. This solution path is not followed here because of the identified difficulty in finding a closed form solution to the generalized immersion map.

4. Therefore according to Serrani, (2005), when a generalized immersion is impossible to find in building a regulator, a suitable approximation can be substituted for the stabilizer using Khalil's observer(Khalil and Praly, 2013).

### 3.3.5 Output error feedback control law

The QUAV is a known non-square and MIMO system. Also, the solvability of the output regulation problem was analysed and tested according to the already discussed principles in sections 2.2.1.2, 2.2.1.3, 2.2.2.3 and 3.1.6.3. The conditions described by Serrani (2005) were:

1. The existence of an observer regulator given by the nonlinear form in equation (2.21), with the linear equivalent given by equation (2.16). Such an observer in the expanded form is given by

$$\dot{\xi} \equiv \begin{pmatrix} \dot{\xi}_0 \\ \dot{\xi}_1 \end{pmatrix} = \left( \begin{pmatrix} A & P \\ 0 & S \end{pmatrix} - \begin{pmatrix} G_0 \\ G_1 \end{pmatrix} \begin{bmatrix} C & Q \end{bmatrix} \right) \begin{pmatrix} \xi_0 \\ \xi_1 \end{pmatrix} + \begin{pmatrix} G_0 \\ G_1 \end{pmatrix} e + \begin{pmatrix} B \\ 0 \end{pmatrix} u \qquad (3.189)$$

   is confirmed to exist and is called the internal model. The significance of the internal model is that, it represents the dynamics that are both stable and unstable while ensuring the asymptotic stability of the measurement system by the feedback gain $L = [G_0 \quad G_1]$.

2. Its existence is such that, all trajectories of the closed loop system $\dot{w}, \dot{x}, \dot{\xi}, e$,originating within a neighborhood of the origin are bounded and satisfies equation (2.8) for all uncertanties $\mu$ in an open neighborhood $P \subset R^p$ of $\mu = 0$.

3. That $\dot{\mu} = 0$, s.t. $\mu$ and $w$ are not separated but $\mu$ is incorporated into the exosystem state $w$.

4. Existence of this internal model or observer regulator implies that the observer regulator given by $\xi$ and $u$, locally exponentially stabilizes the origin of the unforced closed loop system given by

$$\begin{pmatrix} A & BH & P \\ GC & F & GQ \\ 0 & 0 & S \end{pmatrix} \equiv \begin{pmatrix} J & * \\ 0 & S \end{pmatrix} \tag{3.190}$$

with the following spectra defined $spec(J) \subset C^{-}$ and $spec(S) \subset C^{0}$ forming a center manifold at the origin that is defined by $M = (x, \xi, w) \in R^{n+v+d} : x = \pi(w), \xi = \sigma(w), w \in W$

5. the center manifold $M$ is invariant with respect to the flow of the closed-loop system

6. the invariant manifold defines a diffeomorphism with the exosystem

7. the nonlinear and linear regulator equations of Isidori and Byrnes (1990) given by equation (**??**) and equation (**??**) have a solution satisfying the various relations in both equations.

### 3.3.6 Immersion-invariance controller for the quadrotor

The developed immersion invariance stabilizing controller for the QUAV is described here. Firstly is presented the structure of the controller for the nonlinear QUAV system which can be recalled as given by equation (3.191).

$$\begin{pmatrix} \dot{x}_1 \\ \dot{x}_2 \\ \dot{x}_3 \\ \dot{x}_4 \\ \dot{x}_5 \\ \dot{x}_6 \\ \dot{x}_7 \\ \dot{x}_8 \\ \dot{x}_9 \\ \dot{x}_{10} \\ \dot{x}_{11} \\ \dot{x}_{12} \end{pmatrix} = \begin{pmatrix} x_7 \\ x_8 \\ x_9 \\ x_{10} \\ x_{11} \\ x_{12} \\ (cx_4sx_5cx_6 + sx_4sx_6)\frac{u_1}{m} \\ (cx_4sx_5sx_6 - sx_4cx_6)\frac{u_1}{m} \\ -g + (cx_4cx_5)\frac{u_1}{m} \\ x_{11}x_{12}\frac{J_y - J_z}{J_x} + \frac{u_2}{J_x} \\ x_{10}x_{12}\frac{J_z - J_x}{J_y} + \frac{u_3}{J_y} \\ x_{10}x_{11}\frac{J_x - J_y}{J_z} + \frac{u_4}{J_z} \end{pmatrix} \tag{3.191}$$

The total thrust and torques given by $u_1, \quad u_2, \quad u_3, \quad u_4$ in the equation (3.191) were nominally expressed by Ozbek *et al.*,(2015) as:

$$u_1 = b(\Omega_1^2 + \Omega_2^2 + \Omega_3^2 + \Omega_4^2) \tag{3.192}$$

$$u_2 = b(-\Omega_2^2 + \Omega_4^2) \tag{3.193}$$

$$u_3 = b(\Omega_1^2 - \Omega_3^2) \tag{3.194}$$

$$u_4 = d(-\Omega_1^2 + \Omega_2^2 - \Omega_3^2 + \Omega_4^2) \tag{3.195}$$

where another design modification made, ensured that the velocities $\Omega_i = \Omega_1, \Omega_2, \Omega_3, \Omega_4$ were replaced by their corresponding state angular velocity variables from the four DC motor actuators given by $x_{13}, x_{14}, x_{15}, x_{16}$ and $b, d$ being thrust and drag coefficients respectively.

### 3.3.7 Actuator model formulation

The introduction of the dynamic model for rotors or propellers resulted in the addition of four extra equations. While different models for the motor and propeller dynamic exist in literaure, two variants are explained here. The propeller model as given and described in Bouabdallah *et al.*, (2004a)

$$\dot{\Omega}_m = -\frac{1}{\tau}\Omega_m - \frac{d}{\eta r^3 J_t}\Omega_m^2 + \frac{1}{K_m \tau}u \tag{3.196}$$

with $1/\tau = K_m^2/RJ_t$, $\Omega_m$ is the rotor angular velocity of the ith rotor, $\eta$ is the gear box efficiency , $K_m$ is the torque constant, $R$, is the internal resistance and $J_t$, the total inertia. For a more complete actuator model, this work adopted the example in Sugawara and Shimada, (2017);

$$V_m = R_m i_m + L_a \frac{di}{dt} + K_e w_m \tag{3.197}$$

$$\tau_m = K_T i_m \tag{3.198}$$

$$\tau_m = J_m \frac{dw_m}{dt} + C_m w_m + \tau_l \tag{3.199}$$

$$\tau_l = J_r \frac{dw_r}{dt} + C_r w_r + \frac{b}{4n} \rho w_m^2 R^4 c \left( \frac{d}{2} + a\phi_t(\theta_t - \phi_t) \right) \tag{3.200}$$

Let the constants $b, n, \rho, R, c, d, a, \phi_t, \theta_t$ be represented by $P_{prop}$. Then the actuator equation can be described by

$$V_m = R_m i_m + L_a \frac{di}{dt} + K_e w_m \tag{3.201}$$

$$\tau_m = K_T i_m \tag{3.202}$$

$$\tau_m = J_m \frac{dw_m}{dt} + C_m w_m + \tau_l \tag{3.203}$$

$$\tau_l = J_r \frac{dw_r}{dt} + C_r w_r + P_{prop} w_m^2 \tag{3.204}$$

in which the last equation is nonlinear in $w_m$. Linearization by Taylors expansion and simplifying the equation gives

$$V_m = R_m i_m + L_a \frac{di}{dt} + K_e w_m \tag{3.205}$$

$$\tau_m = K_T i_m \tag{3.206}$$

$$\tau_m = J_m \frac{dw_m}{dt} + C_m w_m + \tau_l \tag{3.207}$$

$$\tau_l = J_r \frac{dw_r}{dt} + C_r w_r \tag{3.208}$$

from which the following derivations are made $i = \frac{1}{K_T}(J_m + \frac{J_r}{n})\frac{dw_m}{dt} + \frac{1}{K_T}(C_m + \frac{C_r}{n})w_m$ from which we deduce the derivative of $i$ for backward substitution and replacement of the $i$ variable in

equation ( 3.205). The resulting actuator equation now becomes

$$V_m = \frac{R_m}{K_T}(J_m + \frac{J_r}{n})\dot{w}_m + \frac{R_m}{K_T}(C_m + \frac{C_r}{n})w_m + \frac{L_a}{K_T}(J_m + \frac{J_r}{n})\ddot{w}_m + \frac{L_a}{K_T}(C_m + \frac{C_r}{n})\dot{w}_m + K_e w_m \tag{3.209}$$

from which convenient constants are introduced to simplify the look of the equation

$$V_m = K_1\dot{w}_m + K_2 w_m + K_3\ddot{w}_m + K_4\dot{w}_m + K_e w_m \tag{3.210}$$

which by Laplace transform yields the transfer function equivalent

$$V_m = K_3\ddot{w}_m + K_1\dot{w}_m + K_4\dot{w}_m + K_2 w_m + K_e w_m \tag{3.211}$$

$$V_m = K_3\ddot{w}_m + (K_1 + K_4)\dot{w}_m + (K_2 + K_e)w_m \tag{3.212}$$

$$V_m(s) = s^2 K_3 W_m(s) + s(K_1 + K_4)W_m(s) + (K_2 + K_e)W_m(s) \tag{3.213}$$

$$\frac{W_m(s)}{V_m(s)} = \frac{1}{s^2 K_3 + s(K_1 + K_4) + (K_2 + K_e)} \tag{3.214}$$

Another assumption could be made, taking into consideration the small size of the actuators providing the needed thrust vectors and the negligible electrical inductance parameter. Equation (3.209), is replaced by

$$V_m = \frac{R_m}{K_T}(J_m + \frac{J_r}{n})\dot{w}_m + \frac{R_m}{K_T}(C_m + \frac{C_r}{n})w_m + K_e w_m \tag{3.215}$$

which led to the form

$$V_m = K_1\dot{w}_m + K_2 w_m + K_e w_m \tag{3.216}$$

and finally,

$$V_m = K_1\dot{w}_m + K_2 w_m + K_e w_m \tag{3.217}$$

$$V_m(s) = sK_1 W_m(s) + (K_2 + K_e)W_m(s) \tag{3.218}$$

$$V_m(s) = \left(sK_1 + (K_2 + K_e)\right) W_m(s) \tag{3.219}$$

$$\frac{W_m(s)}{V_m(s)} = \frac{1}{sK_1 + (K_2 + K_e)} \tag{3.220}$$

### 3.3.8 Augmented system model

Representing the new system with actuator dynamics considered gives the augmented UAV dynamic system

$$\begin{pmatrix} \dot{x}_1 \\ \dot{x}_2 \\ \dot{x}_3 \\ \dot{x}_4 \\ \dot{x}_5 \\ \dot{x}_6 \\ \dot{x}_7 \\ \dot{x}_8 \\ \dot{x}_9 \\ \dot{x}_{10} \\ \dot{x}_{11} \\ \dot{x}_{12} \\ \dot{x}_{13} \\ \dot{x}_{14} \\ \dot{x}_{15} \\ \dot{x}_{16} \end{pmatrix} = \begin{pmatrix} x_7 \\ x_8 \\ x_9 \\ x_{10} \\ x_{11} \\ x_{12} \\ (cx_4 sx_5 cx_6 + sx_4 sx_6)\frac{u_1}{m} \\ (cx_4 sx_5 sx_6 - sx_4 cx_6)\frac{u_1}{m} \\ -g + (cx_4 cx_5)\frac{u_1}{m} \\ x_{11}x_{12}\frac{J_y - J_z}{J_x} + \frac{u_2}{J_x} \\ x_{10}x_{12}\frac{J_z - J_x}{J_y} + \frac{u_3}{J_y} \\ x_{10}x_{11}\frac{J_x - J_y}{J_z} + \frac{u_4}{J_z} \\ -\frac{1}{\tau}x_{13} - \frac{d}{\eta r^3 J_t}x_{13}^2 + \frac{1}{K_m \tau}V1 \\ -\frac{1}{\tau}x_{14} - \frac{d}{\eta r^3 J_t}x_{14}^2 + \frac{1}{K_m \tau}V2 \\ -\frac{1}{\tau}x_{15} - \frac{d}{\eta r^3 J_t}x_{15}^2 + \frac{1}{K_m \tau}V3 \\ -\frac{1}{\tau}x_{16} - \frac{d}{\eta r^3 J_t}x_{16}^2 + \frac{1}{K_m \tau}V4 \end{pmatrix} \tag{3.221}$$

these modifications gave rise to the set of augmented linear equations re-written as

$$\begin{pmatrix} \dot{x}_1 \\ \dot{x}_2 \\ \dot{x}_3 \\ \dot{x}_4 \\ \dot{x}_5 \\ \dot{x}_6 \\ \dot{x}_7 \\ \dot{x}_8 \\ \dot{x}_9 \\ \dot{x}_{10} \\ \dot{x}_{11} \\ \dot{x}_{12} \\ \dot{x}_{13} \\ \dot{x}_{14} \\ \dot{x}_{15} \\ \dot{x}_{16} \end{pmatrix} = \begin{pmatrix} x_7 \\ x_8 \\ x_9 \\ x_{10} \\ x_{11} \\ -x_{12} \\ (cx_4sx_5cx_6 + sx_4sx_6)\frac{b}{m}(x_{13}^2 + x_{14}^2 + x_{15}^2 + x_{16}^2) \\ (cx_4sx_5sx_6 - sx_4cx_6)\frac{b}{m}(x_{13}^2 + x_{14}^2 + x_{15}^2 + x_{16}^2) \\ -g + (cx_4cx_5)\frac{b}{m}(x_{13}^2 + x_{14}^2 + x_{15}^2 + x_{16}^2) \\ x_{11}x_{12}\frac{J_y - J_z}{J_x} + \frac{b}{J_x}(-x_{14}^2 + x_{16}^2) \\ x_{10}x_{12}\frac{J_z - J_x}{J_y} + \frac{b}{J_y}(x_{13}^2 - x_{15}^2) \\ x_{10}x_{11}\frac{J_x - J_y}{J_z} + \frac{d}{J_z}(-x_{13}^2 + x_{14}^2 - x_{15}^2 + x_{16}^2) \\ -\frac{1}{\tau}x_{13} - \frac{d}{\eta r^3 J_t}x_{13}^2 + \frac{1}{K_m \tau}V1 \\ -\frac{1}{\tau}x_{14} - \frac{d}{\eta r^3 J_t}x_{14}^2 + \frac{1}{K_m \tau}V2 \\ -\frac{1}{\tau}x_{15} - \frac{d}{\eta r^3 J_t}x_{15}^2 + \frac{1}{K_m \tau}V3 \\ -\frac{1}{\tau}x_{16} - \frac{d}{\eta r^3 J_t}x_{16}^2 + \frac{1}{K_m \tau}V4 \end{pmatrix} \tag{3.222}$$

### 3.3.9 Selection of target dynamic for the quadrotor

The target dynamic system is now selected after the already established map given by$x_1 = \pi(\xi_1), x_2 = \pi(\xi_2), x_3 = \pi(\xi_3), x_4 = \pi(\xi_4), x_5 = \pi(\xi_5), x_6 = \pi(\xi_6), x_7 = \pi(\xi_7), x_8 = \pi(\xi_8), x_9 = \pi(\xi_9), x_{10} = \pi(\xi_{10}), x_{11} = \pi(\xi_{11}), x_{12} = \pi(\xi_{12}), x_{13} = \pi(w_1), x_{14} = \pi(w_2), x_{15} = \pi(w_3), x_{16} = \pi(w_4)$. The target system was derived from the derivative of these maps which resulted in:

$$\begin{pmatrix} \dot{\xi}_1 \\ \dot{\xi}_2 \\ \dot{\xi}_3 \\ \dot{\xi}_4 \\ \dot{\xi}_5 \\ \dot{\xi}_6 \\ \dot{\xi}_7 \\ \dot{\xi}_8 \\ \dot{\xi}_9 \\ \dot{\xi}_{10} \\ \dot{\xi}_{11} \\ \dot{\xi}_{12} \end{pmatrix} = \begin{pmatrix} \xi_7 \\ \xi_8 \\ \xi_9 \\ \xi_{10} \\ \xi_{11} \\ -\xi_{12} \\ (c_4s_5c_6 + s_4s_6)\frac{b}{m}(\Omega_1^2 + \Omega_2^2 + \Omega_3^2 + \Omega_4^2) \\ (c_4s_5s_6 - s_4c_6)\frac{b}{m}(\Omega_1^2 + \Omega_2^2 + \Omega_3^2 + \Omega_4^2) \\ -g + (c_4c_5)\frac{b}{m}(\Omega_1^2 + \Omega_2^2 + \Omega_3^2 + \Omega_4^2) \\ \xi_{11}\xi_{12}\frac{J_y - J_z}{J_x} + \frac{b}{J_x}(-\Omega_2^2 + \Omega_4^2) \\ \xi_{10}\xi_{12}\frac{J_z - J_x}{J_y} + \frac{b}{J_y}(\Omega_1^2 - \Omega_3^2) \\ \xi_{10}\xi_{11}\frac{J_x - J_y}{J_z} + \frac{d}{J_z}(-\Omega_1^2 + \Omega_2^2 - \Omega_3^2 + \Omega_4^2) \end{pmatrix} \tag{3.223}$$

In equation (3.223), the state variables $x_{13}, x_{14}, x_{15}, x_{16}$ were replaced by $\Omega_1 + \Omega_2 + \Omega_3 + \Omega_4$.

### 3.3.10 UAV state feedback controller design for immersion invariance

The immersion condition used equation (**??**) to confirm the validity of the selected target system. While section 3.3.9 briefly touched on the derivation of the immersion maps, a detailed look at how the immersions were obtained has been presented for clarity in section C.2 of the appendix. After some calculation and subsequent inspection, the selected choice of maps were seen to properly match the target equations selected earlier. The design of the state feedback was made with the condition to be satisfied being the Hurwitz stability criterion of $A - BF$. Where $A$ is the system transmission matrix, $B$ is the input matrix and $F$ the feedback gain vector or matrix. The selected pole locations for the system feedback gain were -19 ; -17 ; -13 ; -12 ; -14 ; -10 ; -8 ; -16 ; -11 ; -18 ; -9 ; -7. $C_i(s)$, represents the controls that render the manifold invariant while the off-manifold control, given by $\psi(x, z)$, is the sought after control law that is developed subsequently.

For the development of the off manifold control law, a set of suitable manifolds were selected, as informed by the immersion invariance condition and FBI equations given in equations (2.42)-(2.45). These zero dynamics manifolds are defined as

$$z_{13} = \phi_1(x) = x_{13} - \Omega_1 \equiv 0 \tag{3.224}$$

$$z_{14} = \phi_2(x) = x_{14} - \Omega_2 \equiv 0 \tag{3.225}$$

$$z_{15} = \phi_3(x) = x_{15} - \Omega_3 \equiv 0 \tag{3.226}$$

$$z_{16} = \phi_4(x) = x_{16} - \Omega_4 \equiv 0 \tag{3.227}$$

Equations (3.224)-(3.227), captured the fast actuator subsystem which supplied the currents for the four actuators. These currents provided the needed torques to drive the UAV towards its control target. With subscripts on the variables ignored, the design of the off-manifold control law is presented here for the first UAV actuator dynamic system given by equation (3.224).

$$z \equiv \phi(x) = x - w \tag{3.228}$$

$$\dot{z} \equiv \frac{\partial \phi(x)}{\partial x}.\frac{dx}{dt} \equiv \dot{x} - \dot{w} \tag{3.229}$$

$$\dot{z} = \dot{x}_{13} - \dot{w}_1 \tag{3.230}$$

$$\dot{z} = -\frac{1}{\tau}x_{13} - \frac{d}{\eta r^3 J_t}x_{13}^2 + \frac{1}{K_m \tau}V1 - \dot{w}_1 \tag{3.231}$$

where $\dot{x}$ in equation (3.234) has been replaced by the state variable $\dot{x_{13}}$ from equation (3.222). Furthermore, $V_1$ was substituted for $\psi(x, z)$

$$\dot{z} = -\frac{1}{\tau}x_{13} - \frac{d}{\eta r^3 J_t}x_{13}^2 + \frac{1}{K_m \tau}\phi(x, z) - \dot{w}_1 \tag{3.232}$$

$$\frac{\psi(x, z)}{K_m \tau} = \dot{z} + \frac{1}{\tau}x_{13} + \frac{d}{\eta r^3 J_t}x_{13}^2 + \dot{w}_1 \tag{3.233}$$

$$\frac{\psi(x, z)}{K_m} = \tau\dot{z} + x_{13} + \frac{d\tau}{\eta r^3 J_t}x_{13}^2 + \tau\dot{w}_1 \tag{3.234}$$

setting $\dot{z} = -\frac{1}{\tau}z$ and $w_1 = x_{13} - z$, the immersion invariance controller becomes

$$\frac{\psi(x, z)}{K_m} = -z + x_{13} + \frac{d\tau}{\eta r^3 J_t}x_{13}^2 + \tau\dot{w}_1 \tag{3.235}$$

$$\frac{\psi(x, z)}{K_m} = -z + x_{13} + \frac{d\tau}{\eta r^3 J_t}x_{13}^2 + \tau\dot{w}_1 \tag{3.236}$$

$$\psi_1(x, z) = K_m w_1(x) + \frac{K_m d\tau}{\eta r^3 J_t}x_{13}^2 + K_m\tau\dot{w}_1 \tag{3.237}$$

$$\psi_2(x, z) = K_m w_2(x) + \frac{K_m d\tau}{\eta r^3 J_t}x_{14}^2 + K_m\tau\dot{w}_2 \tag{3.238}$$

$$\psi_3(x, z) = K_m w_3(x) + \frac{K_m d\tau}{\eta r^3 J_t}x_{15}^2 + K_m\tau\dot{w}_3 \tag{3.239}$$

$$\psi_4(x, z) = K_m w_4(x) + \frac{K_m d\tau}{\eta r^3 J_t}x_{16}^2 + K_m\tau\dot{w}_4 \tag{3.240}$$

Equation (3.237)-(3.240) properly designed formed the stabilizing nonlinear robust immersion invariance state feedback-based controller for the QUAV actuation system. It would be recalled from equation (3.224), that $z = x - w$. Further reparameterizing the system dynamic model in equation (3.222) with $\eta = x - w$. The dynamic equation of the QUAV can then be represented as

$$\begin{pmatrix} \dot{x}_1 \\ \dot{x}_2 \\ \dot{x}_3 \\ \dot{x}_4 \\ \dot{x}_5 \\ \dot{x}_6 \\ \dot{x}_7 \\ \dot{x}_8 \\ \dot{x}_9 \\ \dot{x}_{10} \\ \dot{x}_{11} \\ \dot{x}_{12} \\ \dot{x}_{13} \\ \dot{x}_{14} \\ \dot{x}_{15} \\ \dot{x}_{16} \\ \dot{z} \end{pmatrix} = \begin{pmatrix} x_7 \\ x_8 \\ x_9 \\ x_{10} \\ x_{11} \\ -x_{12} \\ (cx_4sx_5cx_6 + sx_4sx_6)\frac{b}{m}(x_{13}^2 + x_{14}^2 + x_{15}^2 + x_{16}^2) \\ (cx_4sx_5sx_6 - sx_4cx_6)\frac{b}{m}(x_{13}^2 + x_{14}^2 + x_{15}^2 + x_{16}^2) \\ -g + (cx_4cx_5)\frac{b}{m}(x_{13}^2 + x_{14}^2 + x_{15}^2 + x_{16}^2) \\ x_{11}x_{12}\frac{J_y - J_z}{J_x} + \frac{b}{J_x}(-x_{14}^2 + x_{16}^2) \\ x_{10}x_{12}\frac{J_z - J_x}{J_y} + \frac{b}{J_y}(x_{13}^2 - x_{15}^2) \\ x_{10}x_{11}\frac{J_x - J_y}{J_z} + \frac{d}{J_z}(-x_{13}^2 + x_{14}^2 - x_{15}^2 + x_{16}^2) \\ -\frac{1}{\tau}z - \dot{w}_1 \\ -\frac{1}{\tau}z - \dot{w}_2 \\ -\frac{1}{\tau}z - \dot{w}_3 \\ -\frac{1}{\tau}z - \dot{w}_4 \\ -\frac{1}{\tau}z \end{pmatrix} \tag{3.241}$$

and in new coordinates $(z, \eta, x_1, x_2, x_3, x_4, x_5, x_6, x_7, x_8, x_9, x_{10}, x_{11}, x_{12})$

$$\begin{pmatrix} \dot{x}_1 \\ \dot{x}_2 \\ \dot{x}_3 \\ \dot{x}_4 \\ \dot{x}_5 \\ \dot{x}_6 \\ \dot{x}_7 \\ \dot{x}_8 \\ \dot{x}_9 \\ \dot{x}_{10} \\ \dot{x}_{11} \\ \dot{x}_{12} \\ \dot{z}_i \\ \dot{\eta}_i \end{pmatrix} = \begin{pmatrix} x_7 \\ x_8 \\ x_9 \\ x_{10} \\ x_{11} \\ x_{12} \\ (c_4s_5c_6 + s_4s_6)\, b/m\, (4\eta^2 + 2\eta(x_{13} + x_{14} + x_{15} + x_{16}) + (x_{13}^2 + x_{14}^2 + x_{15}^2 + x_{16}^2)) \\ (c_4s_5s_6 - s_4c_6)\, b/m\, (4\eta^2 + 2\eta(x_{13} + x_{14} + x_{15} + x_{16}) + (x_{13}^2 + x_{14}^2 + x_{15}^2 + x_{16}^2)) \\ -g + (c_4c_5)\, b/m\, (4\eta^2 + 2\eta(x_{13} + x_{14} + x_{15} + x_{16}) + (x_{13}^2 + x_{14}^2 + x_{15}^2 + x_{16}^2)) \\ x_{11}x_{12}Jyzx + Lb/Jx\, (2\eta(x_{16} - x_{14}) - x_{14}^2 + x_{16}^2) \\ x_{10}x_{12}Jzxy + Lb/Jy\, (2\eta(x_{15} - x_{13}) - x_{13}^2 + x_{15}^2) \\ x_{10}x_{11}Jxyz + d/Jz\, (2\eta(-x_{13} + x_{14} - x_{15} + x_{16}) + (-x_{13}^2 + x_{14}^2 - x_{15}^2 + x_{16}^2)) \\ -\frac{1}{\tau}z_i \\ -\frac{1}{\zeta\tau}z_i \end{pmatrix} \tag{3.242}$$

$w_1 = x_{13} - z$, thereby giving the final equation for the off-manifold control law as

$$\psi(x, z) = K_m w_1 + \frac{K_m d\tau}{\eta r^3 J_t} x_{13}^2 + K_m \tau \dot{w}_1 \tag{3.243}$$

with $\tau = RJ_t/K_m^2$. Equation (3.243), is the control law that steers the states of the system on the prescribed or selected manifold as forced by the actuator dynamic coupled with the dynamic of the system. It ensures all the off-manifold state variables are brought back to this surface or zeroed. This control law is state feedback-based, such that the variable $w_1$ is a state feedback based controller which when properly expressed was;

$$w_i(x_j) = -Kx_j \tag{3.244}$$

with $i \in R^{1-12}$ and $j \in R^{1-4}$. $x_j$ is a function of all the other state variables in the system that must be bounded by the designed feedback control law that has been designed to keep all the system trajectories bounded. Equation (3.244), written otherwise can be represented in terms of the error feedback,

$$w_i(x_j) = -K(x_{rj} - x_j) \equiv -Ke_j \tag{3.245}$$

the variables $x_{rj}$ and $x_j$, are the reference and feedback state respectively while $K$ represents a positive constant control parameter which must be designed for and carefully chosen as explained in section 3.3.2. The other control variables $w_{i=2...4}$ are similarly derived and form the structure of equation (3.242). While the control signals were designed independent of Lyapunov's method, Lyapunov's approach was applied to confirm the stability of the controller. System boundedness of the dynamic model was also studied.

### 3.3.11 Proof of boundedness and stability of immersion invariance control law

The boundedness and stability of the immersion invariance control law is proved by applying tools from differential calculus. It is well established that given $\dot{x} = Ax$, a solution to this differential

equation is obtained as $x = \exp^{Ax}$. Similarly, with $\dot{x} = -Ax$, a possible solution becomes $x = \exp^{-Ax}$. While $x = \exp^{Ax}$, represents an exponential growth curve, $x = \exp^{-Ax}$ represents an exponential decay curve which is desired in a stable system. This decay was forced by the introduction of $z$ and $\eta$ dynamic equations found in equation (3.242). Regulating the speed of decay was the magnitude of the term $\tau$ given in

$$\dot{z}_i = -\frac{1}{\tau} z_i \tag{3.246}$$

$$\dot{\eta}_i = -\frac{1}{\tau} z_i \tag{3.247}$$

The control manifold formed by $w_1 = x_{13} - z$ when properly designed guarantees that all trajectories of the system

$$\dot{z} = \frac{\partial \phi}{\partial x}[f(x) + g(x)\psi(x, z)] \equiv \frac{\partial \phi}{\partial x}[f(x) + g(x)\psi(x, \phi(x))] \tag{3.248}$$

$$\dot{x} = f(x) + g(x)\psi(x, z) \tag{3.249}$$

are bounded and in equations (3.247)- (3.249),

$$\lim_{t \to \infty} z(t) = 0 \tag{3.250}$$

is satisfied. The boundedness of these dynamic equations is backpropagated to the rest of the dynamic system and forms an adaptive tool for self regulating the behavior of the states of the QUAV. It also implies (Astolfi & Ortega, 2003), that $x^*$, is a globally asymptotically stable equilibrium equation (4.250). Since the immersion invariance controller is based on state feedback, stability of the designed controller was ascertained using Lyapunov techniques on the state feedback controller in equation (3.244). Similar stabilizing design and careful control parameter selection such as described in section 3.3.1, ensured the resultant immersion invariance control law was stabilizing.

### 3.3.12 Synthesis of immersion invariance output feedback observer-based control

The description of the developed controller firstly derived from the synthesis of a stabilizing output error feedback observer. The output error is derived from the expression $e = Cx + Qw$. This error is required to be regulated to zero by the designed observer regulator/controller. The structure of the standard regulator was given as

$$\dot{\xi} = G_1\xi + G_2 e; u = K\xi \tag{3.251}$$

where in equation (3.251), $\xi \in R^{n+s}$ and s.t. $v = (n+s)$ (Chen, Z. & Huang, J., 2004). From work on nonlinear regulators by Brynes and Isidori (1990), (Huang, J. & Chen, Z. 2004), the following robust regulator was proposed by Serrani, (2005)

$$\dot{\xi}_0 = \phi(\xi_0) + \Theta e \equiv \Phi\xi_0 + \Theta e \tag{3.252}$$

$$\dot{\xi}_1 = L\xi_1 + Me \tag{3.253}$$

$$u = \gamma(\xi_0) + N\xi_1 \tag{3.254}$$

in equations (3.252)-(3.254), $\phi(\xi_0)$ or its linearized equivalent $\Phi\xi_0$ makes up the immersion map that must be found with characteristics described as continuously differentiable and invertible. . . otherwise referred to as a nonlinear diffeomorphism. $L$ and $M$ are analogues of $G_1$ and $G_2$ in equation (3.251).

The form of the regulator in equation (3.251) has been completely designed for in this work with the results showing that the regulator is stabilizing from whatever start condition. However for tracking experiments, further sufficiency results are demanded from the regulator so that active rejection of the exosystem disturbance was ensured. This led to the design of the second regulator in equations (3.252) - (3.254). This regulator was found to be difficult to completely define in practice especially for large systems and systems with transcedental or trigonometric terms in their input function maps (Serrani, 2005; Castillo-Toledo *et al.*, 2004). The difficulty resides in the search for

a suitable immersion function or generalized immersion that forms a suitably diffeomorphism of the exosystem input. Therefore this work innovated, using an immersion invariance controller in place of the immersion functional map $\Phi(\xi_0)$ of equation (3.252). This was how the immersion invariance error feedback regulator was constructed.

Next, the state output from the observer was used as feedback to the immersion invariance controller. This immersion invariance controller being a state feedback controller, took for input the feedback error derived according to equations (3.121) - (3.132). However the equation is slightly modified according to the rotor actuator terms whch occur in the immersion invariance controller as given by equation (3.237). The boundedness of the QUAV dynamic model was investigated using the model in equation (3.242). This boundedness which was explained in section 3.3.11, has a direct dependence on the fast decay of the $z$ and $\eta$ dynamic of equation (3.242). The boundedness and stability of the immersion invariance feedback control law was proved by application of Lyapunov techniques and further confirmation tests carried out with the aid of Lasalles invariance principle. Graphical proof is provided in the results section to show the profile of the derived immersion invariance error feedback control signals.

### 3.3.13 Design of the error feedback observer

In theory, a complete solution of the error feedback problem exists if a suitable immersion map $\Phi(\omega)$, can be found for the exosystem (Serrani, (2005);Castillo-Toledo *et al.*, (2004) ). However in practice finding this immersion map is a difficult and cumbersome task especially for large systems and systems with trigonometric or transcedental terms (Serrani, 2005; Castillo-Toledo *et al.*, 2004). Avoiding this obstruction requires the setting up of a suitable device for estimation of the generated feedback error signals. This device is an observer, examples of which abound in literature e.g. Hammouri-Gauthier-Kupka, Khalil's high gain observer (HGO), . Based on past

works, this work has selected Khalil's HGO for estimation of the error state variables. The observer regulator described in section 3.1.1.5 has the general structure given in Figure 3.4. The design of

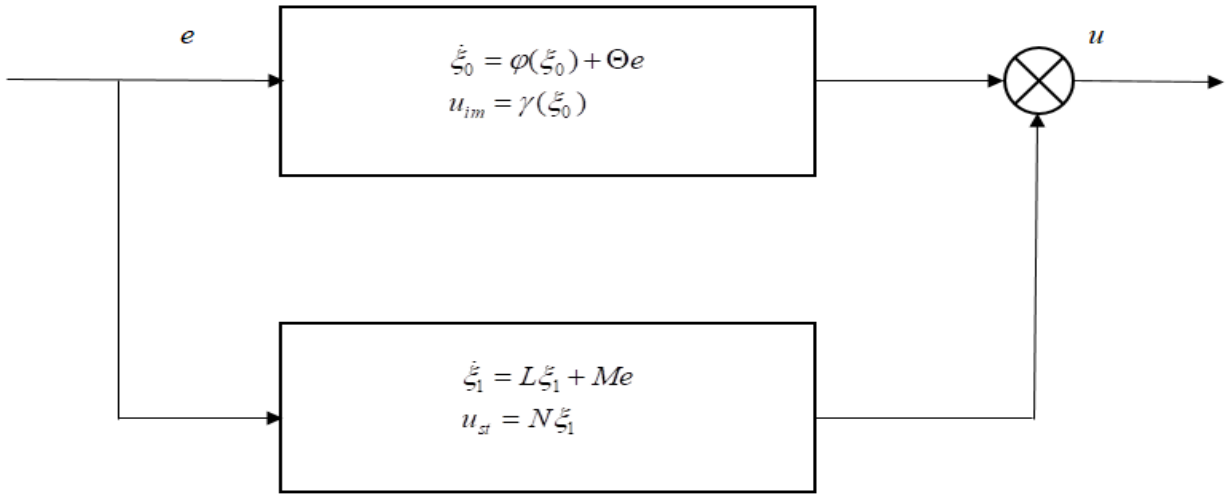



Figure 3.4: Composite Regulator Controller Schematic (Serrani, 2005)

the regulator takes the form of a composite controller with a stabilizer shown in the lower block and an internal model as the upper block. Equation (3.251) gave a complete definition of the stabilizer. The internal model was designed as Khalil's observer with an immersion invariance control law.

*3.3.13.1 Design of the feedback observer*

The QUAV model in equation (3.163), was considered and adopted for the design of the Khalil-type HGO (Khalil and Praly, 2013) developed here. The observer model for equation (3.163), has the form

$$\begin{pmatrix} \dot{\hat{x}}_1 \\ \dot{\hat{x}}_2 \\ \dot{\hat{x}}_3 \\ \dot{\hat{x}}_4 \\ \dot{\hat{x}}_5 \\ \dot{\hat{x}}_6 \\ \dot{\hat{x}}_7 \\ \dot{\hat{x}}_8 \\ \dot{\hat{x}}_9 \\ \dot{\hat{x}}_{10} \\ \dot{\hat{x}}_{11} \\ \dot{\hat{x}}_{12} \end{pmatrix} = \begin{pmatrix} \hat{x}_7 + P_1\omega + h_1(y - \hat{x}) \\ \hat{x}_8 + P_2\omega + h_2(y - \hat{x}) \\ \hat{x}_9 + P_3\omega + h_3(y - \hat{x}) \\ \hat{x}_{10} + P_4\omega + h_4(y - \hat{x}) \\ \hat{x}_{11} + P_5\omega + h_5(y - \hat{x}) \\ \hat{x}_{12} + P_6\omega + h_6(y - \hat{x}) \\ (c\hat{x}_4 s\hat{x}_5 c\hat{x}_6 + s\hat{x}_4 s\hat{x}_6)\frac{u_1}{m} + P_7\omega + h_7(y - \hat{x}) \\ (c\hat{x}_4 s\hat{x}_5 s\hat{x}_6 + s\hat{x}_4 c\hat{x}_6)\frac{u_1}{m} + P_8\omega + h_8(y - \hat{x}) \\ -g + (c\hat{x}_4 c\hat{x}_5)\frac{u_1}{m} + P_9\omega + h_9(y - \hat{x}) \\ \hat{x}_{11}\hat{x}_{12}\frac{J_y - J_z}{J_x} - \frac{J_r}{J_x}\hat{x}_{11}\Omega_r + \frac{L}{J_x}u_2 + P_{10}\omega + h_{10}(y - \hat{x}) \\ \hat{x}_{10}\hat{x}_{12}\frac{J_z - J_x}{J_y} + \frac{J_r}{J_y}\hat{x}_{10}\Omega_r + \frac{L}{J_y}u_3 + P_{11}\omega + h_{11}(y - \hat{x}) \\ \hat{x}_{10}\hat{x}_{11}\frac{J_x - J_y}{J_z} + \frac{u_4}{J_z} + P_{12}\omega + h_{12}(y - x) \end{pmatrix} \tag{3.255}$$

where $e_i \equiv (y_i - x_i)$ is a function of $x_1, x_2, x_3, x_4, x_5, x_6$ and forms the output error to be regulated. The equation ( 3.255) has the general form given by

$$\dot{\hat{x}} = M_g\hat{x} + L_g e \tag{3.256}$$

where the pair $(M_g, L_g)$ must be observable and $M_g$ is Hurwitz stable. The pair $(M_g, L_g)$, is analogous to the pair $(\Phi(\omega), \Gamma)$, found in literature (Serrani, 2005; Castillo-Toledo *et al.*, 2004). The goal was to stabilize the error dynamic associated with the estimation or observation of plant parameters. The following algorithm describes the construction of the observer.

1. Given the plant output space space vector as $x = [x, y, z, \phi, \theta, \psi, \dot{x}, \dot{y}, \dot{z}, \dot{\phi}, \dot{\theta}, \dot{\psi}]$ being equivalent to $[x_1, x_2, x_3, x_4, x_5, x_6, x_7, x_8, x_9, x_{10}, x_{11}, x_{12}]$

2. The observation error was then computed as $e_i = x_i - \hat{x}_i$. With $i \in R^{1-12}$

3. subsequent differentiation of the observation error resulted in $\dot{e}_i = \dot{x}_i - \dot{\hat{x}}_i$. An example of which is $x_7 - \hat{x}_7 - h_1(y - \hat{x})$, that results in $-h_1(y - \hat{x}) + e_7 \equiv -h_1 e_1 + e_7$. Other error dynamics are similarly derived.

4. careful selection was made of a matrix whose characteristic polynomial was globally Hurwitz. The coefficients of this characteristic polynomial were applied to form the matrix $M_g$

in the algorithm in section B.1.27 of the appendix.

5. Furthermore, to prevent the occurence of finite escape times or peaking phenomenon, the estimates were correctly saturated at the output (Serrani, 2005). The saturation applied for this work ensured that the output of the plant and observer state remained within the bounds of the desired output or reference inputs.

6. The formaulation of the matrix $L_g$ has also been derived in section B.1.27 of the appendix.

7. subsequently, the control input $u_{im}$, was derived as $u = -K\hat{x}$

The immersion-invariance control law was then synthesized from

$$\dot{\hat{x}} = M_g\hat{x} + L_g e \tag{3.257}$$

and replacing $u = -K\hat{x}$ with equation ( 3.243),

$$\psi(x, z) = K_m w_1 + \frac{K_m d\tau}{\eta r^3 J_t} x_{13}^2 + K_m \tau \dot{w}_1 \equiv Uii \tag{3.258}$$

thereby completing the synthesis of the controller.

$$\dot{\hat{x}} = M_g\hat{x} + L_g eUii = K_m w_1(\hat{x}) + \frac{K_m d\tau}{\eta r^3 J_t} x_{13}^2 + K_m \tau \dot{w}_1 \tag{3.259}$$

Equation (3.259) properly designed was a stabilizing error feedback regulator for the QUAV system.

### 3.4 Validation of the Developed Immersion Invariance Output Feedback Control Law

The validation of the designed control law was made on a model of the quadrotor unmanned aerial vehicle (QUAV) given in Figure 3.3. Several past works were consulted to come up with a workable and realistic simulation platform for the control law. Major works consulted and ideas

used are described here. The original dynamic model was adopted from Ozbek *et al.*,(2015) . The structure of the control system followed ideas from Sugawara and Shimada (2016) and has the basic form of Figure 3.2. However the following details were added as needed to implement the output feedback design. In the forward path, a feedforward input was used as described by Tengis and Batmunkh (2016)

$$G = -B^{-1}(A - BKx)C^{-1} \tag{3.260}$$

Equation (3.260) forces correspondence between the feedback states and the reference signals. The next block in the model is a controller block with the green background. This block contains both the nominal state feedback given by equation (3.152) and the immerison invariance controller in equations (3.237)-(3.240). The output from this block formed the initial pseudo-input control law. Next is the block which calculates the reference angular velocities for the rotor's motors. With $U_{f1}, U_{f2}, U_{f3}, U_{f4}$, as pseudo control inputs coming from the nominal controller, the following reference angular velocity equations were applied

$$\Omega_{rd_1} = \frac{\sqrt{d(U_{f1} - U_{f3}) - bU_{f4}}}{2\sqrt{bd}} \tag{3.261}$$

$$\Omega_{rd_2} = \frac{\sqrt{d(U_{f1} - U_{f2}) + bU_{f4}}}{2\sqrt{bd}} \tag{3.262}$$

$$\Omega_{rd_3} = \frac{\sqrt{d(U_{f1} - U_{f3}) - bU_{f4}}}{2\sqrt{bd}} \tag{3.263}$$

$$\Omega_{rd_4} = \frac{\sqrt{d(U_{f1} + U_{f2}) + bU_{f4}}}{2\sqrt{bd}} \tag{3.264}$$

The reference velocity computation block was derived from equations (4.262)-(3.264) as given in Sugawara and Shimada (2016) and has four signals which are fed to the input of the four rotors's motors. The next block in the QUAV closed loop structure comprised four brushless direct current (BLDC) motors. These principle actuating component of the QUAV system were modelled using transfer function between the rotor output velocity $W_m$ and the input voltage $V_m$. The detailed analysis of the actuator was given in section 3.3.7. The control of the actuator formed the inner loop of the closed loop structure. This work innovated with a hybrid control algorithm for the

actuators using both a standard Proportional-integral-derivative (PID) controller in the forward path and a pole placement algorithm in the feedback path.

$$U_{act} = K_p(1 + \frac{1}{s}K_i + sK_d) + (-K_{pp}x) \tag{3.265}$$

The structure of the actuator control algorithm was made to increase robustness of the inner loop to disturbances and uncertainties and also force faster dynamic in the inner loop than the outer loop. In equation (3.265), $K_p, K_i, K_d, K_{pp}$ are defined as the proportional, integral, derivative and pole placement gains respectively.

The next block in the control structure is the force calculation block. The forces which produce the lifts and attitude manouvers are the thrusts and torques. Computation of the correct thrusts and torques was necessary to produce the correct control input to the QUAV. The final control inputs were defined in equation (3.195). The next block in the control diagram is the QUAV system to be controlled as defined by the working model in equation (3.120).

The observer regulators were placed in the feedback path. Three different observer regulators were designed. The first was described in equation (3.251) and whose algorithm can be found in section B.1.17 of the appendix. The second regulator consisted of a robust regulator following the form in equation (3.254). However due to the obvious approximation in deriving a generalized immersion map, Serrani, (2005) proposed adopting Khalil's observer to compute the needed derivatives or state estimates. Details for construction of such an observer was given in Khalil and Praly (2013) and detailed in section 3.3.13.1 of this report.

Parameter effect on the simulation experiment was significant. Specific parameters which required careful selection in order to obtain the correct response were; the backstepping control parameters $k_1$ - $k_{12}$, motor scale factor, $msf$, torque scale factor, $tsf$, ,motor controller PID parameters, $k_p$, $k_i$ and $k_p$. These parameters can be found in the code listing of section B.1.5. They also constitute a takeoff point for system optimization.

# CHAPTER 4

# RESULTS AND DISCUSSION

## 4.1 Introduction

In this chapter, the results obtained from all the experiments are presented and discussed. The experiments were all made using Matlab for the scripting and Simulink for the symbolic modeling and simulations. The order of results presentation has been made according to the sequence of stated objectives for this report and in accordance with the laid down methodology. The output regulation results are first presented for the RTAC, CIP and UAV systems. Next are the results for immersion invariance stabilization control as implemented on the RTAC model. Third and last are results for the proposed immersion invariance error feedback controller (IIEFCL) and control law validation on the QUAV system.

## 4.2 Output Regulation Experiments

This section presents the results for the output regulation experiments carried out on the RTAC, CIP and UAV control benchmark models. Output regulation design on these models was to enforce the stability of the closed loop system of the various plant models discussed. This stability is tested by injecting into the closed loop system signals of various magnitudes so as to test the transient stability response of the closed loop system. The desired result in every stabilization experiment of this kind was required to have all states settle down to the equilibrium position as time tends to infinity. This stabilization was made in the presence of disturbance and reference signals modeled by an exosystem. Such a result is used to confirm the validity of the regulator design and confirm the internal stability of the closed loop system.

### 4.2.1 RTAC Regulation Experiments

The results for the RTAC regulation experiment are presented for the given RTAC system parameters. The system under initial perturbation was unstable. Therefore an output feedback regulator was designed using both static and dynamic output feedback. The output error feedback regulator(OEFR) for the RTAC system was designed and simulated in Matlab. The developed observer internal model was tested for stability using the static and dynamic state and error output feedback presented in equations (2.31) and (**??**). The size of the observer was found to be $n_z = 6$. Stability tests for the internal model observer gave the following computed eigenvalues;

eig(Aobsv+Bobsv*Kxv) =

$$\begin{aligned}
-2.9943e+000+i \\
-18.5310e+000+i \\
-15.3013e+000+i \\
-13.0912e+000+i \\
0.0000e+000+1.0000e+000i \\
0.0000e+000-1.0000e+000i
\end{aligned}$$

eig(Aobsv-G2*Cobsv) =

$$\begin{aligned}
-144.6227e+000+94.7115e+000i \\
-144.6227e+000-94.7115e+000i \\
-60.0796e+000+i \\
-25.8172e+000+i \\
-12.4289e+000+783.7299e-003i \\
-12.4289e+000-783.7299e-003i
\end{aligned}$$

The displayed results for the stability of the observer showed good stability properties for the observer internal model. Since all the eigenvalues were suitably located in the LHCP, the system assuredly gave suitable asymptotic stability result. These stability results of the designed observer internal model was further confirmed for stabilization and tracking experiments as shown in the following response profiles;

Figure 4.1 depicts the stabilization experiment for the initial condition $ic = (0.051, 0, pi/8, 0)$ for

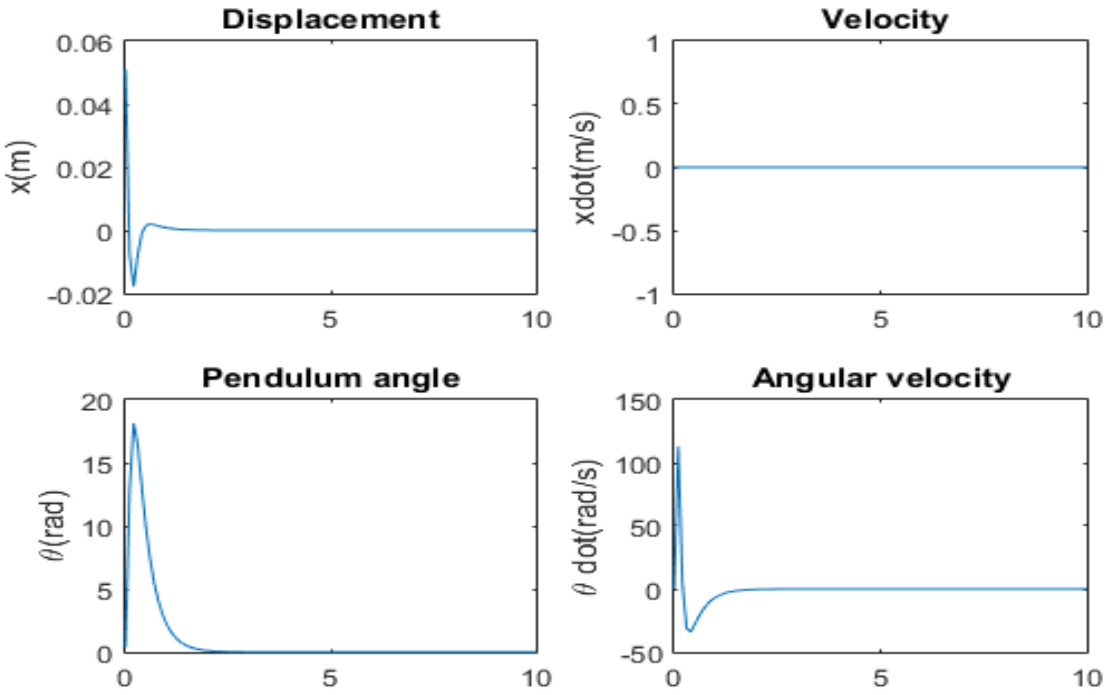



Figure 4.1: RTAC OEFR Stabilization with ic=(0.051 0 pi/8 0)

the four states of the RTAC system. The four states are the displacement ($x$), velocity ($\dot{x}$), angular displacement ($\theta$) and angular velocity ($\dot{\theta}$). It was deduced from the results that the developed output regulator was able to in every case stabilize to the origin from whatever starting intiial condition. The closed loop states were seen to decay to zero in 2.7s from the initial transient phase at the start of the simulation. The behavior of this controller conformed to the results obtained from the regulator equation solutions in section 3.1.1.4 which were unique and the stability test performed on the eventual closed loop system. Figure 4.2 depicts the stabilization experiment for another initial condition of $(0.2, 0, 15, 0)$. This fast decay of the transients was verified by the asymptotic stability response curves of Figure 4.1 and 4.2.

The poles for determination of the state feedback gain were chosen as $-19, -3, -15, -13$. After some calculation, the obtained gain $Kx$ was $237.3198, 17.3309, 0.0910, 0.0482$. This gain resulted in the feedback with the closed loop system $A + BKx$ that was stable and had the eigenvalues $-2.9943e + 000, -18.5310e + 000, -15.3013e + 000, -13.0912e + 000$. The next computed pa-

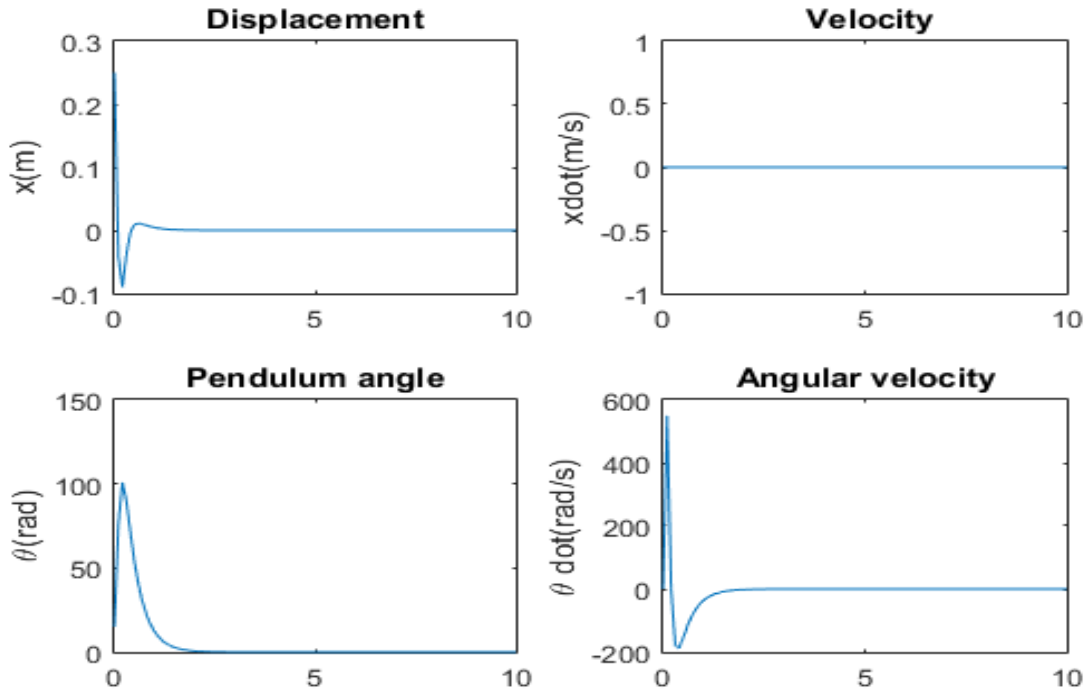



Figure 4.2: RTAC OEFR Stabilization with ic=(0.2 0 15 0)

rameter was the disturbance gain $Kv$. This gain parameter was necessary to drive the disturbances generated by the exosystem to zero. This gain when evaluated from the solution of equation (3.19), was found to be $Kv = [0.1773, -9.8259e + 16]$. The Luenberger observer gains $G1$ and $G2$ were calculated but not displayed here due to size constraints ( see calculation in section A.0.10 of the appendix. However, the observer poles were selected as 8-times the magnitude of the feedback poles. This is done so as to make the estimation faster than the computation of the control signal generation. After completion of all computations, the overall closedloop system $Aclsys$, was confirmed stable by the position of all the eigenvalues which were properly placed in the LHCP as follows:

stabAclsys =

$$
\begin{aligned}
&-2.9943e+000+i\\
&-18.5310e+000+i\\
&-15.3013e+000+i\\
&-13.0912e+000+i\\
&-144.6227e+000+94.7115e+000i\\
&-144.6227e+000-94.7115e+000i\\
&-60.0796e+000+i\\
&-25.8172e+000+i\\
&-12.4289e+000+783.7299e-003i\\
&-12.4289e+000-783.7299e-003i
\end{aligned}
$$

these results comfirmed the existence of the unique set of RTAC regulator solutions obtained in section 3.1.1.4. All other intermediate simulation results are presented in the appendix of this report.

### 4.2.2 CIP Output Regulation

The sections that follow describe the output regulation results on the CIP. Uncompensated, the CIP system is inherently unstable. This led to the development of a stabilizing controller which was developed as an error feedback internal model based controller. The Hurwitz test on the closed loop CIP with the designed regulator was confirmed by the following eigenvalues:

stabAclsys =

$$
\begin{aligned}
-19.2756e+000+i\\
-16.4122e+000+i\\
-15.3208e+000+i\\
-8.9966e+000+i\\
-170.5082e+000+i\\
-151.1266e+000+i\\
-126.0149e+000+i\\
-66.5615e+000+i\\
-894.4208e-003+3.5947e+000i\\
-894.4208e-003-3.5947e+000i
\end{aligned}
$$

where these eigenvalues consist of the poles for the plant, observer and exosystem taken together.

With the regulator confirmed, stability experiments gave the following results. Figure 4.3 gives the stability results and response for an initial perturbing signal of $(0.5, 2.66, pi/4)$ Figure 4.3 showed

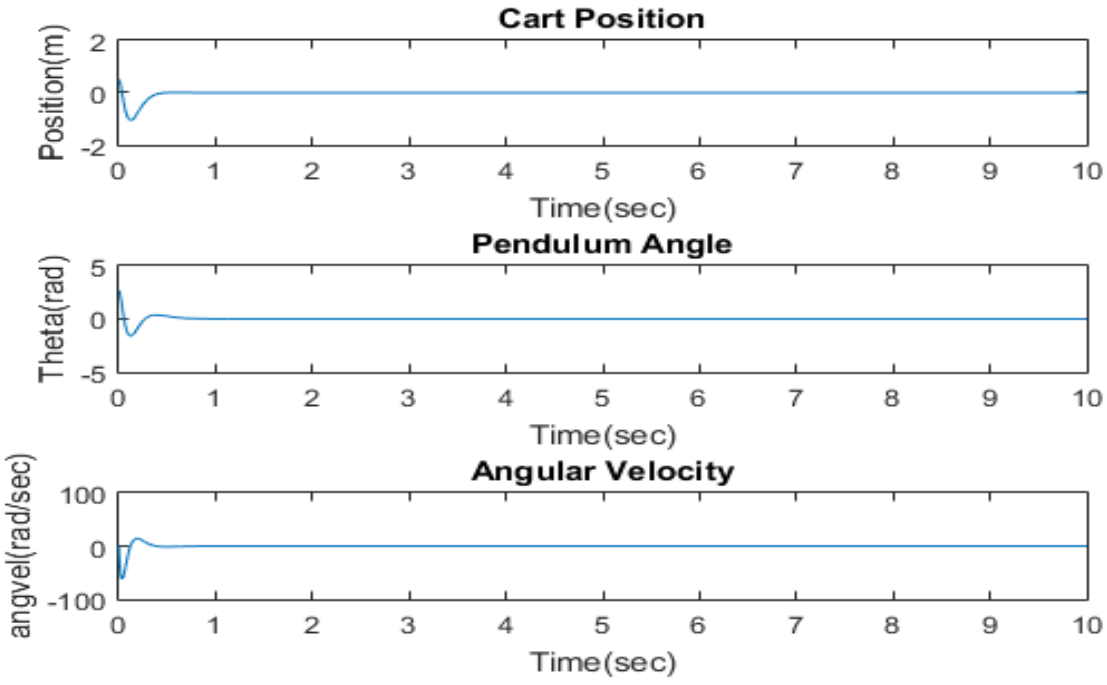



Figure 4.3: CIP OEFR Stabilization with ic=(0.5 2.66 pi/4)

the settling of all system states to zero in under 1.113 seconds. A new set of initial conditions were tested. Figure 4.4 gives the stability results and response for an initial perturbing signal of $(0.2, 1.3, pi/2)$ Figure 4.4 highlights the settling of all system states to zero in 1.113 second. This

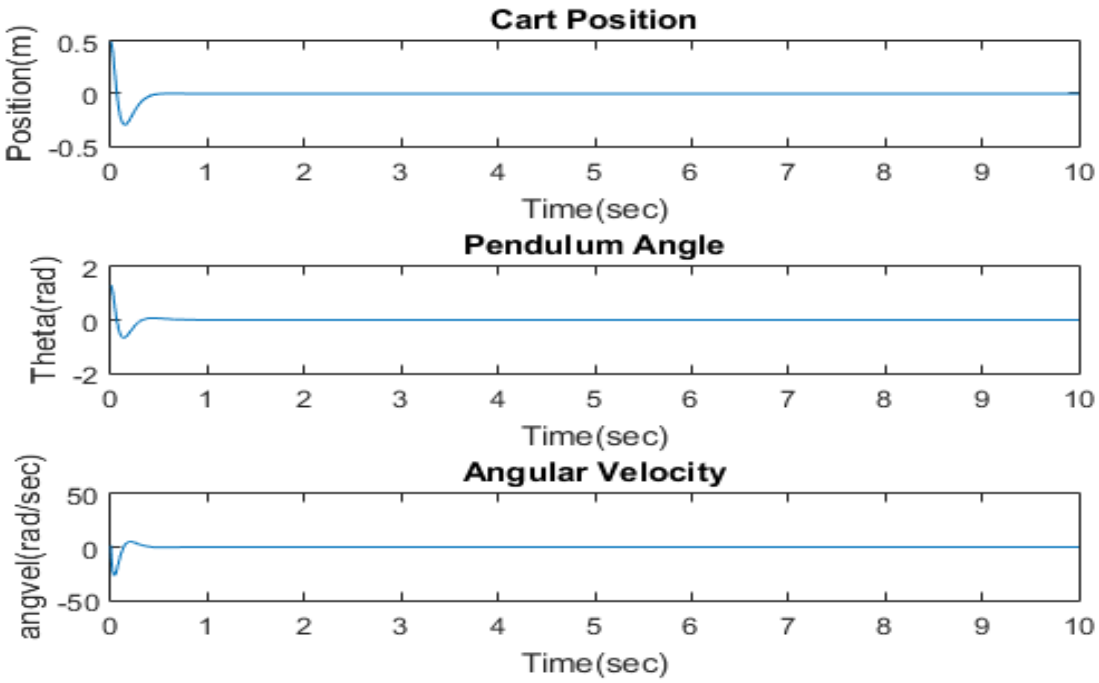



Figure 4.4: CIP OEFR Stabilization with ic=(0.2 1.3 pi/2)

second result showed the sensitivity of stability response to the magnitude of the perturbing signal. From the developed feedback regulator solutions which were shown to be unique in section 3.1.4 and Hurwitz test on the CIP closed loop system, it was shown that all the eigenvalues of the system were suitably located in the LHCP. This confirms the total internal structural stability of the designed CIP regulator.

### 4.2.3 Quadrotor UAV Output Regulation

The regulator for the UAV was designed with an observer internal model. Test for stability revealed all eigenvalues of the system occured in the LHCP. All poles were stable except for the pole allocated to the yaw feedback that turned out an unstable positive eigenvalue.The following

results were obtained after experimentation for different initial conditions with the selected states chosen as the $x$,$y$,$z$ displacement and the $\phi$, $\theta$ and $\psi$ orientation angles. These states are otherwise known as the in-plane (x and y) displacement, the altitude,roll angle, pitch angle and yaw angle respectively: Figure 4.5 shows the first experiment for testing the developed stabilizing regulator

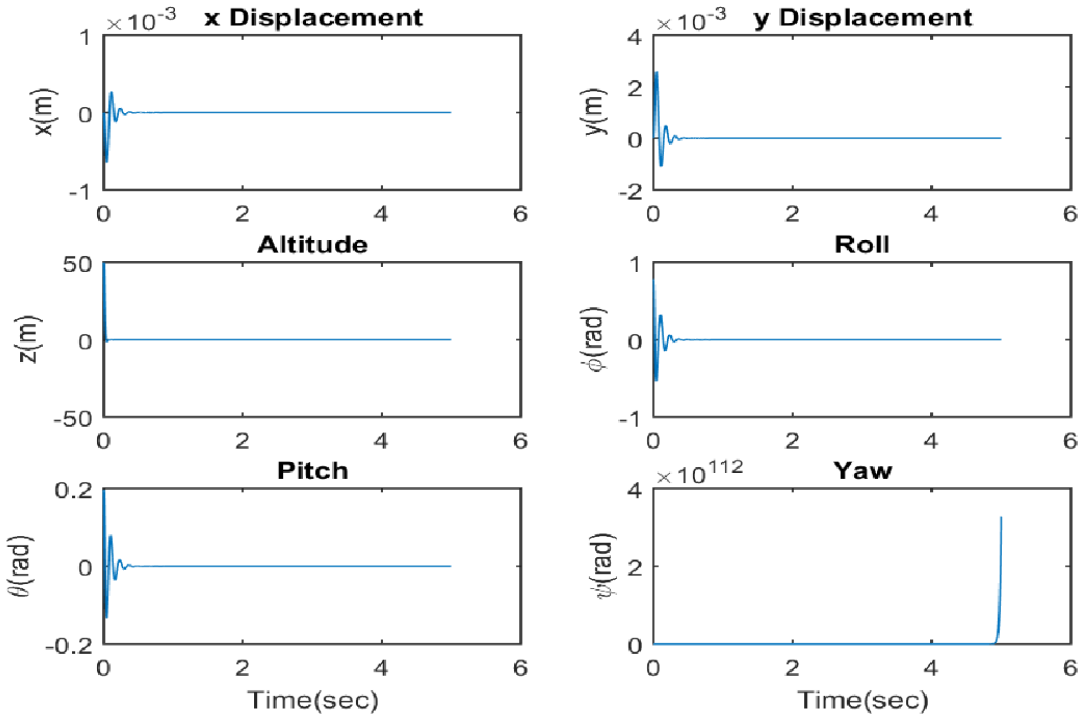



Figure 4.5: Regulation Control; ic=(0,0,50,0.785,0.196,0.131) and fc=(0,0,0,0,0,0)

for the quadrotor states: $x, y, z, roll, pitch, yaw$. The initial and final condition values used were $ic1 = (0, 0, 50, pi/4, pi/16, pi/24)$ and $fc = (0, 0, 0, 0, 0, 0)$ respectively. Figure 4.6 shows the second experiment for testing the developed stabilizing regulator on the same states but utilizing different initial condition values: $ic1 = (0, 0, 19, 7.5, 15, pi/45)$ and $fc = (0, 0, 0, 0, 0, 0)$ respectively. From the results, all the states settled down to zero except the yaw which was seen to be unstable. All system states asymtptotically converged to the equilibrium in 0.6435 seconds. On further investigation, several experiments were performed which changed the position of the selected poles. However the eigenvalues associated with the yaw control torque remained fixed in the positive right hand complex plane (RHCP). The poles for the determination of the state feedback

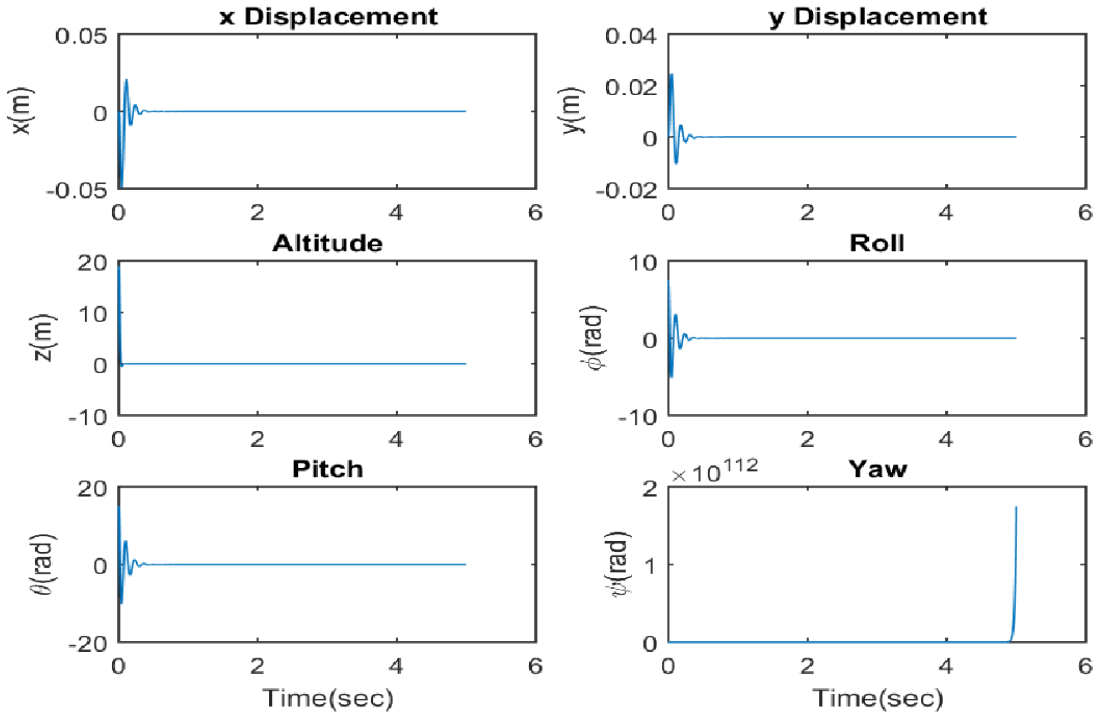



Figure 4.6: Regulation Control; ic=(0,0,19,7.5,15,0.07) and fc=(0,0,0,0,0,0)

gain were chosen as (-19, -17 , -13 , -12 , -14 , -10 , -8 , -16 , -11 ,-18 , -9 ,-7 ). After some calculation, the gains $Kx$ was obtained. This gain resulted in the feedback with the closed loop system $A + BKx$ that was stable in all its eigenvalues but one. The next computed parameter was the disturbance gain $Kv$. This gain parameter was necessary to drive the disturbances generated by the exosystem to zero, thereby forcing convergence to the equilibrium. This gain was evaluated from solving the Sylvester equations (equation (3.19)), as $Kv = U - Kx\Pi$. The internal model observer gains $G1$ and $G2$ were next calculated but not displayed here due to size constraints. However, the observer poles were selected as ten times the magnitude of the feedback poles. This is done so as to make the estimation faster than the computation of the control signal generation. After all computations, the overall closeloop system $Aclsys$, was confirmed stable by the position of all the eigenvalues which were properly placed in the LHCP except for the yaw state pole that could not stabilize the target state. The computed regulator solution for the selected output state of the quadrotor were in section 3.1.6.2 confirmed to be non-unique in the obtained regulator solu-

tions.

stabAclsys =

$$
\begin{aligned}
&-64.5387e+000+29.2162e+000i\\
&-64.5387e+000-29.2162e+000i\\
&-12.4613e+000+48.8871e+000i\\
&-12.4613e+000-48.8871e+000i\\
&-77.0014e+000+69.6558e+000i\\
&-77.0014e+000-69.6558e+000i\\
&-12.4613e+000+48.8871e+000i\\
&-12.4613e+000-48.8871e+000i\\
&-64.5387e+000+29.2162e+000i\\
&-64.5387e+000-29.2162e+000i\\
&-206.2670e+000+i\\
&***52.2670e+000+i***\\
&-399.9791e+000+i\\
&-384.8450e+000+i\\
&-181.2824e+000+i\\
&-163.1018e+000+i\\
&-132.0642e+000+11.0355e+000i\\
&-132.0642e+000-11.0355e+000i\\
&-127.1296e+000+13.1191e+000i\\
&-127.1296e+000-13.1191e+000i\\
&-105.4073e+000+i\\
&-85.4687e+000+i\\
&-35.7197e-003+1.0262e+000i\\
&-35.7197e-003-1.0262e+000i\\
&-25.3029e+000+i\\
&-36.1537e+000+i
\end{aligned}
$$

All code listings can be found in the appendix of this report.

### 4.2.4 Summary of Output Regulation Experiments

The results for the output regulation experiments have been summarized in Table 4.1

Table 4.1: Table of Results for Output Error Feedback Stabilization Control)

| Param/System | RTAC | CIP | UAV | Unit |
|---|---|---|---|---|
| Settling time | 2.7 | 1.113 | 0.6435 | sec |
| SSE | 0 | 0 | 0 | |

## 4.3 Immersion Invariance Stabilization Experiments

The immersion invariance control experiments was performed on the RTAC model only. The experimental results are here presented in full.

### 4.3.1 RTAC Immersion Invariance

The immersion invariance design was built in four parts which are given as follows;

1. Linear immersion invariance controller without and with observer

2. Nonlinear immersion invariance controller without and with observer

### 4.3.2 RTAC immersion invariance stabilization controller

Experiments for the linear RTAC system immersion invariance controller were developed and presented next

*4.3.2.1 Linear immersion invariance controller without observation*

Figure 4.7 show the profile of the state output. This profile was obtained from simulation of the linear RTAC model without observation.

*4.3.2.2 Linear immersion invariance controller with observation*

Figure 4.8 shows the profile of the signal for state output. These profiles are obtained from simulation of the linear RTAC model with the Luenberger observer used for estimation.

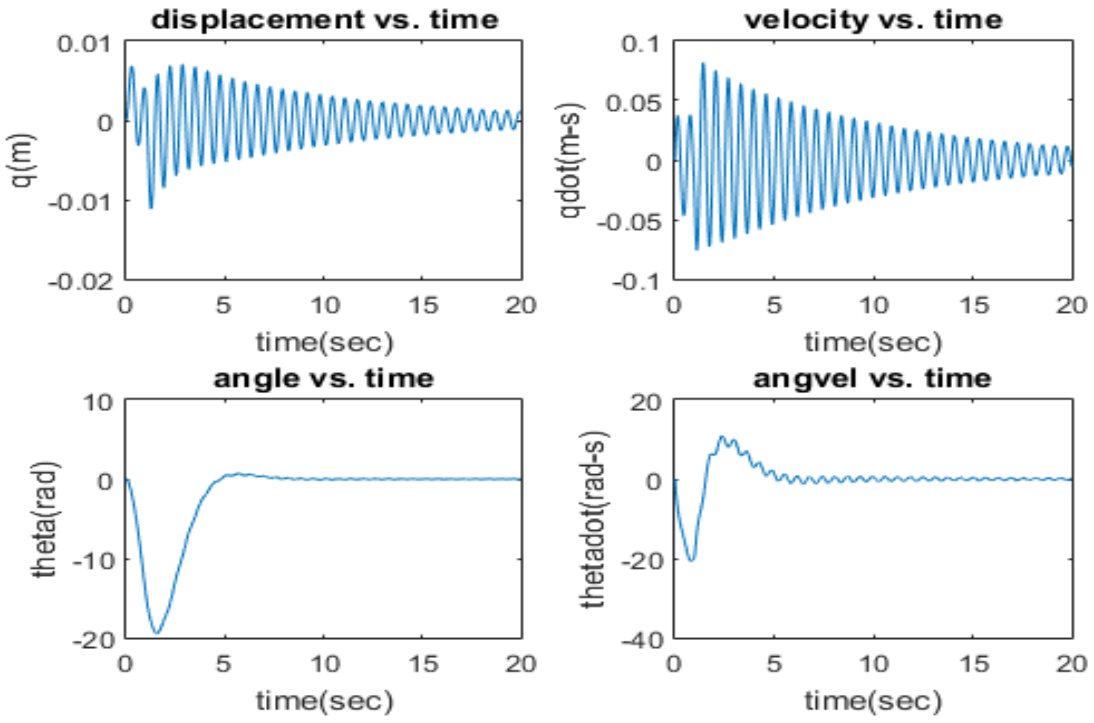



Figure 4.7: State Output from Immersion Invariance Linear Controller

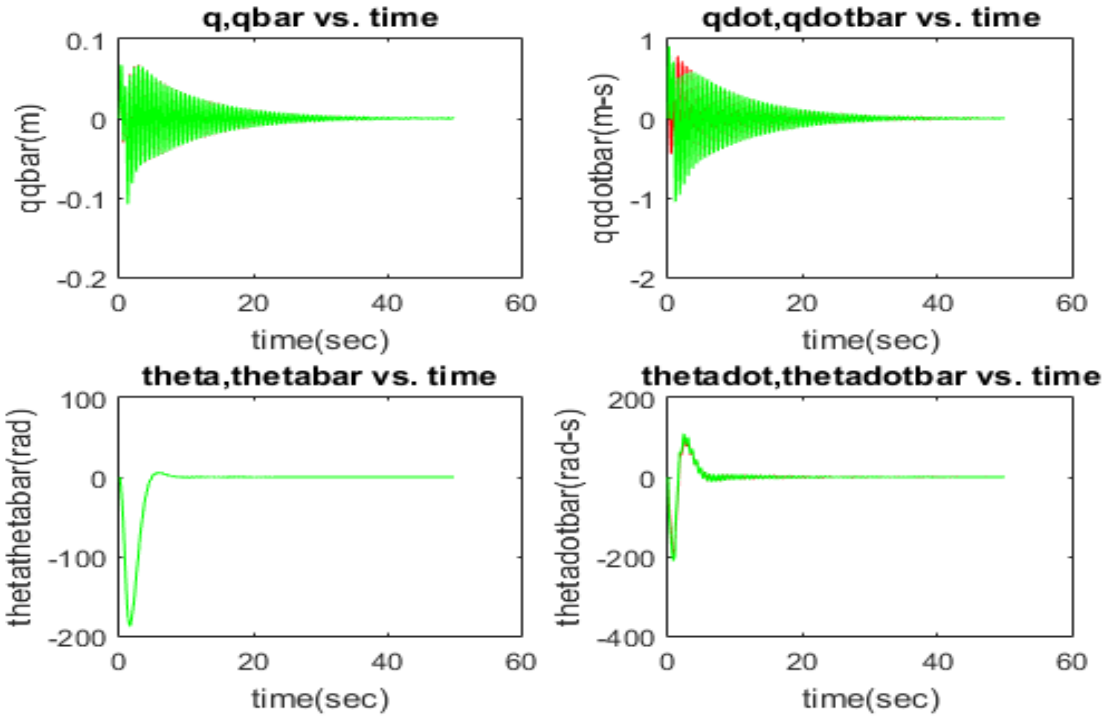



Figure 4.8: Plant and Observer Output from Immersion Invariance Linear Controller

*4.3.2.3 Nonlinear immersion invariance controller without observation*

Figure 4.9 shows the profile of the signal for state output. This profile was obtained from simulation of the nonlinear RTAC model without observation. The effect of the nonlinearities were clearly obvious as seen in the plot.

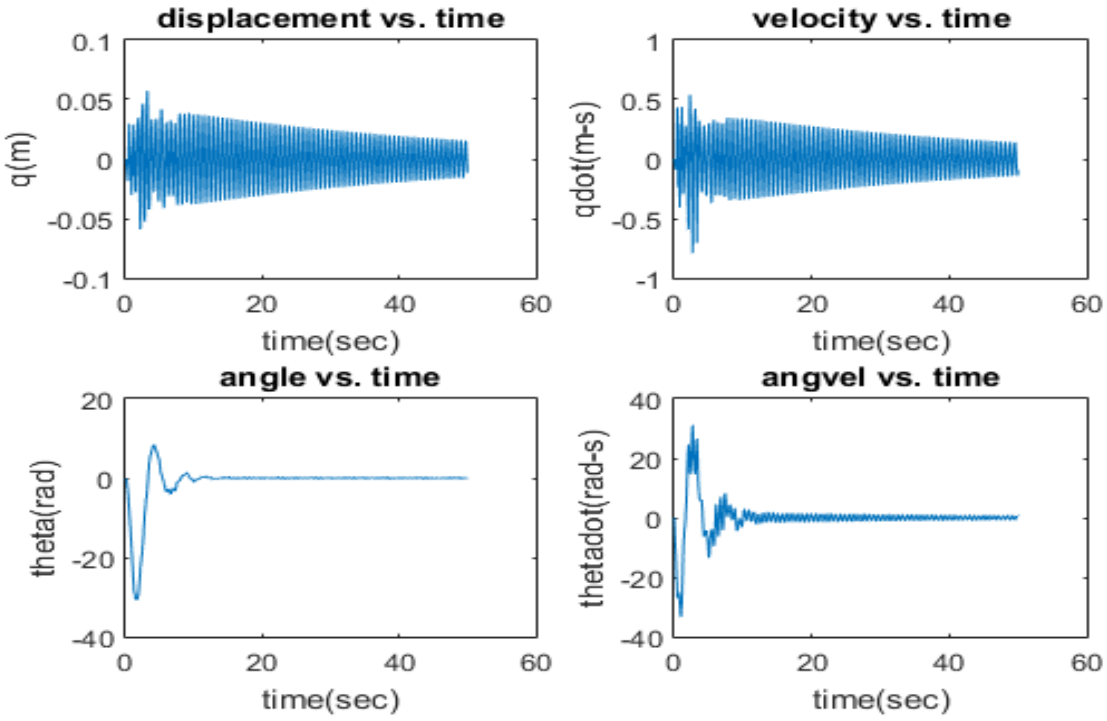



Figure 4.9: Nonlinear State Output from Immersion Invariance Controller without Observer

*4.3.2.4 Nonlinear immersion invariance controller with observation*

Figure 4.10 shows the profile of the system states signal obtained from simulation of the nonlinear RTAC model with the Luenberger observer used for estimation. The execution time was set to 50 seconds, so as to show the eventual stabilization to the origin of the error signal involved. Figure 4.11 shows the profile of the system states signal obtained from simulation of the nonlinear RTAC model with the Luenberger observer used for estimation. The execution time was set to 500 seconds, so as to show the eventual stabilization to the origin of the error signal involved.

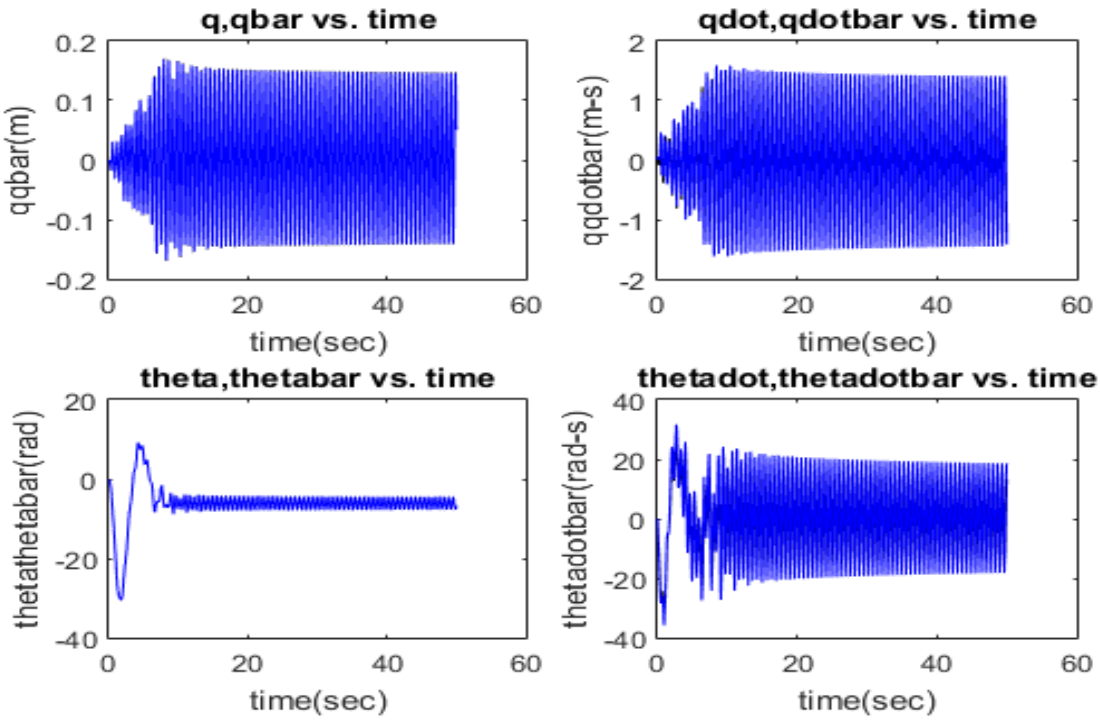



Figure 4.10: Nonlinear States Stabilization for 50sec with Observation

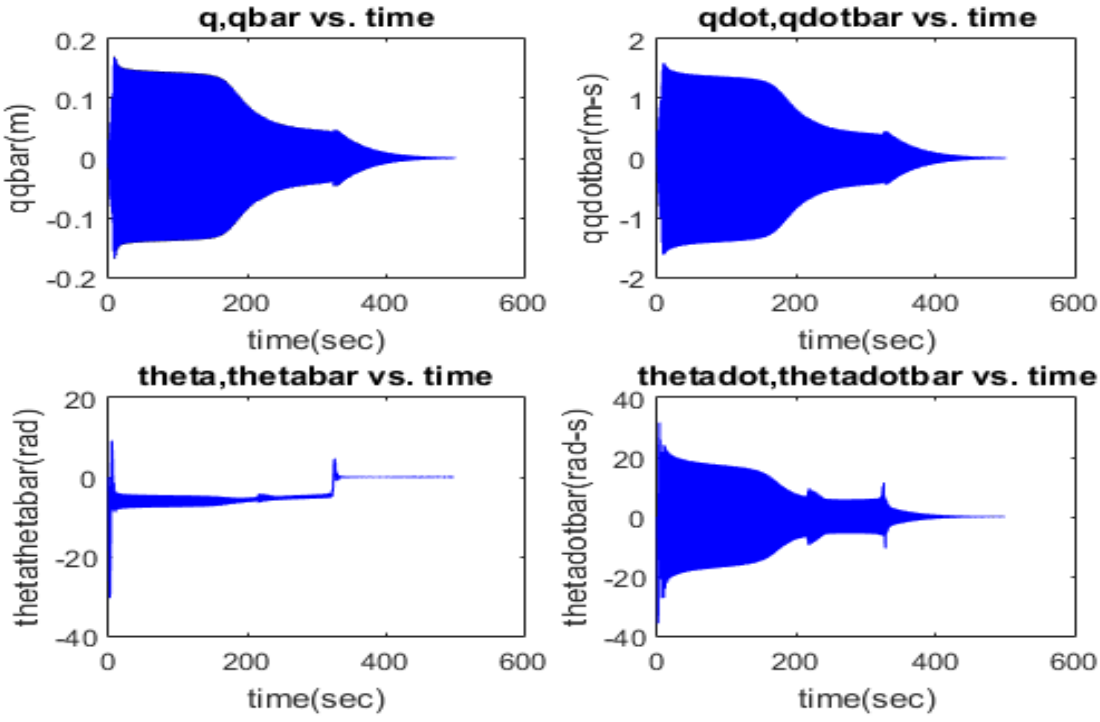



Figure 4.11: Nonlinear States Stabilization for 500sec with Observation

### 4.3.3 Linear immersion invariance Tracking control with observation

Tracking experiments were performed for the RTAC system and displayed here. Figure 4.12

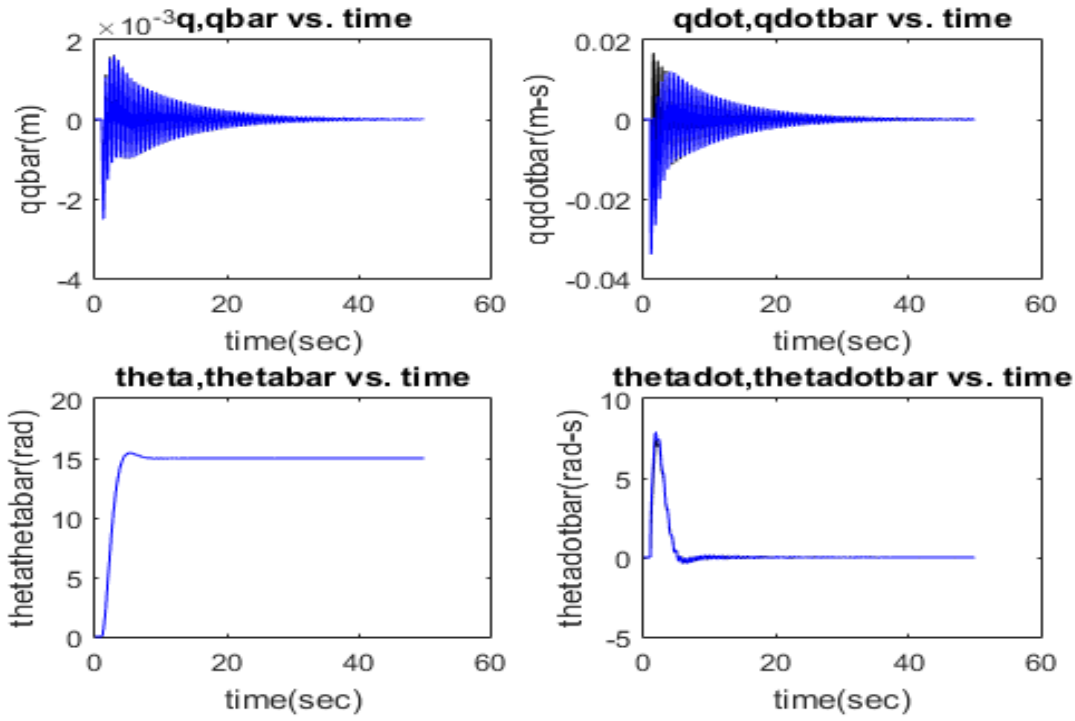



Figure 4.12: Linear Tracking Control with Conditions; ic=(0,0,0,0), fc1=(0,0,15,0)

presents the results from the immersion invariance controller during state setpoint tracking . The performed experiments used the initial condition, $(0, 0, 0, 0)$ while the final condition were set to $(0, 0, 15, 0)$. Figure 4.13 presents the the second result from the immersion invariance controller during state setpoint tracking . The performed experiments used the initial condition, $(0, 0, 0, 0)$ while the final condition were set to $(0, 0, 7.5, 0)$.

### 4.3.4 Robust RTAC stabilization and tracking experiments with disturbance injection

Following the previous experiments on the RTAC model, the system output was perturbed by different magnitudes of disturbances. These disturbances were injected at the output in order to study the stability behavior of the system under the influence of selected disturbance regime and while under the designed immersion invariance control law. These tests were carried out to test robust-

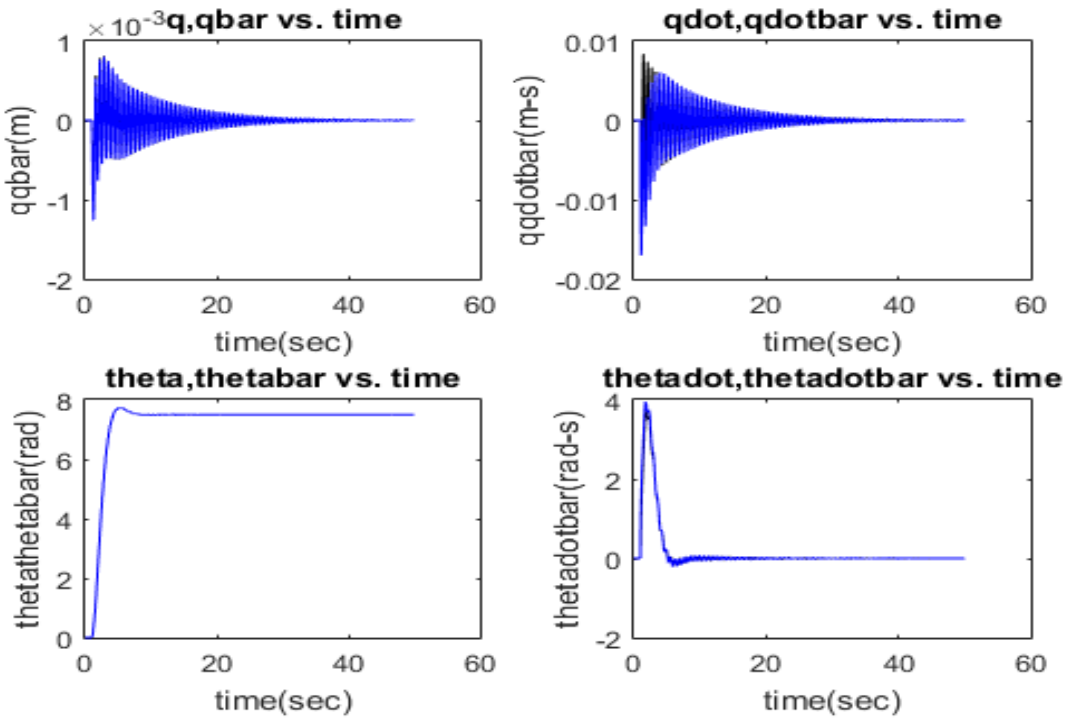



Figure 4.13: Linear Tracking Control with Conditions; ic=(0,0,0,0), fc2=(0,0,7.5,0)

ness of the designed control laws to injected disturbances. The resulting control action considered two control laws: the first was driven by only the immersion invariance design while the second control law had an outer loop PID controller which was made robust by the inclusion of an inner loop dynamic state immersion invariance feedback controller. Under similar input conditons, both control actions were compared and formed the basis for the developed immerison invariance output feedback control law synthesized in methodology items 3 and 4.

Figure 4.14 shows the behavior of the immersion invariance control law acting alone in a stabilization experiment. All the states of the system are clearly shown to stabilize to zero. This confirms the stabilizing function of the designed control law. However the magnitude of oscillations was large.

Figure 4.15 shows the behavior of the immersion invariance control law acting as a robustifier to a PID outer loop in a stabilization experiment. All the states of the system are clearly shown to stabilize to zero. While confirming the stabilizing function of the designed control law, the magni-

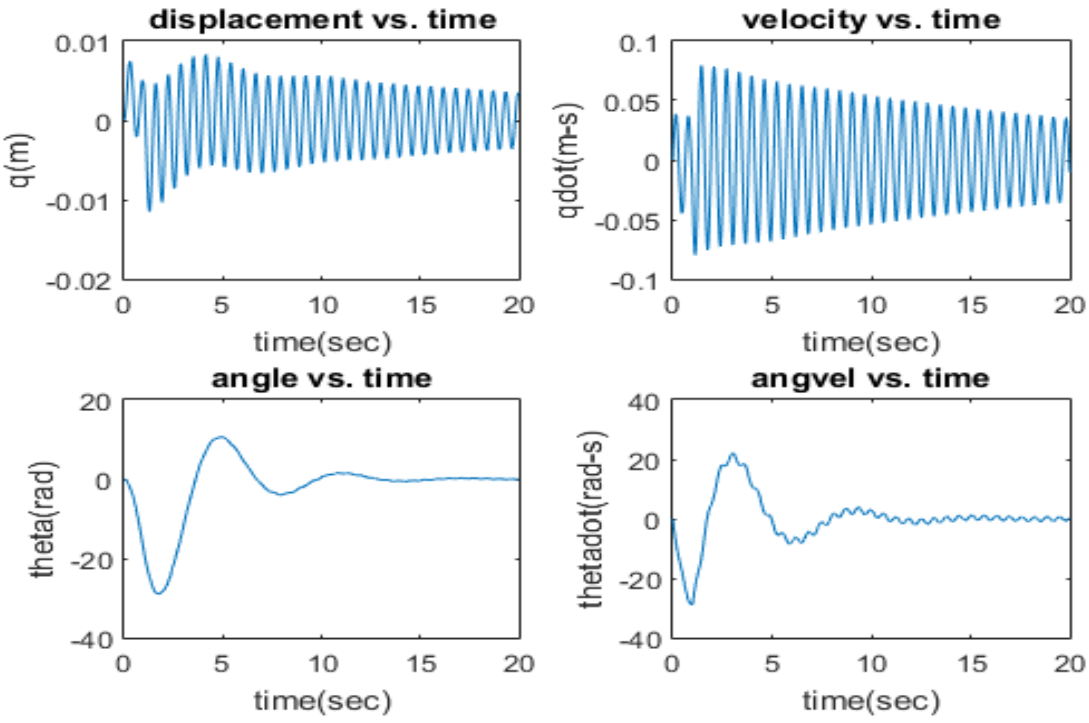



Figure 4.14: Non-robust Stability Control; ic=(0.051,0,0.393,0), disturbance=0.1units

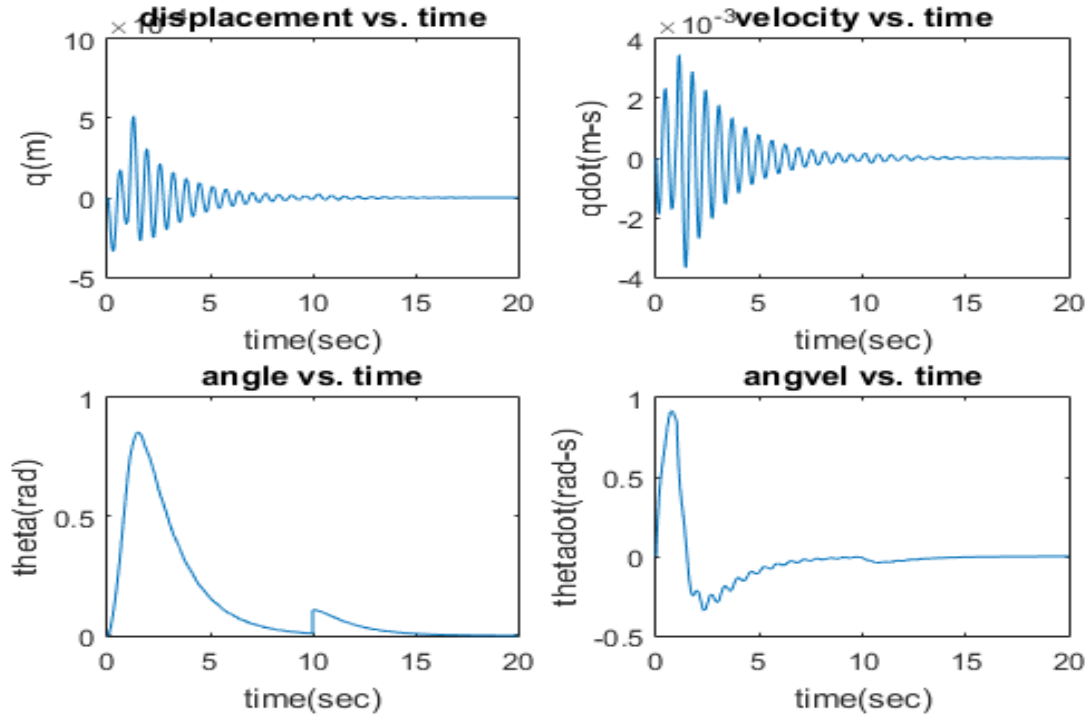



Figure 4.15: Robust Stability Control; ic=(0.051,0,0.393,0), disturbance=0.1units

tude of oscillations were demished as compared to the non-robust case in Figure 4.14.

Figure 4.16 shows the behavior of the immersion invariance control law acting alone in a tracking

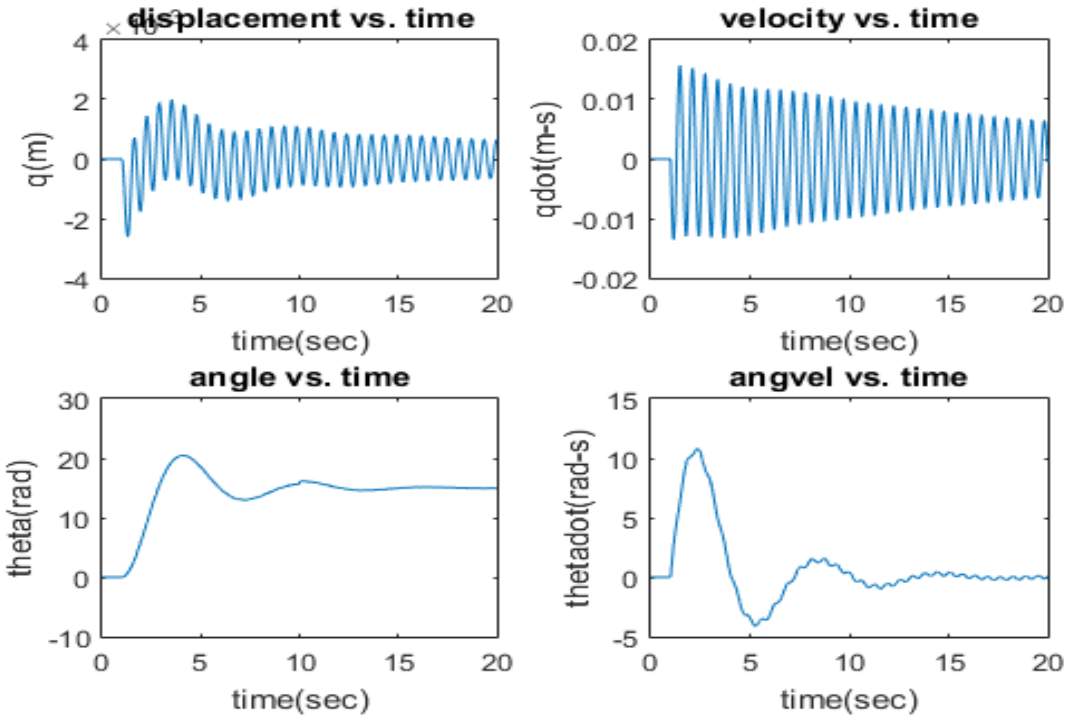



Figure 4.16: Non-robust Tracking Control; ic=(0,0,0,0), fc=(0,0,15,0)

experiment. With intial conditions set to [0 0 0 0] and final conditions set to [0 0 15 0], all the states of the system are clearly shown to track the desired reference commands. This confirmed the tracking function of the designed control law. However the magnitude of oscillations was large.

Figure 4.17 shows the behavior of the immersion invariance control law acting as a robustifier to a PID outer loop in a tracking experiment. With initial conditions set to [0 0 0 0] and final conditions set to [0 0 15 0], all the states of the system are clearly shown to track the desired reference commands. While confirming the tracking function of the designed control law, the magnitude of oscillations were demished as compared to the non-robust case in Figure 4.16. All the main results for the nonrobust and robust stabilization and tracking experiments have been summarized in Table 4.2.

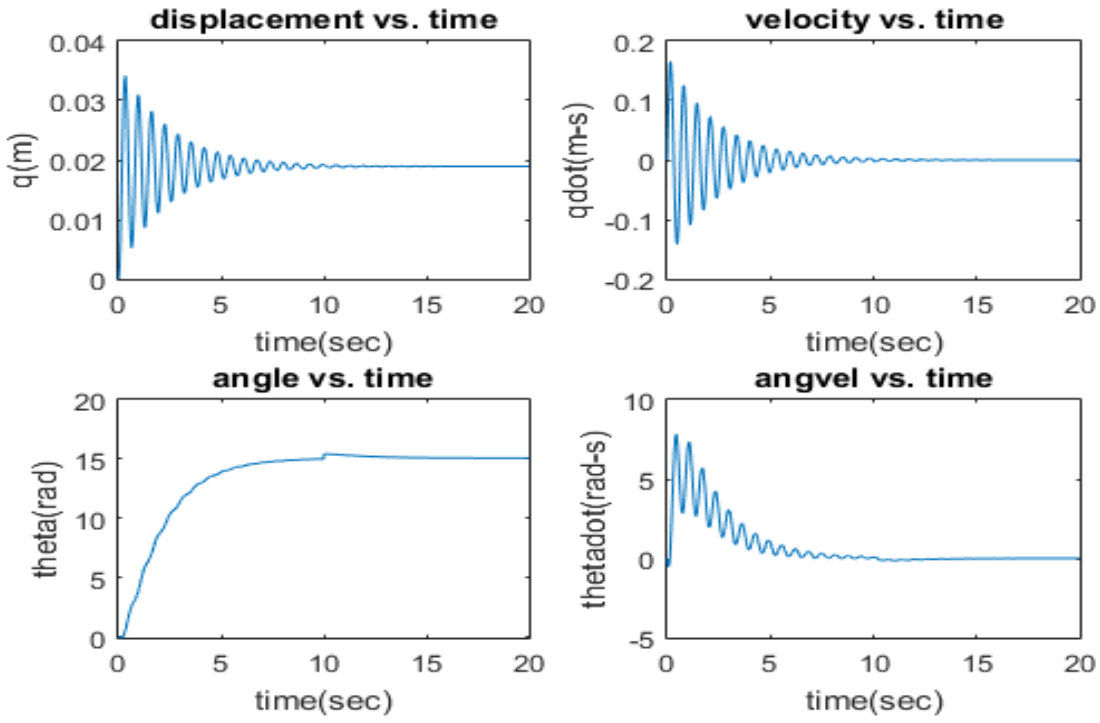



Figure 4.17: Robust Tracking Control; ic=(0,0,0,0), fc=(0,0,15,0)

Table 4.2: RTAC Immersion Invariance Results for Robust-R and Nonrobust-NR

| Description | NR-stability | R-stability | NR-tracking | R-tracking | Unit |
|---|---|---|---|---|---|
| Overshoot | | | yes(36.27) | no(0) | percent |
| SSE | no | no | yes | no | |
| Settling time | 15 | 10 | 18 | 8 | seconds |

## 4.4 Immersion Invariance Error Feedback Control Results

Prior to implementing the proposed IIEFCL on the QUAV system, several nonlinear control laws were developed and tested. These include; a nominal nonlinear control law (NLCL), an error feedback control law (EFCL) and an immersion invariance stabilizing control law(IICL). The test model for all described controllers in this and all subsequent sections of this thesis is the QUAV model. (Ozbek *et al.*, 2015; Sugawara and Shimada, 2016).

### 4.4.1 QUAV unforced stabilization results

The initial design of the output feedback observer regulator was tested for internal stability performance. While the previous QUAV stabilization result showed instability for the rotation about the z-axis (yaw motion), the model utilized here from Ozbek *et al.*, (2015), responded to the designed regulator with stability on all six states of interest. Figures 4.18 and 4.19 are results for the initial condition of $(0, 0, 19, 0.5236, 0.5236, 0.07)$ settling to zero. Overall settling time for all states was under 0.6 seconds.

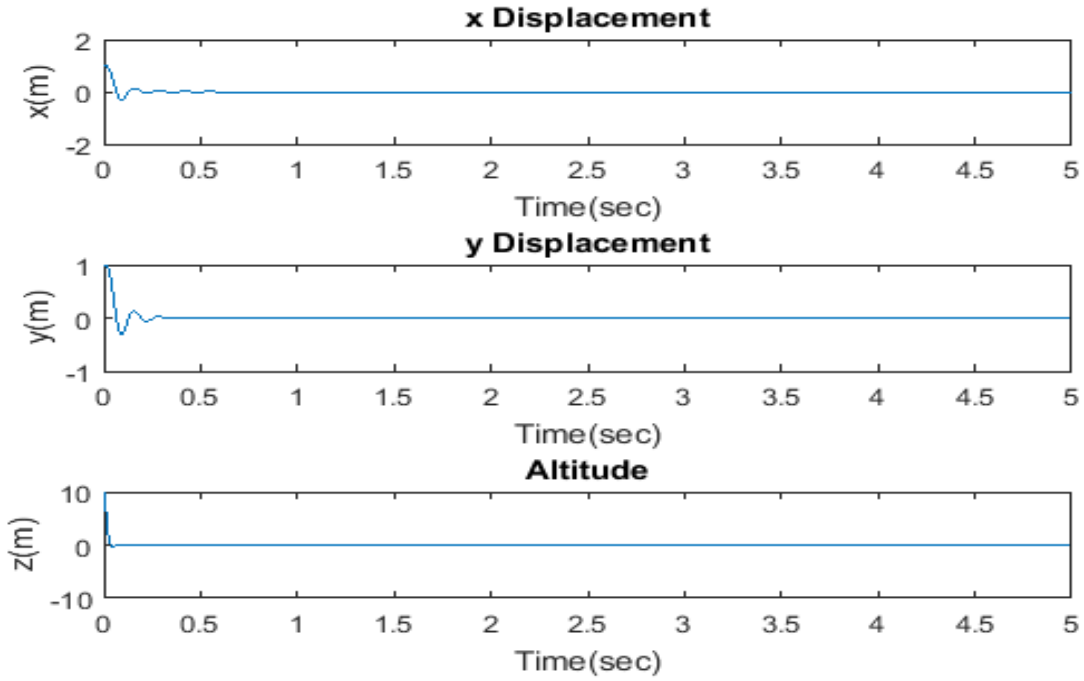



Figure 4.18: Unforced X-Y-Z Stabilization for the QUAV

Figure 4.18 gives the transient reponse for the translation x,y and z component of the QUAV while Figure 4.19 gave the attitude roll-pitch and yaw component transient response of the QUAV.

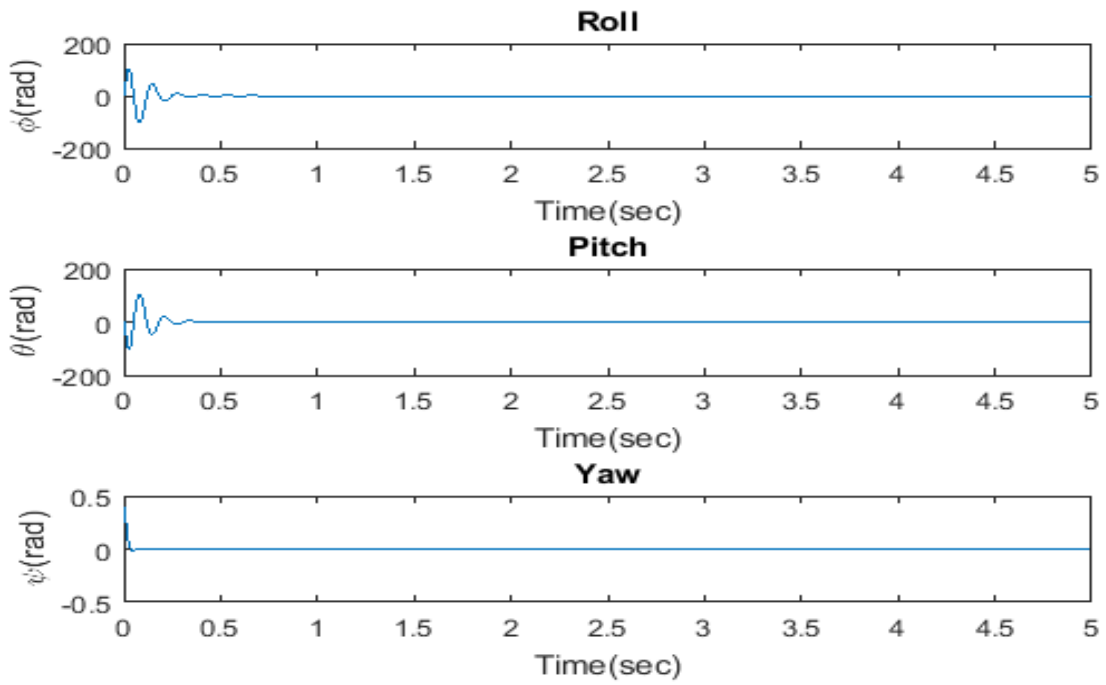


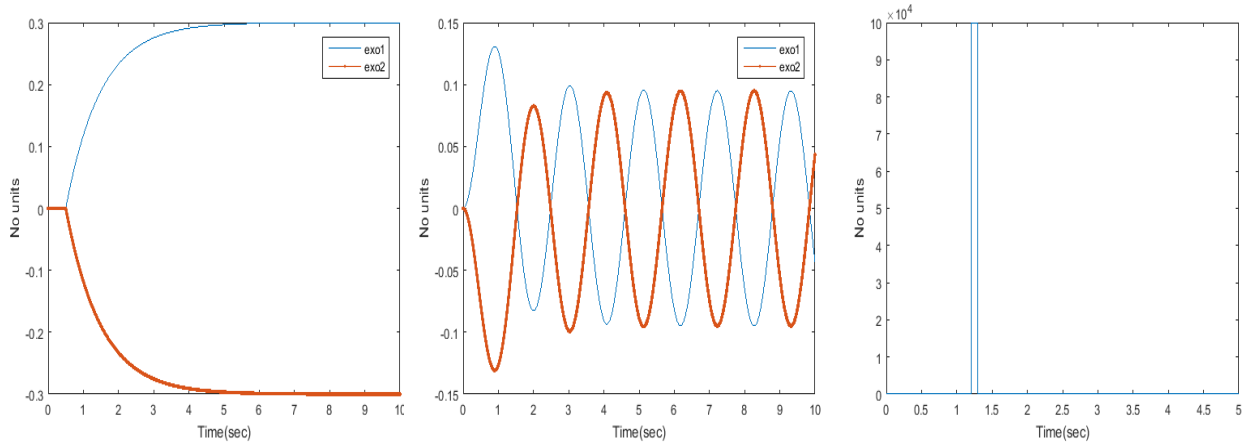

Figure 4.19: Unforced Attitude Roll-Pitch-Yaw Stabilization for the QUAV

Although all states were stabilizable, the feedback regulation studied here used a static exosystem matrix for the internal stability analysis and results in Figures 4.18 and 4.19. In practical applications the presence of a dynamic exosystem such as given in equation ( 3.162) must be used. This requirement meant the rejection of the generated disturbance input resulting from the exosystem.

### 4.4.2 Exosystem profile

An exosystem is a structured or unstructured disturbance generator. Although there are different exosystem profiles in existence, selecting a profile depends on the type of disturbance to be investigated. in this work, three types of exosystem profiles have been investigated. These are the smoothed step, impulse- and sinusoidal- type exosystem. The smoothed step exosystem represents a slow starting but constant disturbance. The impulse-type exosystem mimics a variable magni-

tude disturbance that occurs infinitesimally such as a sudden shock which is instantaneous. The sinusoidal-type exosystem mimics a periodic or oscillatory type disturbance profile such as a low amplitude, high frequency fluctuating signal (Khalil and Praly, 2013). The goal is to inject a disturbance signal whose purpose was to affect the system response and simultaneously be rejected by the developed controllers. Figure 4.20 represents the profiles of the considered exosystem. The




(a) Smoothed Step-type (b) Sinusoidal-type (c) Impulse-type

Figure 4.20: Disturbance Generator Profiles

QUAV stabilization and tracking experiments were performed under disturbance injection. The regulator experiments were done for the whole output made up of $x, y, z, \phi, \theta, \psi$. The aim of these experiments was to make the system output settle down to zero after the initial perturbation and also track the supplied reference signals. Two sets of results will be presented for all the controllers applied in this work. The first set of experiments studied the output error while the second set of experiments studied the correct characterizaton of the developed control laws with respect to the selected disturbance.

### 4.4.3 Immersion-invariance error feedback regulator results

The immersion invariance control law developed was used for output error regulation experiment.

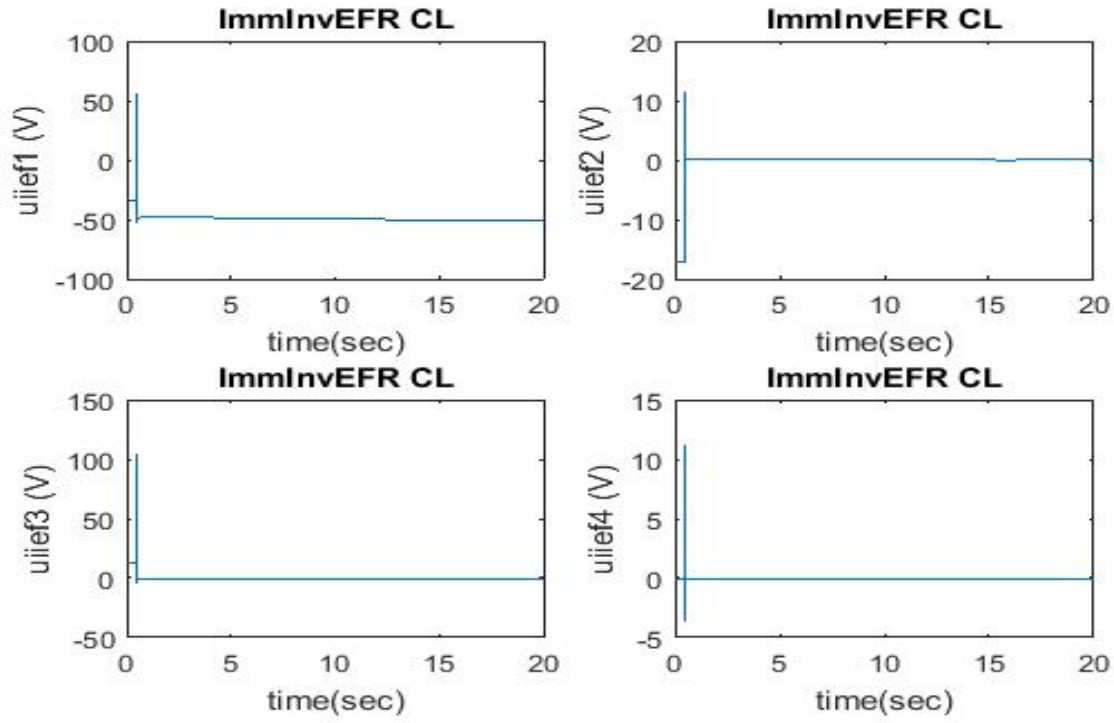



Figure 4.21: Control Effort of Immersion-Invariance Error Feedback Regulator

Figure 4.21 represents the profle of the immersion invariance error feedback control law. Figure 4.21 shows that each control variable $u_1 \ldots u_4$ were stable and bounded. The respective error output to be regulated was the $z, \phi, \theta, \psi$ state output of the system.

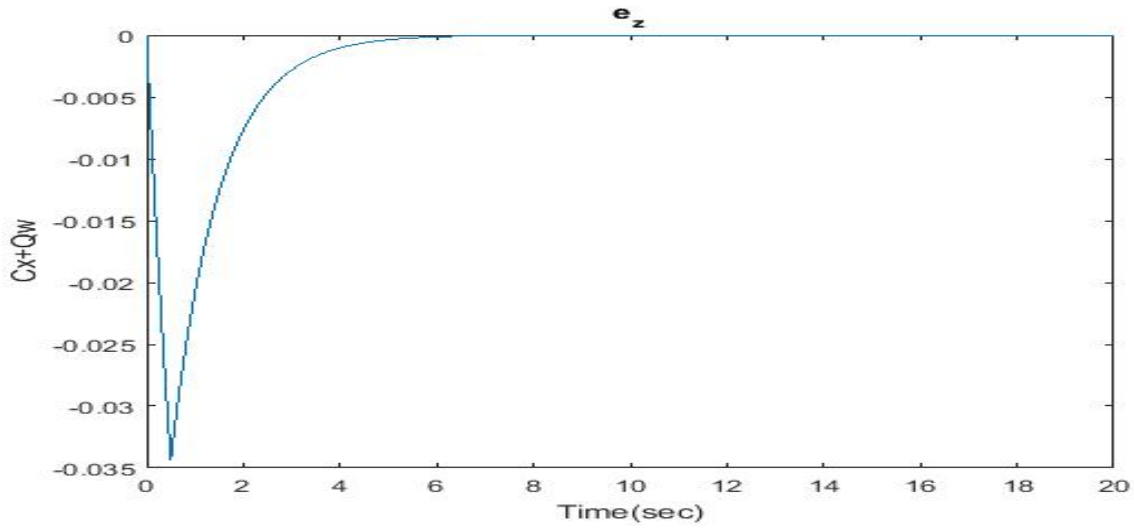



Figure 4.22: Z-axis Output Error

Figure 4.22 shows the translational stabilization of the output error along the z axis of the QUAV when using the immerison invariance error feedback controller. The altitude output error here is shown to settle to zero as time goes to infinity.

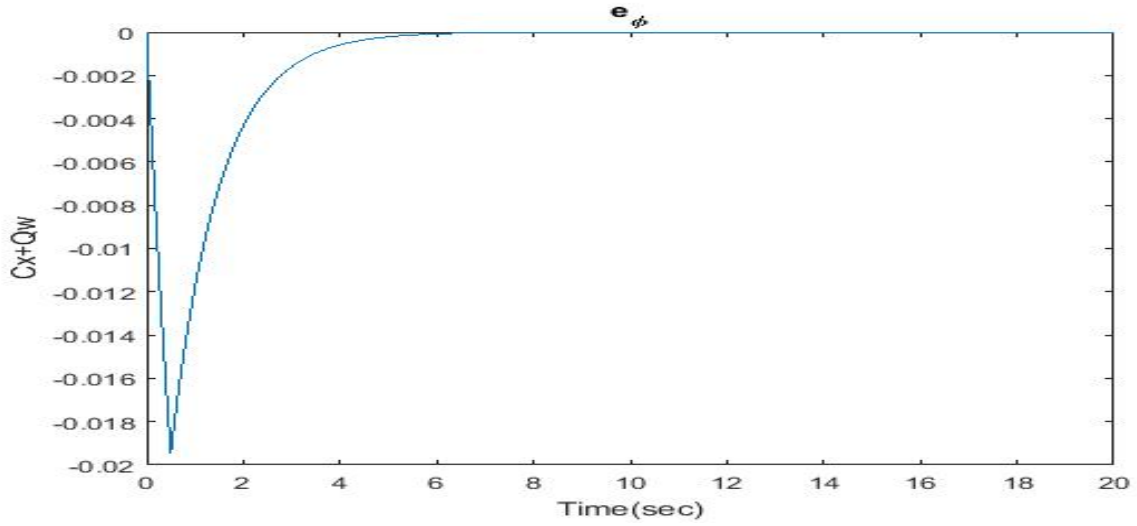



Figure 4.23: Roll Output Error

Figure 4.23 shows the rotational stabilization of the output error about the x-axis of the QUAV when using the immerison invariance error feedback controller.

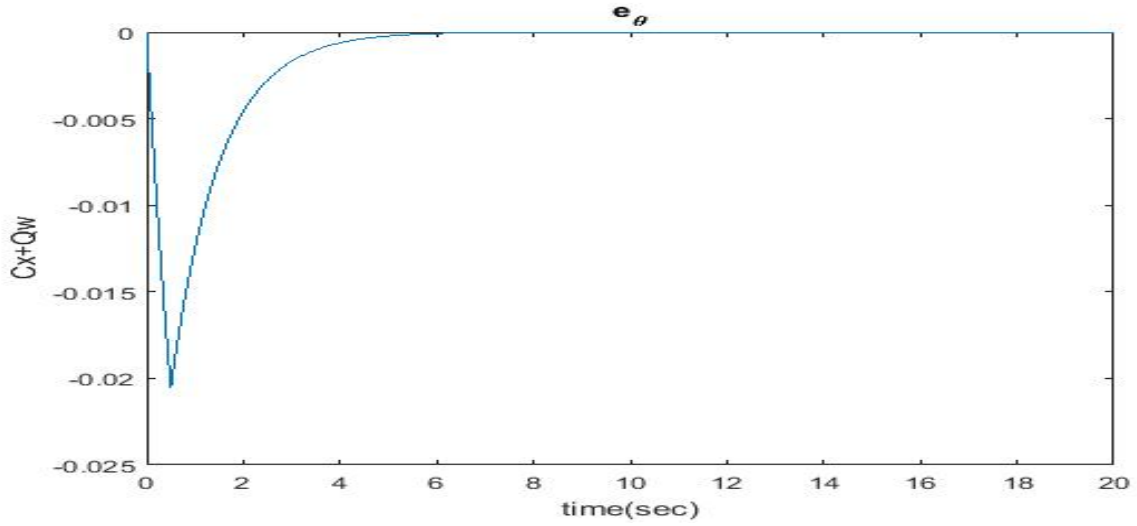



Figure 4.24: Pitch Output Error

Figure 4.24 shows the rotational stabilization of the output error about the y-axis of the QUAV

when using the immerison invariance error feedback controller.

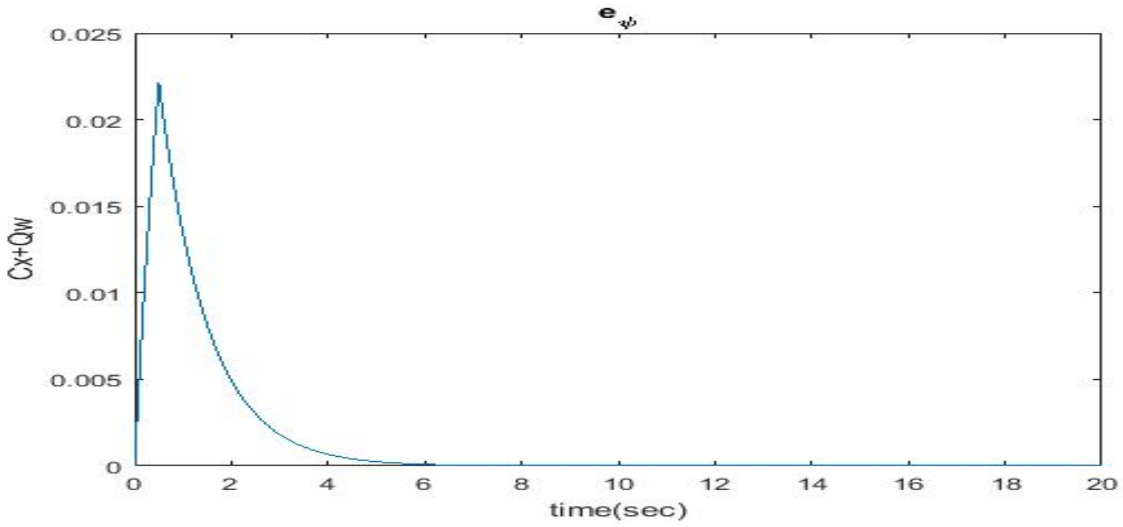



Figure 4.25: Yaw Output Error

Figure 4.25 shows the rotational stabilization of the output error about the z-axis of the QUAV when using the immerison invariance error feedback controller.

### 4.4.4 IIEFCL state output results

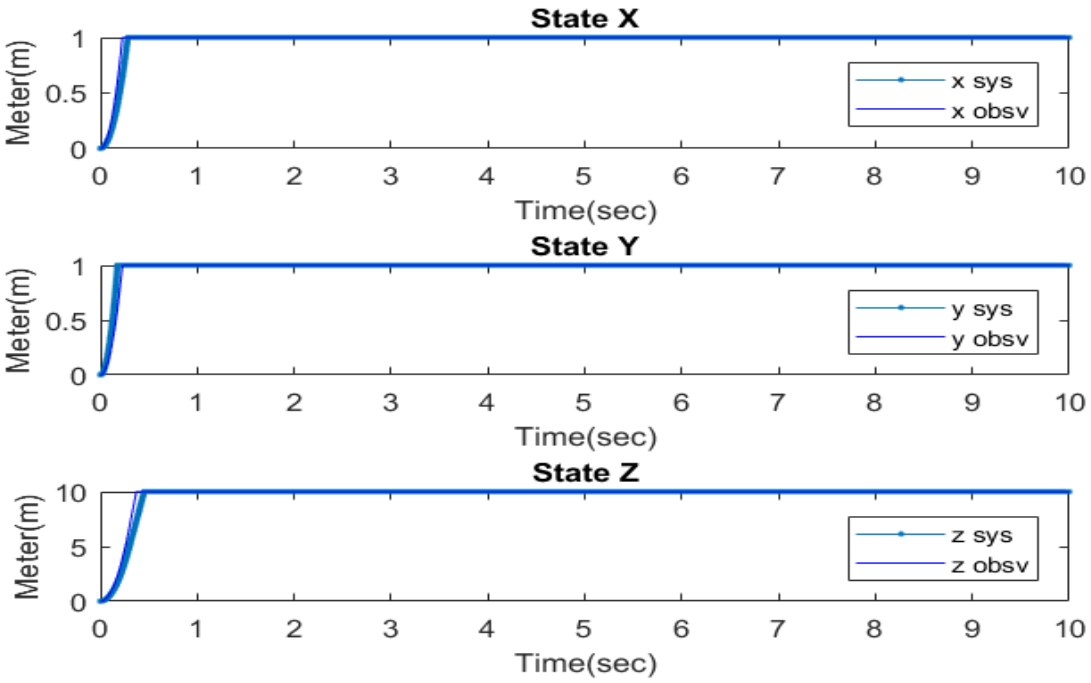



Figure 4.26: Translational Output Response for (x,y,z)=(1,1,10)

Figure 4.26 shows the output response from the IIEF controller for the three translational axes. The system response is bounded. The output response has a rise time of , no overshoot and a zero steady state error.

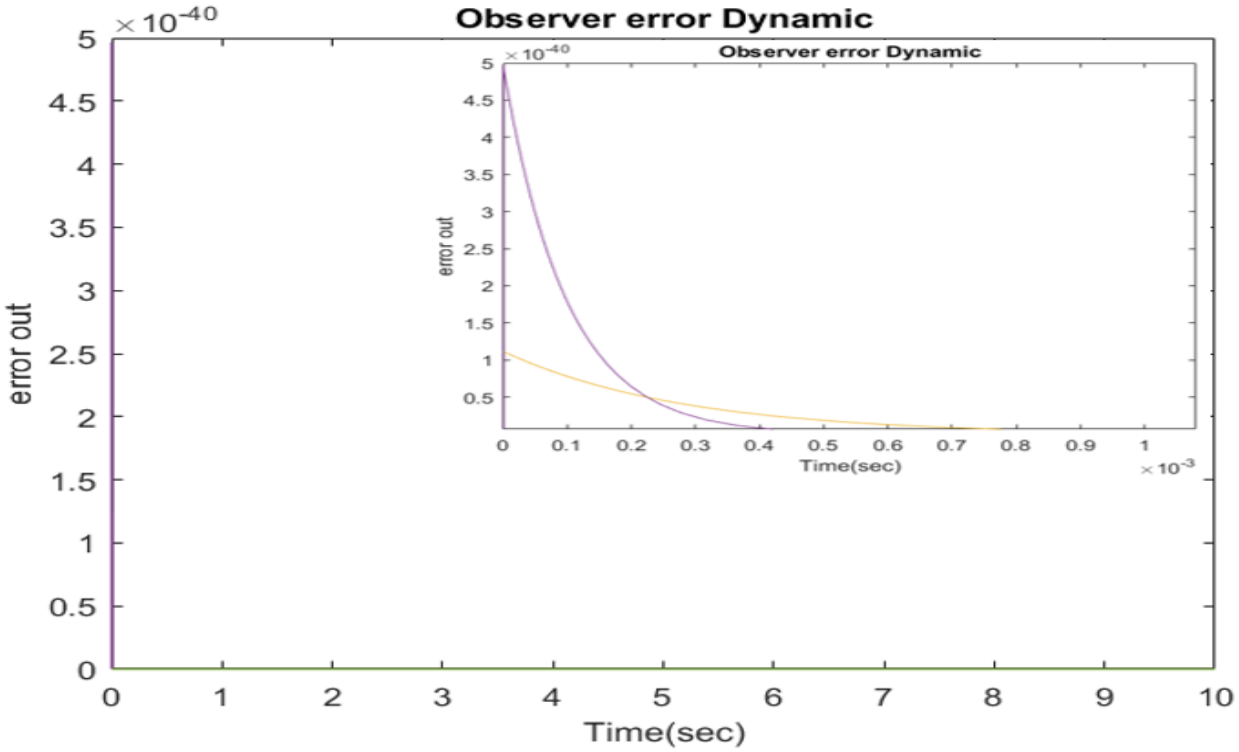



Figure 4.27: Translational Observer Output Error Response for (x,y,z)=(1,1,10)

The observer error dynamic which drives the state convergence is given in Figure 4.27. Asymptotic convergence of the error to zero at 0.85ms is clearly discernible and underscores the practicability of the HGO giving fast estimation.

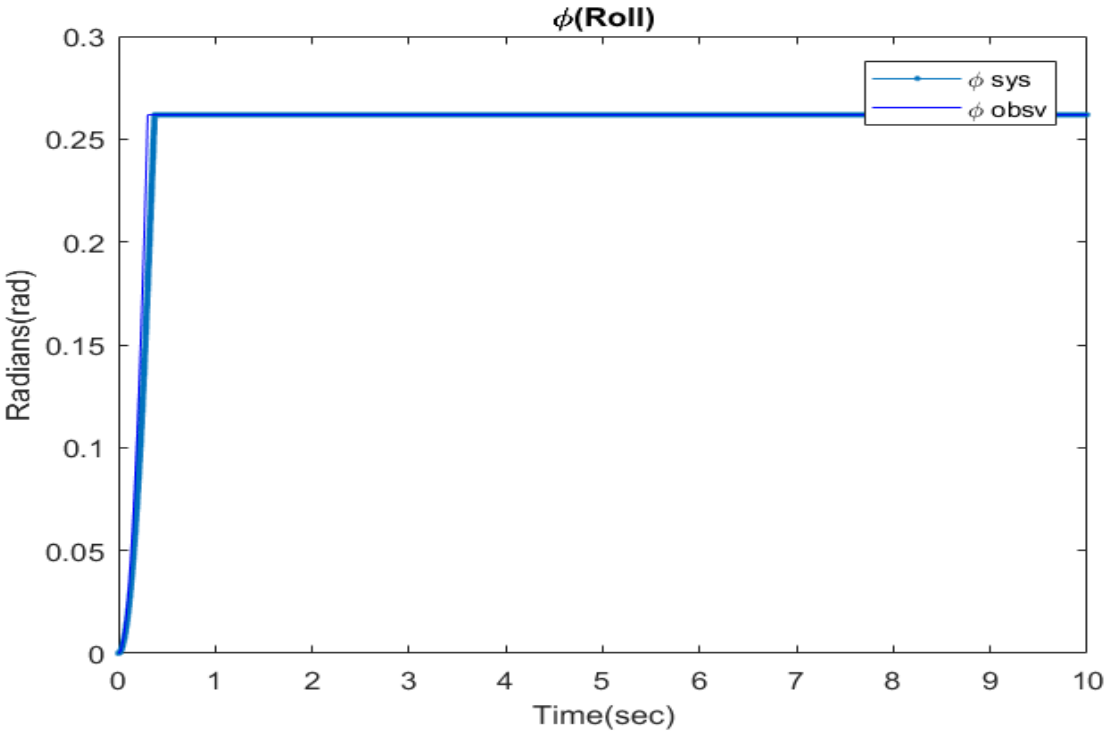



Figure 4.28: Attitude (Roll) Output Response for $\phi = \pi/12$

Figure 4.28 shows the output response from the IIEF controller for the roll axis. The system response is bounded. The output response has a rise time of , no overshoot and a zero steady state error.

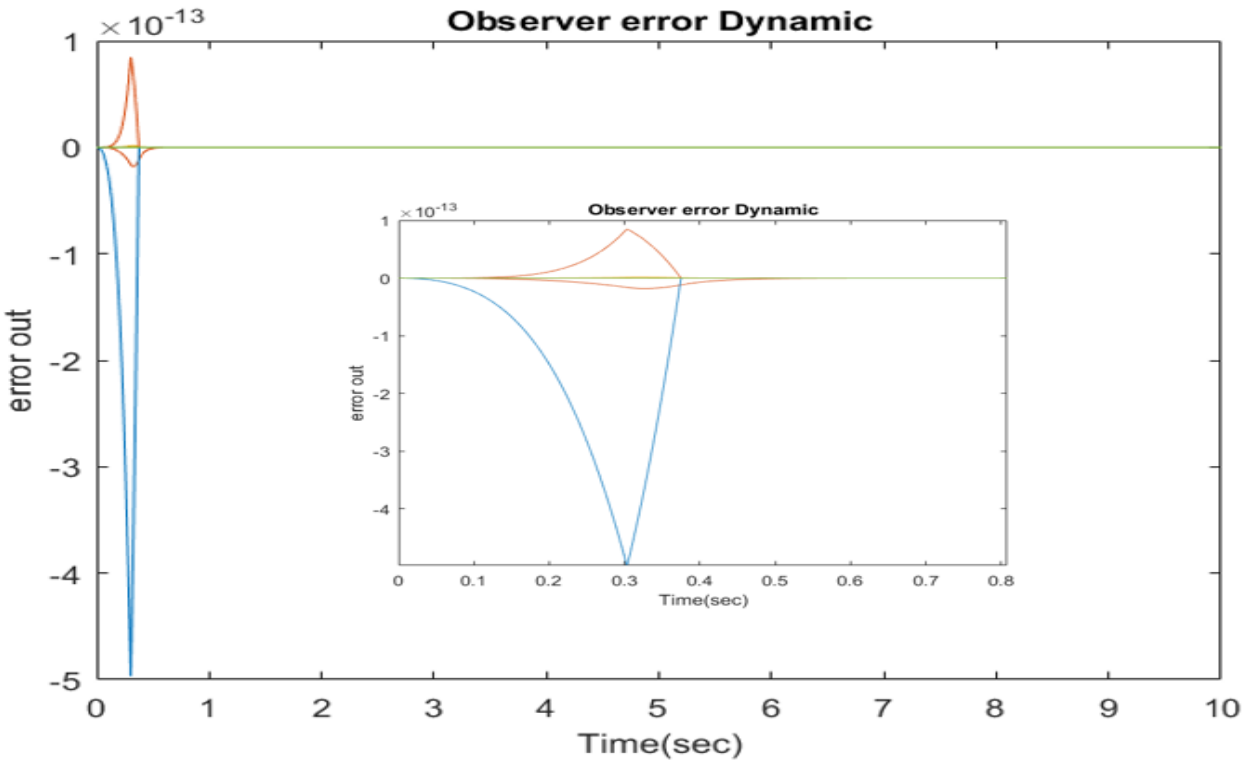



Figure 4.29: Roll Observer Output Error Response for $\phi = \pi/12$

The observer error dynamic which drives the attitude-roll convergence is given in Figure 4.29. Asymptotic convergence of the error to zero as given by the theory was proved with the observation error dynamic settling down to zero in 0.576s.

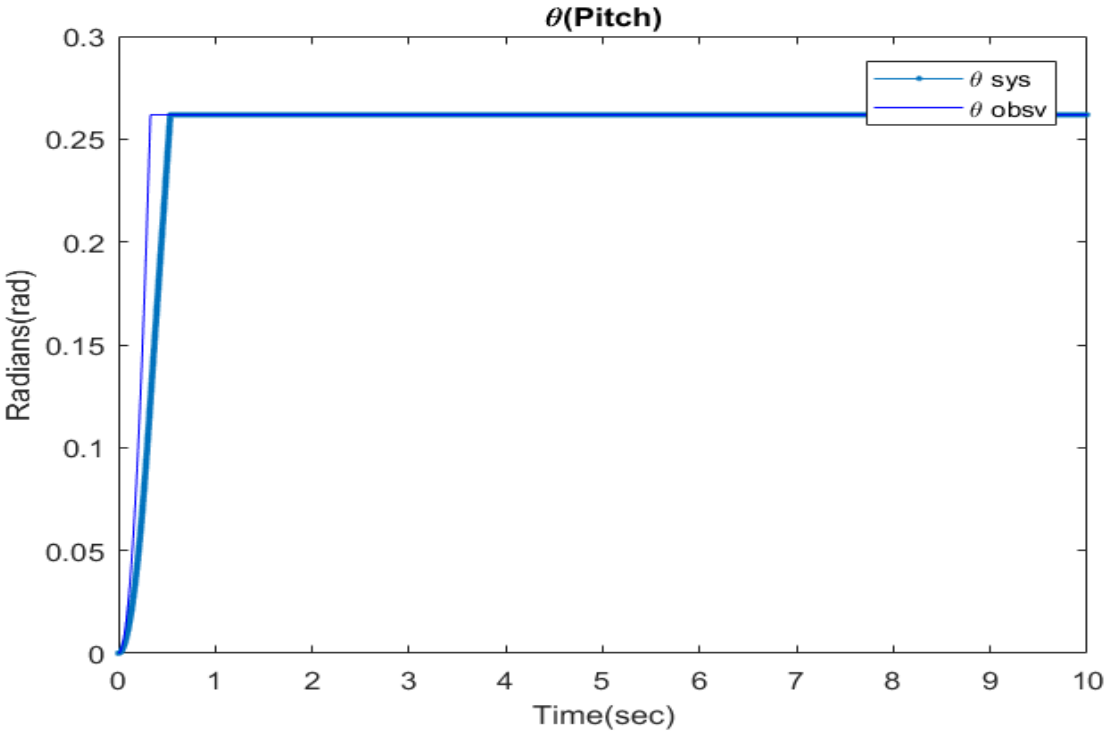



Figure 4.30: Attitude (Roll) Output Response for $\phi = \pi/12$

Figure 4.30 shows the output response from the IIEF controller for the pitch axis. The system response is bounded. The output response has a rise time of , no overshoot and a zero steady state error.

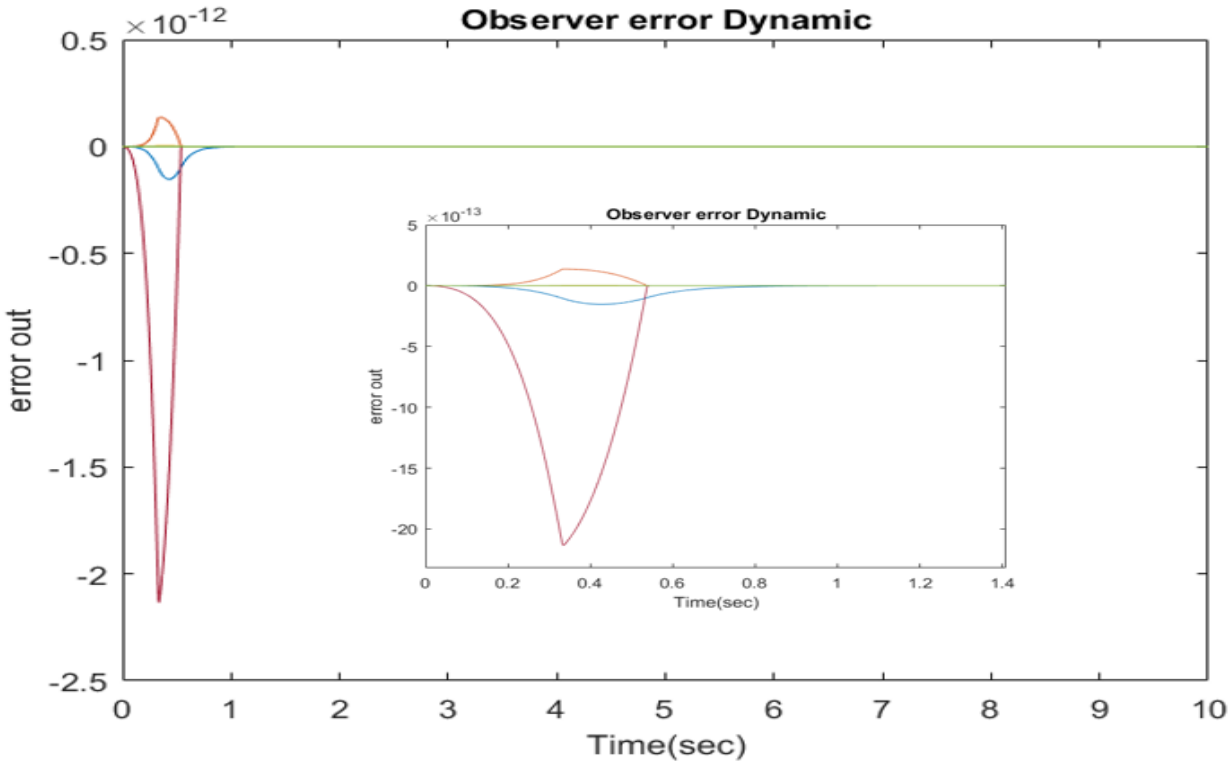



Figure 4.31: Pitch Observer Output Error Response for $\phi = \pi/12$

The observer error dynamic which drives the attitude-pitch convergence is given in Figure 4.31. The asymptotic convergence of the error to zero occured at 1.15s.

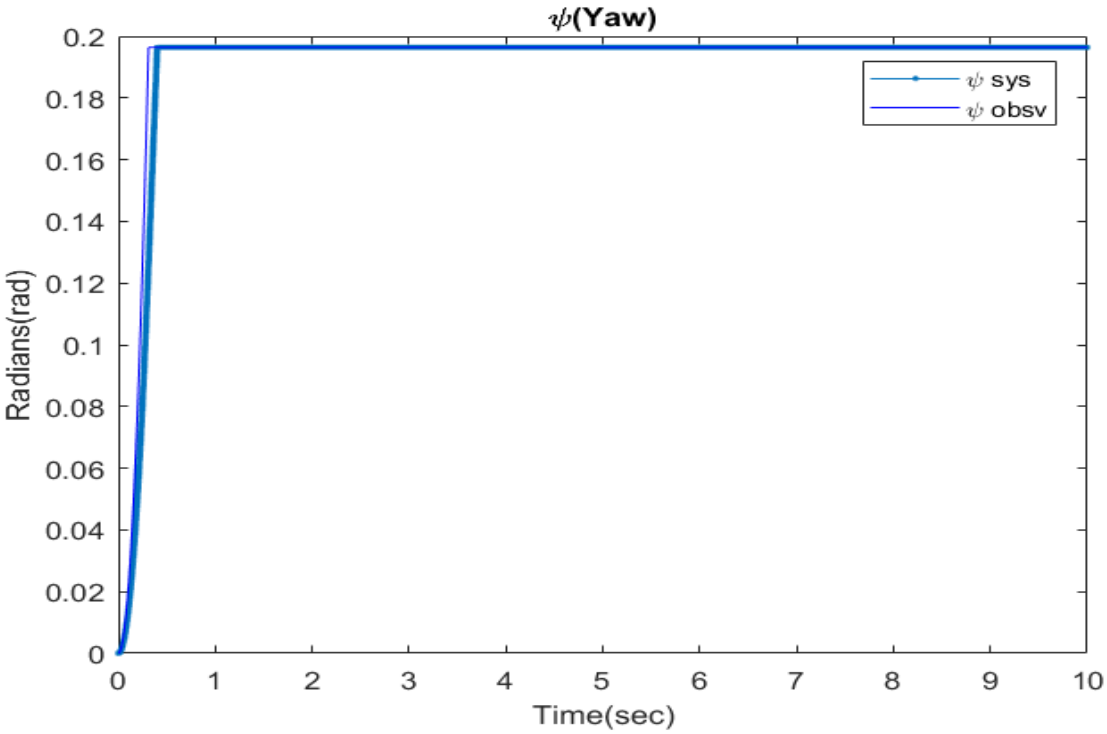



Figure 4.32: Attitude (Yaw) Output Response for $\phi = \pi/12$

Figure 4.32 shows the output response from the IIEF controller for the yaw axis. The system response is bounded. The output response has a rise time of , no overshoot and a zero steady state error.

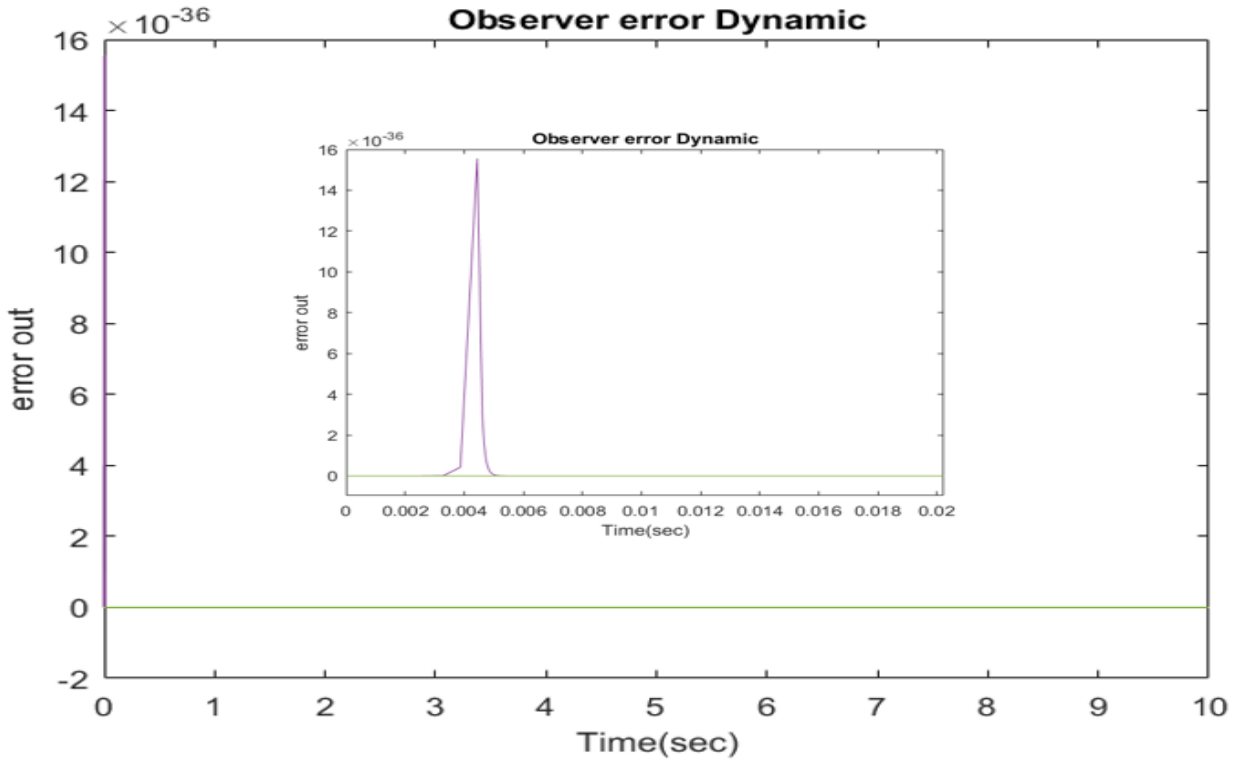



Figure 4.33: Yaw Observer Output Error Response for $\phi = \pi/16$

The observer error dynamic which drives the attitude-yaw convergence is given in Figure 4.33. The asymptotic convergence of the error to zero occured at 5.5ms. In every case, the HGO gave very fast response and error convergence which forced the output states of the QUAV to have fast convergence to the desired values as evidenced in Figures 4.26, 4.28, 4.30, 4.32.

### 4.4.5 Characterization of the control laws

The characterization of the control laws was both qualitative and quantitative. Qualitatively, the profiles of the various control laws has been displayed as plots.Figure 4.34 is a smoothed step function mimicking a constant magnitude and non-oscillating disturbance.

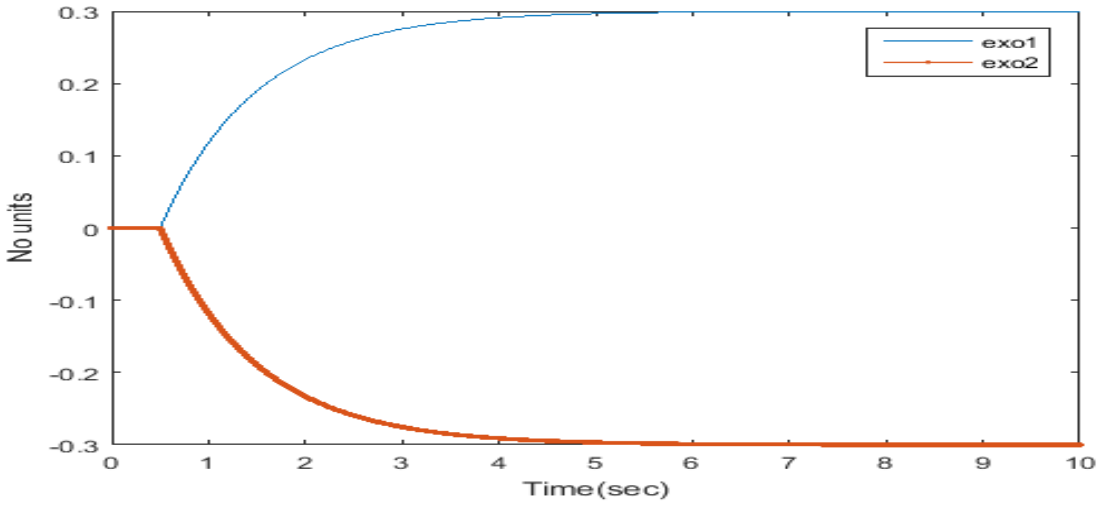



Figure 4.34: Smoothed Step Exosystem

The profile of the control laws when Figure 4.34 was applied as disturbance is given in Figure 4.35- 4.38.

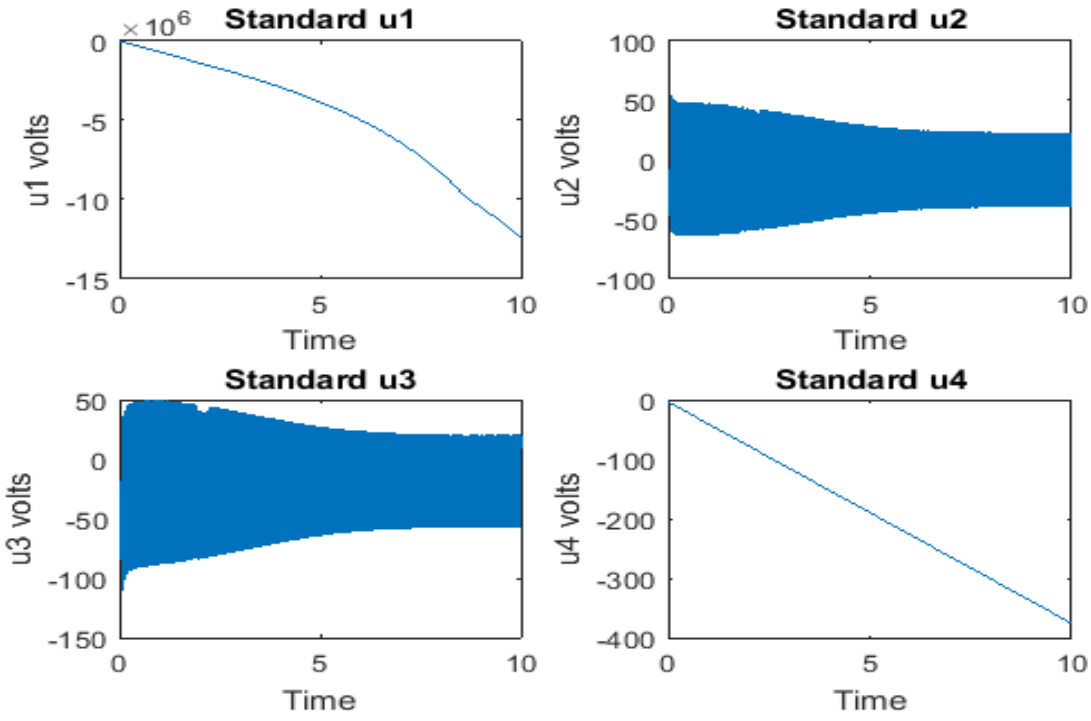



Figure 4.35: Backstepping NLCL for Step Input

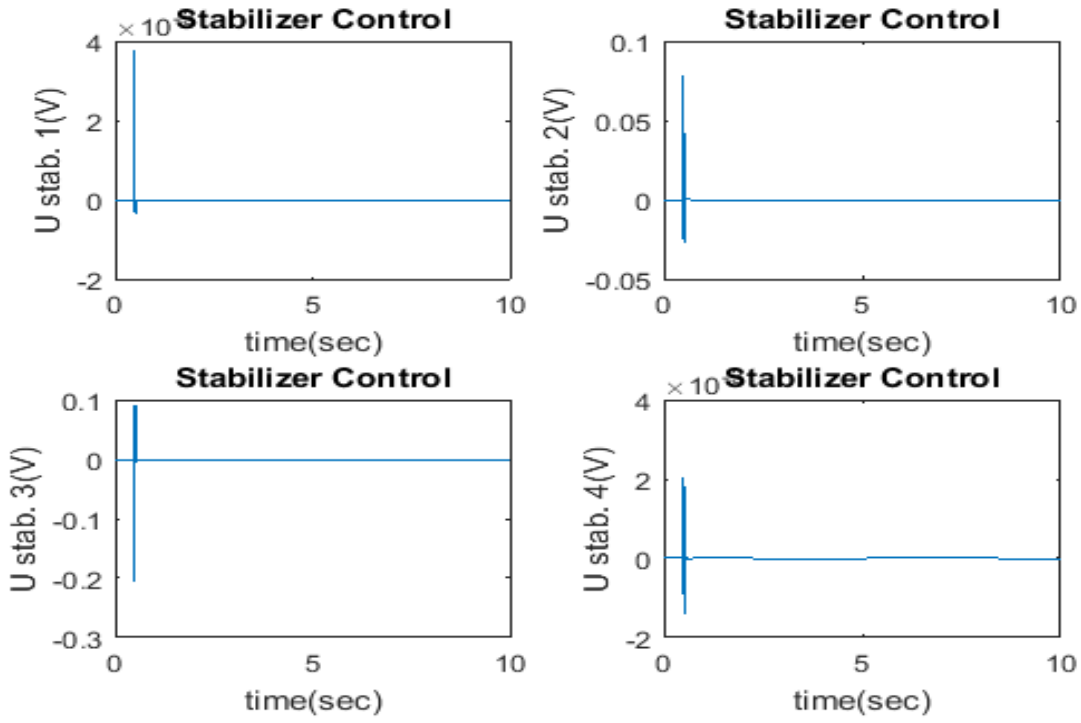



Figure 4.36: EFCL for Step Input

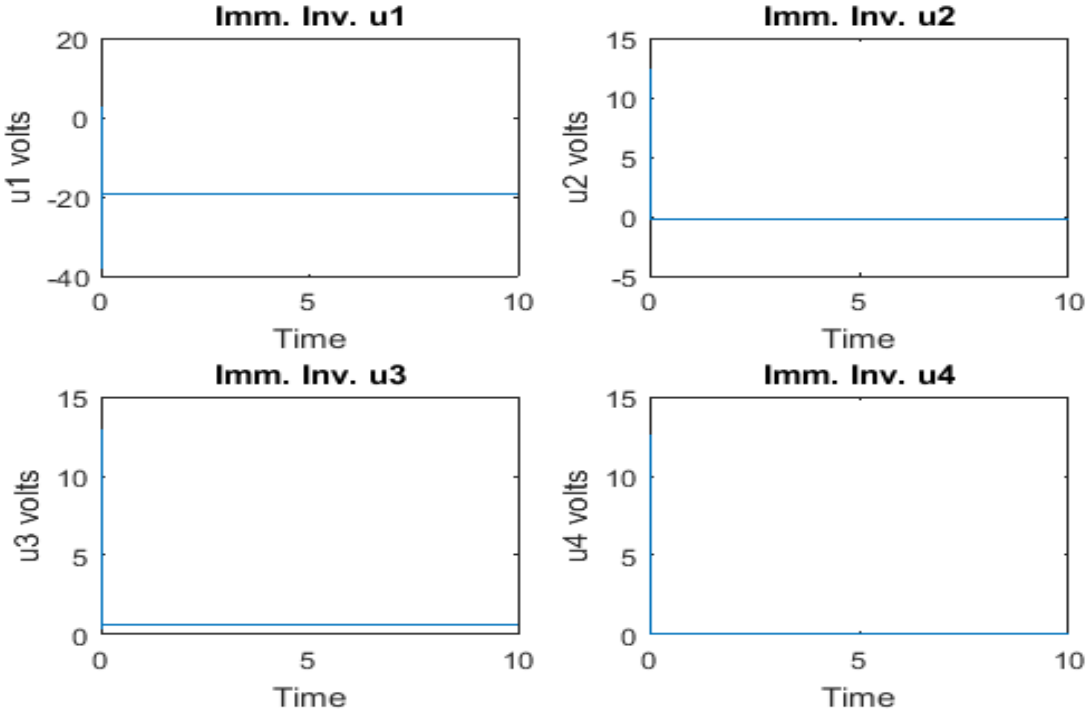



Figure 4.37: IICL for Step Input

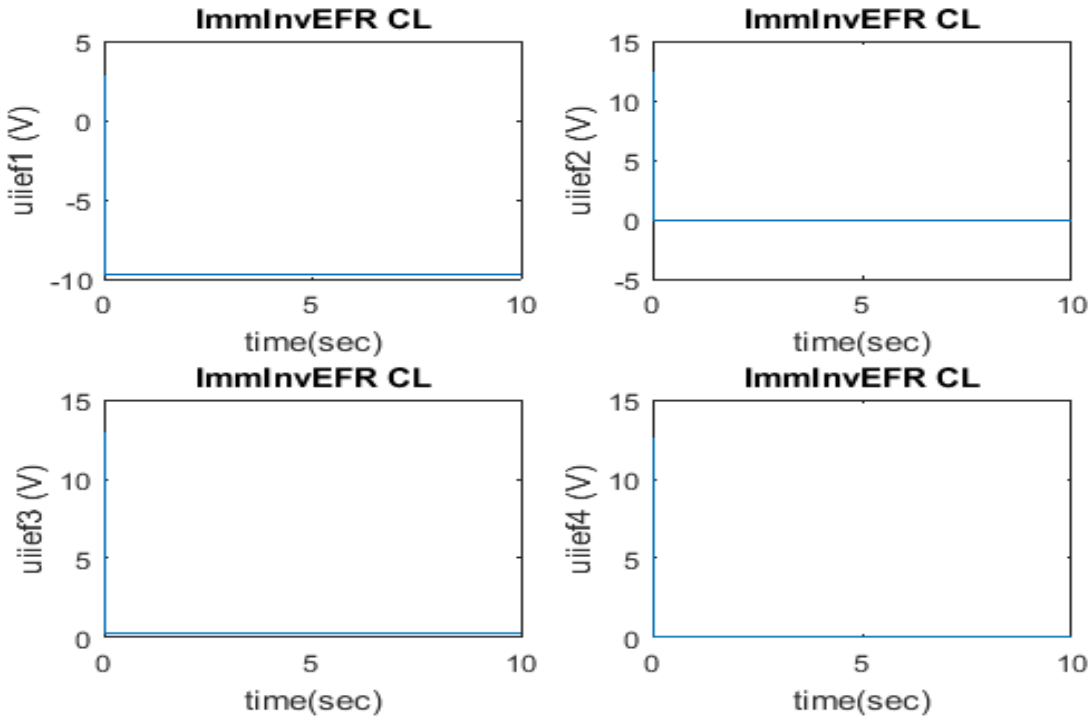



Figure 4.38: IIEFCL for Step Input

Figure 4.39 is a sinusoidal function mimicking a small amplitude but high frequency (oscillatory) disturbance.

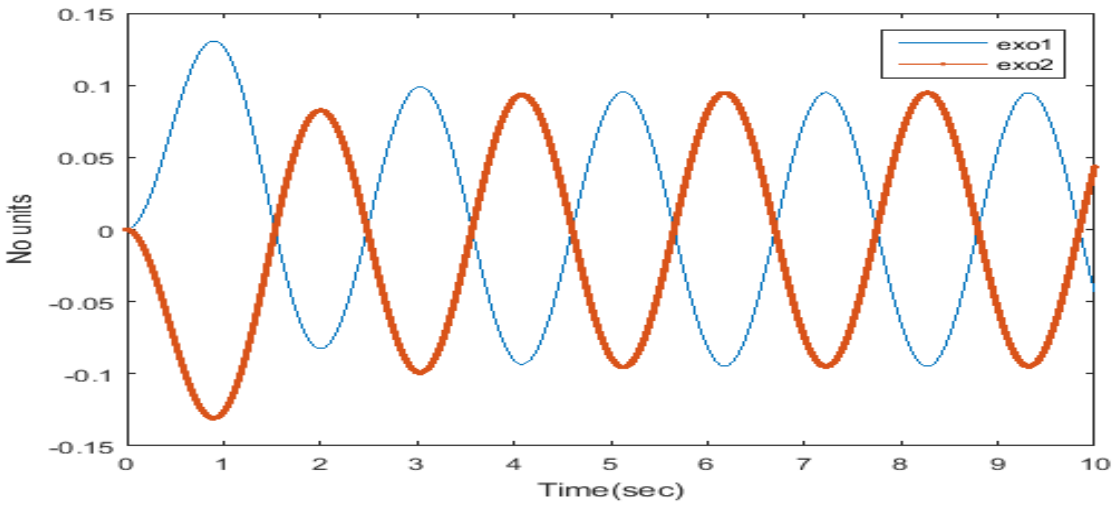



Figure 4.39: Sinosoidal Exosystem

Similarly, the profile of the control laws when Figure 4.39 was applied as disturbance is given

in Figure 4.40-4.43.

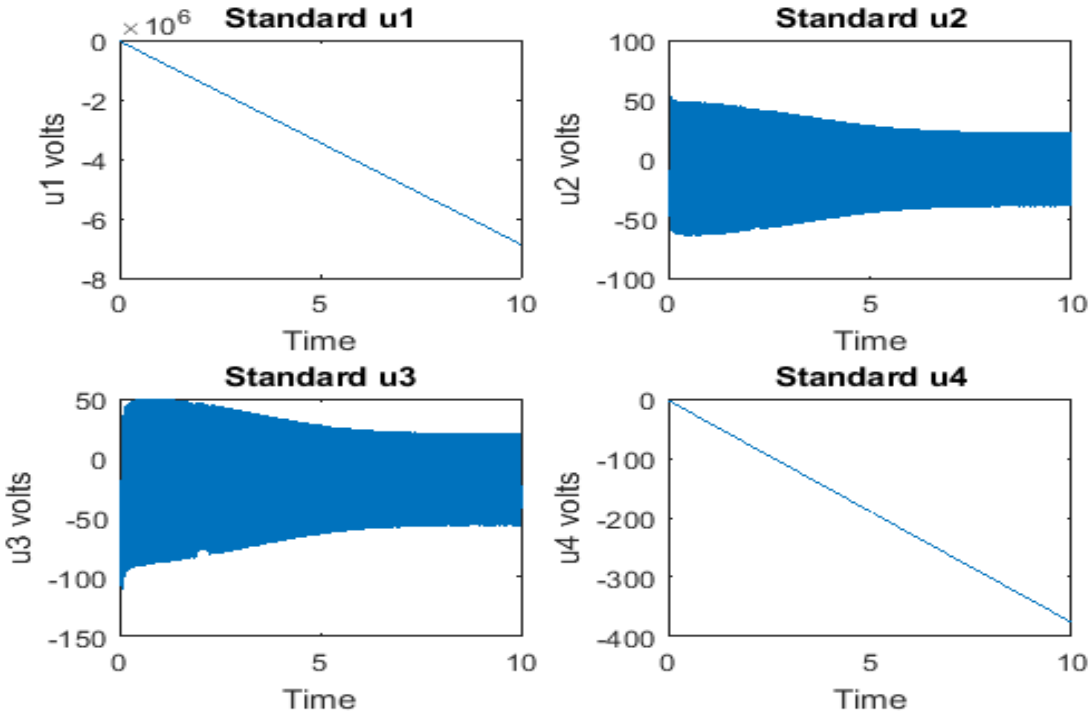



Figure 4.40: Backstepping NLCL for Sinusoidal Input

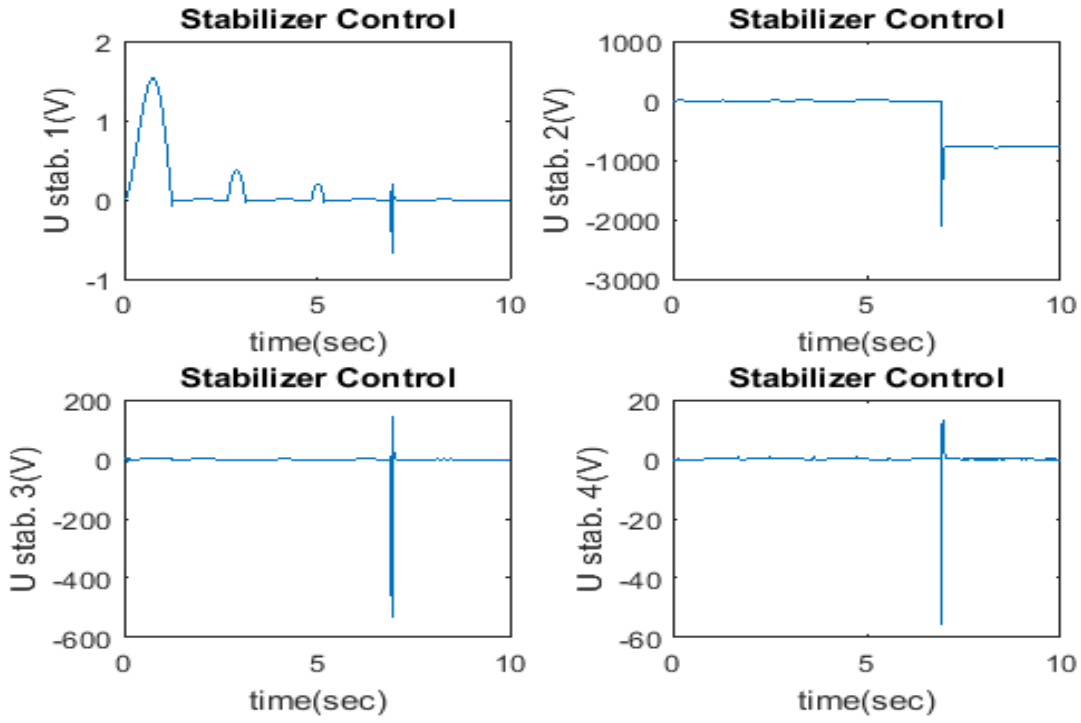



Figure 4.41: EFCL for Sinusoidal Input

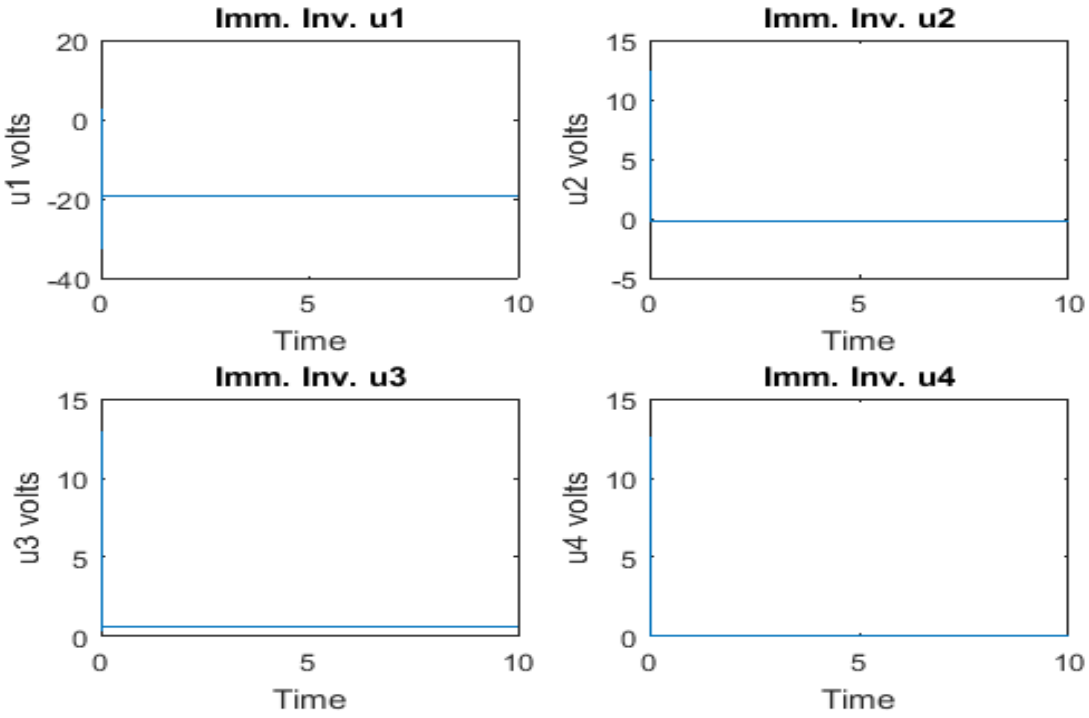



Figure 4.42: IICL for Sinusoidal Input

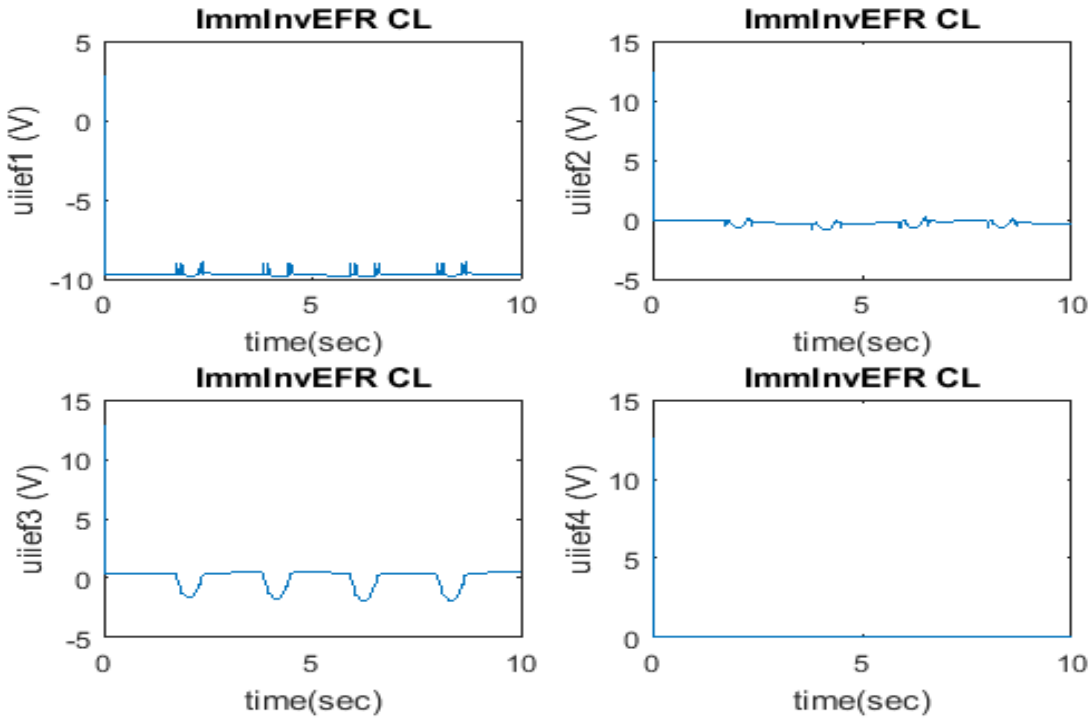



Figure 4.43: IIEFCL for Sinusoidal Input

Figure 4.44 is an impulse function mimicking sudden high amplitude, shock-type disturbance.

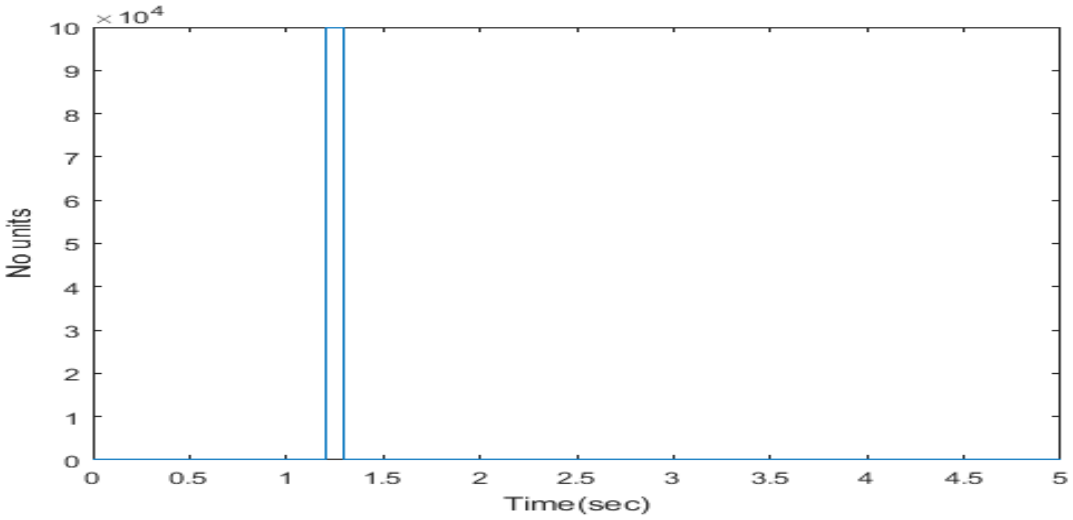



Figure 4.44: Impulse Exosystem

Finally, the profile of the control laws when Figure 4.44 was applied as disturbance is given in Figure 4.45-4.48.

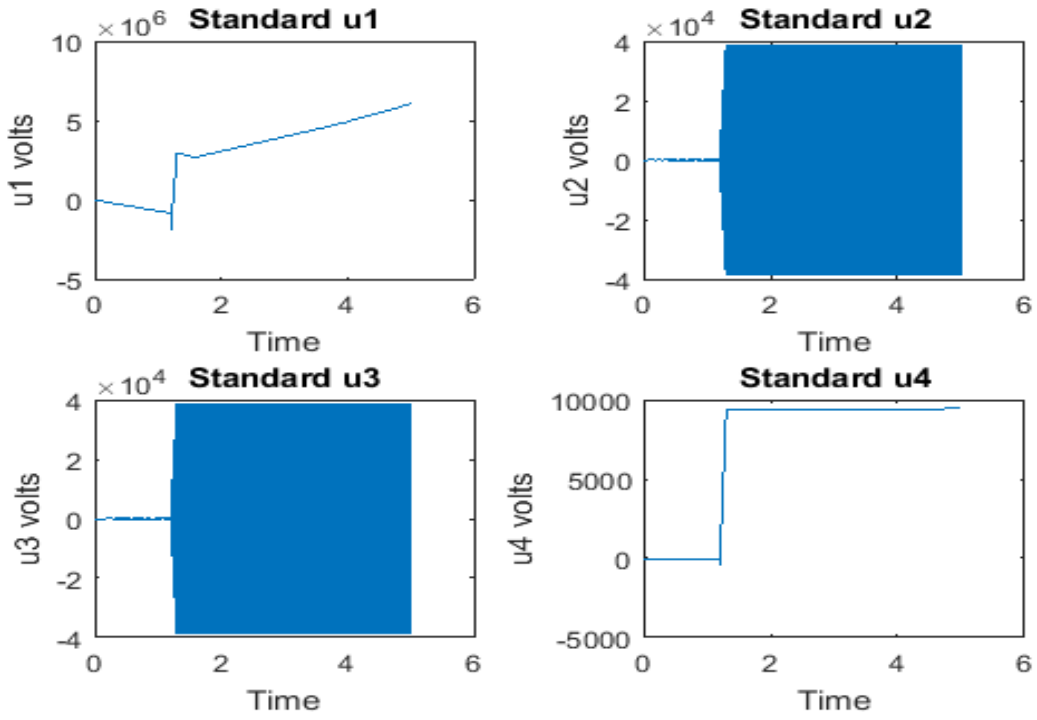



Figure 4.45: Backstepping NLCL for Impulse Input

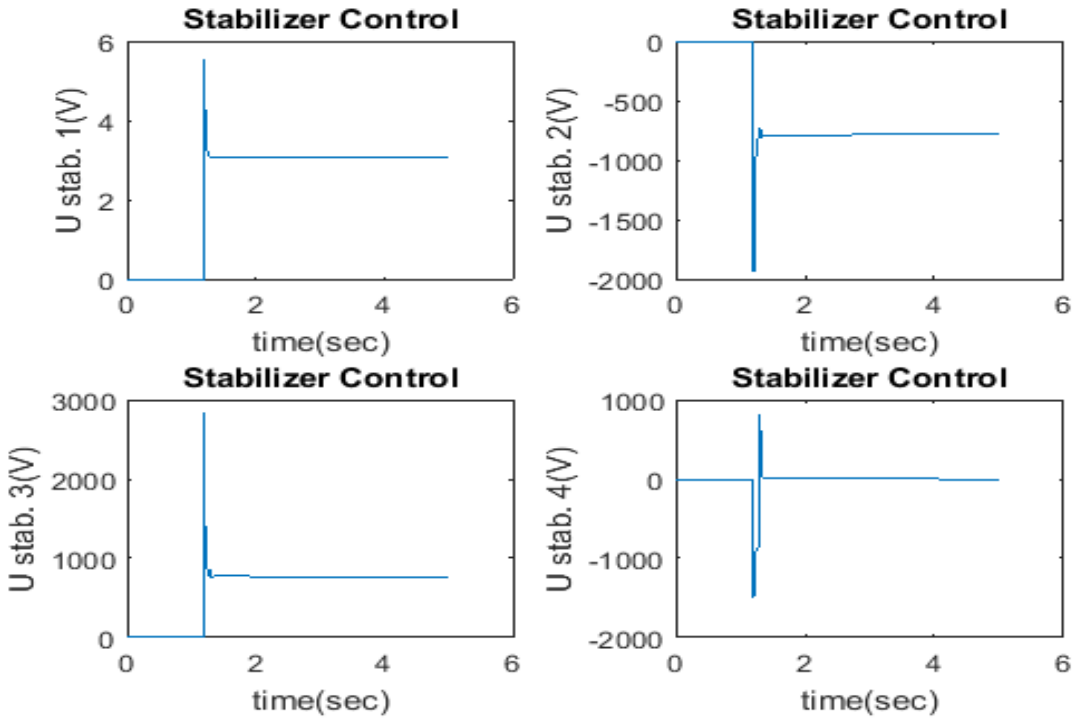



Figure 4.46: EFCL for Impulse Input

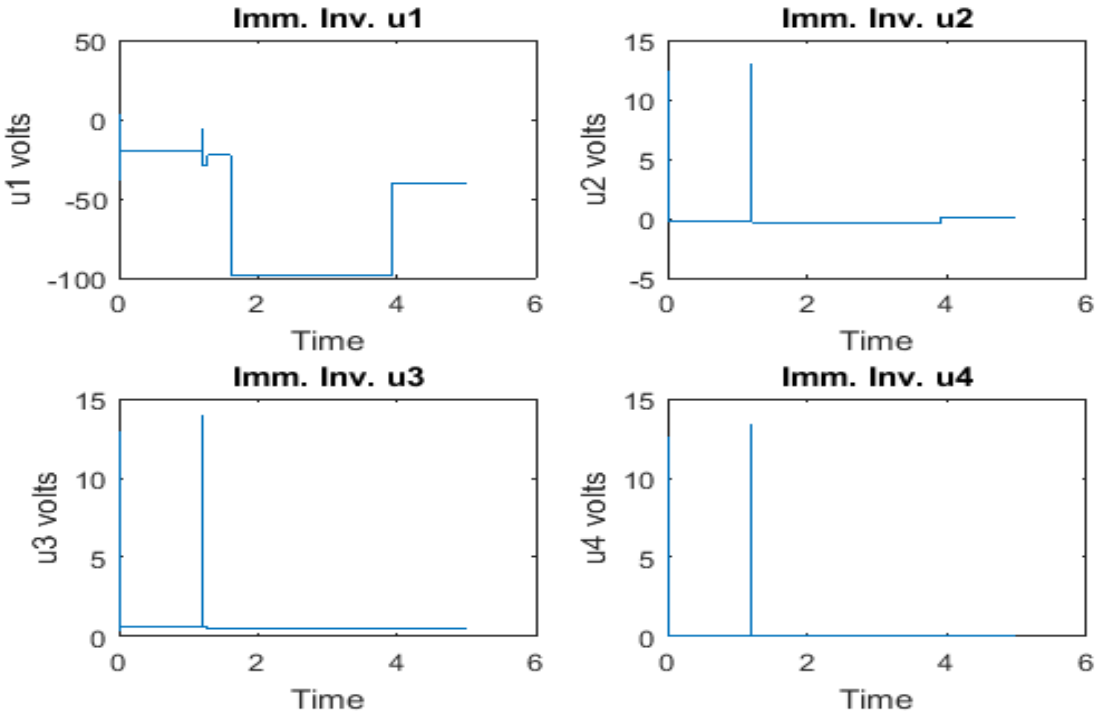



Figure 4.47: IICL for Impulse Input

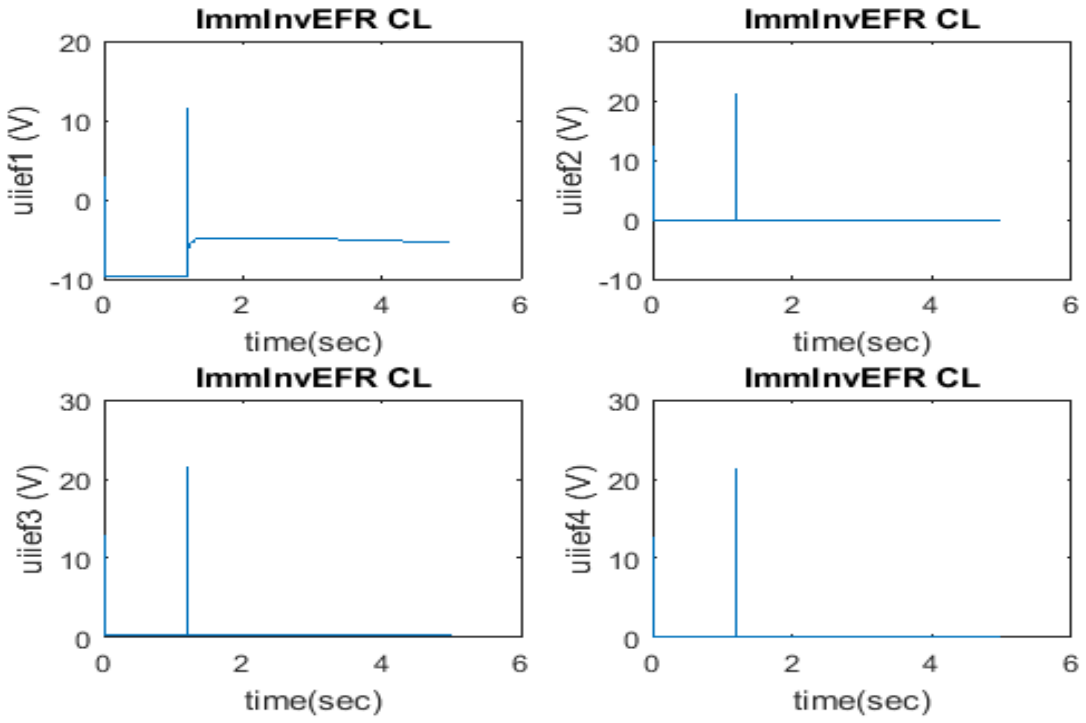



Figure 4.48: IIEFCL for Impulse Input

The results shows that the various control laws could be graded from good to best according to the displayed profiles when smoothed disturbance was present, next was when the instantaneous impulse disturbance was present and finally with the sinusoidal disturbance present.

Quantitatively, analysis of the control laws was made by computing the integral of the squared control input(ISCI) and the standard deviation of the ISCI. The ISCI metric is an energy function of the control inputs and was computed for each of the four control inputs $U1, U2, U3, U4$ of the QUAV. $U_1$ is equivalent to the translational control torque, $U_x, U_y, U_z$. $U_2, U_3, U_4$ are equivalent to the rotational attitude control torques, $U_\phi, U_\theta, U_\psi$. This computation was made by taking the integral of the square for each control signal. This energy signal was then analyzed by computing certain performance metrics such as the mean energy and standard deviation. Three different exosystem profiles were investigated and are displayed in Figure 4.20 of section 4.4.2. Table 4.3 summarizes the values of standard deviation for the energies of the four controllers used when a smoothed step exosystem was applied.

Table 4.3: Standard Deviation for a Smoothed Step Exosystem

| S/No | Cont. Law | Std. Dev. 1 | Std. Dev. 2 | Std. Dev. 3 | Std. Dev. 4 | Mean Dev. | Comment |
|---|---|---|---|---|---|---|---|
| 1 | NLCL | 1.45e15 | 2.8e3 | 5.35e3 | 1.13e6 | 3.63e14 | *** |
| 2 | EFR | 545.5e-12 | 1.82e-6 | 351e-9 | 359e-12 | 5.43e-7 | * |
| 3 | II | 319.6e9 | 4.23e15 | 6.6e15 | 246.75 | 2.71e15 | **** |
| 3 | IIEF | 452.6 | 62.6e-3 | 510.7e-3 | 8.65e-3 | 113.293 | ** |

Table 4.4 summarizes the values of standard deviation for the energies of the four controllers used when a sinusoidal low amplitude but high frequency exosystem was applied.

Table 4.4: Standard Deviation Results for a Sinusoidal Exosystem

| S/No | Cont. Law | Std. Dev. 1 | Std. Dev. 2 | Std. Dev. 3 | Std. Dev. 4 | Min. Dev. | Comment |
|---|---|---|---|---|---|---|---|
| 1 | NLCL | 377.62e12 | 2.81e3 | 5.34e3 | 1.131e6 | 9.441e13 | **** |
| 2 | EFR | 9.17 | 696.7 | 2.6e6 | 77.38e-3 | 6.5e5 | *** |
| 3 | II | 1.81e3 | 250.4e-3 | 2.0 | 34.62e-3 | 453.07 | ** |
| 3 | IIEF | 452.3 | 62.9e-3 | 499.12e-3 | 8.63e-3 | 113.23 | * |

Table 4.5 summarizes the values of standard deviation for the energies of the four controllers used when an impulse exosystem was applied.

Table 4.5: Standard Deviation Results for an Impulse Exosystem

| S/No | Cont. Law | Std. Dev. 1 | Std. Dev. 2 | Std. Dev. 3 | Std. Dev. 4 | Min. Dev. | Comment |
|---|---|---|---|---|---|---|---|
| 1 | NLCL | 19.44e12 | 803.51e6 | 803.51e6 | 95.66e6 | 4.86e12 | **** |
| 2 | EFR | 4.61e3 | 642.8e3 | 672.12e3 | 10.1 | 3.299e5 | *** |
| 3 | II | 8.67e3 | 148.51e-3 | 254.18e-3 | 7.05e-3 | 2.17e3 | ** |
| 3 | IIEF | 27.3524 | 0.012 | 0.0905 | 0.0016 | 6.8641 | * |

The comments in Tables 4.3 ,4.4 and 4.5 grades the performance of the control effort from best $(*)$ to worst $(****)$.

### 4.4.6 Comparison of results from various control laws

Table 4.6 has summarized the results from the mean standard deviation computation

Table 4.6: Average Standard Deviation Results for Each Exosystem

| S/No | Cont. Law | Equation | Step | Sinusoidal | Impulse | |
|---|---|---|---|---|---|---|
| 1 | NLCL | equations (3.147)-(3.152) | 3.63e14 | 9.441e13 | 4.86e12 | **** |
| 2 | EFCL | equation (3.251)-(3.254) | 5.43e-7 | 6.5e5 | 3.299e5 | *** |
| 3 | IICL | equation (3.243) | 2.71e15 | 453.07 | 2.17e3 | ** |
| 3 | IIEFCL | equation (3.259) | 113.293 | 113.23 | 6.8641 | * |

Overall the best performance amongst all controllers was the IIEFCL followed by the IICL , the EFCL and finally the NLCL. Ozbek *et al.*, (2015) compared some linear and nonlinear feedback control laws used for QUAV-type systems. Their results used several metric for the evaluation. Two of those metrics were the integral of the squared control input (ISCI) and the control signal variance were used to analyse the control signal. The results obtained in this thesis were compared to that obtained by Ozbek *et al.*, (2015). The quantitative analyses benchmarks the ISCI results obtained from the developed IIEFCL against the best performing results from Ozbek *et al.*, (2015) using the variables: $\%$ improvement, bench mark value(BMV) and developed value(DV) in the relation:

$$\% = \frac{BMV - DV}{BMV} * 100 \tag{4.1}$$

Table 4.7: Integral of the Squared Control Input(ISCI) for Three Different Sets of Controllers

| S/No | Cont. Law | Researcher | ISCI U1 | ISCI U2 | ISCI U3 | ISCI U4 | Mean |
|---|---|---|---|---|---|---|---|
| 1 | FBL1 | Ozbek *et. al.* | 4.647e4 | 513.9530 | 197.7108 | 0.0350 | 11.7954e3 |
| 2 | FBL2 | ″ | 4.6572e4 | 551.6272 | 194.7696 | 0.0161 | 11.8296e4 |
| 3 | FBL3 | ″ | 4.7247e4 | 618.3654 | 227.3134 | 0.0129 | 12.0231e4 |
| | | | | | | | |
| 1 | BS1 | ″ | 9.81e4 | 28.7015 | 21.4519 | 0.97380 | 24.5378e4 |
| 2 | BS2 | ″ | 9.81e4 | 29.166 | 22.5848 | 0.3052 | 24.538e4 |
| 3 | BS3 | ″ | 9.8971e4 | 32.8089 | 30.4720 | 0.04020 | 24.7586e4 |
| | | | | | | | |
| 1 | SMC1 | ″ | 4.3523e4 | 63.9705 | 152.3928 | 0.0012 | 10.9348e3 |
| 2 | SMC2 | ″ | 4.36e4 | 66.9137 | 56.4994 | 0.0046 | 10.9308e3 |
| 3 | SMC3 | ″ | 4.5957e4 | 107.55 | 93.23 | 0.2386 | 11.5395e3 |
| | | | | | | | |
| 1 | IIEF(step) | Proposed | 1.89e3 | 260.8e-3 | 2.09 | 36.1e-3 | 473.096 |
| 2 | IIEF(sin) | ″ | 1.88e3 | 261.9e-3 | 2.08 | 35.995e-3 | 470.59 |
| 3 | IIEF(imp) | ″ | 209.99 | 0.0577 | 0.4414 | 0.0079 | 52.62425 |

Using equation (4.1), the developed IIEFCL with step input disturbance vs. FBL1 showed a 95.95% improvement on U1, 99.95% improvement on U2, 98.94% improvement on U3 and underperformed by -3.14% on U4. The developed IIEFCL with step input disturbance vs. BS1 showed a 98% improvement on U1, 99.1% improvement on U2, 90.3% improvement on U3 and 96.3% improvement on U4. The developed IIEFCL with step input disturbance vs. SMC1 showed a 95.7% improvement on U1, 99.6% improvement on U2, 98.6% improvement on U3 and underperformed by -29.08% on U4. It was however observed that in every case, the proposed IIEFCL has significantly lower average energy values compared to the baseline controllers against which it was compared. On average, the IIEFCL was 95.99%, 99.81% and 95.57% more energy efficient than the FBL1, BS1 and SMC1 controllers respectively.

# CHAPTER 5
# SUMMARY AND CONCLUSIONS

## 5.1 Summary

A constructive approach for the development of a dynamic output feedback internal model-based observer regulator has been developed for the RTAC, CIP and QUAV systems. The design goals included internal stability, output stability and tracking with an observer internal model as the regulating element. The concept of immersion invariance stabilization was also demonstrated in the RTAC system with the underlying design principles and robustness characteristics shown. System immersion was established as a tool in both internal model-based regulator design and immersion invariance design. Finding exact solution to the regulator problem in the presence of disturbance generator was discussed and mention was made of the difficulty in finding a closed solution to the generalized immersion problem especially as it concerned the QUAV. Control law design then proceeded to replace the search for an immersion map with immersion invariant control law. This synergy used a base error feedback regulator as the core of the developed controller.

The RTAC and CIP are single-input multiple-output (SIMO) nonlinear systems since they have a single input and four possible outputs to select from. As such, they do not qualify to be called multiple-input multiple-output (MIMO) systems. MIMO systems must have at least two or more inputs and outputs. The QUAV system is a MIMO nonlinear system having four inputs and six possible outputs to choose from. The unbalanced number of inputs and outputs in the QUAV made it the selected candidate for a non-square MIMO system. Each implementation of the controllers on the QUAV system utilized a high fidelity model with a double loop configuration.

The inner loop is the actuator control loop with four QUAV rotors that were driven by four brushless D.C motors. A PID and state feedback controller was used in this inner loop with PID gains

tuned with Matlab's PID tuner giving the values $kp = 1.76e + 04, ki = 75.7, kd = 9.45e + 05$. The state feedback controller utilized poles placed at $-19.970, -20.18$ respectively. The poles were placed at this location to make them faster than the system poles.

For the outer loop control, three standard control laws and a fourth proposed control law were developed for control of the QUAV system. The first three control laws are the nominal nonlinear backstepping controller (NLCL) , a standard nonlinear error feedback observer regulator (EFCL) and an immersion invariance controller (IICL). The fourth controller developed was an immersion invariance error feedback regulator (IIEFCL), which is being proposed as a suitable candidate for substitution of the existing controllers. The nominal nonlinear controller was theoretically stabilizing and confirmed by Lyapunov stability analysis. However with the introduction of disturbance into the system model the nonlinear controller showed considerably significant maximum energy across all disturbance profiles used. The total mean energy was $3.63e14$watt-sec for step disturbance, $9.441e13$watt-sec for sinusoidal disturbance and $4.86e12$watt-sec for impulse disturbance. The standard EFRCL had average energy values of $5.43e^{-7}$,$6.5e5$ and $3.299e5$watt-sec respectively. The IICL gave average energy values of $2.71e15$,$453.07$ and $2.17e3$watt-sec respectively while the IIEFCL had average maximum energy values of $113.293$,$113.23$ and $6.8641$watt-sec respectively. Experiments confirmed that in every case the nominal NLCL gave the worst results with an elevated control energy effort while the IIEFCL had the least total energy for the control signal.

## 5.2 Conclusions

This thesis has addressed the development of all set out objectives. It has successfully established the suitability of the designed controllers for stabilization and tracking as specified in objective items (1)-(4) for the selected benchmark models. The control schemes which have been implemented include a nominal Lyapunov based nonlinear controller (NLCL), an output feedback regulator control law (EFCL), an immersion invariance control law (IICL) and finally the

immersion-invariance output feedback regulator (IIEFCL). All controllers were developed using the mathematical tools of linear algebra, geometric control theory, linear and nonlinear control theory and implemented using Matlab scripts and Simulink block sets.

The simulations confirmed the analytical results obtained with respect to the availability of stabilizing internal model observers that could ensure good error convergence from any start condition. Output regulation results in section 4.2.1, 4.2.2 and 4.2.3 formed the basis for subsequent regulator development. The regulator developed showed considerable stabilization for the RTAC, CIP and UAV systems with time for the initial transients to settle obtained as 2.7s, 1.113s and 0.6435s respectively for the three benchmark systems mentioned.

An IICL was developed for reference trajectory tracking and stabilization in both unperturbed and perturbed systems state. The perturbation comprised injection of a disturbance signal into the output to be regulated. The IICL for regualtion of the RTAC system was used in two configurations. It was used in standalone mode as the sole controller and in a cascade control structure together with a PID where it increased robustness of the PID controller. The utilized PID gains were $1, 0, 0.0059$, which were obtained using Matlab's PID tuner and fine tuned through a trial and error process until satisfactory results were obtained. The increased robustness from such an arrangement was evident in the stability and tracking results of sections 4.3.2, 4.3.3 and 4.3.4 respectively. The controller served as an effective control tool for direct application to nonlinear systems stabilization. The IICL was tested on the RTAC system. It proved to be stabilizing and properly handled the off-manifold state components by regulating them to zero. In the non-robust stability experiments no visible steady state error was recorded however a steady state error was present during nonrobust tracking. Non-robust experiment had a remarkable overshhot of 36.27% but no overshoot in robust experiments. Settling time for the nonrobust and robust stability experiments were 15 and 10 seconds respectively while settling times for the nonrobust and robust tracking was 18 and 8 seconds respectively.

The development of the output feedback observer regulator using an immersion invariance controller for supply of the control input to the system was made. Characterizing the developed contoller in ternms of energy efficiency, the total mean energy computed was $3.63e14$ for step disturbance, $9.441e13$ for sinusoidal disturbance and $4.86e12$ for impulse disturbance. The standard EFRCL had average energy values of $5.43e^{-7}$,$6.5e5$ and $3.299e5$respectively. The IICL gave average energy values of $2.71e15$,$453.07$ and $2.17e3$ respectively while the IIEFCL had average maximum energy values of $113.293$,$113.23$ and $6.8641$ respectively.

A validation model was implemented to test the IIEFCL in simulation experiments that used a high fidelity nonlinear MIMO QUAV model. The integral of the squared control input(ISCI) was used as the test metric on the four control inputs $U1, U2, U3, U4$. The results obtained were benchmarked against results in Ozbek *et al.*, (2015) with the following findings made;the developed IIEFCL with step input disturbance vs. feedback linearization (FBL) controller showed a 95.95% improvement on U1, 99.95% improvement on U2, 98.94% improvement on U3 and -3.14% degradation on U4. The developed IIEFCL with step input disturbance vs. backstepping(BS) showed a 98% improvement on U1, 99.1% improvement on U2, 90.3% improvement on U3 and 96.3% improvement on U4. The developed IIEFCL with step input disturbance vs. sliding mode controller(SMC) showed a 95.7% improvement on U1, 99.6% improvement on U2, 98.6% improvement on U3 and -29.08% degradation on U4. The IIEFCL therefore proved to be an improvement over those obtained in Ozbek *et al.*, (2015).

## 5.3 Limitation

The limitation encountered in this work concerns the inconclusive search for a generalized immersion function for the QUAV internal model. However a high gain observer which met the requirement of the internal model was synthesized to provide quasi-immersion and state estimates for feedback.

## 5.4 Contribution to Knowledge

The following are some of the contributions to knowledge made in this work:

1. Development of a practical framework to be applied towards achieving robust regulation in the presence of uncertainties and disturbance sources. To the best of my knowledge the structure of the developed immersion invariance error feedback control law (IIEFCL) has not been used previously.

2. Strictly non-square systems were considered in this work with particular treatment of a non-square MIMO QUAV system. Internal stability of the system was guaranteed on the QUAV with all eigenvalues satisfying the Hurwitz stability criterion at the end of the design. Initial value response tests gave settling time of 0.6345s.

3. Table 4.7 shows the IIEFCL outperformed two of the modern nonlinear controllers in 10 out of 12 instances. The average energy of the proposed controller was less than the baseline controllers with the IIEFCL being 95.99%, 99.81% and 95.57% more energy efficient than the FBL1, BS1 and SMS1 controllers respectively. The meaning of this in real world terms is significant energy savings for the QUAV employing the IIEFCL, which in practice means better battery life, longer flying times and ability to get more value out of the QUAV per battery charge.

4. Exosystem characterization studies of the IIEFCL with respect to energy efficiency (minimal energy used), in producing the control effort. It proved to be less efficient with respect to the EFR when a step-type disturbance was injected into the system with $113.293 >>> 5.43e{-}7$. IIEFR in comparison to the EFR alone was more energy efficient when a sinusoidal disturbance was injected with ($113.23 <<< 6.5e5$). IIEFR was again more energy efficient in comparison to the EFR when an impulse disturbance was injected with $6.8641 <<< 3.99e5$.

5. Characterization of the effect of the various exosystems showed that a IIEFCL outperformed

the standard IICL and standard EFCL in every exosystem choice except when the step-type disturbance was injected into the system. As a result, the IIEFCL gave a smooth and asymptotically stable control profile that benefited the QUAV system in the form of lower energy consumption and reduced oscillations in the control effort. This implied reduced wear and tear on the actuators from the application of the IIEFCL as against the others. Reduced energy means lower battery and system temperatures which physically translates into longer service life of the QUAV

6. It also has economic significance since the controller can be applied in renewable or alternative power systems which employ inverter-battery combination to prolong the life of such systems.

## 5.5 Recommendation for Future Work

1. Although the developed controller met the minimum standards for selecting control parameters, no optimization technique has been used in this work. Future work could consider optimization of some of the parameters mentioned in this work such as the PID gains, the NLCL control parameters given by $k_1\tilde{k}_{12}$, the motor scale factor, torque scale factor represented by $msf$ and $tsf$ in the Matlab script in section B.1.5 of the appendix. This is recommended to see how much improvement such optimization could give the system.

2. The developed IIEFCL is classified as a composite control law in the same composite family as sliding mode control. Comparison could be made to investigate the stabilization characteristics and robustness of both controllers since they both possess the unique property of invariance and invariant manifolds.

3. Utilization of the developed IIEFCL for the stabilization of similar non-square systems such as induction machines, aircraft spacecraft and satellites utilizing control moment gyroscopes (CMGs) and generally for systems with primary actuators supplying the control signal.

4. Generalized immersion for the QUAV should still be looked into and better algorithms developed towards this search.

## REFERENCES


[1] M. Abdelkhalek, M. El-Demerdash, and T. Dief, "Attitude stability of quadcopter using classic control with angular acceleration.," *International Journal of Computer Science and Information Technology and Security (IJCSITS)*, 5, no., pp. 325–331, 4 2015.

[2] A. Al-Tahir, "Semi-global output feedback nonlinear stabilization of variable speed grid connected direct drive wind turbine generator systems.," *International Journal of Dynamics and Control.*, no., 2016.

[3] J. Avis, S. Nersesov, R. Nathan, and H. Ashrafiuon, "A comparison study of nonlinear control techniques for the rtac system.," *Nonlinear Analysis: Real World Applications.*, 11, no., pp. 2647–2658, 2010.

[4] A. Astolfi and R. Ortega, "Immersion and invariance: A new tool for stabilization and adaptive control of nonlinear systems.," *IEEE TRANSACTIONS ON AUTOMATIC CONTROL*, 48, no., pp. 590–606, 4 2003.

[5] C. Aguilar and A. Krener, "Patchy solution of a francis byrnes isidori partial differential equation.," *Int. J. Robust. Nonlinear Control.*, 13, no., 10461061, 2013.

[6] ——, "Model predictive regulation.," *The International Federation of Automatic Control.*, no., 2014.

[7] D. Astolfi and L. Praly, "Integral action in output feedback for multi-input multi-output nonlinear systems.," *IEEE TRANSACTIONS ON AUTOMATIC CONTROL.*, 62, no., pp. 1559–1574, 4 2017.

[8] A. Bemporad, "Lecture: Observability analysis.," *Automatic Control 1*, no., 2011.

[9] S. Bouabdallah, P. Murrieri, and R. Siegwart, "Design and control of an indoor micro quadrotor.," no., 2004a.

[10] C. Byrnes, F. Priscoli, and A. Isidori, "Output regulation of uncertain nonlinear systems.," *Systems and control foundations and applications*, 26, no., pp. 963–972, 6 1990.

[11] C. Byrnes and A. Isidori, "Output regulation for nonlinear systems: An overview.," *Int. J. Robust Nonlinear Control*, no., pp. 323–337, 2000.

[12] A. Calise, N. Hovakimyan, and M. Idan, "Adaptive output feedback control of nonlinear systems using neural networks.," *Preprint submitted to Elsevier*, 14, no., 2001.

[13] D. Carnevale, S. Galeani, and L. Menini, "Output regulation for a class of linear hybrid systems. part 2: Stabilization.," *IEEE Conference on Decision and Control*, 51, no., 2012.

[14] E. Castaneda-Toledo, V. Kucera, and J. Ruiz-Leon, *Realization of full column rank precompensators using stabilizing static state feedback.* Elsevier Ltd., 2015, vol. 76, 4246.

[15] B. Castillo-Toledo, S. Celikovsky, and S. Di-Gennaro, *Generalized Immersion and Nonlinear Robust Output Regulation Problem.* 2004, vol. 40, pp. 207–220.

[16] J. Chang, C. Wua, and C. Shih, "Output feedback high-gain proportional integral control for minimum phase uncertain systems.," *Journal of the Franklin Institute*, 352, no., pp. 2314–2328, 2015.

[17] Z. Chen and J. Huang, "Robust output regulation with nonlinear exosystems.," *Proceedings of the 2004 American control conference*, no., 2004.

[18] ——, "Global robust output regulation for output feedback systems.," *IEEE TRANSACTIONS ON AUTOMATIC CONTROL.*, 50, no., pp. 117–121, 1 2005.

[19] A. Chovancova, T. Fico, T. Hubinsky, and F. Duchon, "Comparison of various quaternion-based control methods applied to quadrotor with disturbance observer and position estimator.," *Robotics and Autonomous Systems*, no., 2016.

[20] A. Daasch, F. Svaricek, and M. Schultalbers, *Strong Structural Non-Minimum Phase Systems.* Elsevier Ltd., 2016, vol. 49, 051055.

[21] B. Elsayed, M. Hassan, and S. Mekhilef, "Fuzzy swinging up with sliding mode control for third order cart-inverted pendulum system.," *International Journal of Control, Automation and Systems.*, 13, no., pp. 238–248, 1 2015.

[22] M. Fliess, J. Levine, P. Martin, and P. Rouchon, "Flatness and defect of nonlinear systems; introductory theory and examples.," *Int. J. Control.*, 61, no., pp. 1327–1361, 6 1995.

[23] B. Francis, "The linear multivariable regulator problem.," *Siam J. Control and Optimization.*, 15, no., pp. 486–505, 3 1977.

[24] B. A. Francis and W. M. Wonham, "The internal model principle of control theory.," *Automatica.*, 12, no., pp. 457–465, 1976.

[25] B. Friedland, "Full-order state observers.," *Control Systems, Robotics and Automation*, VIII, no., ND.

[26] J. Gauthier, H. Hammouri, and S. Othman, "A simple observer for nonlinear systems: Applications to bioreactors.," *Proceedings of the 2006 American Control Conference*, 37, no., 6 1992.

[27] J. Hoagg and D. Bernstein, "Deadbeat internal model control for command following and disturbance rejection in discrete-time systems.," *Proceedings of the 2006 American Control Conference*, no., 2006.

[28] J. Huang, "Nonlinear output regulation: Theory and applications..," *SIAM*, no., 2004.

[29] J. Huang and Z. Chen, "A general framework for tackling the output regulation problem.," *IEEE Transactions on Automatic Control*, 49, no., 12 2004.

[30] J. Huang and W. Rugh, "Stabilization on zero-error manifolds and the nonlinear servomechanism problem.," *Proceedlngs of the 29th Conference on Decision and Control*, 29, no., pp. 1262–1267, 1990.

[31] ——, "On a nonlinear multivariable servomechanism problem.," *Automatica,lntemational Federation of Automatic Control*, 26, no., pp. 963–972, 6 1990.

[32] A. Isidori, "The zero dynamics of a nonlinear system:from the origin to the latest progresses of a long successful story.," *European Journal of Control.*, 19, no., 369378, 2013.

[33] ——, "The zero dynamics of a nonlinear system:from the origin to the latest progresses of a long successful story.," *Proceedings of the 30th Chinese Control Conference.*, 30, no., 2011.

[34] A. Isidori and C. Byrnes, "Output regulation of nonlinear systems.," *IEEE TRANSACTIONS ON AUTOMATIC CONTROL.*, 35, no., pp. 131–140, 2 1990.

[35] A. Isidori and L. Marconi, *Nonlinear Output Regulation.* 2010, vol. 2.

[36] A. Isidori, L. Marconi, and A. Serrani, *Robust Autonomous Guidance. An Internal Model Approach*. 2007.

[37] A. Isidori and L. Marconi, *System Regulation and Design: Geometric and Algebraic Methods.*

[38] A. Isidori, L. Marconi, and L. Praly, "Robust design of nonlinear internal models without adaptation.," *Automatica*, 48, no., pp. 2409–2419, 2012.

[39] N. Jeurgens, "Implementing a simulink controller in an ar.drone 2.0.," *Journal of the Franklin Institute.*, no., 2016.

[40] X. Jiang, B. Hua, Z. Guana, D. He, and X. Zhang, "Optimal tracking performance for non-square plant models with input disturbance and feedback channel noise.," *Journal of the Franklin Institute.*, no., 29712984, 352 2015.

[41] Z. Jiang, I. Mareels, D. Hill, and J. Huang, "A unifying framework for global regulation via nonlinear output feedback: From iss to iiss.," *IEEE TRANSACTIONS ON AUTOMATIC CONTROL.*, 49, no., pp. 549–562, 4 2004.

[42] N. Kazantzis and C. Kravaris, "Nonlinear observer design using lyapunov's auxiliary theorem.," *Systems and Control Letters*, 34, no., pp. 241–247, 1998.

[43] H. Kim, "Output regulation: Into the internal model principle.," *CDSL, SNU NST*, no., 2009.

[44] P. Kokotovic, "Recent trends in feedback design: An overview.," *International Journal of Automatic Control. Automatica*, 21, no., pp. 225–236, 3 1985.

[45] P. Kokotovic and M. Arcak, "Nonlinear and adaptive control: An abbreviated status report.," *The 9th Mediterranean Conference on Control and Automation*, no., 2001.

[46] A. J. Krener, "The existence of optimal regulators.," *Proceedings of the 37th IEEE conference on decision and control*, no., 1998.

[47] A. Kaldmae and U. Kotta, "Input-output linearization by dynamic output feedback.," *European Control Conference (ECC)*, no., 2013.

[48] H. K. Khalil and P. L., "High-gain observers in nonlinear feedback control.," *Int. J. Robust. Nonlinear Control.*, no., 2013.

[49] H. K. Khalil and L. Praly, "High-gain observers in nonlinear feedback control.," *Int. J. Robust. Nonlinear Control.*, 24, no., pp. 993–1015, 6 2014.

[50] B. Kernighan and D. Ritchie, *The C Programming Language Second Edition*. Prentice-Hall, Inc., 1988.

[51] A. Lefeber, "Controlling of a single drone: Hovering the drone during flight modes.," *Department of Mechanical Engineering Dynamics and Control.*, no., 2015.

[52] B. Liu, J. Li, and X. Luo, "General integral control design via feedback linearization.," *Intelligent Control and Automation.*, no., pp. 19–23, 5 2014.

[53] Y. Leu, W. Wang, and T. Lee, "Observer-based direct adaptive fuzzy-neural control for nonaffine nonlinear systems.," *IEEE TRANSACTIONS ON NEURAL NETWORKS*, 16, no., 4 2005.

[54] C. Lobry and T. Sari, "The peaking phenomenon and singular perturbations: An extension of tikhonov's theorem.," *Unit de recherche INRIA Sophia Antipolis*, no., 2004.

[55] A. Luzi, D. Peaucelle, J. Biannic, C. Pittet, and J. Mignot, "Structured adaptive attitude control of a satellite.," *INTERNATIONAL JOURNAL OF ADAPTIVE CONTROL AND SIGNAL PROCESSING.*, no., 2013.

[56] L. Marconi, L. Praly, and A. Isidori, "Output stabilization via nonlinear luenberger observers.," *Siam Journal of Control Optimal Control and Industrial and Applied Mathematics*, 45, no., 22772298, 6 2007.

[57] E. Moshksar and M. Guay, *Almost invariant manifold approach for adaptive estimation of periodic and aperiodic unknown time-varying parameters.* Wiley Online Library, 2015, vol. 30, 7692.

[58] S. Nazrulla and H. Khalil, "Robust stabilization of non-minimum phase nonlinear systems using extended high gain observers.," *American Control Conference*, no., 2008.

[59] T. Oliveira, A. Peixoto, and L. Hsu, "Peaking free output-feedback control of uncertain nonlinear systems.," *American Control Conference*, no., 2008.

[60] T. Oliveira, L. Hsu, and A. Peixoto, "Peaking free high gain observer based sliding mode control for uncertain systems with strong nonlinearities.," *American Control Conference*, no., 2008.

[61] N. Ozbek, M. Onkol, and M. Efe, "Feedback control strategies for quadrotor-type aerial robots: A survey.," *Transactions of the lnstitute of Measurement and Control.*, no., 2015.

[62] Y. Pan, T. Sun, and H. Yu, "Peaking-free output-feedback adaptive neural control under a nonseparation principle.," *IEEE Transactions on Neural Networks and Learning Systems*, no., 2015.

[63] L. Paunonen, "The role of exosystems in output regulation.," *IEEE TRANSACTIONS ON AUTOMATIC CONTROL.*, no., 2013.

[64] A. Peixoto, T. Oliveira, and L. Hsu, "Global tracking output-feedback sliding mode control design via norm estimators and variable high gain observer.," *Joint 48th IEEE Conference on Decision and Control and 28th Chinese Control Conference*, no., 2009.

[65] D. Peaucelle and Y. Ebihara, "Lmi results for robust control design of observer-based controllers, the discrete-time case with polytopic uncertainties.," no., 2014.

[66] C. Prieur and A. Teel, "Uniting local and global output feedback controllers.," no., 2010.

[67] J. Primbs, "Survey of nonlinear observer design techniques.," *American Control Conference*, no., 1996.

[68] Z. Qu, A. Annaswamy, and E. Lavretsky, "Adaptive output-feedback control for a class of multi-input-multi-output plants with applications to very flexible aircraft.," *IEEE American Control Conference.*, 30, no., 2016.

[69] I. Sarras, E. Nuno, M. Kinnaert, and L. Basanez, "Output-feedback control of nonlinear bilateral teleoperators.," *American Control Conference*, no., 2012.

[70] A. Serrani, "The nonlinear output regulation problem: Local and structurally stable regulation.," *Collaborative Center for Control Sciences The Ohio State University*, no., 2005.

[71] ——, "Output regulation for over-actuated linear systems via inverse model allocation.," *IEEE Conference on Decision and Control*, no., 2012.

[72] ——, "Nested zero-dynamics redesign for a non-minimum phase longitudinal model of a hypersonic vehicle.," *IEEE Conference on Decision and Control*, 52, no., pp. 4833–4838, 6 2013.

[73] L. Shead and J. Rossiter, "Feasibility for non-square linear mpc.," no., 2006.

[74] H. Shim, G. Park, Y. Joo, J. Back, and N. Jo, "Yet another tutorial of disturbance observer: Robust stabilization and recovery of nominal performance.," no., 2015.

[75] S. Srinivasa, "Observers for non-linear systems manipulation lab talk.," *The Robotics Institute Carnegie Mellon University*, no., 2002.

[76] Y. Sugawara and A. Shimada, "Attitude control of quadrotor in consideration of the effects of a pole based on limited pole placement.," *Electrical Engineering in Japan*, 198,135-D, no., pp. 827–835, 1 2017.

[77] N. Sun, Y. Wu, Y. Fang, H. Chen, and B. Lu, "Nonlinear continuous global stabilization control for underactuated rtac systems: Design, analysis, and experimentation.," *IEEE/ASME TRANSACTIONS ON MECHATRONICS.*, 22, no., pp. 1104–1115, 2 2016.

[78] H. J. Sussmann and P. V. Kokotovic, "The peaking phenomenon and the global stabilization of nonlinear systems.," *IEEE Transactions on Automatic Control*, 36, no., 4 1991.

[79] A. Teel and L. Praly, "Global stabilizability and observability imply semi-global stabilizability by output feedback.," *Systems & Control Letters*, no., 1993.

[80] ——, "Tools for semi-global stabilization by partial state and output feedback.," *Siam Journal on Control*, no., 1995.

[81] A. Tanwani and D. Liberzon, "Invertibility of nonlinear switched systems.," *Automatica*, no., 2010.

[82] J. Trumpf, H. Trentelman, and J. Willems, "An internal model principle for observers.," *IEEE Conference on Decision and Control and European Control Conference (CDC-ECC)*, 50, no., pp. 3992–3999, 2011.

[83] A. Udrea, A. Ticlea, C. Flutur, and V. Tanasa, *On the nonlinear output regulation problem-part 1: MIMO nonlinear systems normal forms and a discussion on the necessary conditions for solving the control problem.* 2012, vol. 74.

[84] S. Vaidyanathan, "State feedback controller design for the output regulation of sprott-h system.," *International Journal of Information Sciences and Techniques (IJIST) Vol.1, No.3, November 2011.*, 1, no., 3 2011.

[85] G. Valmorbida and S. Galeani, "Nonlinear output regulation for over-actuated linear systems.," *IEEE Conference on Decision and Control*, 52, no., pp. 10–13, 2013.

[86] D. Wiese, A. Annaswamy, J. Muse, M. Bolender, and E. Lavretsky, "Adaptive output feedback based on closed-loop reference models for hypersonic vehicles.," no., 2015.

[87] D. Wiese, A. Annaswamy, J. Muse, and M. Bolender, "Adaptive output feedback based on closed-loop reference models for hypersonic vehicles.," no., 2015.

[88] L. Wang, A. Isidori, H. Su, and W. Xu, "Partial-state observer for a class of mimo nonlinear systems.," *The International Federation of Automatic Control.*, no., pp. 3676–3681, 2014.

[89] X. Wu and X. He, "Cascade-based control of a benchmark system.," *28th Chinese Control and Decision Conference (CCDC)*, no., pp. 5027–5031, 2016.

# Appendices

# APPENDIX A
# CODE LISTING FOR THE RTAC OUTPUT FEEDBACK REGULATOR PROBLEM

### A.0.1 RTAC parameters are defined here from Avis *et al.*, 2013

```
M=1.7428;
mp=0.2739;
l=0.0537;
J=0.000884;
ks=339.4;

M1=M+mp;
M2=J+mp*l^2;

Dl=(M1*M2-mp^2*l^2);
```

### A.0.2 Substitution of params

```
A=[0 1 0 0 ; M2*ks/Dl 0 0 0 ; 0 0 0 1 ; mp*l*ks/Dl 0 0 0];
B=[0 -mp*l/Dl 0 M1/Dl]';
C=[1 0 1 1];
Cmat=[1 0 0 0 ; 0 0 0 0  ; 0 0 1 0 ; 0 0 0 1 ];
D=[0 0 0 0]';
P=[0 0  ;M2/Dl 0  ;0 0;-mp*l/Dl 0 ];
Q=[0 0;0 0;0 0 ;0 0 ];
```

### A.0.3 Definition of the exosystem matrix as either constant or variable

```
Sexo=[0 1 ; -1 0];
```

### A.0.4 Computing controllability

```
poles=eig(A)
Wr=ctrb(A,B);
rnkWr=rank(Wr);
if rnkWr==4
    disp('System is full rank and Controllable')
else
    disp('System is NOT full rank and NOT controllable')
end
```

### A.0.5 Discussion

By Kalman's rank test for controllability, we say that the system is controllable and a stabiizing feedback can be found for the system

### A.0.6 Computing observability

```
Wo=obsv(A,C);
rnkWo=rank(Wo);
if rnkWo==4
    disp('System is full rank and Observable')
else
    disp('System is NOT full rank and NOT observable')
end

% By Kalman's rank test for observability, we say that the system is
% observable and a stabiizing gain can be found for the system internal stat
```

### A.0.7 Computing observability

```
Wow=obsv(Aw,Cw);
rnkWow=rank(Wow)
if rnkWow==4
    disp('System is full rank and Observable')
else
    disp('System is NOT full rank and NOT observable')
end
```

### A.0.8 Construct a stabilizing gain Kx for A+BKx

use place Matlab command eigenwert=2;

```
pval=[-19 -3 -15 -13]'

Kx=place(A,B,pval)

stabAB=eig(A+B*Kx)

for i=1:4
    if real(stabAB(i)>0)
        disp('System is NOT stabilizable by choice of poles')
    else
        disp('System is stabilizable by selected poles')
    end
end
```

### A.0.9 Developed method for matching the poles

```
syms kx1 kx2 kx3 kx4
clear Kx
Kxsym=[kx1 kx2 kx3 kx4];
mmat1=A+B*Kxsym;
chplymmat1=charpoly(mmat1);
lenmmat1=length(chplymmat1);

% pmmat1=poly_select(2,lenmmat1)
pmmat1=poly(pval);

eqn1=4.66*kx2-638.34*kx4==pmmat1(2);
eqn2=4.66*kx1-638.34*kx3==pmmat1(3)+179.82;
eqn3=122140*kx4==pmmat1(4);
eqn4=122140*kx3==pmmat1(5);

[Amat,Bmat] = equationsToMatrix([eqn1,eqn2,eqn3,eqn4], [kx1,kx2,kx3,kx4]);

Xvec = linsolve(Amat,Bmat);
Kxavis=[237.3198 17.3309  0.0910  0.0482]

stabAB=eig(A+B*Kxavis)

for i=1:4
    if real(stabAB(i)>0)
        disp('System is NOT stabilizable by choice of poles')
    else
        disp('System is stabilizable by selected poles')
    end
end
```

### A.0.10 Computing the values in the gains L,L1,L2,G1,G2

```
La=place(A',C',8*pval)'
stabALC=eig(A-La*C)
```

### A.0.11 Computing the gains L=L1

the size of L1 is n*p

```
Lb=place(A',Cmat',8*pval)'
stabALpmatC=eig(A-Lb*Cmat)
L=Lb
```

### A.0.12 Computing the gains L1 and L2 for the matrix G2

the size of L1 is n*p the size of L2 is q*p

```
syms l1 l2 l3 l4 l5 l6 l7 l8 l9 l10 l11 l12 l13 l14 l15 l16 l17 l18 l19 l20
L1sym=[l1 l2 l3 l4 ; l5 l6 l7 l8; l9 l10 l11 l12; l13 l14 l15 l16];
Al1=A-L1sym*Cmat;
chplyl1=charpoly(Al1);
lenal1=length(chplyl1);
pal1=poly(8*pval);

syms a b c d e f g h k m n p q r s t u v w x an ck at dq nt ps cp dn as cq e
syms gk et hq gp hn es gq nt ps ant aps ckt cpq dks dns ent eps gkt gpq hks

eqnl1a=a+n+t==pal1(2);
eqnl1b=1580.1*d+e+s+an-ck+at-dq+nt-ps==pal1(3)+179.82;
eqnl1c=1580.1*c+1580.1*h-179.82*n-179.82*t-1580.1*cp+1580.1*dn+as-cq+en-gk+e
eqnl1d=1580.1*g-179.82*s-1580.1*gp+1580.1*hn+es-gq-179.82*nt+179.82*ps+ent-e

[Amat,Bmat] = equationsToMatrix([eqnl1a,eqnl1b,eqnl1c,eqnl1d], [a,b,c,d,e,f,

Xvec = linsolve(Amat,Bmat);

L1=[ 400  0  1.9072e+03    35.2711 ;  0   0 2.8813e+04  0 ;      0      0

stabAL1=eig(A-L1*Cmat)
```

### A.0.13 Compute the L2 gain from developed method

L2sym=[l1 l2 l3 l4 ; l5 l6 l7 l8; l9 l10 l11 l12; l13 l14 l15 l16; l17 l18 l19 l20]

```
L2sym=[l1 l2 l3 l4 ; l5 l6 l7 l8] ;% this stabilizes the exosystem component
pval=[-19 -3 -15 -13 -pi/2 -pi/2]';
Al2=[A-L1*Cmat P-L1*Q; -L2sym*Cmat Sexo-L2sym*Q];
chplyl2=charpoly(Al2);
lenal2=length(chplyl2);
pal2=poly(8*pval);

eqnl2a=-4.656*l4==pal2(3)-5.5553e+04;
eqnl2b=164.7378*l1-4.656*l3-1.8622e+03*l4-4.656*l8==pal2(4)-3.0140e+06;
eqnl2c= 8.8792e+03*l1-1.8622e+03*l3+1.6743e+03*l4+164.7378*l5-4.656*l7-1.862
eqnl2d=1.3414e+05*l1+ 1.6743e+03*l3+8.8792e+03*l5-1.8622e+03*l7+1.6743e+03*l
eqnl2e=1.3414e+05*l5+ 1.6743e+03*l7==pal2(7)- 4.5528e+07;

[Amat,Bmat] = equationsToMatrix([eqnl2a,eqnl2b,eqnl2c,eqnl2d,eqnl2e], [l1,l2
```

```
Xvec = linsolve(Amat,Bmat);

L2=[ -1.9568e+04 0   -1.2864e+05  -2.1929e+03 ;  7.8462e+04 0 -2.0194e+06 0

Lg=[L1;L2];

G2=Lg
```

### A.0.14 Computing Kv

```
syms kv1 kv2
Kvsym=[kv1 kv2  ]
matkv1=[B*Kxavis B*Kvsym;A-L1*Cmat P-L1*Q ];
% augment the matkv matrix to allow for characteristic polynomial computatio
matkv1aug=[matkv1 zeros(8,2)];
chplymatkv1=charpoly(matkv1aug);
lenplykv1=length(chplymatkv1);
pval=[-13 -11 -9 -17 -15 -pi*5 -6 -pi*3]'
pcoeffkv1=poly(pval)
eqnkva=2.2520e+04*k1==pcoeffkv1(3)+4.2471e-14;
eqnkvb=-2.5916e-11*k1+   1.1931e+04*k2==pcoeffkv1(4);
eqnkvc=- 1.3731e-11*kv2==pcoeffkv1(5);
[Amat,Bmat] = equationsToMatrix([eqnkva, eqnkvb, eqnkvc], [k1,k2]);
Xveckv1 = linsolve(Amat,Bmat);
Kv1=[ 0.1773 -9.8259e+16 ];
%
matkv2=[B*Kxavis B*Kvsym;-L2*Cmat Sexo-L2*Q ];
chplymatkv2=charpoly(matkv2);
lenplykv2=length(chplymatkv2);
pval=[-13 -11 -9 -17 -15 -pi*5 ]';
pcoeffkv2=poly(pval);
eqnkva=-1.3998e+06*kv1==pcoeffkv2(3)-1;
eqnkvb=1.6110e-09*kv1+1.3998e+06*kv2==pcoeffkv2(4)-49.9178;
eqnkvc=-1.6110e-09*kv2==pcoeffkv2(5)+4.2471e-14;
[Amat,Bmat] = equationsToMatrix([eqnkva, eqnkvb, eqnkvc], [k1,k2]);
Xveckv2 = linsolve(Amat,Bmat);
Kv2=[2.5111e+29 -2.8900e+14 ];
Kv3=[-0.0019 -2.8900e+14 ];
%
```

### A.0.15 Compute the global K matrix Kavis=[Kxavis Kvavis]

```
Kvavis=Kv1;
Kxv=[Kxavis Kvavis]
```

```
K1=Kxavis;
K2=[Kxavis Kvavis]
Kz=K2;
```

### A.0.16 Solve the sylvester equations from knowlwegde of Kx and Kv

Solve Sylvester equation AX + XB = C for X X = sylvester(A,B,C)

```
Asyl=A+B*Kxavis;
Bsyl=B*Kvavis+P;
Csyl=Cmat+D*Kxavis;
Dsyl=D*Kvavis+Q;

Xsyl = sylvester(Asyl,-Sexo,-Bsyl)
Usyl=Kxavis*Xsyl+Kvavis

syms x11 x12 x21 x22 x31 x32 x41 x42
Xsyms=[x11 x12 ;x21 x22 ;x31 x32; x41 x42];
xsymSexo=Xsyms*Sexo;
axsym=A*Xsyms;

bkvsym=B*Kvsym;
cxsym=Cmat*Xsyms;
```

### A.0.17 Computing the other gain of the observer G1

```
Aobsv=[A P ; zeros(2,4) Sexo]
Bobsv=[B ; zeros(2,1)]

Cobsv=[Cmat Q]
DKxv=D*Kxv


Lobj=G2*(Cobsv+DKxv)

G1=Aobsv +Bobsv*Kxv-Lobj
```

### A.0.18 Test for the controllability of Aobsv, Bobsv

```
Wrobsv=ctrb(Aobsv,Bobsv)
rnkobsv=rank(Wrobsv)
```

### A.0.19 Test for stability of G1 and G2 matrices

```
stabab_obsv1=eig(Aobsv+Bobsv*Kxv)
stabALobsv=eig(Aobsv-Lobj)
```

### A.0.20 Check for Hurwitz stability of the closed loop system matrix below

```
%according to Jie Huang
Kk=[Kxavis Usyl]
Aclsys=[A+B*Kxavis B*Kxavis B*(Usyl-Kxavis*Xsyl) ; zeros(4,4) A-L1*Cmat P-L
stabAclsys=eig(Aclsys)
```

### A.0.21 Calling model here

```
simtime=10;
Fdist=0;

x1ref=0.2;
x2ref=0;
x3ref=15;
x4ref=0;

Xref=[x1ref x2ref x3ref x4ref 0 0 0 0 0 0]';


sys=ss(Aclsys,[Bobsv;zeros(4,1)],[Cobsv zeros(4,4)],0)
x0=Xref;
xhat0=[0 0 0 0 0 0 0 0 0 0];
figure(1)
initial(sys,Xref,simtime)

figure(2)
t=(0:simtime)';
v=ones(size(t));
lsim(sys,v,t);
```

# APPENDIX B
# CODE LISTING FOR THE UAV OUTPUT ERROR FEEDBACK REGULATOR PROBLEM

## B.1 QUAV smulation script

### B.1.1 Symbolic variables used

```
syms x_1 x_2 x_3 x_4 x_5 x_6 x_7 x_8 x_9 x_10 x_11 x_12
syms mp gg I_xx I_yy I_zz
syms A_x A_y A_z
syms u_1 u_2 u_3 u_4
syms k_f k_t l
syms omega_1 omega_2 omega_3 omega_4
syms k1 k2 k3 k4 k5 k6 k7 k8 k9 k10 k11 k12
syms lambda
syms Jx Jy Jz Jxyz Jyzx Jzxy
```

### B.1.2 Derived variables from Lefeber, (2015) prepared for linearization

```
f1=cos(x_6)*cos(x_5)*x_7+(-sin(x_6)*cos(x_4)+cos(x_6)*sin(x_5)*sin(x_4))*x_8
f2=sin(x_6)*cos(x_5)*x_7+(cos(x_6)*cos(x_4)+sin(x_6)*sin(x_5)*sin(x_4))*x_8+
f3=-sin(x_5)*x_7+sin(x_4)*cos(x_5)*x_8+cos(x_5)*cos(x_4)*x_9;
f4=x_10+x_11*sin(x_4)*tan(x_5)+x_12*cos(x_4)*tan(x_5);
f5=x_11*cos(x_4)-x_12*sin(x_4);
f6=x_11*sin(x_4)*1/cos(x_5)-x_12*cos(x_4)*1/cos(x_5);
f7=x_12*x_8-x_11*x_9-gg*sin(x_5);
f8=-x_12*x_7+x_10*x_9+gg*sin(x_4)*cos(x_5);
f9=x_11*x_7-x_10*x_8+gg*cos(x_5)*cos(x_4)-u_1/mp;
f10=x_11*x_12*Jyzx+u_2/Jx;
f11=x_10*x_12*Jzxy+u_3/Jy;
f12=x_10*x_11*Jxyz+u_4/Jz;


u_1_fixed_point=mp*gg-(k_f*((omega_1)^2+(omega_2)^2+(omega_3)^2+(omega_4)^2)
u_2_fixed_point=k_f*((omega_3)^2-(omega_1)^2)*l;
u_3_fixed_point=k_f*((omega_4)^2-(omega_2)^2)*l;
u_4_fixed_point=k_f*k_t*((omega_1)^2-(omega_2)^2+(omega_3)^2-(omega_4)^2);
u=solve(u_1_fixed_point==0, u_2_fixed_point==0, u_3_fixed_point==0,u_4_fixed
u=[u.omega_1 u.omega_2 u.omega_3 u.omega_4];
```

### B.1.3 Derived variables from Ozbek *et al.*, (2015) prepared for linearization

```
% Model from Ozbek et al., (2015)
```

```
f1=x_7;
f2=x_8;
f3=x_9;
f4=x_10;
f5=x_11;
f6=-x_12;
f7=(cos(x_4)*sin(x_5)*cos(x_6)+sin(x_4)*sin(x_6))*u_1/mp;
f8=(cos(x_4)*sin(x_5)*sin(x_6)-sin(x_4)*cos(x_6))*u_1/mp;
f9=-gg+(cos(x_5)*cos(x_4))*u_1/mp;
f10=x_11*x_12*Jyzx-(Jr/Jx)*x_11*u_5+la*u_2/Jx;
f11=x_10*x_12*Jzxy+(Jr/Jy)*x_10*u_5+la*u_3/Jy;
f12=x_10*x_11*Jxyz+u_4/Jz;


u_1_fixed_point=mp*gg-(b*((omega_1)^2+(omega_2)^2+(omega_3)^2+(omega_4)^2))
u_2_fixed_point=b*((omega_3)^2-(omega_1)^2)*la;
u_3_fixed_point=b*((omega_4)^2-(omega_2)^2)*la;
u_4_fixed_point=b*d*((omega_1)^2-(omega_2)^2+(omega_3)^2-(omega_4)^2);
u_5_fixed_point=omega_1-omega_2+omega_3-omega_4;

u=solve(u_1_fixed_point==0, u_2_fixed_point==0, u_3_fixed_point==0,u_4_fixe
u=[u.omega_1 u.omega_2 u.omega_3 u.omega_4];
```

### B.1.4 Matrix of vector fields

```
A=jacobian([f1 ;f2 ;f3 ;f4 ;f5 ;f6 ;f7 ;f8 ;f9 ;f10 ;f11 ;f12],[x_1 x_2 x_3

B=jacobian([f1 ;f2 ;f3 ;f4 ;f5 ;f6 ;f7 ;f8 ;f9 ;f10 ;f11 ;f12],[u_1 u_2 u_3
```

### B.1.5 Load system parameter values

```
% run('param_lefeber')
run('param_ozbek')
%% parameter file for Lefeber

A_x=1;
A_y=1;
A_z=1;
gg=9.81;
%%%%%%%%%%%%%%%%%%
%% Ozbek
mp=0.8;
Jx=0.001567;
Jy=0.001567;
Jz=0.002834;
```

```
Jr=6.01*10^-5;
la=0.30;
%%%%%%%%%%%%%%%%
Jxyz=(Jx-Jy)/Jz;
Jyzx=(Jy-Jz)/Jx;
Jzxy=(Jz-Jx)/Jy;
u_1=mp*gg-A_z; u_2=0;  u_3=0; u_4=0; u_5=0; x_1=0; x_2=0; x_3=0;  x_4=0;
x_5=0;  x_6=0; x_7=0;x_8=0; x_9=0;x_10=0; x_11=0;x_12=0;x_13=0;x_14=0;
x_15=0;x_16=0;x_17=0;x_18=0;x_19=0;x_20=0;



 % electric motor constant
La=30*10^-6;
Ra=0.16;
Ja=0.000000712;
ba=0.3;
Ke=0.0168;
Km=Ke;
rho=Ra/La;
mu=Ke/La;
alpha=Km/Ja;
beta=ba/Ja;


b=192.32*10^-7;
d=4.003*10^-7;
% tsf=90000000000;
% msf=95000;

vsf=(2*pi)/60;

ptsf=1;
tsf=1e3;
msf=1;

Jm=0.40076725;
N1=1100; % motor gear tooth count
N2=25; % output gear tooth count
n=N2/N1; % reduction or gear ratio 44 teeth
rr=Jm+Jr/n^2; % total inertia of the motor
eff=0.97; % gear box efficiency
Jt=Ja+Jm+Jr/n^2;
tau=(Ra*Jt)/Km^2;
c1=d*tau/(eff*n^3*Jt);
```

```
c3=d/(eff*n^3*Jt);
c4=1/(Km*tau);
c2=1/tau;


rj=Jm+Jr/n; % total inertia of the motor
Cm=0.000015;
Cr=0.0000158;
rm=Cm+Cr/n; % total inertia of the motor

%% blade aero params

bia=0.15;% blade inflw angle <0.2 rad-1
ro=1.25; % air density
nrb=2; % number of rotor blades
Rr=0.15; % 0.14 to 0.16 blade radius
bhr=Rr/2; % blade half radius
chdlen=(0.0357-(bhr/Rr)*0.0148);
% chdlen1=(0.0348-(bhr/Rr)*0.0158);

bpa=asin(chdlen/(2*Rr))

a=5.73; % 2-dim lift slope
Cprop=(nrb/4)*ro*a*Rr^3*chdlen*(bpa+bia)
%% for full motor dynamics
K_1=(La/Km)*rj;
K_2=(Ra/Km)*rj+(La/Km)*rm;
K_3=(Ra/Km)*rm+Ke;

%% for simple motor dynamics
q1=(Ra/Km)*rj;
q2=(Ra/Km)*rm;
q3=Ke



%% PID params

kp=19.474
ki=3.626
kd=0.073
Tf=100

jcx=1/Jx;
jcy=1/Jy;
```

```
jcz=1/Jz;
```

### B.1.6 Evaluating the transmission and input matrices

```
A=eval(A)
B=eval(B)

plsA=eig(A)
for i=1:12
    if plsA(i)>0
        disp('Open loop system is unstable')
    elseif plsA(i)<0
        disp('Open loop system is stable')
    else
        disp('Open loop system is critically stable')
    end
end
```

### B.1.7 Controllability & observability computation

```
Wr=ctrb(A,B);
rnkWr=rank(Wr)

if (rnkWr==12)
    disp('Rank is full and system is controllable');
else
    disp('System is not controllable')
end

Cvec=[1 1 1 1 1 1 0 0 0 0 0 0];
Cmat=[1 0 0 0 0 0  ; 0 1 0 0 0 0  ; 0 0 1 0 0 0  ; 0 0 0 1 0 0  ; 0 0 0 0 1
% size of D is p x m
D=zeros(6,4);
aleph=1;
Sexo=[0 aleph ; -aleph 0]
plsexo=eig(Sexo)

% the size of P is n*q
% the size of Q is p*q
rng(1,'twister'); % fixing the value of the random number generator
s = rng;
P=rand(12,2)
Q=rand(6,2)
Pob=rand(12,2)
```

```
Qob=rand(6,2)
Perr=P-Pob;
Qerr=Q-Qob;
```

### B.1.8 Computation of canonical form matrices

```
Apoly=poly(A);
pval=[-19 ; -17 ; -13 ; -12 ; -14 ; -10 ; -8 ; -16 ; -11 ; -18 ; -9 ; -7 ];

%%%%%%%%%%end of CCF design %%%%%%%%%%%%%%%%%%%%%%%%%%%%
```

### B.1.9 Output error feedback regulator design

```
Wr1=ctrb(A,B(:,1));
rnkWr1=rank(Wr1)

if (rnkWr1==12)
    disp('Rank is full and system is controllable');
else
    disp('System is not controllable');
end

Wr2=ctrb(A,B(:,2));
rnkWr2=rank(Wr2)

if (rnkWr2==12)
    disp('Rank is full and system is controllable');
else
    disp('System is not controllable');
end

Wr3=ctrb(A,B(:,3));
rnkWr3=rank(Wr3)

if (rnkWr3==12)
    disp('Rank is full and system is controllable');
else
    disp('System is not controllable');
end

Wr4=ctrb(A,B(:,4));
rnkWr4=rank(Wr4)

if (rnkWr4==12)
    disp('Rank is full and system is controllable');
```

```
else
    disp('System is not controllable');
end
```

### B.1.10 State feedback Kx

Kx is m * n vector Kv is a m * q vector

```
syms kx1 kx2 kx3 kx4 kx5 kx6 kx7 kx8 kx9 kx10 kx11 kx12
syms kx13 kx14 kx15 kx16 kx17 kx18 kx19 kx20 kx21 kx22 kx23 kx24
syms kx25 kx26 kx27 kx28 kx29 kx30 kx31 kx32 kx33 kx34 kx35 kx36
syms kx37 kx38 kx39 kx40 kx41 kx42 kx43 kx44 kx45 kx46 kx47 kx48

Kxsym1=[kx1 kx2 kx3 kx4 kx5 kx6 kx7 kx8 kx9 kx10 kx11 kx12];
Kxsym2=[kx13 kx14 kx15 kx16 kx17 kx18 kx19 kx20 kx21 kx22 kx23 kx24];
Kxsym3=[kx25 kx26 kx27 kx28 kx29 kx30 kx31 kx32 kx33 kx34 kx35 kx36 ];
Kxsym4=[kx37 kx38 kx39 kx40 kx41 kx42 kx43 kx44 kx45 kx46 kx47 kx48];

pcoeff=poly(pval);

matab1=A+B(:,1)*Kxsym1;
chplyab1=charpoly(matab1);
eqnb1a=-1.25*kx9==pcoeff(2);
eqnb1b=-1.25*kx3==pcoeff(3);

[Amat,Bmat]=equationsToMatrix([eqnb1a,eqnb1b],[kx1, kx2, kx3, kx4, kx5, kx6,
Xvecb1= linsolve(Amat,Bmat);
Kx1=[0 0 -8.6248e+03 0 0 0 0 0  -123.2 0 0 0];



matab2=A+B(:,2)*Kxsym2;
chplyab2=charpoly(matab2);
eqnb2a=-191.4486*kx22 ==pcoeff(2);
eqnb2b=-191.4486*kx16==pcoeff(3);
eqnb2c=1.6388e+03*kx20==pcoeff(4);
eqnb2d=1.6388e+03*kx14==pcoeff(5);
[Amat,Bmat]=equationsToMatrix([eqnb2a,eqnb2b,eqnb2c,eqnb2d],[kx13, kx14, kx1
Xvecb2= linsolve(Amat,Bmat);
Kx2=[0  7.7948e+03 0 -56.3128 0 0 0  276.7964  0 -0.8044 0 0];


matab3=A+B(:,3)*Kxsym3;
chplyab3=charpoly(matab3);
eqnb3a=-191.4486*kx35 ==pcoeff(2);
```

```
eqnb3b=-191.4486*kx29==pcoeff(3);
eqnb3c=-1.6388e+03*kx31==pcoeff(4);
eqnb3d=-1.6388e+03*kx25==pcoeff(5);
[Amat,Bmat]=equationsToMatrix([eqnb3a,eqnb3b,eqnb3c,eqnb3d],[kx25, kx26, kx
Xvecb3= linsolve(Amat,Bmat);
Kx3=[  -7.7948e+03 0 0 0  -56.3128 0  -276.7964 0 0 0  -0.8044 0];


matab4=A+B(:,4)*Kxsym4;
chplyab4=charpoly(matab4);
eqnb4a=-352.8582*kx48 ==pcoeff(2);
eqnb4b=352.8582*kx42==pcoeff(3);
[Amat,Bmat]=equationsToMatrix([eqnb4a,eqnb4b],[kx37, kx38 ,kx39 ,kx40, kx41,
Xvecb4= linsolve(Amat,Bmat);
Kx4=[0 0 0 0 0  30.5533 0 0 0 0 0  -0.4364];
```

### B.1.11 Compute the augmented Kxi gain

```
Kx=[ Kx1;Kx2;Kx3;Kx4];
```

### B.1.12 Check stability of the gain Kx(i) and global Kx

```
stabab1=eig(A+B(:,1)*Kx1);
stabab2=eig(A+B(:,2)*Kx2);
stabab3=eig(A+B(:,3)*Kx3);
stabab4=eig(A+B(:,4)*Kx4);
stabab=eig(A+B*Kx)
```

### B.1.13 Regulator equations solving the sylvester equations for X and U in the format

XS=AX+BU+P and 0=CX+Q is given by

```
Qaug=[ Q ; zeros(6,2) ];

Xc=-Cmat\Q;

Xcaug=[Xc; zeros(6,2)];

rhs=-A*Xcaug+Xcaug*Sexo-P;

bpseudo=inv(B'*B)*B';

Usyl=bpseudo*rhs

Kv=Usyl-Kx*Xcaug;
```

```
Xsyl=Xcaug;
```

### B.1.14 Check FBI solution results

```
eq1lhs1=Xc*Sexo
eq1lhs2=Xcaug*Sexo;
eq2rhs1=Cmat*Xc+Q;
```

### B.1.15 Compute the gains L1 and L2 for the matrix G2

the size of L1 is n*p the size of L2 is q*p note that L1 and L2 are solved from the matrix Al=[A-L1C P-L1Q ; -L2C S-L2Q]

```
Lpmat=place(A',Clmat',20*pval)';
L1=Lpmat
stabAL1C=eig(A-L1*Clmat)

pal2b=[-19 ; -17 ]';
L2mat=place(Sexo',Q',20*pal2b)';


%
% %% check stability
% stabSLQ1=eig(Sexo-L2mat1*Q)
stabSLQ2=eig(Sexo-L2mat*Q)

L2=L2mat
```

### B.1.16 Observer gain matrices or internal model matrices can now be formed for G2

```
G2=[L1;L2]

Kxv=[Kx Kv];
Kxv2=[Ksf Kv];
```

### B.1.17 Internal model design

```
Aobsv=[A P ; zeros(2,12) Sexo];
Bobsv=[B ; zeros(2,4)];
CQ=[Clmat Q];
Cobsv=CQ;

DK=D*Kxv;
Dobsv=DK;
```

```
Lobj=G2*(Cobsv+Dobsv);

Atransobsv=Aobsv-G2*Cobsv;
specObsv=eig(Atransobsv)


G1=Aobsv+Bobsv*Kxv-Lobj;
stab_G1=eig(G1)
```

### B.1.18 Test the stability of the overall closed loop system

```
Jint=[A B*Kxv ; G2*Clmat G1];
stabJint=eig(Jint)

Aclsys=[A+B*Kx B*Kx B*(Usyl-Kx*Xsyl) ;...
            zeros(12,12) A-L1*Clmat P-L1*Q ;...
            zeros(2,12) -L2*Clmat Sexo-L2*Q];
stabAclsys=eig(Aclsys)
```

### B.1.19 Exosystem reference inputs

wref=0.001*cos(pi/6);

```
wref=0.3;
% wref=0;

ref1=1;
ref2=1;
ref3=10;
ref4=pi/4;
ref5=pi/4;
ref6=0.3927;

disp('Flight Mode Keys')
fprintf('1 or u for upward\n');
fprintf('2 or b for backward pitch\n');
fprintf('3 or f for forward pitch\n');
fprintf('4 or l for left roll\n');
fprintf('5 or r for right roll\n');
fprintf('6 or y for yaw motion\n');
fprintf('7 or a for combined trans and attitude motion\n');


mode=input(sprintf('Enter desired flight mode: '));
```

```
switch mode
    case 1
        x1ref=ref1;
        x2ref=ref2;
        x3ref=ref3;
       x4ref=0;
       x5ref=0;
       x6ref=0;
    case {2,'b'}
       x1ref=ref1;
x2ref=ref2;
x3ref=ref3;
x4ref=0;
x5ref=ref5; % pitch back
x6ref=0;
    case 3
       x1ref=ref1;
x2ref=ref2;
x3ref=ref3;
x4ref=0;
x5ref=-ref5;% pitch forward
x6ref=0;
    case 4
       x1ref=ref1;
x2ref=ref2;
x3ref=ref3;
x4ref=ref4;% roll left
x5ref=0;
x6ref=0;
    case 5
       x1ref=ref1;
x2ref=ref2;
x3ref=ref3;
x4ref=-ref4;% roll right
x5ref=0;
x6ref=0;

    case 6
       x1ref=ref1;
x2ref=ref2;
x3ref=ref3;
x4ref=0;
x5ref=0;
x6ref=ref6;% yaw
    case 7
```

```
       x1ref=ref1;
x2ref=ref2;
x3ref=ref3;
x4ref=ref4;
x5ref=ref5;
x6ref=ref6;

    otherwise
        warning('Not a known flight mode')
end


Xref12=[x1ref x2ref x3ref x4ref x5ref x6ref 0 0 0 0 0 0]';
Xref14=[x1ref x2ref x3ref x4ref x5ref x6ref 0 0 0 0 0 0 0 0]';
Xref26=[x1ref x2ref x3ref x4ref x5ref x6ref 0 0 0 0 0 0 0 0 0 0 0 0 0 0 0 0 0 0
Xref20=[x1ref x2ref x3ref x4ref x5ref x6ref 0 0 0 0 0 0 0 0 0 0 0 0 0 0 0 0]';
Xinit=[ref1 ref2 ref3 ref4 ref5 ref6 ]'

Flight Mode Keys
1 or u for upward
2 or b for backward pitch
3 or f for forward pitch
4 or l for left roll
5 or r for right roll
6 or y for yaw motion
7 or a for combined trans and attitude motion
```

### B.1.20 Execution of various commands in script

```
sys1=ss(A,B,Clmat,0);
sys2=ss(Aclsys,[Bobsv;zeros(12,4)],[Cobsv zeros(6,12)],0);
sys3=ss(Aobsv,Bobsv,Cobsv,0);
sys4=ss(Aclsys);

figure(1)
initial(sys1,Xref12,simtime), title('Uncompensated QUAV Initial Response')

[ys,ts,xs]=initial(sys2,Xref26,simtime);
figure(2)
subplot(311)
plot(ts,ys(:,1)),title('x Displacement'),xlabel('Time(sec)'),ylabel('x(m)')
subplot(312)
plot(ts,ys(:,2)),title('y Displacement'),xlabel('Time(sec)'),ylabel('y(m)')
subplot(313)
plot(ts,ys(:,3)),title('Altitude'),xlabel('Time(sec)'),ylabel('z(m)')
```

```
figure(3)
subplot(311)
plot(ts,ys(:,4)),title('Roll'),xlabel('Time(sec)'),ylabel('\phi(rad)')
subplot(312)
plot(ts,ys(:,5)),title('Pitch'),xlabel('Time(sec)'),ylabel('\theta(rad)')
subplot(313)
plot(ts,ys(:,6)),title('Yaw'),xlabel('Time(sec)'),ylabel('\psi(rad)')
```

### B.1.21 Battery value

```
Vbatt=12.6; % volts
Vmin=9.9;
```

### B.1.22 Inverse matrix for torque generation in plus configuration

```
ct1=2.9107*10^-2;
ct2=2.7543*10^-2;
ct3=3.6171*10^-2;
ct4=4.0559*10^-2;


fwdmat=[1 1 1 1 ;...
                 0 -la 0 la;...
                 -la 0 la 0;...
                 ct1 -ct2 ct3 -ct4];

invmat=inv(fwdmat)
```

### B.1.23 Compute feedforward generator for the QUAV

```
G_fwd=-pinv(B)*(A-B*Kx)*pinv(Clmat)
```

### B.1.24 Gains for the nominal back stepping controller

```
k1=20.68;
k2=6.05;
k3=35.53;
k4=9.84;
k5=33.22;
k6=8.17;
k7=30.22;
k8=9.39;
k9=45.55;
k10=3.84;
k11=34.42;
```

```
k12=5.73;
k13=0.1178;
k14=0.1475;
```

### B.1.25 Pole placement for the actuators

```
% Aact=[-rho -mu ; alpha -beta];
Aact=[-rho -mu ; (n*Km)/(Jr+n*Jm) -beta];
Bact=[1/La 0]';
pact=[-19.970 ; -20.18];
Fact=place(Aact,Bact,pact)

Aii=[A+B*Kx P+B*Kv; zeros(2,12) Sexo];
rank(ctrb(Aobsv,Bobsv))
kii=-1*[k1 k2 k3 k4 k5 k6 k7 k8 k9 k10 k11 k12]';
Fim=place(A,B,pval)
stabkii=eig(A-B*Fim)
```

### B.1.26 Stabilizer analysis

using sylvester equation MQ-G1M=G2R

```
w1ref=wref;
w2ref=wref;
Gamm=[1 0 0 0 0 0 0 0 0 0 0 0 0 0;...
                0 1 0 0 0 0 0 0 0 0 0 0 0 0;...
                0 0 1 0 0 0 0 0 0 0 0 0 0 0;...
                0 0 0 1 0 0 0 0 0 0 0 0 0 0];

Gi=[0 1 0 0 0 0 0 0 0 0 0 0 0 0 ;...
        0 0 1 0 0 0 0 0 0 0 0 0 0 0 ;...
        0 0 0 1 0 0 0 0 0 0 0 0 0 0 ;...
        0 0 0 0 1 0 0 0 0 0 0 0 0 0 ;...
        0 0 0 0 0 1 0 0 0 0 0 0 0 0 ;...
        0 0 0 0 0 0 1 0 0 0 0 0 0 0 ;...
        0 0 0 0 0 0 0 1 0 0 0 0 0 0 ;...
        0 0 0 0 0 0 0 0 1 0 0 0 0 0 ;...
        0 0 0 0 0 0 0 0 0 1 0 0 0 0 ;...
        0 0 0 0 0 0 0 0 0 0 1 0 0 0 ;...
        0 0 0 0 0 0 0 0 0 0 0 1 0 0 ;...
        0 0 0 0 0 0 0 0 0 0 0 0 1 0 ;...
        0 0 0 0 0 0 0 0 0 0 0 0 0 1 ;...
        -6*w1ref*w2ref 0 0 0 0 0 0 0 0 0 0 0 0 0];

tstctrb=ctrb(Gi,G2)
```

```
rnktst=rank(tstctrb)
```

### B.1.27 Khalil's Observer gain

```
rank(obsv(A,Cvec))
% Lkh=place(A',Cvec',100*pval)'
kh=-1*rand(17,1)
hg=2;

Mg12=[kh(1) 0 0 0 0 0 0 0 0 0 0 0;...
            0 kh(2) 0 0 0 0 0 0 0 0 0 0 ;...
            0 0 kh(3) 0 0 0 0 0 0 0 0 0;...
            0 0 0 kh(4) 0 0 0 0 0 0 0 0 ;...
            0 0 0 0 kh(5) 0 0 0 0 0 0 0 ;...
            0 0 0 0 0 kh(6) 0 0 0 0 0 0 ;...
            0 0 0 0 0 0 kh(7) 0 0 0 0 0  ;...
            0 0 0 0 0 0 0 kh(8) 0 0 0 0  ;...
            0 0 0 0 0 0 0 0 kh(9) 0 0 0 ;...
            0 0 0 0 0 0 0 0 0 kh(10) 0 0 ;...
            0 0 0 0 0 0 0 0 0 0 kh(11) 0 ;...
            0 0 0 0 0 0 0 0 0 0 0 kh(12)];
cply12=poly(Mg12)

        stabMg12=eig(Mg12)

Mg14=[kh(1) 0 0 0 0 0 0 0 0 0 0 0 0 0;...
            0 kh(2) 0 0 0 0 0 0 0 0 0 0 0 0;...
            0 0 kh(3) 0 0 0 0 0 0 0 0 0 0 0;...
            0 0 0 kh(4) 0 0 0 0 0 0 0 0 0 0;...
            0 0 0 0 kh(5) 0 0 0 0 0 0 0 0 0;...
            0 0 0 0 0 kh(6) 0 0 0 0 0 0 0 0;...
            0 0 0 0 0 0 kh(7) 0 0 0 0 0 0 0 ;...
            0 0 0 0 0 0 0 kh(8) 0 0 0 0 0 0 ;...
            0 0 0 0 0 0 0 0 kh(9) 0 0 0 0 0;...
            0 0 0 0 0 0 0 0 0 kh(10) 0 0 0 0;...
            0 0 0 0 0 0 0 0 0 0 kh(11) 0 0 0 ;...
            0 0 0 0 0 0 0 0 0 0 0 kh(12) 0 0;...
            0 0 0 0 0 0 0 0 0 0 0 0 kh(13) 1;...
            0 0 0 0 0 0 0 0 0 0 0 0 -1 kh(14)];
cply14=poly(Mg14)
          stabMg14=eig(Mg14)


          %%%%%%%%%%%%%%%%%%%%%%
```

```
M1=[hg*cply12(1) 0 0 0 0 0 1 0 0 0 0 0;...
         hg^2*cply12(2) 0 0 0 0 0 0 1 0 0 0 0;...
         hg^3*cply12(3) 0 0 0 0 0 0 0 1 0 0 0;...
         hg^4*cply12(4) 0 0 0 0 0 0 0 0 1 0 0;...
         hg^5*cply12(5) 0 0 0 0 0 0 0 0 0 1 0;...
         hg^6*cply12(6) 0 0 0 0 0 0 0 0 0 0 1;...
         hg^7*cply12(7) 0 0 0 0 0 0 0 0 0 0 0;...
         hg^8*cply12(8) 0 0 0 0 0 0 0 0 0 0 0;...
         hg^9*cply12(9) 0 0 0 0 0 0 0 0 0 0 0;...
         hg^10*cply12(10) 0 0 0 0 0 0 0 0 0 0 0;...
         hg^11*cply12(11) 0 0 0 0 0 0 0 0 0 0 0;...
         hg^12*cply12(12) 0 0 0 0 0 0 0 0 0 0 0];

M2=[0 hg*cply12(1) 0 0 0 0 1 0 0 0 0 0;...
         0 hg^2*cply12(2)  0 0 0 0 0 1 0 0 0 0;...
         0 hg^3*cply12(3)  0 0 0 0 0 0 1 0 0 0;...
         0 hg^4*cply12(4)  0 0 0 0 0 0 0 1 0 0;...
         0 hg^5*cply12(5)  0 0 0 0 0 0 0 0 1 0;...
         0 hg^6*cply12(6)  0 0 0 0 0 0 0 0 0 1;...
         0 hg^7*cply12(7)  0 0 0 0 0 0 0 0 0 0;...
         0 hg^8*cply12(8)  0 0 0 0 0 0 0 0 0 0;...
         0 hg^9*cply12(9)  0 0 0 0 0 0 0 0 0 0;...
         0 hg^10*cply12(10)  0 0 0 0 0 0 0 0 0 0;...
         0 hg^11*cply12(11)  0 0 0 0 0 0 0 0 0 0;...
         0 hg^12*cply12(12)  0 0 0 0 0 0 0 0 0 0];

M3=[0 0 hg*cply12(1) 0 0 0 1 0 0 0 0 0;...
         0 0 hg^2*cply12(2)  0 0 0 0 1 0 0 0 0;...
         0 0 hg^3*cply12(3)  0 0 0 0 0 1 0 0 0;...
         0 0 hg^4*cply12(4)  0 0 0 0 0 0 1 0 0;...
         0 0 hg^5*cply12(5)  0 0 0 0 0 0 0 1 0;...
         0 0 hg^6*cply12(6)  0 0 0 0 0 0 0 0 1;...
         0 0 hg^7*cply12(7)  0 0 0 0 0 0 0 0 0;...
         0 0 hg^8*cply12(8)  0 0 0 0 0 0 0 0 0;...
         0 0 hg^9*cply12(9)  0 0 0 0 0 0 0 0 0;...
         0 0 hg^10*cply12(10) 0 0 0 0 0 0 0 0 0;...
         0 0 hg^11*cply12(11) 0 0 0 0 0 0 0 0 0;...
         0 0 hg^12*cply12(12) 0 0 0 0 0 0 0 0 0];

M4=[0 0 0 hg*cply12(1) 0 0 1 0 0 0 0 0;...
         0 0 0 hg^2*cply12(2)  0 0 0 1 0 0 0 0;...
         0 0 0 hg^3*cply12(3)  0 0 0 0 1 0 0 0;...
         0 0 0 hg^4*cply12(4)  0 0 0 0 0 1 0 0;...
         0 0 0 hg^5*cply12(5)  0 0 0 0 0 0 1 0;...
```

```
          0 0 0 hg^6*cply12(6)  0 0 0 0 0 0 0 1;...
          0 0 0 hg^7*cply12(7)  0 0 0 0 0 0 0 0;...
          0 0 0 hg^8*cply12(8)  0 0 0 0 0 0 0 0;...
          0 0 0 hg^9*cply12(9)  0 0 0 0 0 0 0 0;...
          0 0 0 hg^10*cply12(10) 0 0 0 0 0 0 0 0;...
          0 0 0 hg^11*cply12(11) 0 0 0 0 0 0 0 0;...
          0 0 0 hg^12*cply12(12) 0 0 0 0 0 0 0 0];

M5=[0 0 0 0 hg*cply12(1) 0 1 0 0 0 0 0;...
          0 0 0 0 hg^2*cply12(2)  0 0 1 0 0 0 0;...
          0 0 0 0 hg^3*cply12(3)  0 0 0 1 0 0 0;...
          0 0 0 0 hg^4*cply12(4)  0 0 0 0 1 0 0;...
          0 0 0 0 hg^5*cply12(5)  0 0 0 0 0 1 0;...
          0 0 0 0 hg^6*cply12(6)  0 0 0 0 0 0 1;...
          0 0 0 0 hg^7*cply12(7)  0 0 0 0 0 0 0;...
          0 0 0 0 hg^8*cply12(8)  0 0 0 0 0 0 0;...
          0 0 0 0 hg^9*cply12(9)  0 0 0 0 0 0 0;...
          0 0 0 0 hg^10*cply12(10) 0 0 0 0 0 0 0;...
          0 0 0 0 hg^11*cply12(11) 0 0 0 0 0 0 0;...
          0 0 0 0 hg^12*cply12(12) 0 0 0 0 0 0 0];

M6=[0 0 0 0 0 hg*cply12(1) 1 0 0 0 0 0;...
          0 0 0 0 0 hg^2*cply12(2)  0 1 0 0 0 0;...
          0 0 0 0 0 hg^3*cply12(3)  0 0 1 0 0 0;...
          0 0 0 0 0 hg^4*cply12(4)  0 0 0 1 0 0;...
          0 0 0 0 0 hg^5*cply12(5)  0 0 0 0 1 0;...
          0 0 0 0 0 hg^6*cply12(6)  0 0 0 0 0 1;...
          0 0 0 0 0 hg^7*cply12(7)  0 0 0 0 0 0;...
          0 0 0 0 0 hg^8*cply12(8)  0 0 0 0 0 0;...
          0 0 0 0 0 hg^9*cply12(9)  0 0 0 0 0 0;...
          0 0 0 0 0 hg^10*cply12(10) 0 0 0 0 0 0;...
          0 0 0 0 0 hg^11*cply12(11) 0 0 0 0 0 0;...
          0 0 0 0 0 hg^12*cply12(12) 0 0 0 0 0 0];

 Mkh=M1+M2+M3+M4+M5+M6

Lkh=-1.*[hg*cply12(1) hg*cply12(1) hg*cply12(1) hg*cply12(1) hg*cply12(1) hg
        hg^2*cply12(2) hg^2*cply12(2) hg^2*cply12(2) hg^2*cply12(2) hg^2*cpl
        hg^3*cply12(3) hg^3*cply12(3) hg^3*cply12(3) hg^3*cply12(3) hg^3*cpl
        hg^4*cply12(4) hg^4*cply12(4) hg^4*cply12(4) hg^4*cply12(4) hg^4*cpl
        hg^5*cply12(5) hg^5*cply12(5) hg^5*cply12(5) hg^5*cply12(5) hg^5*cpl
        hg^6*cply12(6) hg^6*cply12(6) hg^6*cply12(6) hg^6*cply12(6) hg^6*cpl
        hg^7*cply12(7) hg^7*cply12(7) hg^7*cply12(7) hg^7*cply12(7) hg^7*cpl
        hg^8*cply12(8) hg^8*cply12(8) hg^8*cply12(8) hg^8*cply12(8) hg^8*cpl
        hg^9*cply12(9) hg^9*cply12(9) hg^9*cply12(9) hg^9*cply12(9) hg^9*cpl
```

```
hg^10*cply12(10) hg^10*cply12(10) hg^10*cply12(10) hg^10*cply12(10)
hg^11*cply12(11) hg^11*cply12(11) hg^11*cply12(11) hg^11*cply12(11)
hg^12*cply12(12) hg^12*cply12(12) hg^12*cply12(12) hg^12*cply12(12)
```

# APPENDIX C
# PRESENTATION OF IMMERSION INVARIANCE SCRIPT

## C.1 Immersion Invariance Controller Design for RTAC System

```
[rw,col]=size(A);
Wr=ctrb(A,B)
rnkWr=rank(Wr)

if rnkWr==col
    disp('Rank is full')
    disp('System input is stabilizable by state feedback')
else
    disp('Rank is not full')
    disp('System input is NOT stabilizable by state feedback')
end
```

### C.1.1 Test for observability or detectability

```
[rw,col]=size(A);
Wo=obsv(A,C)
rnkWo=rank(Wo)

if rnkWo==col
    disp('Rank is full')
    disp('System output is stabilizable ')
else
    disp('Rank is not full')
    disp('System output is NOT stabilizable')
end
```

### C.1.2 Using matlabs place command find a feedback F with specified poles

```
pval=[-19 -3 -10 -13]';
F=place(A,B,pval)
stabAB=eig(A-B*F)
```

### C.1.3 Using matlabs place command, find an obsrver gain L

```
L1=place(A',Caug',pval)'
L2=place(A',C',pval)'
```

```
stabACL1=eig(A-L1*Caug)
stabACL2=eig(A-L2*C)
```

### C.1.4 Call model here

```
simtime=20.0
sim('rtac_imminv_lin') % time runs for simtime seconds
```

## C.2 Proof of Immersion Condition

Section 3.3.3 made mention of the immersion condition for the QUAV. Proof of the existence of such an immersion has been provided here. The immersion maps given in section 3.3.3 for the exosystem $\dot{w}_1 = w_2$ and $\dot{w}_2 = -w_1$ were $x_1 = \pi_1(w), x_2 = \pi_2(w), x_3 = \pi_3(w), x_4 = \pi_4(w), x_5 = \pi_5(w), x_6 = \pi_6(w), x_7 = \pi_7(w), x_8 = \pi_8(w), x_9 = \pi_9(w), x_{10} = \pi_{10}(w), x_{11} = \pi_{11}(w), x_{12} = \pi_{12}(w), e_1 = x_1 - w_1, e_2 = x_2 - w_1, e_3 = x_3 - w_1, e_4 = x_4 - w_1, e_5 = x_5 - w_1, e_6 = x_6 - w_1$. Application of the FBI immersion condition of equation ( **??**) .....

$$\dot{x}_1 = \frac{\partial \pi_1}{\partial w}\frac{dw}{dt} \equiv \pi_7 \tag{C.1}$$

since from the map relations $\frac{\partial \pi_1}{\partial w} = 1$ and $\frac{dw}{dt} = w_2$, it becomes conclusive that $\pi_7 = w_2$. With similar computation for $\dot{x}_2 \ldots 6$, it is proven that $\pi_7 \equiv \pi_8 \equiv \pi_9 \equiv \pi_{10} \equiv \pi_{11} \equiv \pi_{12} = w_2$. By similar reasoning the input immerison functions was derived as

$$\dot{x}_7 = \frac{\partial \pi_7}{\partial w}\frac{dw}{dt} \equiv (c\pi_4 s\pi_5 c\pi_6 + s\pi_4 s\pi_6)\frac{u_x(w)}{m} \tag{C.2}$$

but since $\pi_4 = \pi_5 = \pi_6 = w_1$ from the map relations and $u_x(w) \equiv c_x(w)$, equation ( C.2) can be re-writen as

$$-w_1 = (-sw_1c^2w_1 + s^2w_1)\frac{c_x(w)}{m} \tag{C.3}$$

from which $c_x(w) = \frac{-mw_1}{-sw_1c^2w_1 + s^2w_1}$. The same computation method was used to obtain $c_y(w), c_z(w), c_2(w), c_3(w)$, in section 3.3.3.

[1], [2],[3], [4], [5], [6], [7], [8], [9], [**ref10**], [10], [11], [12], [13],[14], [15], [16], [17], [18], [19] , [20] , [21] , [22], [23], [24],[25], [26], [27],[28],[29],[30],[31],[32],[33],[34],[35],[36],[37],[38], [39],[40],[41],[42],[43],[44],[45],[46],[47],[48],[49],[50],[51],[52],[53],[54],[55],[56],[57],[58],[59],[60],[61],[62 ,[83] ,[84],[85],[86],[87],[88],[89],